Phenotypic Plasticity in Economically and Ecologically Important Bivalves in Response to Changing Environments

Lindsay Alma

A dissertation

submitted in partial fulfillment of the

requirements for the degree of

Doctor of Philosophy

University of Washington

2022

Reading Committee:

Jacqueline Padilla-Gamiño, Chair

Steven Roberts

Paul Mcelhany

Program Authorized to Offer Degree:

School of Aquatic and Fishery Sciences

University of Washington

ABSTRACT

Phenotypic Plasticity in Economically and Ecologically Important Bivalves in Response to Changing Environments

Lindsay Alma

Chair of the Supervisory Committee:

Associate Professor, Jacqueline Padilla Gamiño

School of Aquatic and Fishery Sciences

Marine bivalves are ecologically important, providing ecosystem services like filtering water, stabilizing substrate, and creating hard structure for epibionts. Cultured bivalves are also economically important, supporting thousands of aquaculture jobs nationwide and providing valuable protein sources for our growing human population. However, recent shifts in the environment such as temperature, ocean acidification, hypoxia, and extreme environmental variation have greatly affected bivalve physiology, reproduction, and survival across multiple lifestages. Bivalves in the Northeast Pacific are increasingly vulnerable climate change related stressors like intensifying upwelling and weather extremes, defined stratification, and unique

geography which causes distinct spatial and seasonal variation. I seek to investigate if higher degrees of phenotypic plasticity and parental carryover will have the potential to improve bivalve's fitness and tolerance as climate change progresses. My goal is to evaluate plastic capacity by taking a multi-method approach to assessing the physiological metrics of several important bivalve species, using both field and laboratory experiments. Early lifestages are greatly influenced by parental environmental history leading to carryover effects, favoring phenotypes that have a higher likelihood of surviving. In addition to natural selection in the wild, commercial and restoration aquaculturists may select for beneficial phenotypes in adults and offspring which would yield the most desirable characteristics. In our experiment, I focus on three different species: the purple-hinge rock scallop *Crassadoma gigantea*, the Mediterranean mussels *Mytilus galloprovincialis,* and the Olympia oyster *Ostrea lurida.* By choosing a suite of native and non-native, inter- and subtidal species, I hope to obtain a broad snapshot of physiological responses to help restore vulnerable species and maximize quality of farmed product. Chapter 1 examines physiological responses of the scallop *C. gigantea* to climate change related stressors in the laboratory. I conducted a full factorial laboratory experiment, manipulating pCO_2 and temperature to mimic current and future ocean acidification and warming levels. After six weeks of acclimation, I found that stressors reduced shell strength and periostracum (outer shell layer) density. Only acidification affected lipids, and fatty acid content varied between treatments. I was the first to quantify microbial composition of a bivalve under multiple stressors and I found differences in the microbiome, especially with temperature stress. Chapter 2 explores physiological responses of *C. gigantea* and *M. galloprovincialis* in a six-month field acclimatation experiment. Shellfish were deployed in cages in Puget Sound, Washington at either 5 or 30 m below the surface. I found that environmental gradients varied

seasonally and spatially and affected growth, shell strength, and isotopic signatures. There were differences between the two species, namely with shell strength and $\delta^{13}C$. I found that no one depth or time period yielded the most desirable traits for culturing, and I highlight the concerning patterns in Puget Sound's most productive region. In Chapter 3, I took my research one step further by introducing a spatial component to a one-year field experiment. I outplanted *O. lurida* in cages at 5 m depth in three different locations in Puget Sound, one of which also had a 20 m depth. Each of these locations had an oceanographic monitoring buoy which allowed me to couple physiological data with high-resolution environmental data. I spawned the oysters to test parental carryover and found evidence in growth rates of larvae, which when acclimated to high temperatures, mirrored their parents. Interestingly, larval survival did not coincide with growth, and through respirometry, I found that 20°C may be a bottleneck for this lifestage. Adult oyster growth, isotopic signatures, and gametogenesis were affected by both seasonal and spatial field conditions. Metabolic responses to pH and temperature depending on recent acclimatization history. This research shows evidence of strong adaptive plasticity which was demonstrated by energetic trade-offs and parental carryover. Chapter 4 acclimatized *M. galloprovincialis* in the field in a similar fashion to *O. lurida*. Growth, shell strength, and isotopes were all affected by season and site. Similar to oysters, acute metabolic rate of each site and season was affected differently between pH and temperature. Shellfish covered in Chapter 3/4 have a high degree of plasticity and results are useful to restoration (oyster) and commercial (mussel) aquaculturists to create selective breeding programs that will withstand climate change. Results of this dissertation demonstrate the rapid degree of phenotypic plasticity and capacity for parental carryover in field and laboratory setting though a wide array of physiological analysis. Outcomes of this research

add to the limited but growing body of literature about multiple-stressors and field experiments, and indents to assist aquaculturists as climate change progresses.

TABLE OF CONTENTS

You may use the chapter/section, and sub-chapter/section designation system of your choice. You may choose to use no numbers, Arabic numbers (1, 2, 3, etc.), Roman Numerals (I, II, III, etc.) or written numbers (One, Two, Three, etc.). You may choose to list some, all, or none of your subchapter titles in the Table of Contents. You may choose to number your sub-headings, or not to number them. Whatever formatting choices you make, you must carry them out consistently through each chapter/section of your document.

LIST OF FIGURES

LIST OF TABLES

ACKNOWLEDGEMENTS

I would like to express my appreciation toward my advisor Jacqueline Padilla-Gamiño, for all your unwavering support, mentorship, and encouragement all these years. I would like to express my sincerest thanks to my committee members: Steven Roberts, Paul Mcelhany, Gordon Holtgrieve, and Parker McCready your their valuable mentorship, support, and feedback.

I would like to first thank my funding sources: Conchologists of America, International Women Fishing Association, UW Victor and Tamara Loosanoff Endowed Fellowship, William H. Pierce Sr. Endowed Fellowship, CSUDH Graduate Research and Development Grant, CSU COAST, CSUPERB, CSUDH College of Natural and Behavioral Sciences, NSF RUI (No. 1715066), Hutton Junior Fisheries Biology Program, NOAA-Saltonstall-Kennedy Grant Program (No. 12493539), Royalty Research Fund Fellowship, the Sloan Foundation Fellowship, and School of Aquatic and Fishery Sciences, and the University of Washington for financial support through multiple TA-ships.

I would like to express my gratitude to all the dozens of amazing people who helped me with this research along the way. A very special thanks to all the young scientist who assisted me with this project: Ashley Barbarino, Sabrina Madrigal, Christopher Mossberg, Fernando Nuñez, Crystal Rodriguez, Manuela Ramirez, Richard Soto, Natalie Whitehead, Lealand Wood, Owen Oliver, Linnea Stavney, Elizabeth Landefeld, Angel Sar, Claudia Penny, Abigail Ames, Leila Arafeh,

Delaney Lawson, Josie Dodd, Davi Borromeo, Andrew Olivero, Lilly Stair, Sarah Elgin, Trevor Derie, Kris Hiromoto, Gabriel McMillen, and Victoria Hsieh. I am deeply grateful for the support of my labmates Jeremy Axworthy, Callum Backstrom, Eileen Bates, Tanya Brown, Courtney Fiamengo, Corinne Klohmann, Miranda Roethler, Sarah Tanja, and Núria Viladrich.

My deepest appreciation goes to my collaborators: to Kelly Stromberg and Phil Cruver at Catalina Sea Ranch, Karen Kram of CSUDH, Rhonda Elliot, Molly Jackson, Benoit Eudeline, and Gordon King of Taylor Shellfish, Simone Alin of NOAA PMEL, Mike Maher of NOAA, Ryan Crim of Puget Sound Restoration Fund, Jan Newton, John Mickett, Chris Archer, Robert Danials, Ryan Newell, Zoe Parsons, Derik Martin, and Wendy Ruef at UW Applied Physics Lab. I'd like to thank everyone else who helped along the way: Jon Wittouck, Julia Hart, Laura Spencer, Yaamini Venkataraman, Ruben Pimentel, Grace Crandall, Beka Stiling, Ruben Pimentel, Brent Vadopalas, of SAFS, Joth Davis of Pacific Hybreed, Betsy Peabody, Olivia Cattau, and Stuart Ryan of Puget Sound Restoration Fund, Danielle Perez, Kate Rovinski, and Kelsey Donahue from NOAA Mukilteo Field Station.

DEDICATION

This dissertation is dedicated to my mom and all my wonderful friends who helped me through this degree. I would not have made it through without you.

1 CHAPTER 1

OCEAN ACIDIZATION AND WARMING EFFECTS ON THE PHYSIOLOGY, SKELETAL PROPERTIES, AND MICROBIOME OF THE PURPLE-HINGE ROCK SCALLOP

A version of this chapter has been published as:
Alma, L., Kram, K. E., Holtgrieve, G. W., Barbarino, A., Fiamengo, C. J., & Padilla-Gamiño, J. L. (2020). Ocean acidification and warming effects on the physiology, skeletal properties, and microbiome of the purple-hinge rock scallop. Comparative Biochemistry and Physiology Part A: Molecular & Integrative Physiology, 240, 110579. https://doi.org/10.1016/j.cbpa.2019.110579

1.1 ABSTRACT

Ocean acidification and increased ocean temperature from elevated atmospheric carbon dioxide can significantly influence the physiology, growth and survival of marine organisms. Despite increasing research efforts, there are still many gaps in our knowledge of how these stressors interact to affect economically and ecologically important species. This project is the first to explore the physiological effects of high pCO_2 and temperature on the acclimation potential of the purple-hinge rock scallop (*Crassadoma gigantea*), a widely distributed marine bivalve, important reef builder, and potential aquaculture product. Scallops were exposed to two pCO_2 (365 and 1050 μatm) and temperature (14 and 21.5°C) conditions in a two-factor experimental design. Simultaneous exposure to high temperature and high pCO_2 reduced shell strength, decreased outer shell density and increased total lipid content. Despite identical diets, scallops exposed to high pCO_2 had higher content of saturated fatty acids, and lower content of polyunsaturated fatty acids suggesting reorganization of fatty acid chains to sustain basic metabolic functions under high pCO_2. Metagenomic sequencing of prokaryotes in scallop tissue revealed treatment differences in community composition between treatments and in the presence of genes associated with microbial cell regulation, signaling, and pigmentation. Results from this research highlight the complexity of physiological responses for calcifying species under global change related stress

and provide the first insights for understanding the response of a bivalve's microbiome under multiple stressors.

1.2 INTRODUCTION

Anthropogenic activities have exponentially increased the carbon dioxide concentration in the atmosphere since the beginning of the Industrial Revolution. Increased CO_2 contributes to the "greenhouse" effect which causes the atmosphere and oceans to warm. Higher levels of CO_2 in the atmosphere lead to higher dissolution of CO_2 into the ocean. Increased CO_2 dissolution into the ocean can change carbon chemistry, making water more acidic and reducing calcium carbonate availability which is critical for many marine calcifiers (Doney et al., 2009).

As the Anthropocene progresses and carbon dioxide levels continue to increase, it is vital that we understand how different stressors associated with increased levels of pCO_2, such as ocean warming and ocean acidification, may interact (or not) and impact the performance of marine species. Identifying limits of physiological flexibility under multiple stressors will help to develop models to realistically predict how species will perform, allocate energy, adapt, and survive in an increasingly changing environment (Sebens et al., 2018). This will help us to quantify tolerance limits and determine under what circumstances the stressors act additively, antagonistically, or synergistically (Gunderson et al., 2015; Todgham and Stillman, 2013). Consequences of decreased physiological and organismal performance metrics in marine organisms due to changing ocean conditions have the potential to negatively impact associated food webs and local human economies.

Previous studies have shown that ocean warming and acidification usually interact additively or synergistically to reduce marine invertebrate fitness. In bivalves, ocean acidification can narrow the thermal tolerance range, resulting in a higher susceptibility to extreme temperatures and impairment in organismal performance (Schalkhausser et al., 2013). Hard shell clams exposed in the laboratory to increased pCO_2 and thermal stress lead to higher organismal energy demands to maintain basic metabolism (Matoo et al., 2013). Decreased fitness was observed in the common cockle which were exposed simultaneously to high pCO_2 and high temperature, where energy uptake and shell strength was reduced, and respiration increased (Ong et al., 2017). In sea urchin larvae, simultaneous exposure to increased temperature and pCO_2 significantly reduced larval metabolism (Padilla-Gamiño et al., 2013).

Marine bivalves are ecologically and economically important calcifiers that are currently being severely impacted by climate change related stressors (Barton et al., 2015; Talmage and Gobler, 2011). Previous studies have shown that near future ocean warming (OW) and ocean acidification (OA) levels predicted by year 2100 will negatively alter bivalve metabolism (Ivanina et al., 2013; Matoo et al., 2013; Timmins-Schiffman et al., 2014), decrease shell integrity and impair biomineralization (Wright et al., 2018, Duckworth and Peterson, 2013; Mackenzie et al., 2014a; Rühl et al., 2017), and cause the organism to be more susceptible to disease (Burge et al. 2014, Mackenzie et al. 2014b, Fuhrmann et al. 2019). To date, however, many knowledge gaps remain, specifically in the linkages between cellular metabolism, energy allocation and stress tolerance (Sokolova et al., 2012). Another important gap in our understanding is how a bivalve's microbiome will respond to OA and OW, and if virulent microbes in shellfish will become more prevalent under global change scenarios. Studies on shellfish microbial responses to single stressors have

just begun to emerge; Asplund et al. (2014) found that a four-month exposure of blue mussels (*Mytilus edulis*) to OA caused a higher incidence of the virulent microbe *Vibrio tubiashii*; and Furhmann et al. (2019) resolved that pacific oysters, *Crassostrea gigas,* exposed to OA treatment had a lower survival rate when exposed to Ostreid herpesvirus type I than those who were not subjected to OA.

The purple-hinge rock scallop *Crassadoma gigantea* (a, b) (Gray 1825, formerly *Hinnites multirugosus,* Gale 1928) is widely distributed across the North American Pacific Coast from Southern Alaska to Baja California, Mexico. They can be found from lower intertidal to 80 m depth (Bourne, 1987; Whyte et al., 1990). *C. gigantea* are ecosystem engineers – they form the foundation of reef structures by clustering on rocks, pilings, and oil rigs and provide habitat for thousands of organisms (**Error! Reference source not found.**c) (Laurén, 2008). Unlike other scallop species which have the ability to swim, *C. gigantea* permanently attach to hard substrate, making it very difficult to actively avoid unfavorable ocean conditions (Culver et al., 2006; RaLonde R., 2012).

C. gigantea is of interest in the aquaculture industry and is considered a seafood delicacy due to its large, sweet-tasting adductor muscle. Despite their ecological importance and growing interest in the aquaculture industry, to the authors' knowledge, there has not been any published research involving the impacts of global change on this species. These scallops are, and will further be, subject to OA and temperature stress throughout their native range along the California Current Large Marine Ecosystem (CCLME), which may affect the reefs they sustain and their future as a harvested aquaculture species (Filgueira et al., 2016). Due to the topographic and geographic nature of the CCLME, this area has already experienced increased upwelling (lowering the levels)

and warming events. This was exemplified during the marine heatwave of 2013-2016 where we observed high temperature anomalies in the CCLME of 1.5°C to 6.2°C (Bond et al., 2015; Di Lorenzo and Mantua, 2016). Studies predict that the CCLME will begin to experience summertime aragonite undersaturation within the optimal habitat depths of *C. gigantea* by year 2050 (Gruber et al., 2012; Hofmann et al., 2014).

In this study we used a multidisciplinary approach to understand the physiological response of *C. gigantea* under ocean warming and ocean acidification. Stressful conditions may cause organisms to reallocate their energy to sustain basic metabolic functions and this in turn can compromise other processes such as calcification, immunity, or growth. This study provides the first insights into the interactive effects of ocean warming and ocean acidification on the physiology, shell integrity and microbiome of *C. gigantea.* We sought to address the following questions: (i) To what extent are shell strength and skeletal density affected by multiple global change stressors in *C. gigantea?* (ii) What are the physiological impacts of simultaneous exposure of multiple stressors in terms of energy reserves and allocation? (iii) How is the microbiome of *C. gigantea* affected by exposure to ocean warming and ocean acidification? Results from this study provide insights into physiological tolerance of *C. gigantea* when subjected to near-future OA and OW conditions and long and short-term consequences to their fitness.

1.3 METHODS

1.3.1 Specimen Collection and Experimental Conditions

Mature adult *C. gigantea* were collected by SCUBA divers (scientific permit No. SC-9758) at 23-25 m depth on August 1, 2016. Collection site was located at Eureka Oil Rig, offshore of Huntington Beach, California (33.56405° N, 118.1158° W). Scallop shell height ranged from 4.1

to 17 cm with an average of 9.5 cm ± 2.7 cm (SD), and shell width range from 15.1 to 3.4 cm with an average of 9.4 cm ± 2.2 cm (SD). Scallops are estimated to be 5 years old on average based on a growth chart published by MacDonald et al. (1991). Following collection, scallops were scraped clean of epibionts and transported into saltwater tanks within 1 hour of collection. Scallops were measured and labeled with Milliput epoxy putty. The organisms were then placed in eight 60 L tanks filled with artificial sea water (n = 7 - 8 per tank) and allowed to acclimate to ambient conditions (14 ± 0.02°C and pCO_2 ~365 µatm) for one week prior to experimental treatments. Scallops were fed using Shellfish Diet 1800 (Reed Mariculture, Campbell, CA: 40% *Isochrysis galbana,* 25% *Tetraselmis, 20% Thalassiosira pseudonana, and* 15% *Pavlova lutheri).* The room was kept on a 14:10 h light: dark cycle and salinity was held constant at 33 ±1 PSU.

Following acclimation, scallops were held for six weeks in one of four treatments: (1) 21.5 °C, 1050 µatm, (2) 21.5°C, 365 µatm, (3) 14°C, 1050 µatm, and (4) 14°C, 365 µatm, which represent factorial combinations of ambient conditions and predictions for year 2100 (IPCC 2013; Stocker et al., 2013). pCO_2 was controlled in each tank by injecting a slow stream of CO_2 gas to a select threshold via a solenoid regulator system in accordance with the Standard Operating Procedure (SOP) for Ocean CO_2 Measurements (Dickson et al., 2007). All tanks were controlled for temperature individually using a closed loop heating and chilling system. Each treatment was performed in replicate, and each tank was completely independent of one another, with separate chillers, heaters, and CO_2 systems (Appendix Figure S1-1). Water samples were collected weekly and poisoned with 100 µl of saturated mercuric chloride ($HgCl_2$) in accordance with Dickson et al. (2007). Samples were tested for alkalinity using 2320 B open cell titration method (APAH 2012). Temperature, salinity, and carbonate chemistry (calculated using CO_2calc software, USGS,

Robbins et al., 2010) of seawater used in experimental treatments can be found in Appendix S1-1, Table S5-1-1.

At the end of the six-week experiment, scallops were removed from their tanks (5-7 individuals per tank), dissected, weighed for wet weight, and samples of ctenidia (gill), adductor muscle, gut, and remaining viscera were flash frozen with liquid nitrogen and stored at -80°C. Shells were cleaned of any tissue using a soft cloth and stored dry.

1.3.2 Shell Strength Analysis

All shells (n = 14 individuals per treatment) were rehydrated for 24 hours in seawater before performing shell strength tests (Ikejima et al., 2003). Each shell was marked using a paint marker at four equally spaced points across its length. A Universal Testing Machine (Instron, model 5585H) was fitted with a 3.9 mm cylindrical steel punch and 4.76 mm die (Carnarius et al., 1996; Ikejima et al., 2003; Wilkie and Bishop, 2012). Shells were removed from the saltwater and immediately placed onto the stage, with the inner side facing upward on a marked point and held perpendicular to the Instron plate. The crosshead was lowered onto the scallop shells at 5 mm s^{-1}, and the force (N) needed to puncture the shell was recorded using Bluehill Software (v.2) (Illinois Tool Works Inc, IL, USA). The puncture force (N) was averaged among 8 puncture points per individual, the 4 punctures made in each shell and in both shell vales of each individual. Shell thickness was measured at the eight marked points using a digital outside caliper gauge (0.01 mm accuracy).

Shell strength at each point was calculated using formulas from (Carnarius et al., 1996; Ikejima et al., 2003; Tyler, 1961). Where S is shell strength measured in megapascals (N mm^{-2}) is equal to F the maximum penetrating force (N) per t is the shell thickness (mm), and d is the diameter of the punch (mm) multiplied by pi to get the circumference of the punch. Shell thickness and maximum force for each treatment were correlated using a linear regression (Sofie Grefsrud and Strand, 2006; Wilkie and Bishop, 2012).

1.3.3 Micro-CT Scanning

Shells were scanned using a micro computerized tomography (Micro-CT) scanner (Skyscan model 1173, Burker, Belgium) to determine relative shell density. Dried shells (n = 14 per treatment) were scanned at an X-ray resolution of 1120x1120 using a 1 mm aluminum filter, a voltage of 65 or 70 kV, and a current of 114 or 123 µA for thinner and thicker shells, respectively. Two phantom rods (SP-4003 Burker, Belgium) of known volumetric density (0.25 and 0.75 g/cm^3) were scanned alongside shells for calibration purposes. Horizontal 2-D stacked images were re-projected into a 3-D image using Burker's NRecon software based on a modified Feldkamp's algorithm (Feldkamp et al., 2008).

To measure relative shell mineral density (g/cm^3), each 3-D image was calibrated by isolating phantom rods into a region of interest (ROI) and entering their known densities and attenuation coefficients (mm^{-1}) into a calibration algorithm within Burker's CT Analyzer v.1.16 software. Ten vertical 2-D cross sections were randomly selected throughout the length of each shell, and the total shell density was measured by tracing a ROI around the perimeter of the shell (Chatzinikolaou et al., 2017; Queirós et al., 2015). To compare the density of the periostracum (rough outer layer

of the shell exposed to the water) to the overall shell density, 15 pixels were selected as the ROI along the outside of the shell (Papageorgiou and Schmidbaur, 2014; Rühl et al., 2017). The ratio of periostracum to total shell density corresponded to the relative dissolution of the outer shell.

1.3.4 Total Lipid and Fatty Acid Analysis

Ctenidia and adductor muscle tissue were freeze dried for 48 hours and ground using a ball mill (Soudant et al., 1999; Tocher and Sargent, 1984; Whyte et al., 1990). A microbalance (sensitivity 10 µg) was used to measure 15 g of ground adductor mussel and ctenidia powder within pre-weighed aluminum tins. Total lipids (n = 11-14 per treatment, 5-7 per tank) were extracted in accordance with methods from Bligh and Dyer (1959). In short, two purification cycles of a 2:1 chloroform/methanol solution and ultrapure water were performed to separate the lower chloroform phase containing the lipids from the rest of the tissue. Total lipids were determined gravimetrically by drying and weighing a subsample.

The relative composition of 14-24 carbon chain fatty acids (FA) of each individual was determined by transmethylation of dry ctenidia lipid samples by acid-catalyzed esterification with a 1% sulfuric acid in methanol incubated at 50°C for 16 hour and extracted into fatty acid methyl esters (FAME) in accordance with methods from Christie (1998). FAMEs were analyzed using a flame ionization detector gas chromatograph (GC) (HP 6890, Agilent DB-23 column 30 m length, 0.25 mm diameter, 0.15 µm film thickness), and output chromatograph peaks were identified with a FA standard mixture (37-component FAME, Supelco, Bellefonte PA) (Galloway et al., 2015). An individual's FA profile was interpreted using a printed output chromatograph and calculated by normalizing each FA peak area by the sum of all FA peak areas.

1.3.5 Microbial enrichment and DNA extraction

To examine microbial taxonomy and functions, ctenidia and gut tissue (n = 3 per treatment and tissue) were homogenized using a sterile disposable mortar and 1.7 mL micro-centrifuge tube. During homogenization 500 mL NaCl saline (8.5%) buffer was added to the tissue. The homogenates were centrifuged at 1,000 RPM for 5 minutes to pellet the large tissue debris. The supernatant was transferred to a new micro-centrifuge tube and centrifuged at 10,000 RPM for 20 minutes to pellet bacterial cells (Oliveira et al., 2013). Genomic DNA was extracted from this pellet with the DNeasy Blood and Tissue kit (Qiagen Valencia, CA, USA) following the Gram-positive bacteria protocol.

1.3.6 Illumina metagenomic sequencing and bioinformatic analysis

Extracted genomic DNA was prepared for sequencing using the Illumina NexteraXT library preparation kit. Prepared libraries were normalized and pooled and sequenced on the Illumina HiSeq 4000, with 150 bp paired end reads. Quality of sequencing reads were assessed with FastQC (Andrews and Babraham Bioinformatics, 2010). Taxonomic and functional classifications were run using the InsideDNA cloud-based platform (https://insidedna.io). Reads were classified against the bacteria NCBI-database at the species and family level using the classify_metagenome script from CLARK 1.2.4 (Ounit et al., 2015).

1.3.7 Functional annotation

DIAMOND 0.9.18 (Buchfink et al., 2014) was used to align sequences against nr (non-redundant protein sequences) database using the script diamond blastx --db nr.dmnd. MEGAN 6.10.10 (Huson et al., 2007) with SEED (Overbeek et al., 2014) database was used to get functional classification using the script daa2rma -a2seed acc2seed-May2015XX.abin.

1.3.8 Statistical Analysis

Statistical analyses on shell strength, CT-scans, lipid, FAs, and bacterial metagenomics were performed in R Version 3.5.3. We applied a linear mixed effects model for each response variable with tank replicate as a random effect and temperature and pCO_2 as fixed effects using the lmer function from the library lme4 (Bates et al., 2014). Hypotheses testing was conducted based on the fixed effects only using a two-way ANOVA. Post-hoc Tukey HSD tests (corrected for multiple comparisons) was performed to determine differences among treatments. A Shapiro-Wilk test was performed to assess normality of the data, and a Levene's test was performed to confirm homogeneity of variance. If needed, values of analysis were log transformed to achieve normality assumptions before the model was run. A non-metric multidimensional scaling analysis (NMDS) was performed using metaMDS Bray-*Curtis* dissimilarity and oridhull functions within vegan library in R (Oksanen et al., 2013) and was used to visualize distribution of FAs and microbes among treatments (Galloway et al., 2015; Timmins-Schiffman et al., 2014). FA's and bacterial community differences among treatments were analyzed using a fixed factor permutational multivariate analysis (PERMANOVA) using R vegan adonis function with 10,000 random permutations of the residuals under the reduced model (Lamb et al., 2017). Shannon index of microbes was calculated using the R vegan diversity function. Both Sorenson and Bray-Curtis

dissimilartiy indices were calculated using the “beta-pair” or “bray.part” function of the R betapart package (Baselga and Orme, 2012) and the vegan betadisper function.

1.4 RESULTS

1.4.1 Shell Strength

Both, high pCO_2 and high temperature decreased shell strength ($p < 0.001$, $p = 0.01$, Figure 1-2a, Table 1-1). At ambient temperature (14°C), shell strength decreased by 24% under high pCO_2 whereas at high temperature (21.5°C), shell strength decreased by 19% under high pCO_2 (Figure 1-2a). The interaction between pCO_2 and temperature was not significant, indicating no synergistic effect ($p = 0.60$, Table 1-1). Linear regression analyses revealed that the force needed to puncture the shell was positively correlated with shell thickness ($p < 0.001$, Figure 1-2b). In this and all other analysis, no significant differences between replicate tanks were observed. Additional variance from multiple tanks was estimated to be zero, indicating no effect of tank on the response variables.

1.4.2 Scallop Growth

Wet weigh of scallops did not change between treatments after 6 weeks ($p=0.88$). We performed shell length and width measurements before and after the experiment and we did not detect any growth during the 6-week experiment (on a millimeter scale).

1.4.3 Micro-CT Scanning

Micro-CT scanning results revealed no significant differences in overall shell density between treatments (p = 0.294, p = 0.793 for pCO_2 and temperature respectively, Table 1-1). However, there was a 14.6% reduction in the ratio of periostracum density:total shell density in scallops acclimated to high pCO_2 ($p < 0.001$ Figure 1-2c, Table 1-1), suggesting that dissolution may occur primarily in this upper layer as opposed to the deeper layers of the shell. The interaction term between pCO_2 and temperature was not significant, indicating no synergistic effect (p = 0.355, Table 1-1). Additional variance from multiple tanks was estimated to be zero, indicating no effect of tank on the response variables.

1.4.4 Total Lipid and Fatty Acid Analysis

Total lipid content was 30.6% higher in the ctenidia than the adductor muscle ($p < 0.001$). Increased pCO_2 had a significant effect on lipids in both ctenidia and adductor muscle ($p < 0.001$). Total lipid content was not significantly affected by temperature, nor the interaction term in either tissue type (Figure 1-3a, Table 1-1). Additional variance from multiple tanks was estimated to be zero, indicating no effect of tank on the response variables.

Despite identical diets, twenty-five individual fatty acid peaks were isolated in the GC profiles of scallop ctenidia (Table 1-2). Eight FAs had significant differences between treatments in the three major classes: saturated fatty acids (SFA), monounsaturated fatty acids (MUFA), and polyunsaturated fatty acids (PUFA). FAs that had significant differences ($p < 0.05$) between treatments were pentadecanoic acid 15:0 (derived from gut dwelling bacteria), iso-16:0 (derived from gut dwelling bacteria), 18:0 (stearic acid), 20:0 (gadoleic acid), 16:1ω7 (palmitoleic acid),

16:2ω4 (9,12-hexadecadienoic acid), 18:2ω6 (linoleic acid), and 22:5ω6 (Docosapentaenoic acid). NMDS analysis of ctenidia FAs (Bray Curtis stress=0.079) showed high similarity between the samples from the control group (14°C/365 µatm) and low similarities among samples exposed to high temperature (21.5°C) (Figure 1-3b). A PERMANOVA comparing the diversity of FA biomarkers between treatments revealed no significant interaction of pCO_2 and temperature ($p = 0.183$, $R^2 = 0.0312$). Scallops exposed to high pCO_2 had 31.7% and 14.7% less PUFAs (21°C and 14°C, respectively) compared to the ambient pCO_2 treatment.

1.4.5 Microbial Analysis

We analyzed changes in the bacterial community of scallops by performing metagenomic sequencing of both ctenidia and gut tissues. Figure 1-4 shows bacterial diversity of each family in both tissue types. Most samples have a similar bacterial community, however there are a few samples that have one dominant taxon. Overall, we can define several prevailing bacterial families present in every individual including Propionibacteriaceae, Mycoplasmataceae, Flavobacteriaceae, Shewanellaceae, Pasteurellaceae, Streptococcaceae, Alteromonadaceae, Rhodobacteraceae, Enterobacteriaceae, and Mycobacteriaceae; each of these families made up at least 2% of total microbial diversity. Within treatments, Vibrionaceae was the dominant family in individuals exposed to 21.5°C, while those exposed to the 14°C treatment had the highest occurrence of Propionibacteriaceae. Vibrionaceae made up an average of 18% of the bacterial community in the 21.5°C treatments when compared to individuals exposed to 14°C where Vibrionaceae only made up 1.3% of its bacterial diversity. In contrast, Propionibacteriaceae made up only 2.8% of the community in the 21.5°C treatment and 15.6% in the 14°C treatment.

PERMANOVAs comparing community composition of gut and ctenidia revealed that there was no significant difference in composition between tissue types (p = 0.212, R^2=0.07). Overall, there were no significant differences in microbial composition between any treatments (p = 0.836, R^2 = 0.02), however temperature had a nearly significant effect (p = 0.055, R^2 = 0.1). Within tissue types regardless of treatment, Mycoplasmataceae (9.24%) and Rhodobacteraceae (4.5%) were the dominant taxon in ctenidia and Vibrionaceae (16.5%) and Propionibacteriaceae (10.8%) were dominant within the gut. The NMDS plots (Figure S1-2a) shows that microbial community composition among individuals is more similar in the ctenidia tissue than in the gut tissue. Organisms exposed to high temperature showed lower similarity in microbial composition compared to organisms under ambient temperature (Figure S1-2b).

In some cases, we found individuals that contained low microbial diversity and were dominated by one main group of bacterial taxa. For example, one individual's bacterial community from the 21.5°C/365 µatm treatment was dominated by Rhodobacteraceae at 46% of the community. The gut of several individuals exposed to 21.5°C was dominated by Vibrionaceae. One individual from the 21.5°C/1050 µatm treatment was dominated by Enterobacteriaceae (*Escherichia spp.*) at 74% of its total bacterial community. Treatments did not lead to a significant difference in microbial Shannon diversity index when measured in tissues together (F = 0.471, p = 0.706), ctenidia tissues only (F = 1.804, p = 0.224), or gut tissues only (F = 1.978, p = 0.196). Further, both the Sorenson's index and the Bray-Curtis dissimilarly index showed no significant differences in abundance and evenness of taxon between treatments (F = 0.548, p = 0.655 and F = 0.861, p = 0.477, respectively).

In our metagenomic analysis, we identified few significant differences in bacterial community genes in the functional categories of ctenidia and gut tissue. The ctenidia tissue had significant differences among pCO_2 treatments in 'Cofactors Vitamins Prosthetic Groups Pigments' (p = 0.003). A higher percentage of reads in the 'Regulation and Cell Signaling' functional group were found in the ctenidia samples from the high temperature/high pCO_2 treatment (21.5°C/1050 µatm) (p = 0.04, Figure 1-5a). There were no significant differences in functional groups tested in the gut tissue.

1.5 DISCUSSION

Multi-stressor experiments can help us to better predict physiological tolerances and associated ecological consequences in a changing and dynamic global environment. Stressors can act independently or interact synergistically or antagonistically to affect the performance of an organism (Todgham and Stillman, 2013). This study is the first to provide evidence that both ocean acidification and ocean warming can work additively to affect metabolism of *C. gigantea.* Our integrative approach revealed three fundamental insights into the effects of simultaneous exposure of multiple stressors to organismal performance and function. First, OA reduced shell strength by 21% and outer shell density by 17%. Second, simultaneous exposure to multiple stressors increased total lipid content in the ctenidia by 41%, and led to a redistribution of the fatty acid profile. Third, there were marginal differences in the microbiome of the scallop under different temperature treatments. This study highlights the importance of performing multi-stressor experiments at different levels of biological organization.

1.5.1 Shell integrity and growth

Shell strength and density are important traits to protect against predators and inclement water conditions. If shells are compromised by acidic or warm waters, organisms may not be able to defend their soft body tissue nor metabolically cope with the energetic demand of biomineralization (Ivanina et al., 2013; Li et al., 2015). We did not detect any shell growth during our 6-week trial most likely due to the slow growing nature of this species (MacDonald et al. 1991) However, both temperature but primarily pCO_2 affected overall strength of the scallop shell, mirroring similar results in other bivalves (Duckworth and Peterson, 2013; Mackenzie et al., 2014a; Melzner et al., 2011).

Micro-CT scans revealed that shell dissolution occurred mainly in the shell's periostracum layer, the scallop's first level of defense and an important substrate for juvenile scallops and other organisms to recruit. The periostracum is made of a complex protein matrix called conchiolin, which binds aragonite to the outer layer of the shell. Based on our experiment's undersaturated aragonite levels, it is plausible that in an extreme scenario of ocean acidification, *C. gigantea* could experience "death by shell dissolution" as suggested by Green et al. (2009). Reduced shell strength and density due to aragonite undersaturation may make scallops more susceptible to boring epibionts (i.e. drilling "date" mussels, boring sponges, tubeworms) (Beuck et al., 2007; Duckworth and Peterson, 2013) and predators (i.e. sea stars, crabs, otters) who optimize their forage habits and preferentially choose to eat weaker shelled organisms based on time and effort required per energy intake (Kroeker et al., 2014).

Corroding and dissolution of the shell due to the undersaturation of aragonite can take a heavy toll on the energy budget of the organism when in a warm and acidified environment. In a time of stress, shell repair and production may be sacrificed to account for other internal and more essential metabolic maintenance processes (Melzner et al., 2011). Weakened shells in acidified and warmed conditions suggests that scallops in our study may have re-allocated their energy from shell biomineralization to sustain basic metabolic functions to cope with environmental stress or high pCO_2 conditions caused shell dissolution (Mackenzie et al., 2014a; Ramajo et al., 2016). Shell integrity measurements in this study should be interpreted with caution given the caveats involved in the use of artificial seawater as opposed to natural seawater. It is well know that artificial seawater has different carbonate chemistry than natural seawater and may have influenced the rapid change we observed in shell integrity, so further research should be conducted using natural seawater.

1.5.2 Energy reserves and metabolism

Bivalves are very dependent on lipids as an energy source (Milke et al., 2004; Rocchetta et al., 2006). In our experiment, exposure to increased pCO_2 led to a significant increase in total lipids, which suggests potential downregulation of metabolic activities as a survival technique to conserve energy (Hand and Hardewig, 1996). A similar result has been seen in eastern oysters, *Crassostrea virginica,* and hard clams, *Mercenaria mercenaria,* exposed to either 400 or 800 μatm and 22 or 27°C; both clams and oysters from the 800 μatm/27°C treatment had significantly higher total lipid content (Ivanina et al., 2013). It is possible that given these stressful conditions, lipids were being preserved, and an increased amount of protein was being burned to sustain metabolic functions, as is the case with pacific oysters exposed to variable pH and temperature conditions in the intertidal

(Clark et al., 2013). Another example of stress induced lipid redistribution has been seen in Pectinids closely related to *C. gigantea*: the spiny pink scallop and bay scallop. In these species, lipids from other organs were transferred to the gonads under stressful conditions over a series of five months to promote gametogenesis (Barber and Blake, 1981; Pernet et al., 2007). This strategy may be a short-term stress response which may benefit scallop populations, however the redistribution of lipids away from other metabolic functions and shell biomineralization will negatively impact populations in longer time scales.

Examining fatty acid constituents within the lipids can help us determine oxidative stress, energy supply, tissue repair, and growth potential (Milke et al., 2004; Nevejan et al., 2003; Whyte et al., 1991). We found an increase in the saturated fatty acid to PUFA ratio in the high temperature and high pCO_2 treatment, suggesting reorganization of fatty acids under stress without altering the total lipid content (Ivanina et al., 2013; Rocchetta et al., 2014, 2006). Scallops and related bivalves have a high requirement for omega-3 long-chain PUFAs such as ALA (α-Linolenic acid), DPA (Docosapentaenoic acid), DHA (Docosahexaenoic acid), and EPA (Eicosapentaenoic acid) to sustain various metabolic functions (Cotonnec, 2002; Milke et al., 2004). Bivalves must acquire PUFAs from their diet, as they have no capability to synthesize them (Chu and Greaves, 1991). A lower ratio of PUFAs compared to SFAs in bivalve tissue occurs as a stress response to unfavorable water quality (Rocchetta et al., 2006; Williams et al., 2016). The largest decline in PUFAs was observed in the multistressor treatment (21.5°C/1050 µatm), where total PUFAs decreased by 31.7% as compared with the control, which is consistent with the concept of homeoviscous adaptation, where unsaturated fatty acid content tends to decrease in warmer conditions (Hazel and Eugene Williams, 1990). However, there was a slight increase in PUFAs in the treatment with

elevated temperature and ambient pCO_2 (5.1%) which may suggest that elevated pCO_2 may have hasten the accumulation of SFAs in the cell membrane within our short experimental time. PUFAs include essential fatty acids, nutritional value, and added taste which are an important attribute to shellfish consumers (Martin et al. 2019), thus future studies should focus on how fatty acid remodeling due to climate change stressor may impact the market and profitability of the *C. gigantea*. Further experiments using natural sea water and live algal feed will improve our understanding of how this species will be affected by pCO_2 and temperature in their natural environment.

1.5.3 Microbial composition

Changes in microbial composition in bivalves exposed to stressors is largely understudied but may offer us a great deal of information on the fitness of the host bivalve (Lokmer and Mathias Wegner, 2015). Exploring the microbial composition in rock scallops provided us with the first map of the microbiome of this species, and the first ever insights to bivalve microbe redistribution and possibly disease susceptibility when subjected to simultaneous thermal stress and acidification treatments. Regardless of treatment the microbiome community of rock scallops, organized as OTUs (operational taxonomic units) at the family level from most to least abundant are: Propionibacteriaceae, Mycoplasmataceae, Flavobacteriaceae, Shewanellaceae, Pasteurellaceae, Streptococcaceae, Alteromonadaceae, Rhodobacteraceae, Enterobacteriaceae, and Mycobacteriaceae, each which made up at least 2% of total microbial diversity. Deviations from this microbiome may suggest pathogenic infection or a change in metabolic processes and help us identify and predict impacts of global change (Shade and Handelsman, 2012). A larger sample size, more tissue types, and spatial and more temporal separation between samples may assist future studies in further defining the microbiome community for this species.

Tissue specific community structure differences between ctenidia and gut microbiomes suggest that the ctenidia may be more representative of the microbiome, while the gut is dominated by low evenness and many OTUs known to harbor disease, as seen in many other studies on organisms (Lokmer and Mathias Wegner, 2015; Xiong et al., 2018). Within the ctenidia tissue, Mycoplasmataceae was the dominant OTU. The Mycoplasmataceae family contains a wide range of species which are ubiquitous in the animal kingdom and usually have fewer metabolic abilities and exist "quietly" with the host (Tatarinova et al., 2016). Similarly, the ubiquitous family Propionibacteriaceae was found as one of the dominant OTUs in the gut. Propionibacteriaceae function in storing phosphate for the host and producing anaerobic byproducts such as propionic and lactic acid (Stackebrandt and Schaal, 2006).

Overall, we saw no differences in microbial diversity in tissue type nor treatment, however there was a marginally significant effect of temperature. Notably, individuals exposed to 14°C had a more species evenness, and none were dominated with large amounts of Vibrionaceae, Rhodobacteraceae, or Enterobacteriaceae, all potentially pathogenic families. Vibrionaceae were not significantly different in the treatment groups, however this group seemed to be more prevalent among individuals acclimated to high temperature (21.5°C). Virulent strains of *Vibrio spp.* are frequently transmitted to humans via consumption of marine bivalves and have been associated with bivalve disease in aquaculture environments (Gradoville et al., 2018). A meta-analysis of thermal stress on oysters has concluded that increasing thermal stress due to global change directly correlates to increased occurrences of *Vibrio* infection in bivalves (Young et al., 2015). Similarly, climate warming perturbations such as El Ni*ño have also proven to increase the occurrence of*

Vibrio (Martinez-Urtaza et al., 2008). Every individual in our study contained at least a trace amount of *Vibrio*, and it is likely that stressful and warmer conditions of the experiment allowed the microbe to proliferate. One individual in our experiment exposed simultaneously to OW and OA had its microbial composition dominated by Enterobacteriaceae. *E. coli* and *Salmonella spp.*, both Enterobacteriaceae, have also been recorded to proliferate as temperature increases (Kumar et al., 2015; Pachepsky et al., 2014). An individual in our 21.5°C/365 µatm treatment was dominated by Rhodobacteraceae, which has also been seen in the spiny lobster, whose microbial diversity decreased and Rhodobacteraceae proliferated when exposed to 34°C thermal stress treatments (Ooi et al., 2019). Differences in the community composition within gut tissues may have contributed to the differences seen in levels of FA that are derived from bacteria in the gut tissues. Future investigation on the progression of Vibrionaceae, Enterobacteriaceae, and Rhodobacteraceae in the context of multiple stressors would be useful in determining the mechanisms behind the transmission and proliferation of these opportunistic bacteria. Feeding the scallops natural diets (as opposed to commercial frozen diets) and using natural sea water may yield different results since gut microbes are known to be strongly influenced by nutrient concentrations in the water and the type of food the shellfish ingest (Simons et al., 2018).

Bivalve's resident microbiome in the wild may vary greatly depending on a multitude of factors such as environmental chemistry, anthropogenic stressors, and type of tissue sampled (Pierce and Ward, 2018). The microbiome of farmed Peruvian scallops (*Argopecten purpuratus) shared similar families with scallops in our study including:* Vibrio, Mycoplasmataceae, and Enterobacteriaceae (Muñoz et al., 2019). A recent study analyzing the microbiome of wild black-lipped pearl oyster (*Pinctada margaritifera) also showed similar families such as*

Flavobacteriaceae and Rhodobacteraceae (Dubé et al., 2019). Overall, there is very little data on bivalve core microbiomes in their natural environment, and how factors such as season, site of collection, depth, diet, age, and health state may influence an individual's microbial community.

When evaluating the results of the bacterial metagenome, it becomes evident that bacterial communities have experienced a narrow but significant shift in functional profiles between treatments. Increased number of biomarker genes encoding cell regulation/signaling in the ctenidia of the high pCO_2 treatments suggests that the members of the microbiome may have increased ability to communicate with each other and/or the host tissue and other bacterial species (Levy et al., 2015). Bacterial communication is mediated by quorum sensing, which involves the production, release and detection of autoinducers (small hormone-like molecules). Using this chemical communication bacteria can detect their environment and respond by changing in population size and/or community structure, which in some instances may be harmful for the host organism (Waters and Bassler, 2005). Decreased numbers of genes in the 'Cofactors, Vitamins, Prosthetic Groups, Pigments' classification in higher pCO_2 treatments may indicate that microbial pigment production is less likely in these communities, which may be associated with pathogenesis within the host tissue (Liu and Nizet, 2009). Due to the limited nature of our metagenomics analysis, we can only predict what these cells have the potential of expressing. Continued research into the metatranscriptome and community proteomics could help us determine precise gene expression.

1.6 CONCLUSION

Future global change scenarios are predicted to lead to more variable and extreme ocean conditions. This study shows that OW and OA can interact or not and affect the overall physiological health of the purple-hinge rock scallop at multiple cellular levels. When these two stressors are combined, lipid metabolism is significantly affected. However, shell weakening and dissolution and microbial composition did not depend on the interactive effects of these stressors. The fact that we observed these effects within a short six-week experiment may indicate that the future survival and physiological performance of this and similar species needs to be closely monitored if carbon dioxide trends continue as predicted by the end of the twenty-first century. Our results suggest that portions of organism's bodies which are in direct contact with the surrounding water (i.e. ctenidia and periostracum) experience observable effects relatively fast, however this may be an artifact of our short exposure time. Given a longer exposure time, we may begin to see the effects of these stressors in deeper layers of the shell and body. Future research using metabolite, transcriptome, proteome, and multi-generational analyses will help to determine the precise mechanisms involved in the dynamic metabolic budget and adaptive potential of *C. gigantea* under multiple stressors. Moreover, experimental research of multiple stressors in the field will be critical to understand how these organisms' physiology respond under natural conditions. pCO_2 fluctuations along the California Current Large Marine Ecosystem are often associated with upwelling events which are paired with colder rather than warmer temperatures, so it is unlikely that we will observe both extreme conditions simulated in this experiment simultaneously at the current time. However IPCC predictions for the CCLME project this as a possibility within this century (Alexander et al., 2018; Stocker et al., 2013). Results from this study are critical in predicting the fate of *C. gigantea,* and similar/associated species as the Anthropocene

progresses. The reef system and epibionts that *C. gigantea* supports may be affected by reallocation of energy to non-shell formation processes. Restructuring of important fatty acids and microbes may diminish the quality of this potential seafood product for the aquaculture industry as well as their nutritional value for predators and long-term survival. This study highlights the importance of integrative multiple-stressor experiments to assess a snapshot of short-term response to climate related stressors at both the organismal and molecular level.

1.7 FIGURES

Figure 1-1 *(a) C. gigantea* shell, (b) interior (15 cm), (c) *C. gigantea* serves host to epibionts (~7 cm)

Table 1-1: Summary of Two-Way ANOVA statistics used in this study. Bolded terms indicate a significant difference ($p < 0.05$)

	df	**Mean Sq**	**F value**	***p***
Shell Strength				
pCO_2	1	0.171	13.706	**< 0.001**
Temperature	1	0.0867	6.943	**0.0110**
Temperature: pCO_2	1	0.0001	0.0154	0.902
Residuals	52	0.01249		
Total Shell Density				
pCO_2	1	0.0431	1.123	0.294
Temperature	1	0.00265	0.0693	0.793
Temperature: pCO_2	1	0.0894	2.336	0.133
Residuals	50			
Periostracum:Total Shell Density				
pCO_2	1	0.0244	15.179	**< 0.001**
Temperature	1	0.00933	0.580	0.451
Temperature: pCO_2	1	0.014	0.871	0.355
Residuals	50	0.0161		
Total Lipids Gill				
pCO_2	1	0.115	21.678	**< 0.001**
Temperature	1	0.0347	6.532	0.0609
Temperature: pCO_2	1	0.0322	6.057	0.0675
Residuals	48	0.0055		
Total Lipids Adductor				
pCO_2	1	0.349	11.536	**< 0.001**
Temperature	1	0.00281	0.0931	0.761
Temperature: pCO_2	1	0.0323	1.0686	0.306
Residuals	50	0.0302		

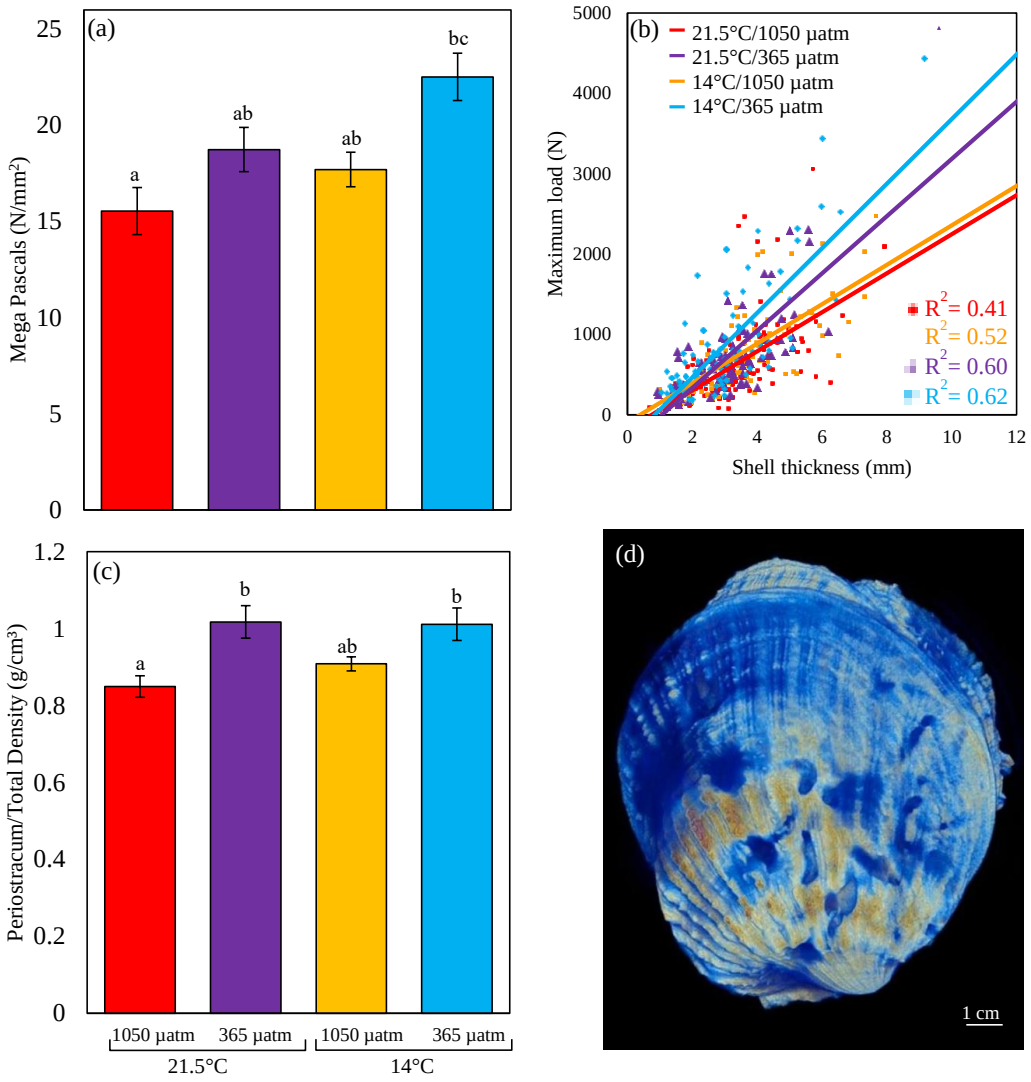

Figure 1-2: Values given as means ± S.E. (n = 14 individuals per treatment). Different letters indicate significant differences ($p < 0.05$). (a) Force needed to puncture a shell at 4 points across the length, normalized by thickness of the shell (mega pascals), (b) Relationship between shell thickness (mm) and maximum load (N) needed to puncture C. gigantea shells. The force needed to puncture the shell was positively correlated with shell thickness. Each point represents one puncture point, and each shell was punctured 4 times and averaged for statistical analysis. (c) Ratio between C. gigantea periostracum and overall shell density after six-week exposure to temperature and pH treatments. (d) A rock scallop shell reprojected and colored using micro-CT imaging and software.

Table 1-2: Total lipids expressed as mg/g of total ctenidia tissue dry weight. Fatty acids reported as normalized values from % of total FA peak areas identified (mean ± s.d.). Trace amounts of FAs < 0.5% of total omitted (—). Different letters indicate significant differences, corrected for multiple comparisons ($p < 0.05$).

	14°C/365 µatm	14°C/1050 µatm	21.5°C/365 µatm	21.5°C/1050 µatm
	n = 14	n = 11	n = 12	n = 14
Total Lipid (mg/g DW)	98.3 ± 4.2^{c}	98.4 ± 3.5^{c}	110.2 ± 3.6^{b}	148.3 ± 8.8^{a}
Saturated Fatty Acids (SFA)				
14:0 (Myristic)	1.8 ± 0.4	2.5 ± 1.-	2.2 ± 1.0	2.3 ± 0.7
15:0	**1.3 ± 0.3^{b}**	**1.6 ± 0.4^{b}**	**1.6 ± 0.3^{b}**	**2 ± 0.4^{a}**
16:0 (Palmitic)	24.9 ± 4	25.7 ± 6.8	27.2 ± 6.7	24.2 ± 5.3
i-16:0	—	—	**0.5 ± 0.4^{b}**	**1.6 ± 0.9^{a}**
17:0	4 ± 0.9	4.1 ± 1.3	4.2 ± 1.1	4.5 ± 1
a-18:0	2.5 ± 1.6	1.8 ± 1.4	2.1 ± 0.9	2.5 ± 1
18:0 (Stearic)	**21.9 ± 6^{ab}**	**18.7 ± 5.6^{b}**	**20.8 ± 4.2^{b}**	**25.6 ± 6.3^{a}**
20:0	**1 ± 0.3^{b}**	**0.6 ± 0.3^{a}**	**0.5 ± 0.3^{a}**	**0.6 ± 0.4^{a}**
Monounsaturated Fatty Acids (MUFA)				
16:1ω7	**1.3 ± 0.5^{a}**	**1.1 ± 0.9^{ab}**	**1.4 ± 0.8^{b}**	**2 ± 0.7^{b}**
17:1	0.7 ± 0.4	—	0.8 ± 0.2	0.8 ± 0.3
18:1ω9 (Oleic)	2.3 ± 0.6	2.4 ± 1.2	2.4 ± 1	1.9 ± 1.1
18:1ω7	2.1 ± 0.7	2.4 ± 1.0	2.8 ± 1	2 ± 1.2
20:1ω11	2.1 ± 0.7	2.4 ± 1	2.8 ± 1.0	2 ± 1.2
20: 1ω9	2.3 ± 0.7	2.2 ± 1.1	2.7 ± 1.0	2 ± 1.2
20:1ω7	2.4 ± 0.9	2.0 ± 1.4	2.7 ± 1.2	2.4 ± 1.7
Polyunsaturated Fatty Acids (PUFA)				
16:2ω4	**1 ± 0.2^{ab}**	**0.9 ± 0.3^{b}**	**1.0 ± 0.2^{ab}**	**1.2 ± 0.2^{a}**
18:2ω6 (LA)	**0.6 ± 0.4^{b}**	**—**	**0.4 ± 0.3^{ab}**	**0.3 ± 0.2^{a}**
18:2ω6c (LA-c)	0.6 ± 0.2	0.7 ± 0.5	0.5 ± 0.2	0.5 ± 0.3
18:3ω3 (ALA)	1.5 ± 1.2	2.3 ± 1.5	1.9 ± 1	1.2 ± 0.7
18:4ω3 (SDA)	—	0.9 ± 1.1	—	—
20:4ω6 (AA)	3.7 ± 1	3.4 ± 1.7	3.1 ± 1.6	3.1 ± 2.1
20:5ω3 (EPA)	2.7 ± 1.1	2.9 ± 2.1	2.4 ± 1.5	1.4 ± 1.1
22:5ω3 (ω3-DPA)	—	0.6 ± 0.3	—	—
22:6ω3 (DHA)	10.3 ± 4.4	10.6 ± 6.5	8.2 ± 7.2	6.2 ± 5.1
22:5ω6 (DPA)	**1.2 ± 0.2^{a}**	**1.0 ± 0.4^{ab}**	**0.9 ± 0.6^{ab}**	**0.7 ± 0.4^{b}**
∑ SFA	58.4 ± 9.5	56.1 ± 12.1	59.9 ± 11.6	64.1 ± 12.9
∑ MUFA	15.8 ± 2.1	16.2 ± 1.9	17.2 ± 3.6	16.1 ± 3.2
∑ PUFA	22.4 ±7.0	23.6 ± 10.4	19.1 ±11.2	15.3 ± 8.9
∑ ω3	15.2 ± 6.1	17.2 ±8.9	13.2 ± 9.4	9.6 ± 6.4
∑ ω6	6.1 ± 1.3	5.7 ± 2.2	5.1 ± 1.3	4.9 ± 2.3

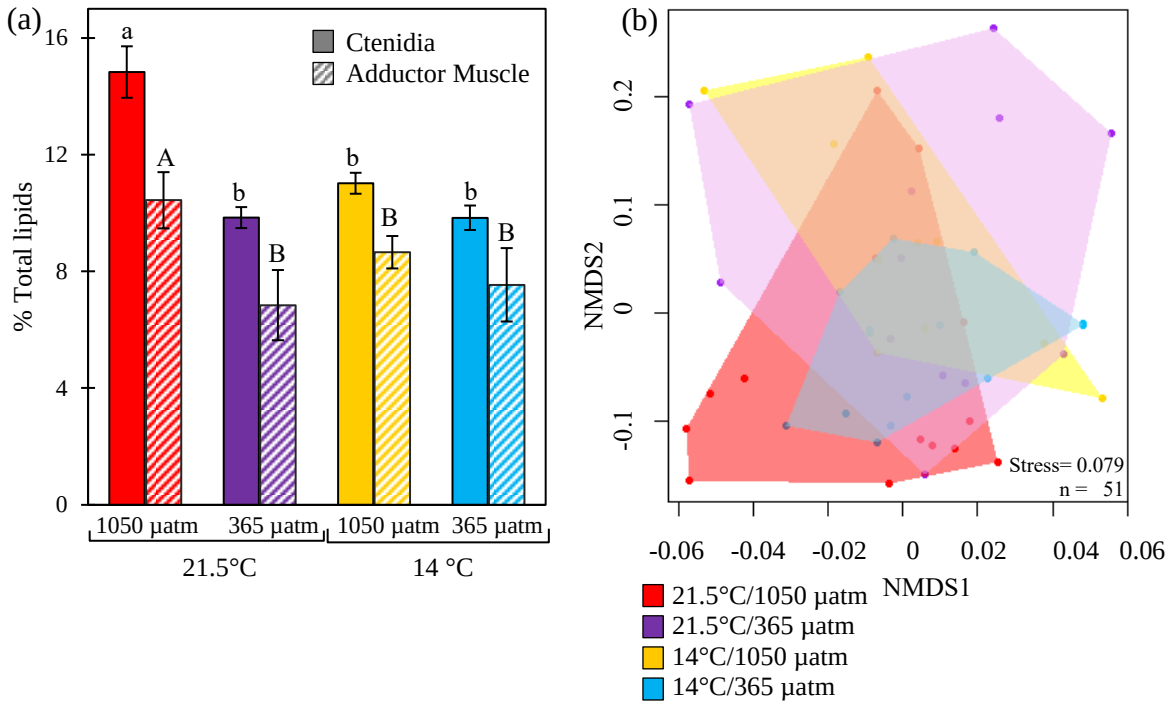

Figure 1-3 (a) Percent total lipids in ctenidia (solid) and adductor muscle (shaded), analyzed from each treatment. Values given as means ± SE (n = 11-14 individuals per treatment). Different letters indicate significant differences (lowercase for ctenidia, uppercase for adductor muscle) ($p < 0.05$). (b) Non-metric multidimensional scaling (NMDS) analysis comparing fatty acid profiles of ctenidia.

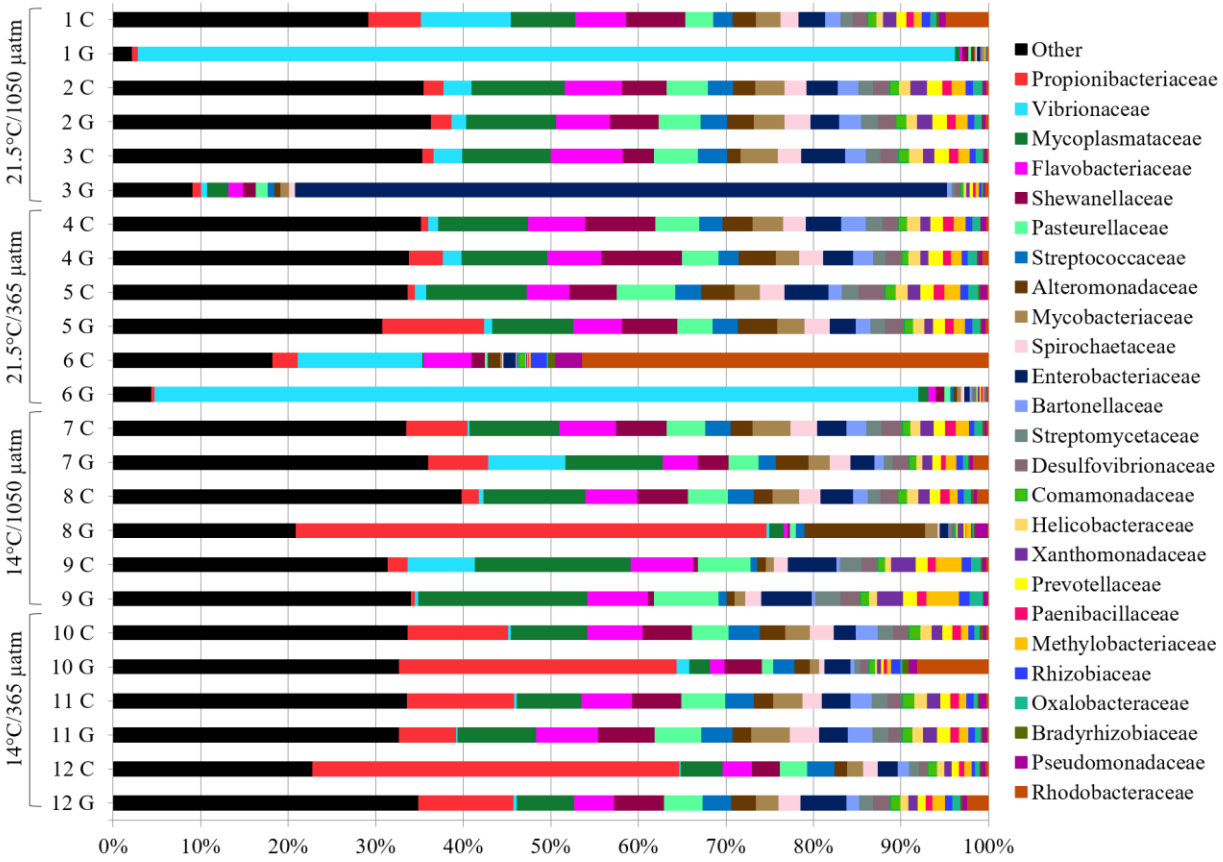

Figure 1-4: Taxonomical bacterial community composition of ctenidia (C) and gut (G) tissue for the four treatments. Each horizontal column represents one individual's bacterial composition of a single tissue, summing to 100%. The named families shown appear > 1% of the bacterial population in at least one sample, whereas the families < 1% and taxa that could not be classified to the family level are included in the "other" group.

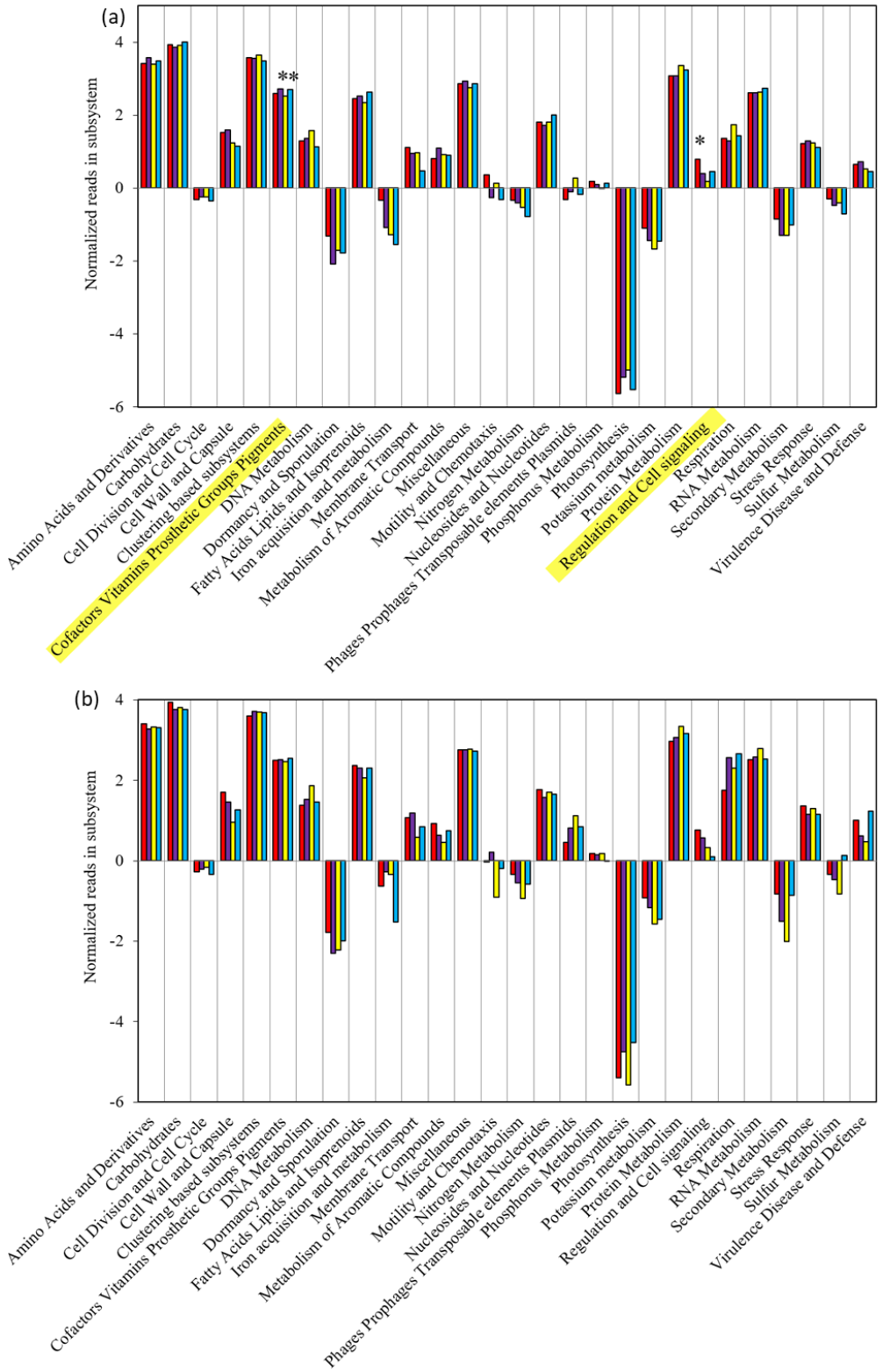

Figure 1-5: Functional analysis of bacterial community genes of (a) ctenidia and (b) gut tissue. Values are expressed as log2 fold. Asterisks indicate significant differences in functional groups ($p < 0.05$).

1.8 REFERENCES

Alexander, M.A., Scott, J.D., Friedland, K.D., Mills, K.E., Nye, J.A., Pershing, A.J., Thomas, A.C., 2018. Projected sea surface temperatures over the 21st century: Changes in the mean, variability and extremes for large marine ecosystem regions of Northern Oceans. Elem Sci Anth. https://doi.org/10.1525/elementa.191

Andrews, S., Babraham Bioinformatics, 2010. FastQC: A quality control tool for high throughput sequence data. Manual. https://doi.org/citeulike-article-id:11583827

Asplund, M.E., Baden, S.P., Russ, S., Ellis, R.P., Gong, N., Hernroth, B.E., 2014. Ocean acidification and host-pathogen interactions: Blue mussels, *Mytilus edulis*, encountering Vibrio tubiashii. Environ. Microbiol. https://doi.org/10.1111/1462-2920.12307

Barber, B.J., Blake, N.J., 1981. Energy storage and utilization in relation to gametogenesis in *Argopecten irradians concentricus* (say). J. Exp. Mar. Bio. Ecol. https://doi.org/10.1016/0022-0981(81)90031-9

Barton, A., Waldbusser, G., Feely, R., Weisberg, S., Newton, J., Hales, B., Cudd, S., Eudeline, B., Langdon, C., Jefferds, I., King, T., Suhrbier, A., McLauglin, K., 2015. Impacts of Coastal Acidification on the Pacific Northwest Shellfish Industry and Adaptation Strategies Implemented in Response. Oceanography. https://doi.org/10.5670/oceanog.2015.38

Baselga, A., Orme, C.D.L., 2012. Betapart: An R package for the study of beta diversity. Methods Ecol. Evol. https://doi.org/10.1111/j.2041-210X.2012.00224.x

Bates, D., Maechler, M., Bolker, B., Walker, S., 2014. lme4: Linear mixed-effects models using Eigen and S4. R package version 1.1-7, http://CRAN.R-project.org/package=lme4. R Packag. version.

Beuck, L., Vertino, A., Stepina, E., Karolczak, M., Pfannkuche, O., 2007. Skeletal response of *Lophelia pertusa* (Scleractinia) to bioeroding sponge infestation visualised with micro-computed tomography. Facies. https://doi.org/10.1007/s10347-006-0094-9

Bligh, E.G., Dyer, W.J., 1959. A rapid method of total lipid extraction and purificationA RAPID. Can. J. Biochem. Physiol. https://doi.org/10.1139/y59-099

Bond, N.A., Cronin, M.F., Freeland, H., Mantua, N., 2015. Causes and impacts of the 2014 warm anomaly in the NE Pacific. Geophys. Res. Lett. https://doi.org/10.1002/2015GL063306

Bourne, N., 1987. Scallop culture in British Columbia. Fourth Alaska Aquac. Conf.

Buchfink, B., Xie, C., Huson, D.H., 2014. Fast and sensitive protein alignment using DIAMOND. Nat. Methods. https://doi.org/10.1038/nmeth.3176

Carnarius, K.M., Conrad, K.M., Mast, M.G., Macneil, J.H., 1996. Relationship of eggshell ultrastructure and shell strength to the soundness of shell eggs. Poult. Sci. https://doi.org/10.3382/ps.0750656

Chatzinikolaou, E., Grigoriou, P., Keklikoglou, K., Faulwetter, S., Papageorgiou, N., 2017. The combined effects of reduced pH and elevated temperature on the shell density of two gastropod species measured using micro-CT imaging. ICES J. Mar. Sci. https://doi.org/10.1093/icesjms/fsw219

Christie, W.W., 1998. Gas chromatography-mass spectrometry methods for structural analysis of fatty acids. Lipids. https://doi.org/10.1007/s11745-998-0214-x

Chu, F.L.E., Greaves, J., 1991. Metabolism of palmitic, linoleic, and linolenic acids in adult

oysters, *Crassostrea virginica*. Mar. Biol. https://doi.org/10.1007/BF01313708
Clark, M.S., Thorne, M.A.S., Amaral, A., Vieira, F., Batista, F.M., Reis, J., Power, D.M., 2013. Identification of molecular and physiological responses to chronic environmental challenge in an invasive species: The Pacific oyster, *Crassostrea gigas*. Ecol. Evol. https://doi.org/10.1002/ece3.719
Cotonnec, G., 2002. Nutritive Value and Selection of Food Particles by Copepods During a Spring Bloom of Phaeocystis sp. in the English Channel, as Determined by Pigment and Fatty Acid Analyses. J. Plankton Res. https://doi.org/10.1093/plankt/23.7.693
Culver, C.S., Richards, J.B., Page, H.M., 2006. Plasticity of attachment in the purple-hinge rock scallop, *Crassadoma gigantea*: Implications for commercial culture. Aquaculture. https://doi.org/10.1016/j.aquaculture.2005.10.022
Di Lorenzo, E., Mantua, N., 2016. Multi-year persistence of the 2014/15 North Pacific marine heatwave. Nat. Clim. Chang. https://doi.org/10.1038/nclimate3082
Dickson, A.G., Sabine, Christian, 2007. Citation Instructions, PICES Special Publication.
Doney, S.C., Fabry, V.J., Feely, R.A., Kleypas, J.A., 2009. Ocean acidification: the other CO_2 problem. Ann. Rev. Mar. Sci. https://doi.org/10.1146/annurev.marine.010908.163834
Dubé, C.E., Ky, C.L., Planes, S., 2019. Microbiome of the black-lipped pearl oyster *Pinctada margaritifera*, a multi-tissue description with functional profiling. Front. Microbiol. https://doi.org/10.3389/FMICB.2019.01548
Duckworth, A.R., Peterson, B.J., 2013. Effects of seawater temperature and pH on the boring rates of the sponge *Cliona celata* in scallop shells. Mar. Biol. https://doi.org/10.1007/s00227-012-2053-z
Feldkamp, L.A., Davis, L.C., Kress, J.W., 2008. Practical cone-beam algorithm. J. Opt. Soc. Am. A. https://doi.org/10.1364/josaa.1.000612
Filgueira, R., Guyondet, T., Comeau, L.A., Tremblay, R., 2016. Bivalve aquaculture-environment interactions in the context of climate change. Glob. Chang. Biol. https://doi.org/10.1111/gcb.13346
Fuhrmann, M., Richard, G., Quéré, C., Petton, B., Pernet, F., 2019. Low pH reduced survival of the oyster *Crassostrea gigas* exposed to the Ostreid herpesvirus 1 by altering the metabolic response of the host. Aquaculture. https://doi.org/10.1016/j.aquaculture.2018.12.052
Galloway, A.W.E., Brett, M.T., Holtgrieve, G.W., Ward, E.J., Ballantyne, A.P., Burns, C.W., Kainz, M.J., Müller-Navarra, D.C., Persson, J., Ravet, J.L., Strandberg, U., Taipale, S.J., Alhgren, G., 2015. A fatty acid based bayesian approach for inferring diet in aquatic consumers. PLoS One. https://doi.org/10.1371/journal.pone.0129723
Gradoville, M.R., Crump, B.C., Häse, C.C., White, A.E., 2018. Environmental Controls of Oyster-Pathogenic *Vibrio* spp. in Oregon Estuaries and a Shellfish Hatchery . Appl. Environ. Microbiol. https://doi.org/10.1128/aem.02156-17
Green, M.A., Waldbusser, G.G., Reilly, S.L., Emerson, K., O'Donnell, S., 2009. Death by dissolution: Sediment saturation state as a mortality factor for juvenile bivalves. Limnol. Oceanogr. https://doi.org/10.4319/lo.2009.54.4.1037
Gruber, N., Hauri, C., Lachkar, Z., Loher, D., Frölicher, T.L., Plattner, G.K., 2012. Rapid progression of ocean acidification in the California Current System. Science. https://doi.org/10.1126/science.1216773
Gunderson, A.R., Armstrong, E.J., Stillman, J.H., 2015. Multiple Stressors in a Changing World: The Need for an Improved Perspective on Physiological Responses to the Dynamic Marine Environment. Ann. Rev. Mar. Sci. https://doi.org/10.1146/annurev-marine-122414-033953

Hand, S.C., Hardewig, I., 1996. Downregulation of Cellular Metabolism During Environmental Stress: Mechanisms and Implications. Annu. Rev. Physiol. https://doi.org/10.1146/annurev.ph.58.030196.002543

Hazel, J.R., Eugene Williams, E., 1990. The role of alterations in membrane lipid composition in enabling physiological adaptation of organisms to their physical environment. Prog. Lipid Res. https://doi.org/10.1016/0163-7827(90)90002-3

Hofmann, G.E., Evans, T.G., Kelly, M.W., Padilla-Gamiño, J.L., Blanchette, C.A., Washburn, L., Chan, F., McManus, M.A., Menge, B.A., Gaylord, B., Hill, T.M., Sanford, E., Lavigne, M., Rose, J.M., Kapsenberg, L., Dutton, J.M., 2014. Exploring local adaptation and the ocean acidification seascape Studies in the California Current Large Marine Ecosystem. Biogeosciences. https://doi.org/10.5194/bg-11-1053-2014

Huson, D.H., Auch, A.F., Qi, J., Schuster, S.C., 2007. MEGAN analysis of metagenomic data. Genome Res. https://doi.org/10.1101/gr.5969107

Ikejima, I., Nomoto, R., McCabe, J.F., 2003. Shear punch strength and flexural strength of model composites with varying filler volume fraction, particle size and silanation. Dent. Mater. https://doi.org/10.1016/S0109-5641(02)00031-3

IPCC, 2013. Summary for Policymakers. In: Climate Change 2013: The Physical Science Basis. Contribution of Working Group I to the Fifth Assessment Report of the Intergovernmental Panel on Climate Change [Stocker, T.F., Qin D., Plattner D.K., Tignor, M., Allen, S.K., Boschung, J., Nauels, A., Xia, Y., Bex, V., Midgley, PM. (eds.)]. Cambridge University Press, Cambridge, United Kingdom and New York, NY, USA

Ivanina, A. V., Dickinson, G.H., Matoo, O.B., Bagwe, R., Dickinson, A., Beniash, E., Sokolova, I.M., 2013. Interactive effects of elevated temperature and CO_2 levels on energy metabolism and biomineralization of marine bivalves *Crassostrea virginica* and *Mercenaria mercenaria*. Comp. Biochem. Physiol. - A Mol. Integr. Physiol. https://doi.org/10.1016/j.cbpa.2013.05.016

Kroeker, K.J., Sanford, E., Jellison, B.M., Gaylord, B., 2014. Predicting the effects of ocean acidification on predator-prey interactions: A conceptual framework based on coastal molluscs. Biol. Bull. https://doi.org/10.1086/BBLv226n3p211

Kumar, R., Datta, T.K., Lalitha, K. V., 2015. Salmonella grows vigorously on seafood and expresses its virulence and stress genes at different temperature exposure. BMC Microbiol. https://doi.org/10.1186/s12866-015-0579-1

Lamb, J.B., Van De Water, J.A.J.M., Bourne, D.G., Altier, C., Hein, M.Y., Fiorenza, E.A., Abu, N., Jompa, J., Harvell, C.D., 2017. Seagrass ecosystems reduce exposure to bacterial pathogens of humans, fishes, and invertebrates. Science (80-.). https://doi.org/10.1126/science.aal1956

Laurén, D.J., 2008. Oogenesis and protandry in the purple-hinge rock scallop, *Hinnites giganteus*, in upper Puget Sound, Washington, U.S.A. . Can. J. Zool. https://doi.org/10.1139/z82-300

Levy, M., Thaiss, C.A., Elinav, E., 2015. Metagenomic cross-talk: The regulatory interplay between immunogenomics and the microbiome. Genome Med. https://doi.org/10.1186/s13073-015-0249-9

Li, S., Liu, C., Huang, J., Liu, Y., Zheng, G., Xie, L., Zhang, R., 2015. Interactive effects of seawater acidification and elevated temperature on biomineralization and amino acid metabolism in the mussel *Mytilus edulis*. J. Exp. Biol. https://doi.org/10.1242/jeb.126748

Liu, G.Y., Nizet, V., 2009. Color me bad: microbial pigments as virulence factors. Trends

Microbiol. https://doi.org/10.1016/j.tim.2009.06.006
Lokmer, A., Mathias Wegner, K., 2015. Hemolymph microbiome of Pacific oysters in response to temperature, temperature stress and infection. ISME J. https://doi.org/10.1038/ismej.2014.160
[a] Mackenzie, C.L., Ormondroyd, G.A., Curling, S.F., Ball, R.J., Whiteley, N.M., Malham, S.K., 2014. Ocean warming, more than acidification, reduces shell strength in a commercial shellfish species during food limitation. PLoS One https://doi.org/10.1371/journal.pone.0086764
[b] Mackenzie, C.L., Lynch, S.A., Culloty, S.C., Malham, S.K. 2014. Future oceanic warming and acidification alter immune response and disease status in a commercial shellfish species, Mytilus edulis L. PLoS One.
Martin V.A.S., Gelcich S., Vásquez Lavín F., Ponce Oliva R.D., Hernández J.I., Lagos N.A., Birchenough S.N.R., Vargas C.A. 2019. Linking social preferences and ocean acidification impacts in mussel aquaculture. Sci Rep. https://doi.org/910.1038/s41598-019-41104-5
Martinez-Urtaza, J., Lozano-Leon, A., Varela-Pet, J., Trinanes, J., Pazos, Y., Garcia-Martin, O., 2008. Environmental determinants of the occurrence and distribution of *Vibrio parahaemolyticus i*n the rias of Galicia, Spain. Appl. Environ. Microbiol. https://doi.org/10.1128/AEM.01307-07
Matoo, O.B., Ivanina, A. V., Ullstad, C., Beniash, E., Sokolova, I.I., 2013. Interactive effects of elevated temperature and CO_2 levels on metabolism and oxidative stress in two common marine bivalves (*Crassostrea virginica* and *Mercenaria mercenaria*). Comp. Biochem. Physiol. - A Mol. Integr. Physiol. https://doi.org/10.1016/j.cbpa.2012.12.025
Melzner, F., Stange, P., Trübenbach, K., Thomsen, J., Casties, I., Panknin, U., Gorb, S.N., Gutowska, M.A., 2011. Food supply and seawater pCO_2 impact calcification and internal shell dissolution in the blue mussel *Mytilus edulis.* PLoS One. https://doi.org/10.1371/journal.pone.0024223
Milke, L.M., Bricelj, V.M., Parrish, C.C., 2004. Growth of postlarval sea scallops, *Placopecten magellanicus*, on microalgal diets, with emphasis on the nutritional role of lipids and fatty acids. Aquaculture. https://doi.org/10.1016/j.aquaculture.2003.11.006
Muñoz, K., Flores-Herrera, P., Gonçalves, A.T., Rojas, C., Yáñez, C., Mercado, L., Brokordt, K., Schmitt, P., 2019. The immune response of the scallop *Argopecten purpuratus* is associated with changes in the host microbiota structure and diversity. Fish Shellfish Immunol. https://doi.org/10.1016/j.fsi.2019.05.028
Nevejan, N., Saez, I., Gajardo, G., Sorgeloos, P., 2003. Supplementation of EPA and DHA emulsions to a Dunaliella tertiolecta diet: Effect on growth and lipid composition of scallop larvae, *Argopecten purpuratus* (Lamarck, 1819). Aquaculture. https://doi.org/10.1016/S0044-8486(02)00585-9
Oksanen, J., Blanchet, F.G., Kindt, R., Oksanen, M.J., Suggests, M., 2013. Package 'vegan.' Community Ecol. Packag. Version.
Oliveira, J.M., Cunha, Â.S., Almeida, A.P., Castilho, F.B., Pereira, M.J., 2013. Comparison of Methodologies for the Extraction of Bacterial DNA from Mussels-Relevance for Food Safety. Food Anal. Methods. https://doi.org/10.1007/s12161-012-9419-1
Ong, E.Z., Briffa, M., Moens, T., Van Colen, C., 2017. Physiological responses to ocean acidification and warming synergistically reduce condition of the common cockle *Cerastoderma edule*. Mar. Environ. Res. https://doi.org/10.1016/j.marenvres.2017.07.001
Ooi, M.C., Goulden, E.F., Smith, G.G., Bridle, A.R., 2019. Haemolymph microbiome of the

cultured spiny lobster *Panulirus ornatus* at different temperatures. Sci. Rep. https://doi.org/10.1038/s41598-019-39149-7
Ounit, R., Wanamaker, S., Close, T.J., Lonardi, S., 2015. CLARK: fast and accurate classification of metagenomic and genomic sequences using discriminative k-mers. BMC Genomics. https://doi.org/10.1186/s12864-015-1419-2
Overbeek, R., Olson, R., Pusch, G.D., Olsen, G.J., Davis, J.J., Disz, T., Edwards, R.A., Gerdes, S., Parrello, B., Shukla, M., Vonstein, V., Wattam, A.R., Xia, F., Stevens, R., 2014. The SEED and the Rapid Annotation of microbial genomes using Subsystems Technology (RAST). Nucleic Acids Res. https://doi.org/10.1093/nar/gkt1226
Pachepsky, Y.A., Blaustein, R.A., Whelan, G., Shelton, D.R., 2014. Comparing temperature effects on Escherichia coli, Salmonella, and Enterococcus survival in surface waters. Lett. Appl. Microbiol. https://doi.org/10.1111/lam.12272
Padilla-Gamiño, J.L., Kelly, M.W., Evans, T.G., Hofmann, G.E., 2013. Temperature and CO_2 additively regulate physiology, morphology and genomic responses of larval sea urchins, *Strongylocentrotus purpuratus*. Proc. R. Soc. B Biol. Sci. https://doi.org/10.1098/rspb.2013.0155
Papageorgiou, N., Schmidbaur, H., 2014. Effects of Ocean Acidification on the calcified structures of benthic organisms (acidiCO_2ceans).
Pernet, F., Tremblay, R., Comeau, L., Guderley, H., 2007. Temperature adaptation in two bivalve species from different thermal habitats: energetics and remodelling of membrane lipids. J. Exp. Biol. https://doi.org/10.1242/jeb.006007
Pierce, M.L., Ward, J.E., 2018. Microbial Ecology of the Bivalvia, with an Emphasis on the Family Ostreidae. J. Shellfish Res. https://doi.org/10.2983/035.037.0410
Queirós, A.M., Fernandes, J.A., Faulwetter, S., Nunes, J., Rastrick, S.P.S., Mieszkowska, N., Artioli, Y., Yool, A., Calosi, P., Arvanitidis, C., Findlay, H.S., Barange, M., Cheung, W.W.L., Widdicombe, S., 2015. Scaling up experimental ocean acidification and warming research: From individuals to the ecosystem. Glob. Chang. Biol. https://doi.org/10.1111/gcb.12675
RaLonde R., 2012. No Title [WWW Document]. Alaska's Purple-Hinge Rock Scallops Consid. Aquac. Dev. URL https://thefishsite.com/articles/alaskas-purplehinge-rock-scallops-considered-for-aquaculture-development
Ramajo, L., Marbà, N., Prado, L., Peron, S., Lardies, M.A., Rodriguez-Navarro, A.B., Vargas, C.A., Lagos, N.A., Duarte, C.M., 2016. Biomineralization changes with food supply confer juvenile scallops (*Argopecten purpuratus*) resistance to ocean acidification. Glob. Chang. Biol. 22, 2025–2037. https://doi.org/10.1111/gcb.13179
Robbins, L.L., Hansen, M.E., Kleypas, J.A., Meylan, S.C., 2010. CO2calc—A user friendly carbon calculator for Windows, Mac OS X and iOS (iPhone). United States Geol. Surv. https://doi.org/10.3133/OFR20101280
Rocchetta, I., Mazzuca, M., Conforti, V., Ruiz, L., Balzaretti, V., De Molina, M.D.C.R., 2006. Effect of chromium on the fatty acid composition of two strains of *Euglena gracilis*. Environ. Pollut. 141, 353–358. https://doi.org/10.1016/j.envpol.2005.08.035
Rocchetta, I., Pasquevich, M.Y., Heras, H., Ríos de Molina, M. del C., Luquet, C.M., 2014. Effects of sewage discharges on lipid and fatty acid composition of the Patagonian bivalve *Diplodon chilensis*. Mar. Pollut. Bull. https://doi.org/10.1016/j.marpolbul.2013.12.011
Rühl, S., Calosi, P., Faulwetter, S., Keklikoglou, K., Widdicombe, S., Queirós, A.M., 2017. Long-term exposure to elevated pCO_2 more than warming modifies early-life shell growth

in a temperate gastropod. ICES J. Mar. Sci. https://doi.org/10.1093/icesjms/fsw242
Schalkhausser, B., Bock, C., Stemmer, K., Brey, T., Pörtner, H.O., Lannig, G., 2013. Impact of ocean acidification on escape performance of the king scallop, *Pecten maximus*, from Norway. Mar. Biol. https://doi.org/10.1007/s00227-012-2057-8
Sebens, K.P., Sarà, G., Carrington, E., 2018. Estimation of fitness from energetics and life-history data: An example using mussels. Ecol. Evol. https://doi.org/10.1002/ece3.4004
Shade, A., Handelsman, J., 2012. Beyond the Venn diagram: The hunt for a core microbiome. Environ. Microbiol. https://doi.org/10.1111/j.1462-2920.2011.02585.x
Simons, A.L., Churches, N., Nuzhdin, S., 2018. High turnover of faecal microbiome from algal feedstock experimental manipulations in the Pacific oyster (*Crassostrea gigas*). Microb. Biotechnol. https://doi.org/10.1111/1751-7915.13277
Toch, E., Strand, Ø., 2006. Comparison of shell strength in wild and cultured scallops *(Pecten maximus*). Aquaculture. https://doi.org/10.1016/j.aquaculture.2005.06.004
Sokolova, I.M., Frederich, M., Bagwe, R., Lannig, G., Sukhotin, A.A., 2012. Energy homeostasis as an integrative tool for assessing limits of environmental stress tolerance in aquatic invertebrates. Mar. Environ. Res. https://doi.org/10.1016/j.marenvres.2012.04.003
Soudant, P., Van Ryckeghem, K., Marty, Y., Moal, J., Samain, J.F., Sorgeloos, P., 1999. Comparison of the lipid class and fatty acid composition between a reproductive cycle in nature and a standard hatchery conditioning of the Pacific Oyster *Crassostrea gigas*. Comp. Biochem. Physiol. - B Biochem. Mol. Biol. https://doi.org/10.1016/S0305-0491(99)00063-2
Stackebrandt, E., Schaal, K.P., 2006. The Family Propionibacteriaceae: The Genera *Friedmanniella, Luteococcus, Microlunatus, Micropruina, Propioniferax, Propionimicrobium and Tessarococcus*, in: The Prokaryotes. https://doi.org/10.1007/0-387-30743-5_18
Stocker, T.F., Qin, D., Plattner, G.K., Tignor, M.M.B., Allen, S.K., Boschung, J., Nauels, A., Xia, Y., Bex, V., Midgley, P.M., 2013. Climate change 2013 the physical science basis: Working Group I contribution to the fifth assessment report of the intergovernmental panel on climate change, Climate Change 2013 the Physical Science Basis: Working Group I Contribution to the Fifth Assessment Report of the Intergovernmental Panel on Climate Change. https://doi.org/10.1017/CBO9781107415324
Talmage, S.C., Gobler, C.J., 2011. Effects of elevated temperature and carbon dioxide on the growth and survival of larvae and juveniles of three species of northwest Atlantic bivalves. PLoS One. https://doi.org/10.1371/journal.pone.0026941
Tatarinova, T. V., Lysnyansky, I., Nikolsky, Y. V., Bolshoy, A., 2016. The mysterious orphans of Mycoplasmataceae. Biol. Direct. https://doi.org/10.1186/s13062-015-0104-3
Timmins-Schiffman, E., Coffey, W.D., Hua, W., Nunn, B.L., Dickinson, G.H., Roberts, S.B., 2014. Shotgun proteomics reveals physiological response to ocean acidification in *Crassostrea gigas*. BMC Genomics. https://doi.org/10.1186/1471-2164-15-951
Tocher, D.R., Sargent, J.R., 1984. Analyses of lipids and fatty acids in ripe roes of some Northwest European marine fish. Lipids. https://doi.org/10.1007/BF02534481
Todgham, A.E., Stillman, J.H., 2013. Physiological responses to shifts in multiple environmental stressors: Relevance in a changing world. Integr. Comp. Biol. https://doi.org/10.1093/icb/ict086
Tyler, C., 1961. Shell Strength: Its Measurement and its Relationship to other Factors. Br. Poult. Sci. https://doi.org/10.1080/00071666109382385
Whyte, J.N.C., Bourne, N., Ginther, N.G., 1991. Depletion of nutrient reserves during

embryogenesis in the scallop *Patinopecten yessoensis* (Jay). J. Exp. Mar. Bio. Ecol. https://doi.org/10.1016/0022-0981(91)90117-F

Whyte, J.N.C., Bourne, N., Hodgson, C.A., 1990. Nutritional condition of rock scallop, *Crassadoma gigantea* (Gray), larvae fed mixed algal diets. Aquaculture. https://doi.org/10.1016/0044-8486(90)90219-D

Wilkie, E.M., Bishop, M.J., 2012. Differences in shell strength of native and non-native oysters do not extend to size classes that are susceptible to a generalist predator. Mar. Freshw. Res. https://doi.org/10.1071/mf12078

Williams, C.M., Buckley, L.B., Sheldon, K.S., Vickers, M., Pörtner, H.O., Dowd, W.W., Gunderson, A.R., Marshall, K.E., Stillman, J.H., 2016. Biological impacts of thermal extremes: mechanisms and costs of functional responses matter, in: Integrative and Comparative Biology. https://doi.org/10.1093/icb/icw013

Wright, J.M., Parker, L.M., O'Connor, W.A., Scanes, E., Ross, P.M., 2018. Ocean acidification affects both the predator and prey to alter interactions between the oyster *Crassostrea gigas* (Thunberg, 1793) and the whelk Tenguella marginalba (Blainville, 1832). Mar. Biol. 165, 1–12. https://doi.org/10.1007/s00227-018-3302-6

Xiong, J., Yu, W., Dai, W., Zhang, J., Qiu, Q., Ou, C., 2018. Quantitative prediction of shrimp disease incidence via the profiles of gut eukaryotic microbiota. Appl. Microbiol. Biotechnol. https://doi.org/10.1007/s00253-018-8874-z

Young, I., Gropp, K., Fazil, A., Smith, B.A., 2015. Knowledge synthesis to support risk assessment of climate change impacts on food and water safety: A case study of the effects of water temperature and salinity on *Vibrio parahaemolyticus* in raw oysters and harvest waters. Food Res. Int. https://doi.org/10.1016/j.foodres.2014.06.035

2 CHAPTER 2

PHYSIOLOGICAL RESPONSES OF SCALLOPS AND MUSSELS TO ENVIRONMENTAL VARIABILITY: IMPLICATIONS FOR FUTURE SHELLFISH AQUACULTURE

Lindsay Alma, Courtney J. Fiamengo, Simone R. Alin, Molly Jackson, Kris Hiromoto, Jacqueline L. Padilla-Gamiño

2.1 ABSTRACT

Puget Sound (Washington, USA) is a large estuary, known for its profitable shellfish aquaculture industry. However, in the past decade, scientists have observed acidification, deoxygenation, and temperatures in Puget Sound that are higher than global modeled predictions for year 2100. These co-occurring environmental stressors are a threat to marine ecosystems and shellfish aquaculture. Our research explores how in situ environmental variability in the Hood Canal fjord reflecting multiple stressors impacts two ecologically and economically important bivalves, the purple-hinge rock scallop (*Crassodoma gigantea*) and Mediterranean mussel (*Mytilus galloprovincialis*). Hood Canal serves as a natural multiple-stressor laboratory, which allowed us to examine acclimatization capacity of shellfish in their natural habitat and provide the aquaculture industry with spatiotemporal parameters to maximize favorable attributes. Bivalves were outplanted at two depths (5 and 30 m) and collected after 3.5 and 7.5 months. To optimize mussel scallop and growth, our results suggest outplanting at 5 m depth, with more favorable oxygen and pH levels. Mussel shell integrity can be improved by acclimatizing to 5 m, regardless of season, however, there were no notable differences between depths in scallops. For both species, $\delta^{13}C$ values were lowest in 5 m in the winter and $\delta^{15}N$ was highest at 30 m regardless of season. Puget Sound's rapidly changing water chemistry is resulting in more extreme ocean chemistry which is already proving to be a

challenge for shellfish farmers. Our study provides crucial information to farmers to optimize aquaculture grow-out as we begin to mitigate the impacts of climate change.

2.2 INTRODUCTION

Coastlines are ideal habitats for most bivalves, where water is shallow, primary production is high, and there is substrate to settle onto (Borges and Gypens, 2010). The natural complexity and variability of coastal systems has allowed bivalves to evolve a wide tolerance to changing oceanographic conditions over millennia. However, rapid anthropogenic disturbances within the last two centuries have caused dramatic spatiotemporal fluctuations in marginal seas leading to changes in temperature, fluctuations in the thermocline, shoaling of the aragonite saturation horizon, and reduced dissolved oxygen with depth (Feely et al., 2012), causing significant stress and mortality outbreaks in shellfish populations (Barton et al., 2015; Soon and Zheng, 2020). Rising atmospheric CO_2 concentration is predicted to result in warmer ocean temperatures, ocean acidification (OA), and extreme weather (Gruber et al., 2012; Melzner et al., 2011; Rykaczewski and Dunne, 2010). Local anthropogenic nutrient load from agriculture, sewage, runoff, and other human activities have increased eutrophication which exacerbates hypoxia and OA in coastal areas (Borges and Gypens, 2010; Wallace et al., 2014).

In Washington state, USA, the shellfish aquaculture industry is an important economic driver with an estimated annual income of $270 million (Barton et al., 2015). Puget Sound, Washington is the second largest estuary in the USA and home to numerous shellfish farms. This area is a natural fjord system and organisms living in the sound frequently experience acidified conditions, temperature fluctuations, and hypoxia levels which can exceed levels predicted by the

Intergovernmental Panel on Climate Change (IPCC, RCP 8.5) global climate models for the end of the century (IPCC, 2014; Wallace et al., 2014). Hood Canal, a large fjord-like channel on the west side of Puget Sound, has recorded some of the most extreme oceanographic conditions in the Pacific Northwest (Feely et al., 2010 ; Alin et al. 2021). Our study was conducted in Hood Canal, just offshore of the Taylor Shellfish Hatchery (Figure 2-1), a large commercial bivalve aquaculture farm. In Hood Canal, environmental variability is influenced by seasonal upwelling, snowmelt, riverine freshwater inputs, anthropogenic activity, and relatively high water residence time. During colder months, the water is well mixed, and the pycnocline is weakly defined (Feely et al., 2010). In contrast, during warm months of the year the water column is characterized by a defined pycnocline, warm upper layer, and cold, hypoxic, acidified bottom-waters. It is predicted that warming will strengthen and lengthen stratification in Puget Sound and may affect bivalve populations (Moore et al., 2015). We chose Hood to conduct our study because Taylor Shellfish has experienced challenges with bivalve production and survival since 2007 due to ocean acidification. Currently they use buffering systems for their hatchery seawater to raise carbonate ion availability for shellfish and combat larval mortality due to acidification of the surrounding waters (Barton et al., 2015; Hoegh-Guldberg et al., 2015). By acclimating shellfish at this commercial hatchery, we hope to provide important information that can assist with the successful continuation of shellfish aquaculture.

In our study, we examined shellfish acclimatization potential to climate change by looking at the effects of environmental variability on the physiological performance of the purple-hinge rock scallop (*Crassodoma gigantea*) and the Mediterranean mussel (*Mytilus galloprovincialis*). These species are considered ecologically important because of their ability to filter water, sequester

nitrogen and carbon, and because their shells form reefs and provide hard surfaces for other organisms to settle, thus increasing biodiversity (Gutiérrez et al., 2003). *C. gigantea* is a native species to the North American Pacific Coast, and the aquaculture industry has great interest in the potential commercial profitability of this species (Culver et al., 2006; Leighton and Phleger, 1977; Walker, 2016). Its large edible adductor muscle is considered a delicacy that is expected to sell at a high market value. Although there is much interest in this species in the aquaculture industry, research on this species is very sparse when compared to many other bivalves, and we are only beginning to understand its responses to oceanographic stressors (Alma et al. 2020). *M. galloprovincialis* is an edible mussel which is highly cultured in the aquaculture industry, and is well-studied due to its ecological and economic importance worldwide. This species of mussels is native to the Mediterranean Sea and Atlantic Ocean and was introduced to Puget Sound in the early 20th century by the aquaculture industry. *M galloprovincialis* is almost indistinguishable from the native *Mytilus trossulus*, and there is some evidence of hybridization between the two species in Puget Sound, mainly around shipyards and aquaculture grow-out locations (Boersma et al., 2006; Anderson et al., 2002; Elliott et al., 2008, 2005).

We seek to explore an important question: what is the spatiotemporal acclimatization potential (or the change in an organism's physiology based upon changes in the environment) of bivalves when subjected to different co-varying stressors in the field? Our study provides a snapshot of potential product quality in a long-line aquaculture setting, which may assist the aquaculture industry in optimally placing their shellfish for grow-out. By holding the two ecologically and economically important species at either 5 m or 30 m depths for 3.5 or 7.5 months in the inland fjord of Hood Canal, we were able to take advantage of this dynamic "natural laboratory" with multiple co-

occurring climate change related stressors. Our experiment spanned December to June at two depths, allowing us to capture both seasonal mixing patterns (well-mixed and stratified). While the quantity of climate change-related multiple stressor experiments has been increasing in the literature, many experiments are performed in the laboratory within carefully controlled conditions that fail to effectively represent the complexity of real-world scenarios where multiple stressors interact and fluctuate (Hofmann et al., 2011; McElhany, 2017; Reum et al., 2014). It is, therefore, critical to study physiological performance in the naturally dynamic environment, where numerous parameters fluctuate simultaneously and interact with each other at various spatiotemporal scales to affect organismal performance (Wernberg et al., 2012). Understanding how in situ environmental variability affects bivalve skeletal properties, growth, physiological performance, and changes in biochemistry is vital to accurately predict the acclimatization potential of these economically and ecologically important species.

2.3 METHODS

2.3.1 Field Conditions and Seawater Chemistry

The study site was located just offshore of Taylor Shellfish Farms in Hood Canal, Puget Sound, Washington (Figure 2-1, 47°49’11” N, 122°49’64” W). Our study was conducted at two depths, 5 and 30 meters, because *M. galloprovincialis* is often grown on long-lines, which can experience a large breadth of oceanographic variation, leading to differences in aquaculture product quality along the long-line with depth (Araújo et al., 2020; Aure et al., 2007). Furthermore, the depth range in our study is consistent with the purple hinge rock scallop habitat, which spans from low intertidal to 80 m depth (Bourne, 1987; Whyte et al., 1990). Chlorophyll-*a* (chl-*a*) data, used to quantify phytoplankton biomass, was not directly measured at our field site, but we used fluorometer data measured in situ by the Dabob Bay Oceanic Remote Chemical Analyzer

(ORCA) buoy located 2.3 km from our study site. The ORCA buoy was not functioning during our study period, so we averaged all available chl-*a* data from years 2010 to 2021 at 5 and 30 m depth to approximate patterns in the area.

2.3.2 Seawater Chemistry

The two depth locations were ~60 m from shallow (5 m) and deep-water (30 m) intake pipes at Taylor Shellfish Hatchery. Water from the two depths was brought up to a fixed shore platform, and weekly oceanographic data was recorded throughout the experiment (temperature, salinity, and dissolved oxygen). Discrete water samples from each depth were collected from the intake lines weekly and preserved with mercuric chloride for carbonate chemistry analysis in accordance with ocean carbon community standard operating procedures (Dickson et al., 2007). Carbonate chemistry bottle samples were processed at NOAA's Pacific Marine Environmental Laboratory (PMEL), Seattle, Washington. Dissolved inorganic carbon (DIC) concentrations were measured on analytical systems consisting of a coulometer (UIC, Inc.) coupled with a Single Operator Multiparameter Metabolic Analyzer (SOMMA) developed to extract DIC from seawater. Total alkalinity (TA) samples were analyzed according to the open-cell titration standard operating procedure (SOP 3b) of the ocean carbon community standards (Dickson et al., 2007), using a custom analytical system built at Scripps Institution of Oceanography (SIO). DIC instruments were calibrated via gas loops. Instrument accuracy and precision for DIC and TA analyses were monitored at regular intervals using Certified Reference Materials (CRMs), consisting of filtered and UV-irradiated seawater supplied by the Dickson Lab (SIO). Uncertainty for DIC and TA measurements is ± 0.1% of measured values (roughly ±2 µmol/kg). More complete description and references on DIC and TA analytical methods can be found in the metadata for Alin et al.

(2021). Using DIC, TA, temperature, and salinity data, we calculated aragonite saturation states (Ω_{Ar}), partial pressures of CO_2 (pCO_2), and pH_T (pH on the total scale) values using the CO_2SYS program (Pelletier et al., 2007) with Lueker et al. (2000) dissociation constants.

2.3.3 Field Experiment and Growth

We obtained eight-month-old, hatchery-raised, purple-hinge rock scallops (*C. gigantea*) and one-year old Mediterranean mussels (*M. galloprovincialis*) from Taylor Shellfish Hatchery in Quilcene, Washington. Scallops were bred in the hatchery from wild broodstock. The non-native mussels are an aquaculture hatchery line, bred using ~1000 individuals from Taylor's farmed populations. We measured shell height (from hinge to apex) using a caliper (0.1 mm precision) and tagged individuals by adhering numbered "bee tags" (Betterbee, Greenwich, New York) to their shells with superglue (Pacer Technology Zap-A-Gap Adhesives). At the beginning of the experiment, December 10, 2016 (T_0), we dissected n = 10 individuals from each species, flash froze their tissue, and placed them in a -80 °C freezer for storage. All individuals were measured and weighed before the start of the field experiment. For scallops (n = 37 - 67), average shell length ± [S.E.] was 40.85 ± 0.34 mm, shell width was 40.05 ± 0.36 mm, and weight was 9.41 ± 0.24 g. For mussels (n = 43 - 62), average shell length was 49.7 ± 0.40 mm, shell width was 27.40 ± 0.22 mm, and weight was 9.80 ± 0.31 g. For the field experiment, shellfish were placed into rigid plastic mesh oyster bags and affixed into to PVC cage structures. On December 11, 2016, the cages (n = 300 shellfish per cage) were deployed to our study sites at 5 and 30 m below the surface using SCUBA. Cages at 5 m were tied onto an anchored buoy using 0.8 cm braided polypropylene rope. Cages at 30 m were lifted ~30 cm from the bottom and fixed to cinderblocks. We collected subsets of scallops and mussels 3.5 and 7.5 months after deployment (March 22, 2017, and June 27, 2017,

respectively). We measured growth rate by recording the shell height of individuals, subtracting from the initial shell height, and dividing by number of months acclimated (Gobler et al., 2017; Hiebenthal et al., 2012; Kim et al., 2013; Riascos and Guzman, 2010). We cleaned all remaining tissue off shells with terrycloth and stored them at room temperature for future shell strength analysis. We then flash froze tissue samples and stored them at -80 °C for further analysis.

2.3.4 Shell Strength

We quantified shell strength by measuring shell thickness and point-crushing the shell with a hydraulic press to quantify the force it took to puncture the shell. Dry shells (n = 44 – 50) were rehydrated in seawater for 24 hours prior to crushing. We used a micro-caliper to measure shell thickness to the nearest 0.01 mm. An Instron Universal Testing Machine measured the force (N) needed to create a hole in the shell (Wilkie and Bishop, 2012). We punctured two holes into the shell (one at 1 cm from the edge of the shell and the other in the middle of the shell) at 30 mm/min using a steel pin with a diameter of 2.5 mm. We averaged the puncture forces for each individual shell and calculated *S* which is shell strength measured in megapascals (N mm^{-2}). *S* can be calculated by normalizing *F* (the maximum penetrating force, newtons), by *t* (shell thickness, mm), and *d* (diameter of the punch, mm) (Carnarius et al., 1996; Ikejima et al., 2003; Tyler, 1961).

2.3.5 Isotopic Signatures

We freeze dried (VirTis Co.) the visceral mass of scallops and mussels (n = 10) and homogenized using a ball-mill (Wig-L-Bug Model MSD). To measure $\delta^{13}C$ and $\delta^{15}N$ stable isotope levels, we weighed 0.6 ± 0.01 mg of freeze dried and ground shellfish tissue (n = 10) using a microbalance

(sensitivity 10 µg) and packed it into a small tin. Glutamic Acid I, II (0.42 µg) and Bristol Bay salmon (0.339 µg) standards of known isotopic composition were packed into tins and interspersed with our samples. Samples were processed at University of Washington's IsoLab on a Finnigan MAT253 mass spectrometer connected to a Costech elemental analyzer in continuous-flow mode (https://isolab.ess.washington.edu/laboratory/solid-CN.php) in accordance with methods highlighted in Fry et al. (1992). $\delta^{13}C$ and $\delta^{15}N$ results are reported as parts per thousand relative to the reference standard Vienna PeeDee Belemnite (VPDB) and atmospheric air, respectively.

2.3.6 Statistical Analysis

Prior to analysis, a Shapiro-Wilks Test was performed to assess normality, and if needed, values of analysis were $\log_{10,}$ arcsign, or square root transformed to achieve normality assumptions before a model was run. We ran an ANOVA and Tukey-HSD test in *R* version 1.0.53 to determine significant differences in growth, shell strength, and isotopic signatures among collection times, depths, and species. A correlation matrix was created to determine co-varying oceanographic conditions using the *corrplot* package in *R* (Taiyun, 2014).

2.4 RESULTS

2.4.1 Field Conditions and Seawater Chemistry

Hood Canal seawater chemical and physical properties varied greatly by depth and season (Table 1). Throughout the winter (December 11, 2016, to March 22, 2017), water at 30 m depth was ~ 1.5 °C warmer than water at 5 m depth; however, in the spring (March 23 to June 27, 2017), water in the shallow depth was ~ 3.8 °C warmer (Figure 2-2A,Table 2-1: Hood Canal seawater chemistry

summary (**mean, standard error [S.E.],** and coefficient of variation [CV]) for shallow (5 m) and deep (30 m) depths in winter (December 11, 2016, to March 22, 2017) and spring (March 23, 2017, to June 27, 2017). Abbreviations are as follows: temperature (Temp), salinity (Sal), dissolved oxygen (DO), dissolved inorganic carbon (DIC), total alkalinity (TA), partial pressure of carbon dioxide (pCO_2), pH_T (pH on the total scale), and aragonite saturation (Ωara).). We found higher variability in temperature at 5 m than 30 m (Figure S1). Water temperature at 5 m fluctuated between 6.8 to 18.8 °C throughout the seven-month study, while temperatures at 30 m remained more consistent at 7.8 to 11.3 °C. The minimum and maximum temperatures recorded in this study, 6.8 and 18.8 °C, were obtained at the shallow depth in January and June, respectively (Figure 2-2A). Salinity was lower and more variable at 5 m depth (22.7 – 29.4 PSU), than at 30 m (28.3 – 30.3 PSU) (Figure 2-2B, Figure S1). Salinity fluctuations at both depths were more prominent in winter when the water column was well-mixed and freshwater input is presumably higher. Dissolved oxygen levels were higher at 5 m than 30 m throughout the experiment; however, we observed more stable and consistently low dissolved oxygen readings at 30 m during the spring due to increased water column stratification (Figure 2-2C, Appendix Figure S2-1, Figure S2-2). Chl-*a*, data collected from the Dabob Bay ORCA monitoring buoy over the last ten years was used as a proxy for phytoplankton biomass (Figure S2-3). There are several years of data missing, and in some instances, there was no data or one years' worth of data for a particular day of the year, namely in December and January. The spike in chl-*a* at 5 m in January may be an artifact of a single year of data and may not be representative of the annual patterns. Overall, 30 m has less chlorophyll than 5 m, and most of the spikes (representing potential algal blooms) can be seen in April and May. pCO_2 levels were consistently higher at the 30 m depth, especially during the spring when levels reached 3738 µatm (pH_T = 7.09, Ωara = 0.20) at 30 m and 1002 µatm (pH_T = 7.62,

Ωara = 0.70) at 5 m on May 30, 2017. pCO_2 levels were more variable at 5 m than 30 m during both seasons (Figure 2-2D, Figure S1). Both pH_T and aragonite saturation state remained higher throughout the experiment at the 5 m depth when compared to 30 m (Figure 2-2E, F). pH_T at the 5 m depth ranged between 7.62 to 8.42, and 30 m depth pH_T ranged between 7.09 to 7.81. Ωara ranged between 0.7 and 2.7 at 5 m and between 0.2 and 0.7 at 30 m. Overall, carbonate parameters, temperature, and DO were strongly correlated, however oceanographic conditions between different depths were not well correlated (Figure 2-3).

2.4.2 Growth

Growth rates based on shell height were 129% and 125% higher across seasons at 5 m when compared to the 30 m depth in mussel and scallops, respectively ($F_{2,213} = 316.3$, $F_{2,182} = 231$, $p < 0.001$, $p < 0.001$, respectively, Figure 2-4A, B). Mussels and scallops at 5 m depth showed higher growth rates in the spring compared to the winter ($p = 0.022$, $p = 0.017$, respectively, Figure 2-4A, B) and no seasonal differences in growth rates were observed at 30 m depth ($p = 0.99$, $p = 0.35$, respectively). Growth rates in mussels were 124% and 132% greater at the 5 m depth than at the 30 m depth in winter and spring, respectively. Growth rates in scallops were 136% and 115% greater at 5 m depth than at the 30 m depth in winter and spring, respectively.

2.4.3 Shell Strength

Shell strength differed based on seasons and depth for mussels (season – $F_{1,247} = 152.49$, $p < 0.001$, depth – $F_{1,247} = 52.34$, Figure 2-4C). Mussel shells acclimatized to 5 m depth were 40% and 22% stronger than deep acclimatized mussels in the winter and spring, respectively ($p < 0.001$, $p <$

0.001, Figure 2-4C). In scallops, shell strength differed between seasons but not depth (season – $F_{1,231} = 6.08$, $p = 0.002$, depth – $F_{1,231} = 2.31$, $p = 0.13$, respectively, Figure 2-4D). Shell strength in scallops only differed between two cohorts, i.e. organisms collected at 30 m in the spring were 37% stronger than those collected from 5 m in the winter ($p = 0.013$, Figure 2-4D).

2.4.4 Isotopic Signatures

Isotopic signatures of mussels changed with both season and depth for $\delta^{13}C$, but only with depth for $\delta^{15}N$ ($\delta^{13}C$ season – $F_{2,45} = 128.1$, $p < 0.001$, depth – $F_{1,45} = 407.8$, $p < 0.001$; $\delta^{15}N$ season – $F_{2,45} = 1.17$, $p = 0.2$, depth – $F_{1,45} = 241.9$, $p < 0.001$, Figure 2-5A, Table S2-1, Figure S2-4). Mussels at 5 m in spring had higher (less negative) $\delta^{13}C$ values than at 5 m in the winter. Overall higher $\delta^{13}C$ values were found at 30 m than 5 m. $\delta^{15}N$ values in mussels differed between depths; higher $\delta^{15}N$ values were found at 30 m than 5 m (both seasons). At 5 m, $\delta^{15}N$ values were higher in the spring than the winter; however, at 30 m, $\delta^{15}N$ values were higher in the winter than the spring ($p < 0.001$, $p = 0.03$, respectively, Figure 2-5A, Table S2-1, Figure S2-4). Samples before the experiment's start (T_0, December 10, 2016) had similar signatures to the 30 m depths for both $\delta^{13}C$ and $\delta^{15}N$.

Scallops showed similar patterns in $\delta^{13}C$ levels to mussels (season – $F_{2,45} = 96.73$, $p < 0.001$, depth – $F_{1,45} = 180.50$, $p < 0.001$, Figure 2-5B, Table S2-1, Figure S2-4). Scallops from 5 m in spring had higher $\delta^{13}C$ values than at 5 m in the winter. Higher $\delta^{13}C$ values were found at 30 m than 5 m. $\delta^{15}N$ values in scallops differed between seasons and depth (season – $F_{2,45} = 11.41$, $p < 0.001$, depth – $F_{1,45} = 196.01$, $p < 0.001$). Similar to $\delta^{13}C$, higher values of $\delta^{15}N$ were observed at 30 m than 5 m ($p = 0.003$, $p < 0.001$, respectively, Figure 2-5B, Table S2-1, Figure S2-4). T_0 scallops had

similar signatures to the 30 m depths for $\delta^{15}N$, and $\delta^{13}C$ signatures were similar to all cohorts except 5 m winter.

In mussels, C:N ratios (Figure S2-4) were affected by both depth and season (depth – $F_{1,36} = 215.2$, $p < 0.001$, season – $F_{1,36} = 222.7$, $p < 0.001$), and had the highest ratio in the 5 m spring cohort. In scallops, C:N ratios were higher in the spring than summer (season – $F_{1,45} = 14.09$, $p < 0.001$,) and were higher at 5 m than 30 m in both seasons (depth – $F_{1,45} = 20.57$, $p < 0.001$).

2.5 DISCUSSION

2.5.1 Seawater Chemistry

Puget Sound's Hood Canal experiences seasonal hypoxia and strong stratification due to warming, upwelling, riverine, and anthropogenic nutrient inputs (Khangaonkar et al., 2018). In our study, we observed strong correlations between OA, deoxygenation, and temperature in Hood Canal. Our results show a relatively well-mixed water column in the winter and increasing stratification as the water warms in the spring. Temperatures experienced by shellfish in our experiment were as high as 18.8 °C and as low as 6.8 °C. In Hood Canal, salinity is typically affected by external freshwater input and precipitation (Reum et al., 2014). The lower salinity values at 5 m in spring are likely due to the outflow of snowmelt and terrestrial runoff which creates a freshwater lens containing high nutrient load (Khangaonkar et al., 2018). Dissolved oxygen was higher at 5 m than at 30 m. Strong spring stratification and warmer surface waters in Hood Canal can lead to increased phytoplankton blooms on the surface and metabolic influences on carbonate chemistry at all depths (Lowe et al., 2019).

The carbonate chemistry parameters (pH_T, pCO_2, and Ωara) fluctuated greatly between spring and winter and between depths. For the majority of the experiment, pCO_2 values were above 1000 µatm (Ωara = 0.2 to 0.6, pH_T = 7.09 to 7.60) at the 30 m depth, which exceeds the global surface ocean pCO_2 levels projected by IPCC (2014) for year 2100. An aragonite saturation state less than 1 is of concern because bivalves biomineralize aragonite to form their hard shells and prolonged undersaturation may lead to shell corrosion, reduced integrity, inability to obtain $CaCO_3$ from the water, and eventual mortality (Feely et al., 2008; Miller et al., 2009). Increased acidification and low Ωara in estuarine conditions like Hood Canal are often associated with eutrophication due to riverine and terrestrial nutrients, stratification, and anomalous upwelling patterns (Feely et al., 2010; IPCC, 2014; Lowe et al., 2019; Miller et al., 2009; Reum et al., 2014; Stevens and Gobler, 2018).

2.5.2 Growth and Shell Strength

Growth of mussels and scallops acclimatized to 5 m was > 100% higher than those from the 30 m depth. In a similar study, giant scallops, *Placopecten magellanicus*, held at different depths in Newfoundland, Canada, had higher growth rates at the shallow 10 m depth when compared to deeper depths (20 and 30 m) (MacDonald and Thompson, 1985). Gallardi et al. (2017) in Notre Dame, Canada found that after one year of acclimatization the blue mussel, *Mytilus edulis* grew more in shallow waters < 20 m when compared to mussels acclimatized to deep waters > 30 m, presumably due to food availability and temperature, however, factors like DO and pH were not measured in this experiment so we cannot rule out those factors as possible factors influencing growth rate. In our study, higher growth at shallow depths is likely due to a combination of multiple factors such as higher aragonite saturation state, dissolved oxygen, food availability, and overall

warmer temperatures, especially during the spring. If growers want fast shellfish growth, it is advisable to place bivalves for grow-out in the top few meters of the water column, shellfish at deeper depths will survive but grow slower.

Low Ωara, as we saw at deeper depths, can impair calcification and growth (Gazeau et al., 2013). With unfavorable carbonate chemistry conditions, more energy may be expended on shell formation and there may be a disruption in extra- and intracellular acid-base equilibria, causing a trade-off of metabolic energy away from growth (Michaelidis et al., 2005; Pörtner et al., 2005; Stevens and Gobler, 2018; Wittmann and Pörtner, 2013). Low DO levels at deeper depths reduces the ability of shellfish's ctenidia to extract oxygen from the water to sustain cellular function, possibly redirecting energy away from growth and toward acclimatory and somatic maintenance processes (Carrington et al., 2015; Froehlich et al., 2016; Sokolova et al., 2012; Stevens and Gobler, 2018). In our study, co-occurring acidification and low DO reduced the growth rate of the bay scallop, *Argopecten irradians*, and hard clam, *Mercenaria mercenaria*. Bivalves exposed to low oxygen and Ωara had lower growth than those acclimatized to ambient conditions or exposed to single stressor treatments (Gobler et al., 2017). A similar study found that *Argopecten irradians experienced significantly lower growth rates when exposed to water collected from Forge River Estuary, New York, which has naturally low DO and pH levels (Gobler et al., 2014).*

Mussels acclimatized to 5 m depth had considerably stronger shells than those from 30 m depth. This is possibly due to favorable aragonite saturation states at the surface. These results are consistent with previous studies in which calcifying species, snail, *Austrocochlea porcata* and blue mussel *Mytilus edulis,* had weaker shells when exposed to acidified conditions (Coleman et al.,

2014; Li et al., 2015). Carbonate chemistry can influence calcification by altering physiological pathways involved in the regulation of ion concentrations along epithelial cells used to secrete shell. As aragonite becomes undersaturated, it is more energetically expensive to maintain this ion balance to calcify (Miller et al., 2009). As suggested by Green et al. (2009) "death by dissolution" is a very real possibility for bivalves as climate change progresses and aragonite undersaturation in coastal waters is exacerbated. In Washington, it is predicted that increased uptake of anthropogenic CO_2 in the next 30 to 100 years will cause the aragonite saturation horizon to shoal further than it already has, causing dissolution and making suitable habitat scarce for calcifiers (Feely et al., 2012).

In contrast to mussels, scallops did not show large differences in shell strength throughout the study or between depths. The strongest shells were found at 30 m depth in the spring, whereas the most fragile shells were found at 5 m during the winter. Similar results have been seen in the gastropod mollusk *Subninella undulata,* whose shell strength was not directly related with pH treatments of 8.2 and 7.7 after 65 days of exposure (Coleman et al., 2014). We did not measure the thickness of the periostracum (organic outermost layer of the shell) layer in our study, however, it may be suggested that if a species has a thick periostracum layer, this may protect the inner layers of the shell from dissolution. It is probable that the scallops from our experiment were protected from dissolution due to their thick periostracum, which led to compromised growth rates but not shell strength (Gazeau et al., 2013). This has been demonstrated in a previous study where *C. gigantea* were exposed to 1050 µatm (pH 8.0) and 365 µatm (pH 7.6) pCO_2 for six weeks and shells were subsequently CT-scanned to measure shell density (Alma et al., 2020). Results of this study showed no significant difference in total shell density; however, a significantly lower

periostracum density was observed in the high pCO_2 treatments suggesting that this outer layer dissolves first when compared to the inner shell layers. Furthermore, *C. gigantea* is known to be more abundant at deeper depths, up to 80 m deep, where aragonite saturation in Hood Canal reaches levels of ~0.5 in the colder, well mixed months, and ~0.6 in the warmer highly stratified months (Feely et al., 2010; Whyte et al., 1990). In comparison, *M. galloprovincialis* can be found up to 40 m deep where aragonite saturation in Hood Canal can reach ~0.7 in the cold months and ~0.8 in the warm months (CABI, 2020; Feely et al., 2010), so it is possible that *C. gigantea* has evolved better biomineralization mechanisms to cope with OA than the more shallow-adapted *M. galloprovincialis*.

2.5.3 Isotopic Signatures

Analysis of stable isotope signatures can provide a time-integrated assessment of an individual's diet origin and insight into the influence of the environment on their assimilation rate (Galimany et al., 2017; Lowe et al., 2019) (Table S3). $\delta^{13}C$ can be used as an indicator of primary production sources, while $\delta^{15}N$ can be used as a proxy for trophic position (Michener and Lajtha, 2008). Scallops and mussels in our study had different isotopic signatures between depths and season. These differences in $\delta^{13}C$ manifested as lower (more negative) $\delta^{13}C$ levels in both species at the 5 m depths, especially in winter, likely due to increased terrestrial C3 plant input. Similar seasonal differences have also been seen in wild-sampled Hood Canal Pacific oyster *C. gigas,* who exhibited lower $\delta^{13}C$ in the winter (November–December) when compared to summer (June–August) (Conway-Cranos et al., 2015), suggesting that the oysters collected in summer had less terrestrial-based organic food sources than the winter. The isotopic pattern seen in the shallow winter cohort may point to increased runoff due to snowmelt or precipitation, directing more

terrestrial nutrients into Hood Canal (Simenstad and Wissmar, 1985). Differences across depths can be seen in both $\delta^{13}C$ and $\delta^{15}N$, in which the 30 m depth had higher isotopic values that the 5 m depth, for both species. A similar isotopic signature to our study was seen in the oyster *C. gigas,* where those grown close to the bottom near a seagrass bed had higher $\delta^{13}C$ and $\delta^{15}N$ when compared to oysters grown offshore (Hori et al., 2019). Oysters grown offshore had a more pelagic-based diet, while those grown on seagrass tidal flats ingested benthic and pelagic matter. An explanation for the low $\delta^{13}C$ values seen in our study at 5 m in winter shellfish is a possible increase in terrestrial salt marsh matter consumption from increased freshwater runoff (Conway-Cranos et al., 2015; Piola et al., 2006). *C. gigas* acclimated to Hood Canal conditions (15 km from our site) are suggested to have relied on a diet of predominantly salt marsh vegetation-derived carbon, resulting in a reduced $\delta^{13}C$ signature (Conway-Cranos et al., 2015). It can also be postulated that cohorts with higher $\delta^{13}C$ were acclimatized to environments with more C4 plant particulate, marsh grass, eelgrass, algal primary productivity, and marine-based POM as photosynthesis releases heavy carbon isotopes into the water and consumers will then integrate those heavier carbon isotopes from their diet into their bodies (Hama et al., 1983; Michener and Lajtha, 2008). This is a plausible hypothesis, as conditions at 5 m in the spring likely had higher phytoplankton productivity than in the winter, and the 30 m locations had a plethora of marine-based POM, while the 5 m location in the winter had mainly terrestrial POM. Furthermore, it may be suggested that those with higher $\delta^{13}C$ and $\delta^{15}N$ may be feeding higher on the food chain due to the trophic enrichment factors (~0.5 – 1‰ and ~2.2 – 3.4‰, respectively) (Fry, 2006; Michener and Lajtha, 2008). Howbeit, it is difficult to verify these assumptions of diet without direct isotopic measurements of food resources.

Typically low $\delta^{15}N$ values are indicative of a more oligotrophic environment while high $\delta^{15}N$ values are indicative of a eutrophic environment, however, in marginal seas we may also correlate enriched $\delta^{15}N$ with nutrients from upwelling (Briant et al., 2018; Michener and Lajtha, 2008). Higher $\delta^{15}N$ values at 30 m may be correlated with POM consumption from upwelling deep waters or sinking biological detritus. (Michener and Lajtha, 2008). Both upwelling and falling POM are linked to excess nutrients and increased metabolic activity of heterotrophic bacteria causing decreased oxygen levels (Zhang et al., 2010). Low DO levels can cause sub-lethal stress responses such as energetic trade-offs away from growth and reproduction, as well as catabolism of macromolecules stored in tissues, which increases nitrogen excretion rates (Patterson and Carmichael, 2018). In this study, low DO values can be seen at the 30 m depth (Figure 2-2), which may be correlated with a higher $\delta^{15}N$ signature in bivalve tissue from that depth. This was also demonstrated in *Crassostrea virginica* who had a higher $\delta^{15}N$ signature when field acclimatized to 3.66 mg/L DO, as opposed to those acclimatized with 6 mg/L DO (Patterson and Carmichael, 2018). Changes in $\delta^{15}N$ may also be attributed to a multitude of factors including changes in agricultural runoff, increased storm activity, or anthropogenic pollution (Piola et al., 2006), therefore, it is difficult to trace changes in $\delta^{15}N$ without discrete water movement data and measurements of food source end-members.

A small change in the C:N ratio may be indicative of environmental stress and alterations in the system's food web dynamics (Patterson and Carmichael, 2018). Food restriction and starvation has been linked with lower C:N ratio (Ek et al., 2015). The increased C:N values in both scallops and mussels in the spring at 5 m may suggest increased food resources due to increased temperature and light in the spring months. High temperature and oxygen is also known to increase metabolism,

growth rates, tissue turnover rates, and the uptake of heavier isotopes (Fry, 2006; Patterson and Carmichael, 2018; Vander Zanden et al., 2015). The highest C:N values in mussels and scallops were observed at 5 m in spring, during the warmest temperatures in the field experiment. Higher temperature is also correlated to an increase in phytoplankton $\delta^{13}C$, whose signature is passed onto the shellfish consumers (Briant et al., 2018). Growth in both species negatively correlates with $\delta^{15}N$ and C:N ratio. From these data, we can infer that the shellfish acclimatized to 30 m grew less and may have lived in an environment with higher nutrient content, low DO, less phytoplankton, and therefore more POM in their diet. Shellfish from the 5 m depth had higher growth, lower $\delta^{15}N$, and C:N, which may be indicative of high phytoplankton abundance and food availability. Isotopic signatures, however, can be modulated by a number of biotic and abiotic factors. A longer-term study of tissue-specific and environmental end-member isotopic signatures may provide further clarification to our assumptions.

2.6 CONCLUSION

Puget Sound acted as a natural multiple-stressor laboratory for our shellfish, and we were able to identify major differences in growth, shell strength, lipids, fatty acids, and stable isotopes across spatiotemporal scales. Overall, we saw higher growth at 5 m in both species. However, shell strength was higher at 5 m in mussels but not scallops, which had the same shell strength at both depths. Both mussels and scallops had low $\delta^{13}C$ levels at the 5 m depth in winter (Figure 2-5, Table S2-1, Figure S2-3). Our study highlights the importance of conducting field-based experiments to highlight spatiotemporal differences in physiology and provide the science community, aquaculture stakeholders, and policy makers with more robust and environmentally relevant results.

This study is unique and relevant because it integrates field-based data with physiological parameters that can be used to improve the culture conditions of shellfish, which ultimately serve as a protein source to feed a growing human population. The acclimatization capability of scallops and mussels have been shown in this study, however future research that acclimatizes bivalves for a longer period of time, and that examines transgenerational effects, metabolism, isotopic end-members, and genetic expression should be implemented. Additionally, it should be noted that this study was constrained for time and results may have differed if we chose to acclimatize during other seasons. These factors will allow us to obtain and better project the adaptive potential of these economically and ecologically important bivalves. This study also offers information to the aquaculture industry to obtain different marketable attributes in shellfish like size and shell integrity. The data are particularly relevant for the burgeoning rock scallop aquaculture market, farms who grow mussels on long lines, and aquaculture locations that are already starting to experience the effects of climate change.

2.7 FIGURES

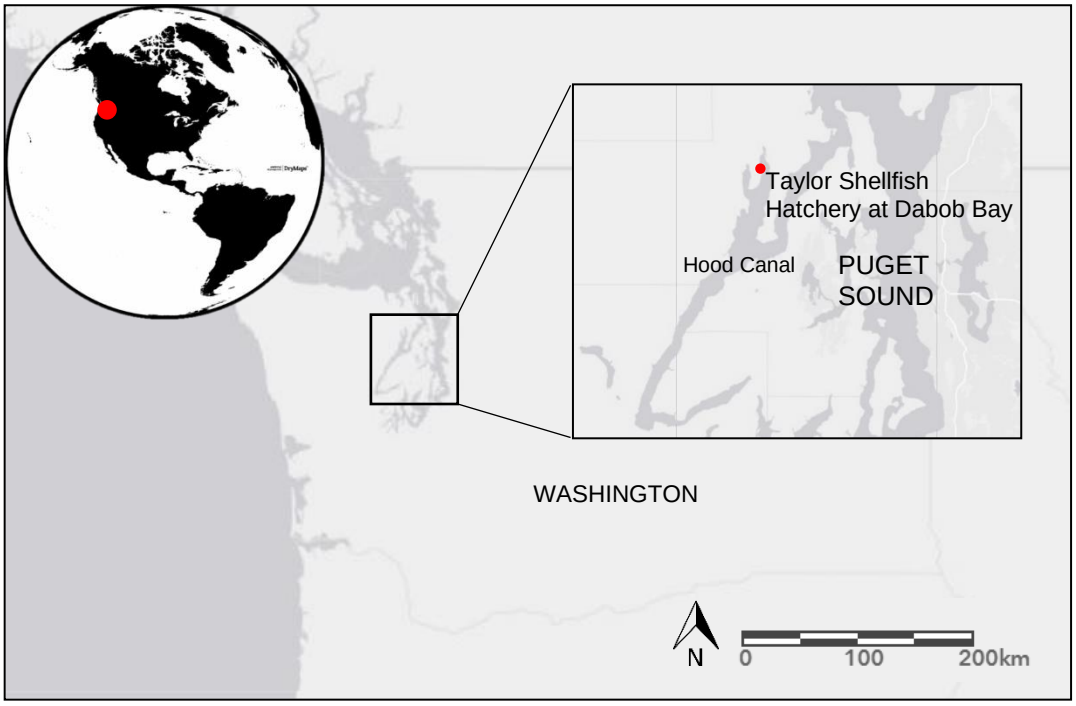

Figure 2-1: Study site located in Puget Sound, Washington USA at the Taylor Shellfish Hatchery in Hood Canal.

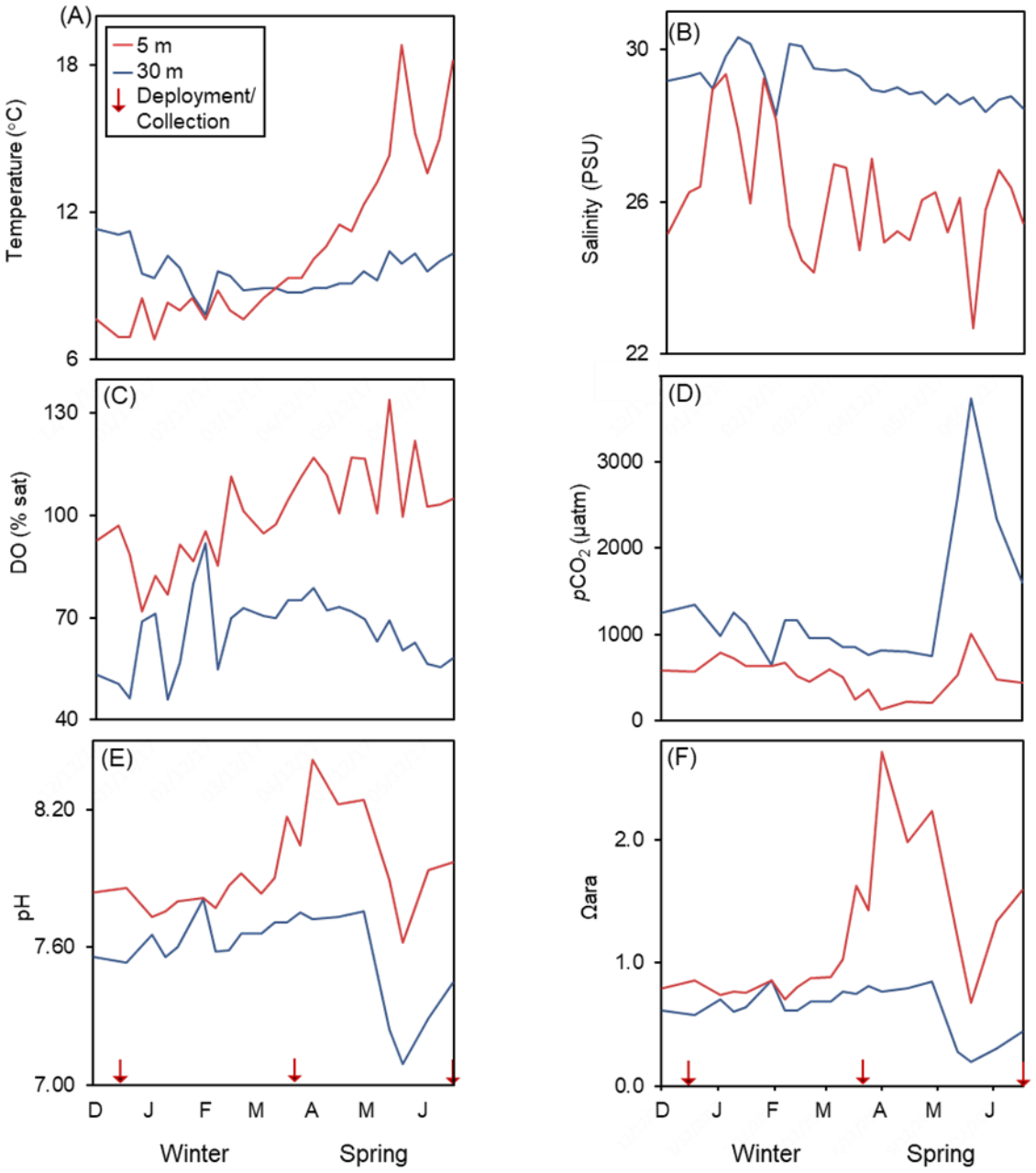

Figure 2-2: Environmental parameters in Hood Canal, Washington from December 2016 to June 2017, at 5 and 30 m depth. (A) Temperature (B) salinity, (C) dissolved oxygen in % saturation, (D) pCO_2, (E) pH, and (F) aragonite saturation (Ωara). Arrows show the time when organisms were deployed (December 11, 2016) and collected (March 22, 2017, and June 27, 2017).

Table 2-1: Hood Canal seawater chemistry summary (**mean, standard error [S.E.],** and coefficient of variation [CV]) for shallow (5 m) and deep (30 m) depths in winter (December 11, 2016, to March 22, 2017) and spring (March 23, 2017, to June 27, 2017). Abbreviations are as follows: temperature (Temp), salinity (Sal), dissolved oxygen (DO), dissolved inorganic carbon (DIC), total alkalinity (TA), partial pressure of carbon dioxide (pCO_2), pH_T (pH on the total scale), and aragonite saturation (Ωara).

	5 m Winter		30 m Winter		5 m Spring		30 m Spring	
Temp (°C)	8.01 ± 0.1	10.4	9.50 ± 0.2	95.0	13.33 ± 0.6	4.6	9.50 ± 0.1	15.8
Sal (PSU)	26.67 ± 0.33	15.3	29.51 ± 0.10	55.7	25.62 ± 0.21	22.9	28.73 ± 0.4	143.7
DO (% Sat)	91.9 ± 2.0	8.9	65.8 ± 2.5	5.0	110.9 ± 2.0	10.8	66.6 ± 1.4	8.7
DIC (µmol/kg)	1815.6 ± 27.8	21.3	2025.8 ± 12.6	46.4	1725.9 ± 30.1	18.0	2040.4 ± 29.4	23.1
TA (µmol/kg)	1877.0 ± 23.9	22.7	2047.8 ± 81.0	72.6	1867.1 ± 24.5	27.0	2021 ± 4.4	164.4
pCO_2 (µatm)	576.0 ± 40.5	4.1	1045.0 ± 59.4	5.1	420.0 ± 92.2	1.5	1677.0 ± 394.7	1.5
pH_T	7.86 ± 0.0	71.5	7.63 ± 0.0	95.4	8.04 ± 0.1	32.2	7.50 ± 0.1	27.8
Ωara	0.89 ± 0.10	3.7	0.68 ± 0.02	8.5	1.64 ± 0.2	2.6	0.56 ± 0.1	2.0

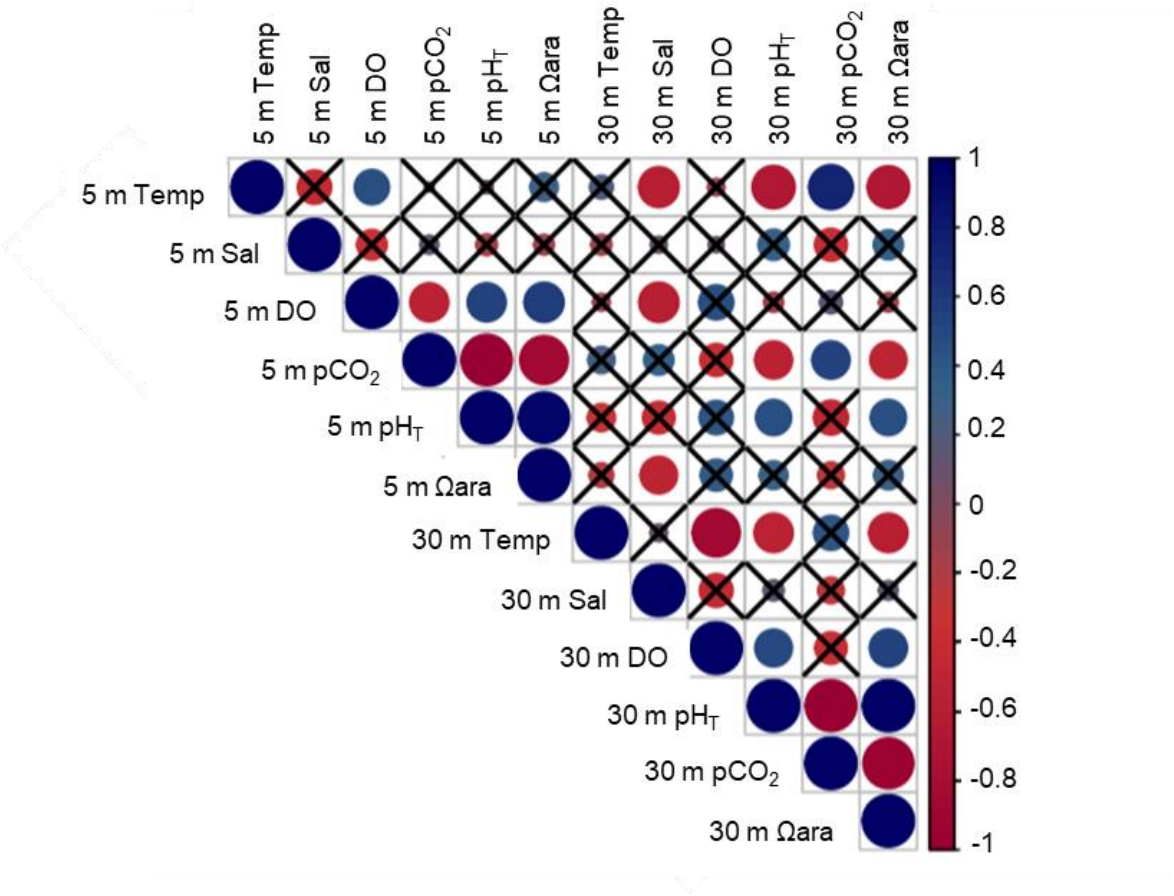

Figure 2-3: Correlation matrix of oceanographic conditions at 5 and 30 m depths. Color scale and circle size represent the Pearson's correlation coefficient, and black X's signify non-significant p-values < 0.05. Abbreviations are as follows: Temperature (Temp), salinity (Sal) dissolved oxygen (DO), partial pressure of carbon dioxide (pCO_2), and aragonite saturation (Ωara).

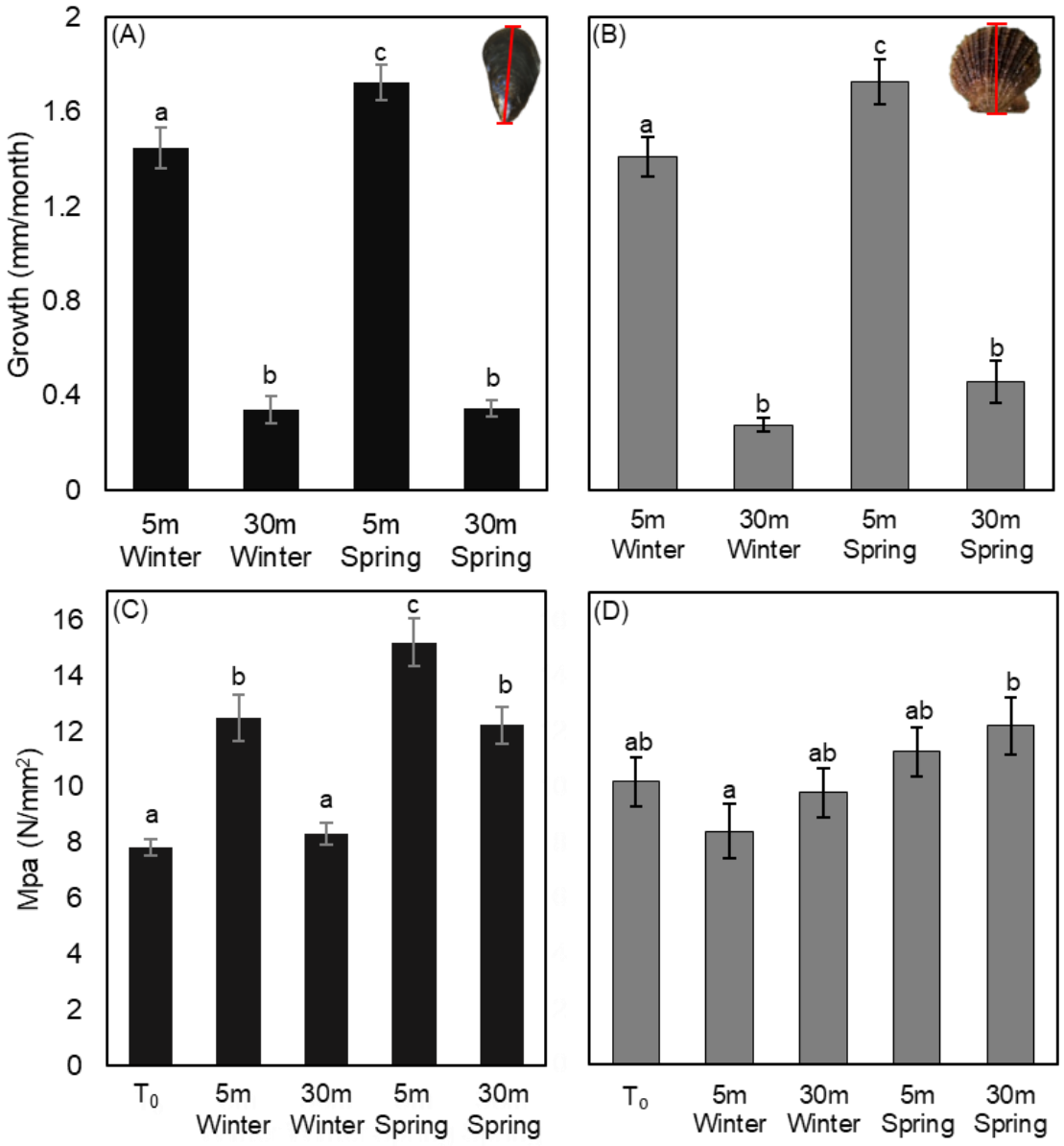

Figure 2-4: Average ± S.E. of (A) Mediterranean mussel (*Mytilus galloprovincialis*) and (B) purple-hinge rock scallop (*Crassodoma gigantea*) growth, (C) mussel and (D) scallop shell strength measured at time periods T_0, (pre-experiment, December 10, 2016), winter (December 11, 2016, March 22, 2017) and spring (March 23, 2017 to June 27, 2017). Bars with no common letters indicate significant differences ($p < 0.05$).

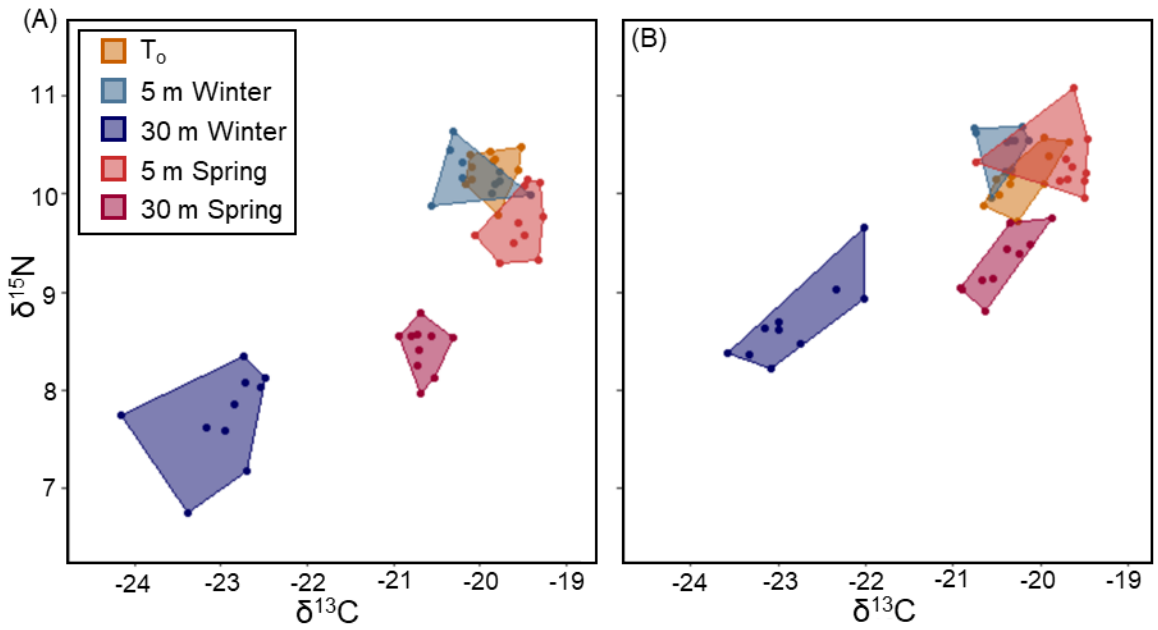

Figure 2-5: $\delta^{13}C$ and $\delta^{15}N$ isotopic signatures in the tissue of (A) Mediterranean mussel (*Mytilus galloprovincialis*) and (B) purple-hinge rock scallop (*Crassodoma gigantea*) analyzed pre-experiment (T_0), shallow (5 m) and deep (30 m) depths in winter (December 11, 2016, to March 22, 2017) and spring (March 23, 2017 to June 27, 2017) in Hood Canal, Washington.

2.8 References

Ab Lah, R., Kelaher, B.P., Bucher, D., Benkendorff, K., 2018. Ocean warming and acidification affect the nutritional quality of the commercially-harvested turbinid snail *Turbo militaris*. Mar. Environ. Res. 141, 100–108. https://doi.org/10.1016/j.marenvres.2018.08.009

Alava, J.J., Cheung, W.W.L., Ross, P.S., Sumaila, U.R., 2017. Climate change–contaminant interactions in marine food webs: Toward a conceptual framework. Glob. Chang. Biol. 23, 3984–4001. https://doi.org/10.1111/gcb.13667

Alin, S.R., Newton, J., Greeley, D., Curry, B., Herndon, J., Kozyr, A., Feely, R.A., 2021. A compiled data product of profile, discrete biogeochemical measurements from 35 individual cruise data sets collected from a variety of ships in the southern Salish Sea and northern California Current System (Washington state marine waters) from 2008-02-04 to 2018-10-19 (NCEI Accession 0238424). NOAA National Centers for Environmental Information. Dataset. https://doi.org/10.25921/zgk5-ep63.

Alin, Simone R.; Newton, Jan; Feely, Richard A.; Mickett, John; Greeley, Dana; Curry, Beth; Herndon, Julian; Ostendorf, M.L., 2019. Dissolved inorganic carbon (DIC), total alkalinity (TA), temperature, salinity, oxygen, nutrient, and CTD data collected from discrete profile measurements during Sound to Sea cruise RBTSN201705 (EXPOCODE 336Q20170502) on R/V Jack Robertson from 2017-05-0 [https://catalog.data.gov/dataset/dissolved-inorganic-

carbon-dic-total-alkalinity-ta-temperature-salinity-oxygen-nutrient-and-ctd29]. NOAA Natl. Centers Environ. Information. Dataset.
Alma, L., Kram, K.E., Holtgrieve, G.W., Barbarino, A., Fiamengo, C.J., Padilla-Gamiño, J.L., 2020. Ocean acidification and warming effects on the physiology, skeletal properties, and microbiome of the purple-hinge rock scallop. Comp. Biochem. Physiol. -Part A Mol. Integr. Physiol. 240. https://doi.org/10.1016/j.cbpa.2019.110579
Anacleto, P., Maulvault, A.L., Bandarra, N.M., Repolho, T., Nunes, M.L., Rosa, R., Marques, A., 2014. Effect of warming on protein, glycogen, and fatty acid content of native and invasive clams. Food Res. Int. 64, 439–445. https://doi.org/10.1016/j.foodres.2014.07.023
Anderson, A.S., Bilodeau, A.L., Gilg, M.R., Hilbish, T.J., 2002. Routes of introduction of the Mediterranean mussel (*Mytilus galloprovincialis*) to Puget Sound and Hood Canal. J. Shellfish Res.
Araújo, J., Soares, F., Medeiros, A., Bandarra, N.M., Freire, M., Falcão, M., Pousão-Ferreira, P., 2020. Depth effect on growth and fatty acid profile of Mediterranean mussel (*Mytilus galloprovincialis)* produced on a longline off south Portugal. Aquac. Int. 28, 927–946. https://doi.org/10.1007/s10499-019-00504-0
Aure, J., Strohmeier, T., Strand, Ø., 2007. Modelling current speed and carrying capacity in long-line blue mussel (*Mytilus edulis*) farms. Aquac. Res. 38, 304–312. https://doi.org/10.1111/j.1365-2109.2007.01669.x
Bachok, Z., Mfilinge, P.L., Tsuchiya, M., 2003. The diet of the mud clam *Geloina coaxans* (Mollusca, Bivalvia) as indicated by fatty acid markers in a subtropical mangrove forest of Okinawa, Japan. J. Exp. Mar. Bio. Ecol. 292, 187–197. https://doi.org/10.1016/S0022-0981(03)00160-6
Barton, A., Waldbusser, G.G., Feely, R.A., Weisberg, S.B., Newton, J.A., Hales, B., Cudd, S., Eudeline, B., Langdon, C.J., Jefferds, I., King, T., Suhrbier, A., McLaughlin, K., 2015. Impacts of coastal acidification on the Pacific Northwest shellfish industry and adaptation strategies implemented in response. Oceanography 28, 146–159. https://doi.org/10.5670/oceanog.2015.38
Bayne, B.L., 2004. Phenotypic flexibility and physiological tradeoffs in the feeding and growth of marine bivalve molluscs, in: Integrative and Comparative Biology. pp. 425–432. https://doi.org/10.1093/icb/44.6.425
Bednaršek, N., Feely, R.A., Beck, M.W., Glippa, O., Kanerva, M., Engström-Öst, J., 2018. El Niño-related thermal stress coupled with upwelling-related ocean acidification negatively impacts cellular to population-level responses in pteropods along the California current system with implications for increased bioenergetic costs. Front. Mar. Sci. 5. https://doi.org/10.3389/fmars.2018.00486
Bligh, E.G., Dyer, W.J., 1959. A rapid method of total lipid extraction and purification. Can. J. Biochem. Physiol. 37, 911–917. https://doi.org/10.1139/y59-099
Boersma, P.D., Reichard, S., Van Buran, A.N., 2006. Invasive species in the Pacific Northwest. University of Washington Press.
Borges, A. V., Gypens, N., 2010. Carbonate chemistry in the coastal zone responds more strongly to eutrophication than to ocean acidification. Limnol. Oceanogr. 55, 346–353. https://doi.org/10.4319/lo.2010.55.1.0346
Bourne, N., 1987. Scallop culture in British Columbia. Fourth Alaska Aquac. Conf.
Briant, N., Savoye, N., Chouvelon, T., David, V., Rodriguez, S., Charlier, K., Sonke, J.E., Chiffoleau, J.F., Brach-Papa, C., Knoery, J., 2018. Carbon and nitrogen elemental and

isotopic ratios of filter-feeding bivalves along the French coasts: An assessment of specific, geographic, seasonal and multi-decadal variations. Sci. Total Environ. 613–614, 196–207. https://doi.org/10.1016/j.scitotenv.2017.08.281

CABI, 2020. *Mytilus galloprovincialis* (Mediterranean mussel): Invasive Species Compendium Datasheet report. Wallingford, UK CAB Int. www.cabi.org/isc. 2020, 1–20.

Canale, C.I., Henry, P.Y., 2010. Adaptive phenotypic plasticity and resilience of vertebrates to increasing climatic unpredictability. Clim. Res. 43, 135–147. https://doi.org/10.3354/cr00897

Carnarius, K.M., Conrad, K.M., Mast, M.G., Macneil, J.H., 1996. Relationship of eggshell ultrastructure and shell strength to the soundness of shell eggs. Poult. Sci. 75, 656–663. https://doi.org/10.3382/ps.0750656

Carrington, E., Waite, J.H., Sarà, G., Sebens, K.P., 2015. Mussels as a model system for integrative ecomechanics. Ann. Rev. Mar. Sci. 7, 443–469. https://doi.org/10.1146/annurev-marine-010213-135049

Chan, C.Y., Wang, W.X., 2019. Biomarker responses in oysters *Crassostrea hongkongensis* in relation to metal contamination patterns in the Pearl River Estuary, southern China. Environ. Pollut. 251, 264–276. https://doi.org/10.1016/j.envpol.2019.04.140

Christie, W.W., 1998. Gas chromatography-mass spectrometry methods for structural analysis of fatty acids. Lipids. https://doi.org/10.1007/s11745-998-0214-x

Coleman, D.W., Byrne, M., Davis, A.R., 2014. Molluscs on acid: Gastropod shell repair and strength in acidifying oceans. Mar. Ecol. Prog. Ser. 509, 203–211. https://doi.org/10.3354/meps10887

Conway-Cranos, L., Kiffney, P., Banas, N., Plummer, M., Naman, S., MacCready, P., Bucci, J., Ruckelshaus, M., 2015. Stable isotopes and oceanographic modeling reveal spatial and trophic connectivity among terrestrial, estuarine, and marine environments. Mar. Ecol. Prog. Ser. 533, 15–28. https://doi.org/10.3354/meps11318

Culver, C.S., Richards, J.B., Page, H.M., 2006. Plasticity of attachment in the purple-hinge rock scallop, *Crassadoma gigantea*: Implications for commercial culture. Aquaculture 254, 361–369. https://doi.org/10.1016/j.aquaculture.2005.10.022

Dickinson, G.H., Ivanina, A. V., Matoo, O.B., Pörtner, H.O., Lannig, G., Bock, C., Beniash, E., Sokolova, I.M., 2012. Interactive effects of salinity and elevated CO 2 levels on juvenile eastern oysters, *Crassostrea virginica*. J. Exp. Biol. 215, 29–43. https://doi.org/10.1242/jeb.061481

Dickson, A.G., Sabine, C.L., Christian, J.R., 2007. Guide to Best Practices for Ocean CO_2 measurements. PICES Special Publication, Guide to Best Practices for Ocean CO_2 measurements. PICES Special Publication.

Domouhtsidou, G.P., Dimitriadis, V.K., 2001. Lysosomal and lipid alterations in the digestive gland of mussels, *Mytilus galloprovincialis* (L.) as biomarkers of environmental stress. Environ. Pollut. 115, 123–137. https://doi.org/10.1016/S0269-7491(00)00233-5

Ek, C., Karlson, A.M.L., Hansson, S., Garbaras, A., Gorokhova, E., 2015. Stable isotope composition in daphnia is modulated by growth, temperature, and toxic exposure: Implications for trophic magnification factor assessment. Environ. Sci. Technol. 49, 6934–6942. https://doi.org/10.1021/acs.est.5b00270

Elliott, J., Holmes, K., Chambers, R., Leon, K., Wimberger, P., 2008. Differences in morphology and habitat use among the native mussel *Mytilus trossulus*, the non-native *M.*

galloprovincialis, and their hybrids in Puget Sound, Washington. Mar. Biol. https://doi.org/10.1007/s00227-008-1063-3

Elliott, J., Rensel, M., Wimberger, P., 2005. Will the introduced mussel *Mytilus galloprovincialis* outcompete the native mussel *M. trossulus* in Puget Sound? A study of relative survival and growth rates among different habitats. Proc. Puget Sound Georg. Basin Conf. Seattle, 2005.

Ezgeta-Balić, D., Najdek, M., Peharda, M., Blažina, M., 2012. Seasonal fatty acid profile analysis to trace origin of food sources of four commercially important bivalves. Aquaculture 334–337, 89–100. https://doi.org/10.1016/j.aquaculture.2011.12.041

Feely, R.A., Alin, S.R., Newton, J., Sabine, C.L., Warner, M., Devol, A., Krembs, C., Maloy, C., 2010. The combined effects of ocean acidification, mixing, and respiration on pH and carbonate saturation in an urbanized estuary. Estuar. Coast. Shelf Sci. 88, 442–449. https://doi.org/10.1016/j.ecss.2010.05.004

Feely, R.A., Sabine, C.L., Byrne, R.H., Millero, F.J., Dickson, A.G., Wanninkhof, R., Murata, A., Miller, L.A., Greeley, D., 2012. Decadal changes in the aragonite and calcite saturation state of the Pacific Ocean. Global Biogeochem. Cycles 26. https://doi.org/10.1029/2011GB004157

Feely, R.A., Sabine, C.L., Hernandez-Ayon, J.M., Ianson, D., Hales, B., 2008. Evidence for upwelling of corrosive "acidified" water onto the continental shelf. Science (80-.). 320, 1490–1492. https://doi.org/10.1126/science.1155676

Franklin, S.T., Martin, K.R., Baer, R.J., Schingoethe, D.J., Hippen, A.R., 1999. Dietary marine algae (*Schizochytrium sp*.) increases concentrations of conjugated linoleic, docosahexaenoic and transvaccenic acids in milk of dairy cows. J. Nutr. 129, 2048–2052. https://doi.org/10.1093/jn/129.11.2048

Froehlich, H.E., Gentry, R.R., Halpern, B.S., 2016. Synthesis and comparative analysis of physiological tolerance and life-history growth traits of marine aquaculture species. Aquaculture 460, 75–82. https://doi.org/10.1016/j.aquaculture.2016.04.018

Fry, B., 2006. Stable isotope ecology, Encyclopedia of Ecology. Springer. https://doi.org/10.1016/B978-0-12-409548-9.10915-7

Fry, B., Mersch, F.J., Tholke, K., Garritt, R., Brand, W., 1992. Automated Analysis System for Coupled δ13C and δ15N Measurements. Anal. Chem. 64, 288–291. https://doi.org/10.1021/ac00027a009

Galimany, E., Lunt, J., Freeman, C.J., Reed, S., Segura-García, I., Paul, V.J., 2017. Feeding behavior of eastern oysters *Crassostrea virginica* and hard clams *Mercenaria mercenaria* in shallow estuaries. Mar. Ecol. Prog. Ser. 567, 125–137. https://doi.org/10.3354/meps12050

Gallardi, D., Mills, T., Donnet, S., Parrish, C.C., Murray, H.M., 2017. Condition and biochemical profile of blue mussels (*Mytilus edulis* L.) cultured at different depths in a cold water coastal environment. J. Sea Res. 126, 37–45. https://doi.org/10.1016/j.seares.2017.07.001

Galloway, A.W.E., Brett, M.T., Holtgrieve, G.W., Ward, E.J., Ballantyne, A.P., Burns, C.W., Kainz, M.J., Müller-Navarra, D.C., Persson, J., Ravet, J.L., Strandberg, U., Taipale, S.J., Alhgren, G., 2015. A fatty acid based bayesian approach for inferring diet in aquatic consumers. PLoS One 10. https://doi.org/10.1371/journal.pone.0129723

Gazeau, F., Parker, L.M., Comeau, S., Gattuso, J.P., O'Connor, W.A., Martin, S., Pörtner, H.O., Ross, P.M., 2013. Impacts of ocean acidification on marine shelled molluscs. Mar. Biol. 160, 2207–2245. https://doi.org/10.1007/s00227-013-2219-3

Gill, S.S., Willette, S., Dungan, B., Jarvis, J.M., Schaub, T., Van Leeuwen, D.M., St Hilaire, R., Omar Holguin, F., 2018. Suboptimal temperature acclimation affects kennedy pathway gene expression, lipidome and metabolite profile of nannochloropsis salina during PUFA enriched TAG synthesis. Mar. Drugs. https://doi.org/10.3390/md16110425

Gobler, C.J., Clark, H.R., Griffith, A.W., Lusty, M.W., 2017. Diurnal fluctuations in acidification and hypoxia reduce growth and survival of larval and juvenile bay scallops (*Argopecten irradians*) and hard clams (*Mercenaria mercenaria*). Front. Mar. Sci. https://doi.org/10.3389/FMARS.2016.00282

Gobler, C.J., DePasquale, E.L., Griffith, A.W., Baumann, H., 2014. Hypoxia and acidification have additive and synergistic negative effects on the growth, survival, and metamorphosis of early life stage bivalves. PLoS One 9. https://doi.org/10.1371/journal.pone.0083648

Green, M.A., Waldbusser, G.G., Reilly, S.L., Emerson, K., O'Donnell, S., 2009. Death by dissolution: Sediment saturation state as a mortality factor for juvenile bivalves. Limnol. Oceanogr. 54, 1037–1047. https://doi.org/10.4319/lo.2009.54.4.1037

Gruber, N., Hauri, C., Lachkar, Z., Loher, D., Frölicher, T.L., Plattner, G.K., 2012. Rapid progression of ocean acidification in the California Current System. Science (80-.). 337, 220–223. https://doi.org/10.1126/science.1216773

Gutiérrez, J.L., Jones, C.G., Strayer, D.L., Iribarne, O.O., 2003. Mollusks as ecosystem engineers: The role of shell production in aquatic habitats. Oikos 101, 79–90. https://doi.org/10.1034/j.1600-0706.2003.12322.x

Halfhill, R., 2007. Wavelength-specific light attenuation, chlorophyll concentration and phytoplankton communities. Univ. Washington.

Hama, T., Miyazaki, T., Ogawa, Y., Iwakuma, T., Takahashi, M., Otsuki, A., Ichimura, S., 1983. Measurement of photosynthetic production of a marine phytoplankton population using a stable 13C isotope. Mar. Biol. 73, 31–36. https://doi.org/10.1007/BF00396282

Hiebenthal, C., Philipp, E., Eisenhauer, A., Wahl, M., 2012. Interactive effects of temperature and salinity on shell formation and general condition in Baltic Sea *Mytilus edulis* and Arctica islandica. Aquat. Biol. https://doi.org/10.3354/ab00405

Hoegh-Guldberg, O., Cai, R., Poloczanska, E.S., Brewer, P.G., Sundby, S., Hilmi, K., Fabry, V.J., Jung, S., 2015. The ocean. In climate change 2014 – Impacts, adaptation and vulnerability: Part B: Regional aspects: Working group II contribution to the IPCC fifth assessment report. Cambridge Univ. Press.

Hofmann, G.E., Smith, J.E., Johnson, K.S., Send, U., Levin, L.A., Micheli, F., Paytan, A., Price, N.N., Peterson, B., Takeshita, Y., Matson, P.G., de Crook, E., Kroeker, K.J., Gambi, M.C., Rivest, E.B., Frieder, C.A., Yu, P.C., Martz, T.R., 2011. High-frequency dynamics of ocean pH: A multi-ecosystem comparison. PLoS One 6. https://doi.org/10.1371/journal.pone.0028983

Hori, M., Lagarde, F., Richard, M., Derolez, V., Hamaguchi, M., Makino, M., 2019. Coastal management using oyster-seagrass interactions for sustainable aquaculture, fisheries and environment. Bull. Japan Fish. Res. Educ. Agency 35–43.

Ikejima, I., Nomoto, R., McCabe, J.F., 2003. Shear punch strength and flexural strength of model composites with varying filler volume fraction, particle size and silanation. Dent. Mater. 19, 206–211. https://doi.org/10.1016/S0109-5641(02)00031-3

IPCC, 2014. Impacts, Adaptation, and Vulnerability: Contribution of working group II to the fifth assessment report of the Intergovernmental Panel on Climate Change. Intergov. Panel Clim. Chang. 1–44.

Kagley, A.N., Snider, R.G., Krishnakumar, P.K., Casillas, E., 2003. Assessment of seasonal variability of cytochemical responses to contaminant exposure in the blue mussel *Mytilus edulis* (complex). Arch. Environ. Contam. Toxicol. 44, 43–52. https://doi.org/10.1007/s00244-002-1303-3

Khangaonkar, T., Nugraha, A., Xu, W., Long, W., Bianucci, L., Ahmed, A., Mohamedali, T., Pelletier, G., 2018. Analysis of Hypoxia and Sensitivity to Nutrient Pollution in Salish Sea. J. Geophys. Res. Ocean. 123, 4735–4761. https://doi.org/10.1029/2017JC013650

Kim, T.W., Barry, J.P., Micheli, F., 2013. The effects of intermittent exposure to low-pH and low-oxygen conditions on survival and growth of juvenile red abalone. Biogeosciences. https://doi.org/10.5194/bg-10-7255-2013

Laing, I., 2000. Effect of temperature and ration on growth and condition of king scallop (*Pecten maximus*) spat. Aquaculture. https://doi.org/10.1016/S0044-8486(99)00262-8

Lamb, J.B., Van De Water, J.A.J.M., Bourne, D.G., Altier, C., Hein, M.Y., Fiorenza, E.A., Abu, N., Jompa, J., Harvell, C.D., 2017. Seagrass ecosystems reduce exposure to bacterial pathogens of humans, fishes, and invertebrates. Science (80-.). 355, 731–733. https://doi.org/10.1126/science.aal1956

Lauren, D.J., 1982. Oogenesis and protandry in the purple-hinge rock scallop, *Hinnites giganteus*, in upper Puget Sound, Washington, USA. Can. J. Zool. 60, 2333–2336. https://doi.org/10.1139/z82-300

Lavaud, R., Artigaud, S., Le Grand, F., Donval, A., Soudant, P., Flye-Sainte-Marie, J., Strohmeier, T., Strand, Ø., Leynaert, A., Beker, B., Chatterjee, A., Jean, F., 2018. New insights into the seasonal feeding ecology *of Pecten maximus* using pigments, fatty acids and sterols analyses. Mar. Ecol. Prog. Ser. 590, 109–129. https://doi.org/10.3354/meps12476

Leighton, D.L., Phleger, C.F., 1977. the Purple-Hinge Rock Scallop: a New Candidate for Marine Aquaculture. Proc. Annu. Meet. - World Maric. Soc. 8, 457–469. https://doi.org/10.1111/j.1749-7345.1977.tb00136.x

Li, S., Liu, C., Huang, J., Liu, Y., Zheng, G., Xie, L., Zhang, R., 2015. Interactive effects of seawater acidification and elevated temperature on biomineralization and amino acid metaboliin the mussel *Mytilus edulis*. J. Exp. Biol. 218, 3623–3631. https://doi.org/10.1242/jeb.126748

Lowe, A.T., Bos, J., Ruesink, J., 2019. Ecosystem metabolidrives pH variability and modulates long-term ocean acidification in the Northeast Pacific coastal ocean. Sci. Rep. 9, 1–11. https://doi.org/10.1038/s41598-018-37764-4

Lueker, T.J., Dickson, A.G., Keeling, C.D., 2000. Ocean pCO_2 calculated from dissolved inorganic carbon, alkalinity, and equations for K1 and K2: Validation based on laboratory measurements of CO_2 in gas and seawater at equilibrium. Mar. Chem. 70, 105–119. https://doi.org/10.1016/S0304-4203(00)00022-0

MacDonald, B., Thompson, R., 1985. Influence of temperature and food availability on the ecological energetics of the giant scallop *Placopecten magellanicus.* I. Growth rates of shell and somatic tissue. Mar. Ecol. Prog. Ser. 25, 279–294. https://doi.org/10.3354/meps025279

Martin, V.A.S., Gelcich, S., Vásquez Lavín, F., Ponce Oliva, R.D., Hernández, J.I., Lagos, N.A., Birchenough, S.N.R., Vargas, C.A., 2019. Linking social preferences and ocean acidification impacts in mussel aquaculture. Sci. Rep. 9. https://doi.org/10.1038/s41598-019-41104-5

McElhany, P., 2017. CO_2 sensitivity experiments are not sufficient to show an effect of ocean acidification. ICES J. Mar. Sci. 74, 926–928. https://doi.org/10.1093/icesjms/fsw085

Melzner, F., Stange, P., Trübenbach, K., Thomsen, J., Casties, I., Panknin, U., Gorb, S.N., Gutowska, M.A., 2011. Food supply and seawater pCO_2 impact calcification and internal shell dissolution in the blue mussel *Mytilus edulis*. PLoS One 6. https://doi.org/10.1371/journal.pone.0024223

Michaelidis, B., Ouzounis, C., Paleras, A., Pörtner, H.O., 2005. Effects of long-term moderate hypercapnia on acid-base balance and growth rate in marine mussels *Mytilus galloprovincialis*. Mar. Ecol. Prog. Ser. 293, 109–118. https://doi.org/10.3354/meps293109

Michener, R., Lajtha, K., 2008. Stable Isotopes in Ecology and Environmental Science: Second Edition, Stable Isotopes in Ecology and Environmental Science: Second Edition. https://doi.org/10.1002/9780470691854

Miller, A.W., Reynolds, A.C., Sobrino, C., Riedel, G.F., 2009. Shellfish face uncertain future in high CO_2 world: Influence of acidification on oyster larvae calcification and growth in estuaries. PLoS One 4. https://doi.org/10.1371/journal.pone.0005661

Moore, S.K., Johnstone, J.A., Banas, N.S., Salathé, E.P., 2015. Present-day and future climate pathways affecting *Alexandrium* blooms in Puget Sound, WA, USA. Harmful Algae 48, 1–11. https://doi.org/10.1016/j.hal.2015.06.008

Oksanen, J., Blanchet, F.G., Kindt, R., Oksanen, M.J., Suggests, M., 2013. Package 'vegan.' Community Ecol. Packag. Version.

Patterson, H.K., Carmichael, R.H., 2018. Dissolved oxygen concentration affects δ15N values in oyster tissues: implications for stable isotope ecology . Ecosphere 9, e02154. https://doi.org/10.1002/ecs2.2154

Pelletier, G.J., Lewis, E., Wallace, D.W.R., 2007. CO^2SYS.XLS: a calculator for the CO_2 system in seawater for Microsoft Excel/VBA. Washingt. State Dep. Ecol. Natl. Lab. Olympia, WA/Upton, NY, USA - Open Access Libr.

Pernet, F., Tremblay, R., Comeau, L., Guderley, H., 2007. Temperature adaptation in two bivalve species from different thermal habitats: Energetics and remodeling of membrane lipids. J. Exp. Biol. 210, 2999–3014. https://doi.org/10.1242/jeb.006007

Piola, R.F., Moore, S.K., Suthers, I.M., 2006. Carbon and nitrogen stable isotope analysis of three types of oyster tissue in an impacted estuary. Estuar. Coast. Shelf Sci. 66, 255–266. https://doi.org/10.1016/j.ecss.2005.08.013

Pörtner, H.O., Langenbuch, M., Michaelidis, B., 2005. Synergistic effects of temperature extremes, hypoxia, and increases in CO_2 on marine animals: From Earth history to global change. J. Geophys. Res. C Ocean. 110, 1–15. https://doi.org/10.1029/2004JC002561

Purroy, A., Najdek, M., Isla, E., Župan, I., Thébault, J., Peharda, M., 2018. Bivalve trophic ecology in the Mediterranean: Spatio-temporal variations and feeding behavior. Mar. Environ. Res. 234–249. https://doi.org/10.1016/j.marenvres.2018.10.011

Reum, J.C.P., Alin, S.R., Feely, R.A., Newton, J., Warner, M., McElhany, P., 2014. Seasonal carbonate chemistry covariation with temperature, oxygen, and salinity in a fjord estuary: Implications for the design of ocean acidification experiments. PLoS One 9. https://doi.org/10.1371/journal.pone.0089619

Riascos, J.M., Guzman, P.A., 2010. The ecological significance of growth rate, sexual dimorphiand size at maturity of *Littoraria zebra* and *L. variegata* (Gastropoda: Littorinidae). J. Molluscan Stud. https://doi.org/10.1093/mollus/eyq011

Rykaczewski, R.R., Dunne, J.P., 2010. Enhanced nutrient supply to the California Current Ecosystem with global warming and increased stratification in an earth system model. Geophys. Res. Lett. 37. https://doi.org/10.1029/2010GL045019

Sajjadi, N., Eghtesadi-Araghi, P., 2011. Determination of Fatty Acid Compositions as Biomarkers in the Diet of *Turbo coronatus* in Chabahar Bay. J. Persian Gulf.
Sherwood, L., Klandorf, H., Yancey, P.H., 2013. Animal Physiology: From Genes to Organisms, Second Edition, Thomson /Brooks/Cole.
Silina, A. V., Zhukova, N. V., 2007. Growth variability and feeding of scallop *Patinopecten yessoensis* on different bottom sediments: Evidence from fatty acid analysis. J. Exp. Mar. Bio. Ecol. 348, 46–59. https://doi.org/10.1016/j.jembe.2007.03.018
Simenstad, C., Wissmar, R., 1985. δ13C evidence of the origins and fates of organic carbon in estuarine and near-shore food webs. Mar. Ecol. Prog. Ser. 22, 141–152. https://doi.org/10.3354/meps022141
Sokolova, I.M., Frederich, M., Bagwe, R., Lannig, G., Sukhotin, A.A., 2012. Energy homeostasis as an integrative tool for assessing limits of environmental stress tolerance in aquatic invertebrates. Mar. Environ. Res. 79, 1–15. https://doi.org/10.1016/j.marenvres.2012.04.003
Soon, T.K., Zheng, H., 2020. Climate Change and Bivalve Mass Mortality in Temperate Regions, in: Reviews of Environmental Contamination and Toxicology. pp. 109–129. https://doi.org/10.1007/398_2019_31
Stevens, A.M., Gobler, C.J., 2018. Interactive effects of acidification, hypoxia, and thermal stress on growth, respiration, and survival of four North Atlantic bivalves. Mar. Ecol. Prog. Ser. 604, 143–161. https://doi.org/10.3354/meps12725
T. Walker, 2016. Rock scallop: Viable candidate for aquaculture? - Aquaculture North America Aquac. North Am.
Taiyun, W., 2014. Visualization of a correlation matrix. CRAN.
Talmage, S.C., Gobler, C.J., 2010. Effects of past, present, and future ocean carbon dioxide concentrations on the growth and survival of larval shellfish. Proc. Natl. Acad. Sci. U. S. A. 107, 17246–17251. https://doi.org/10.1073/pnas.0913804107
Tan, K., Ma, H., Li, S., Zheng, H., 2020. Bivalves as future source of sustainable natural omega-3 polyunsaturated fatty acids. Food Chem. 311, 125907. https://doi.org/10.1016/j.foodchem.2019.125907
Timmins-Schiffman, E., Coffey, W.D., Hua, W., Nunn, B.L., Dickinson, G.H., Roberts, S.B., 2014. Shotgun proteomics reveals physiological response to ocean acidification in *Crassostrea gigas*. BMC Genomics 15. https://doi.org/10.1186/1471-2164-15-951
Tyler, C., 1961. Shell Strength: Its Measurement and its Relationship to other Factors. Br. Poult. Sci. https://doi.org/10.1080/00071666109382385
USGS, 2012. Change to solubility equations for oxygen in water. Tech. Memo. 2001. 03. 2010.
Vale, P., 2010. Profiles of fatty acids and 7-O-acyl okadaic acid esters in bivalves: Can bacteria be involved in acyl esterification of okadaic acid? Comp. Biochem. Physiol. - C Toxicol. Pharmacol. https://doi.org/10.1016/j.cbpc.2009.08.001
Valles-Regino, R., Tate, R., Kelaher, B., Savins, D., Dowell, A., Benkendorff, K., 2015. Ocean warming and CO_2-induced acidification impact the lipid content of a marine predatory gastropod. Mar. Drugs 13, 6019–6037. https://doi.org/10.3390/md13106019
Vander Zanden, M.J., Clayton, M.K., Moody, E.K., Solomon, C.T., Weidel, B.C., 2015. Stable isotope turnover and half-life in animal tissues: A literature synthesis. PLoS One 10. https://doi.org/10.1371/journal.pone.0116182

Wallace, R.B., Baumann, H., Grear, J.S., Aller, R.C., Gobler, C.J., 2014. Coastal ocean acidification: The other eutrophication problem. Estuar. Coast. Shelf Sci. 148, 1–13. https://doi.org/10.1016/j.ecss.2014.05.027

Wernberg, T., Smale, D.A., Thomsen, M.S., 2012. A decade of climate change experiments on marine organisms: Procedures, patterns and problems. Glob. Chang. Biol. https://doi.org/10.1111/j.1365-2486.2012.02656.x

Whyte, J.N.C., Bourne, N., Hodgson, C.A., 1990. Nutritional condition of rock scallop, *Crassadoma gigantea* (Gray), larvae fed mixed algal diets. Aquaculture 86, 25–40. https://doi.org/10.1016/0044-8486(90)90219-D

Wilkie, E.M., Bishop, M.J., 2012. Differences in shell strength of native and non-native oysters do not extend to size classes that are susceptible to a generalist predator. Mar. Freshw. Res. 63, 1201–1205. https://doi.org/10.1071/MF12078

Wittmann, A.C., Pörtner, H.O., 2013. Sensitivities of extant animal taxa to ocean acidification. Nat. Clim. Chang. 3, 995–1001. https://doi.org/10.1038/nclimate1982

Zhang, J., Gilbert, D., Gooday, A.J., Levin, L., Naqvi, S.W.A., Middelburg, J.J., Scranton, M., Ekau, W., Peña, A., Dewitte, B., Oguz, T., Monteiro, P.M.S., Urban, E., Rabalais, N.N., Ittekkot, V., Kemp, W.M., Ulloa, O., Elmgren, R., Escobar-Briones, E., Van Der Plas, A.K., 2010. Natural and human-induced hypoxia and consequences for coastal areas: Synthesis and future development. Biogeosciences. https://doi.org/10.5194/bg-7-1443-2010

Zhukova, N. V., 2019. Fatty acids of marine mollusks: Impact of diet, bacterial symbiosis and biosynthetic potential. Biomolecules. https://doi.org/10.3390/biom9120857

3 CHAPTER 3

PHENOTYPIC PLASTICITY AND CARRYOVER EFFECTS IN AN ECOLOGICALLY IMPORTANT BIVALVE IN RESPONSE TO CHANGING ENVIRONMENTS

Lindsay Alma, Paul McElhany, Ryan Crim, Jan Newton, Michael Mahar, John Mickett, Jacqueline L. Padilla-Gamiño

3.1 ABSTRACT

Phenotypic plasticity can improve organism's fitness when exposed to novel environmental conditions or stress associated with climate change. Our study analyzed spatiotemporal differences in phenotypic plasticity and offspring performance in Olympia oysters *Ostrea lurida*. This species is an ecosystem engineer and is of great interest for commercial and restoration aquaculture. We used a multidisciplinary approach to examine acute and long-term physiological differences in *O. lurida* in response to *in situ* oceanographic conditions in a dynamic inland sea. We outplanted oysters to different areas in Puget Sound, Washington by affixing cages to the anchor lines of oceanographic monitoring buoys. This allowed us to couple high-resolution oceanographic data with organism's phenotypic response. To assess spatiotemporal differences in oyster physiological performance, we collected oysters after six-months and one year of acclimatization at four field sites. During each collection period we evaluated changes in shell properties, diet, metabolism, and reproduction of oysters. Adult growth, $\delta^{13}C$ and $\delta^{15}N$ isotopic signatures, and gametogenesis were affected by both seasonal and environmental conditions. Oysters acclimatized to cold acidified conditions had a higher respiration rate when exposed to acute thermal stress, and lower response to acute pH stress. Lipid content, sex ratio and shell strength did not change across locations. Offspring growth rates between sites (at 20°C), closely reflected parental growth rate

patterns. Offspring survival was not correlated with growth rates suggesting different energetic trade-offs in oyster offspring. Finally, larval metabolic response peaked at 20°C, but plummeted at 25°C, showing higher vulnerability in thermal stress than adult stages and a potential bottleneck for this species in the near future. By deploying genetically similar oysters into distinct environments and employing a wide range of physiological methodologies to examine performance and fitness, our results indicate that oysters exhibit high degree of phenotypic plasticity and show evidence of parental carryover effects.

3.2 INTRODUCTION

In recent years, we have witnessed substantial changes in our environment due to anthropogenically driven climate change (IPCC 2019). The land and sea are warming, the water is becoming more acidic, and we have experienced more extreme and frequent weather events (Doney et al. 2009, Stott et al. 2016, O'Neill et al. 2017). Co-occurring stressors may have unpredictable interactive effects on organismal physiology and their progeny (Todgham and Stillman 2013, Stevens and Gobler 2018). Phenotypic plasticity, or the ability of individual genotypes to produce different phenotypes when exposed to different environmental conditions (Pigliucci et al. 2006), can enable organisms to adapt and survive in rapidly changing environment. However, there is evidence that shows that not all plastic responses area adaptive and some can retard adaptation by modifying the distribution of phenotypes in the population (Sultan 2000, Fox et al. 2019). Novel environments associated with climate change may result in mal-adaptive plasticity (e.g. slow growth), or there may be a lag time between the emergence of novel environments and population level expression of beneficial phenotypes. This can lead to extinction or very rapid adaptive evolution through natural selection (Gibert et al. 2019). Conversely, phenotypic plasticity is also thought to be a means by which the population may expand their

ecological breadth, occupy a wider range of niches, and can drive natural selection (Sultan 2000, Ghalambor et al. 2007, Lancaster et al. 2015, Li et al. 2018, Gibert et al. 2019).

In this study we performed a series of field and laboratory experiments to better understand the role of phenotypic plasticity in a rapidly changing environment. Our experiments were performed in a marginal sea with the ecologically important native species, the Olympia oyster *Ostrea lurida* (Carpenter 1864). Field studies are extremely important because environmental parameters do not occur in isolation and simultaneous exposure to stressors can have unpredictable interactive effects on organismal physiology and potential carryover effects (Todgham and Stillman 2013, Stevens and Gobler 2018). Multi-stressor experiments performed in the lab rarely include realistic physiochemical variation into their design. Although interpretation may be complex, it is crucial to conduct field-based experiments where ocean conditions are spatiotemporally dynamic (Duarte et al. 2013, Gobler 2020). By coupling high resolution environmental data with physiological responses at multiple levels of biological organization, this study fills important gaps in understanding the phenotypic plasticity and carryover effects of *O. lurida*.

Our study was conducted in Puget Sound, an inland fjord-like estuarine system in Washington state, USA with novel geographic and oceanographic conditions (Fassbender et al. 2018, Bednaršek et al. 2021, Cai et al. 2021). Its unique glacial history has resulted in finger-like inlets and channels which have distinct seasonal stratification, and large spatial variations. Significant fluctuations in carbonate chemistry in Puget Sound often result in periods of aragonite undersaturation which greatly affects the calcification capacity of shellfish (Pelletier et al. 2018, Bednaršek et al. 2021, Cai et al. 2021). Generally, in the colder months, the water column in Puget

Sound is well mixed, water is cold, acidified, and has low salinity and dissolved oxygen. Conversely, in the warmer months the water column is highly stratified and surface water is warm with low acidification, and higher salinity and DO relative to the colder months. These variable conditions provide an ideal experimental system to examine how multiple environmental drivers affect (or not) the plasticity of several phenotypic traits including growth, shell strength, physiological performance, reproductive characteristics, and offspring quality.

Washington state is the top producer of farmed shellfish and seed in the country and bivalves are very culturally and economically important in this region (Washington Sea Grant 2015, USDA 2018). As of 2015, the shellfish industry in Washington supports over 2000 jobs and is worth $270 million per year (Barton et al. 2015, Washington Sea Grant 2015). Shellfish growers in Puget Sound experienced large larval die-offs in the early 2000's, which were ultimately found to be due to undersaturated aragonite levels (Barton et al. 2015). Now, many local hatcheries supplement their water with sodium carbonate buffer to combat ocean acidification and keep their product alive (Barton et al., 2015; Gurr et al., 2018; Wallace et al., 2014; Washington State Blue Ribbon Panel, 2012). In addition to aquaculture, bivalves in Washington play an integral part in the food web and serve as ecosystem engineers (Dumbauld et al. 2009, Barber et al. 2016). Recently, in June 2021 a record-breaking heat that hit the Pacific Northwest caused massive mortality of wild and farmed intertidal bivalves and other species that depended on them (Washington Sea Grant 2021, Raymond et al. 2022). This event occurred due to the coincidence of record high temperatures and midday extreme low tides, leading to unusually high lethal temperature levels (Raymond et al. 2022). Events like this are predicted to occur more frequently and increase in intensity as climate change progresses (IPCC 2019).

The Olympia oysters have important ecological roles as they filer water, stabilize substrate, and create reefs for other organisms to recruit (zu Ermgassen et al. 2020). They are endemic from Baja Mexico to British Columbia, and are the only native oyster to Washington (Blake and Bradbury 2012, Pritchard et al. 2016, Becker et al. 2020, Ridlon et al. 2021, Kornbluth et al. 2022). *O. lurida* can be found in estuaries as deep as 71 m, but usually inhabit intertidal or shallow subtidal habitats. Unlike most bivalves, brooding female *O. lurida* release swimming veliger larvae that have a comparatively short planktonic stage than other oysters and therefore are unable to travel far from sedentary parents and potentially harsh environmental conditions. Species with lower dispersal potential like *O. lurida* may have a decreased ability to cope with rapidly changing conditions compared to those with higher dispersal potential and wider environmental tolerance, like the non-native Pacific oyster *C. gigas* (Lefevre 2016, Kornbluth et al. 2022). Exploitation of *O. lurida* occurred around the turn of the century, and wild populations have not been able to recover. In the Pacific Northwest, native Olympia oyster populations have been considered either poor (90-99% lost) or functionally extinct (>99% lost) (Pritchard et al. 2015). In recent years, there has been a significant effort to restore *O. lurida* in the Salish Sea and there is some burgeoning interest in growing this species as an aquaculture product (Peter-Contesse & Peabody 2005, Blake and Bradbury 2012, Spencer et al. 2020, Wasson et al. 2020, McIntyre et al. 2021, Ridlon et al. 2021).

There is growing evidence that environmental stressors like temperature, acidification, and food quantity/quality can affect *O. lurida* fitness, reproduction, offspring performance, susceptibility to predation, and competition for space (especially by non-native Pacific oysters *Crassostrea gigas*)

(Hettinger et al. 2012, 2013, Sanford et al. 2014, Silliman et al. 2018, Spencer et al. 2020, 2021). In Puget Sound, *O. lurida* populations have different growth rates, survival, and reproductive fitness depending on location and it is likely that high thermal tolerance in some populations may be the result of increased stress resilience in offspring from parents exposed to temperature extremes (Heare et al. 2017). Parental acclimatization capacity and carryover effects will likely be essential to ensure the survival of this sensitive species as the environment becomes more extreme. Work by Spencer et al. (2020) found that environmental history of the *O. lurida* parents can affect the tolerance and physiology of the offspring. By understanding the phenotypic plasticity, physiological capacity and multigenerational responses of *O. lurida,* we may further improve selective breeding programs to restore populations to withstand ocean warming and extreme events (Parker et al. 2011, Rossi and Tunnicliffe 2017).

Our study involved outplanting young adult *O. lurida* to four sites in Puget Sound that had considerable spatiotemporal variation. We collected environmental data from monitoring buoys at each site and coupled it with oyster phenotypic characteristics after six months and one year of acclimatization. After six months we moved a subset of oysters from each site to a hatchery where we induced spawning for each cohort to obtain larvae and study carryover effects in offspring quality depending on the parent's environmental history. Specifically, we sought to address these important questions: (i) Will there be differences in phenotypic plasticity and tolerance in *O. lurida* depending on spatiotemporal variation in the field? (ii) Is there evidence of parental carryover in larval offspring based on parent's environmental history?

3.3 METHODS

3.3.1 Oceanographic monitoring

In situ oceanographic readings of temperature, dissolved oxygen (DO), chlorophyll-*a* (chl-*a*), and salinity were acquired from Oceanic Remote Chemical-Optical Analyzer (ORCA) buoys, managed by University of Washington Applied Physics Laboratory, Northwest Association of Networked Ocean Observing Systems (NANOOS), and Integrated Ocean Observing System (IOOS). Three ORCA buoys within Puget Sound were used as our study sites: Carr Inlet (CI) (47° 16.8' N, 122° 43.8' W) in South Puget Sound, Dabob Bay (DB) (47° 48.205' N, 122° 48.175' W) in Hood Canal, and Point Wells (PW) (47° 45.67' N, 122° 23.83' W) in Central Puget Sound (Figure 3-1A). When sensors on ORCA buoys malfunctioned during the course of the study, data from the LiveOcean Model were used instead to estimate a continuous profile of conditions (MacCready et al. 2021). pH, pCO_2, and aragonite saturation state (Ωara) were calculated by entering values for dissolved inorganic carbon (DIC), total alkalinity (TA), temperature, and salinity into *R* package *seacarb version 3.2.14* (Gattuso et al. 2016).

3.3.2 Cage deployment and collection

All individuals in this study were the same age and raised in the same conditions before the outplanting. One-year old *O. lurida* oysters were obtained from Puget Sound Restoration Fund in Manchester, Washington. During their first year these oysters were grown in natural Puget Sound conditions in Clam Bay offshore of Kenneth K. Chew Center for Shellfish Research and Restoration (47° 34.16' N, 122° 33.05' W). We used reared oysters because wild caught animals

may differ in age, environmental history, and nutritive status, and would further confound our results (Byrne 2011).

Before outplanting the oysters, a portion were measured and tagged by adhering numbered "bee tags" (Betterbee, Greenwich, NY) to their shells with superglue (Pacer Technology Zap-A-Gap Adhesives) (n = 400) (Figure 3-1B). Then, shellfish were placed in identical rigid mesh plastic bags and secured inside in a metal cage using cable ties. The cages containing the shellfish were attached with a clamp and tether to the anchor line of the ORCA buoys by SCUBA divers. Cages were affixed to the CI buoy at 5 m and 20 m below the surface on July 13, 2018. Cages were affixed to the DB and PW buoys at 5 m below the surface on July 12, 2018 (Figure 3-1C, D). Cages at 20 m below the surface were affixed at DB and PW, however they sank due to strong current, and were unretrievable by the divers due to the deep depths of the sites (> 100 m). After six months, half of the oysters were removed from the cages and brought back to the lab for physiological analysis. Oysters at CI were collected on January 8, 2019, oysters at DB were collected on January 15, 2019, and oysters in PW were collected on January 23, 2019. The final collections for CI took place on July 11, 2019, for DB on July 18, 2019, and for PW on July 23, 2019 (Figure 3-1D). Tagged shellfish were immediately brought to the laboratory at the School of Aquatic and Fishery Sciences at the University of Washington, dissected, flash frozen, and stored at -80°C for further analysis. Shells containing the numbered tag was cleaned with terrycloth and preserved at room temperature.

3.3.3 Growth

A digital caliper (0.1 mm precision) was used to measure the shell height (length - from hinge to apex) and shell length (from anterior to posterior) of the larger valve. The dissected measurement

was subtracted from the initial shell height and length to obtain total growth. The growth value was divided by the total number of months in the field to obtain a growth rate (n = 70 - 108).

3.3.4 Shell Strength

Shell strength was estimated using a modified method from Alma et al. (2020, 2022a). Dried shells were rehydrated in seawater for 24 hours prior to shell strength tests to mimic the aquatic environment (Ikejima et al. 2003). Hydrated shells were taken to the University of Washington Mechanical Engineering Department where they were point-crushed using an Instron 5585H 250 kN electro-mechanical test frame (Carnarius et al. 1996, Ikejima et al. 2003, Wilkie and Bishop 2012). Shells (n = 170 - 236) were placed on the stage of the Instron and a hydraulic upper mount was pressed down on the shell with one newton of force to hold it in place before crushing. Bluehill Software (v.2) (Illinois Tool Works Inc., IL, USA) recorded newtons it took to create a 2.5 mm puncture hole.

3.3.5 Total Lipids

Total lipids were extracted from whole body tissue (n = 10). Tissue was freeze dried, and ground to a fine powder using a mortar and pestle, then 15 ± 0.2 mg of tissue was weighed out for each individual using a microbalance (sensitivity 10 μg), and lipids were extracted using the Bligh Dyer method (Bligh and Dyer 1959). In short, chloroform:methanol and nanopure water was added, vortexed, and sonicated to extract lipids from the cell. The sample was centrifuged, and polar and non-polar metabolites were separated into phases. The bottom most layer containing the lipids suspended in chloroform was removed using a pasture pipette and placed into a metal tin to dry.

The Bligh Dyer extraction protocol was repeated twice to for each sample to ensure full lipid extraction. Total lipids were quantified gravimetrically by weighing the lipids and subtracting from the initial tissue weight.

3.3.6 Isotopes

Frozen whole body shellfish tissue (n = 10) was freeze-dried and ground in the same fashion as the lipid analysis. Dry tissue was weighed using a microbalance (sensitivity 10 μg) to 0.6 ± 0.01 mg per sample. The tissue was placed into a small tin 8 x 5 mm and the tin was closed and pressed onto itself to create a compact sample. Samples of Glutamic Acid I, II, (0.42 μg) and Bristol Bay Salmon (0.339 μg) of known isotopic values were interspersed in with our samples to serve as a reference. Samples were analyzed at the University of Washington Earth and Space Sciences Department Isolab where they were first placed in a Costech Elemental Analyzer, Conflo III, MAT253 with continuous flow, and then to a Finnigan MAT253 mass spectrometer (Fry et al. 1992). Using an algorithm in Matlab, the output data were corrected to the Air-N_2 scale, for $\delta^{15}N$, and to the VPDB scale, for $\delta^{13}C$. C:N ratio was calculated by dividing the mass of carbon by the mass of nitrogen in the sample.

To determine relative proportions of broad diet categories, we found isotopic signatures of diet end members (diet sources) from the literature. All end member data was collected from the literature within the Salish Sea. We clustered primary production sources based on isotopic values, and created three major categories (Kasai and Nakata 2005); (i) marine phytoplankton and POM (Wright et al. 2011, Conway-Cranos et al. 2015, Eccles et al. 2018, Pelletier et al. 2018, Costalago et al. 2020), (ii) phytobenthos (marine macroalgae, eelgrass) (Liedtke et al. 2011, Mueller 2017,

Costalago et al. 2020), and (iii) terrestrial matter (C3 plant material washed in from land) (Conway-Cranos et al. 2015). Averages and standard deviations were calculated for $\delta^{13}C$ and $\delta^{15}N$ signatures of end members. We plotted the end member and consumer data on a biplot to make estimates of diet proportion. A Monte Carlo mixing model was performed, but the wide variation of end member signatures prevented reliable results, and thus the model was omitted from the analysis.

3.3.7 Respirometry

A subset of outplanted oysters were taken to National Oceanic and Atmospheric Administration (NOAA) Mukilteo Research Station, Mukilteo, Washington (47° 56.56' N, 122° 18.10' W) to perform respiration measurements. Oysters were placed in holding tanks with filtered flow-through seawater. Oysters were starved 24 hours prior to respirometry trials to eliminate signals of metabolic activity due to digestion (Parker et al. 2017). The respirometry system consisted of 650 mL chambers equipped with a temperature and fiberoptic oxygen probes connected to an OXY-10 SMA G2 meter box, which was then connected to a computer with software PreSens Measurement Studio 2 (version 2.0.0.28). Prior to trials, the system was calibrated using a two-point oxygen calibration. 100% oxygen was achieved by leaving a beaker of fresh seawater overnight to equilibrate with the atmosphere. 0% oxygen was achieved by combining 1 g of sodium sulfate (Na_2SO_3) (Sigma-Aldrich) with 50 µl of cobalt standard for ICP ($Co(NO_3)_2$) (Sigma-Aldrich) and 100 mL of DI water. Individual oysters were placed in the water within airtight chambers, and chambers were placed in a water bath controlled by an Aqualogic heat pump (DSHP-4) (± 0.1°C). A magnetic stir bar was also placed into the chamber, and eight chambers were placed onto a custom-made magnetic submersible stir plate. Constant water movement via the stir bar allowed homogenous temperature and oxygen levels within the

chamber. Trials were run for one hour with n = 8 individuals per cohort per trial. We ran blank chambers with seawater to determine a baseline oxygen consumption due to microbial and background respiration; we subtracted that value from each individual's respiration rate. Respirometry trials were run at five different temperatures (3, 8.5, 14, 19.5, and 25°C), and five different pH levels (6.6, 6.9, 7.2, 7.6, and 7.8). Temperatures were achieved by adjusting the heat pump, and pH was achieved by bubbling CO_2 controlled by a solenoid valve. The pH probe (Honeywell) was calibrated with tris buffer and verified using a spectrophotometer and m-cresol purple dye in accordance with Dickson et al., (2007). Temperature treatments were performed at pH 7.8 and pH treatments were performed at 11°C. After respirometry trials were completed, tagged individuals were dissected, and visceral mass was placed in a labeled metal tin. Oyster visceral mass was dried in a 60°C oven for 48 hours to ensure full dehydration, and individual dry weight was measured. Appropriate start and end points were chosen for each individual's respiration curve, and oxygen consumption was converted from % oxygen saturation to mg/L of oxygen, using an equation (Benson and Krause 1984) which takes into account temperature and salinity. Standard metabolic rate (SMR) of each individual (mg O_2 g^{-1} DW h^{-1}) was calculated as oxygen consumption in mg/L per hour and gram of dry weight.

3.3.8 Gonad Histology

A pea-sized piece of gonad (~3 – 12 cm^2) was excised from the visceral mass (n = 10) the day of collection, fixed for 24 hours in 10% formalin and subsequently preserved in with 70% ethanol. Fixed samples were sent to Histology Consultation Services (Everston, WA) for staining with hematoxylin counterstaining with eosin staining, paraffin wax imbedding slicing, and mounting onto slides (da Silva et al. 2009, Hassan et al. 2018a, Spencer et al. 2020). The slides were examined using under a high-powered microscope (Nikon Eclipse Ni) and photographed using the

program NIS-Elements Basic Research. Sex of each individual was recorded and gonad maturation was determined using a scale of 0-5, a scale previously used on *O. lurida* and *Ostrea edulis* (da Silva et al. 2009, Oates 2013, Hassan et al. 2018a). The gonad maturation scale is as follows: (0) no gametes present, (1) some evidence of gametes, (2) moderately developed follicles, (3) ripe gametes, follicles fully expanded, (4) spawning, follicles begin to empty, (5) resorbing, follicles empty and reduced. Since *O. lurida* is a hermaphroditic species, sex was determined using a scale (da Silva et al. 2009, Oates 2013, Spencer et al. 2020); Indeterminate – empty follicles, Male – only spermatogonia found, Hermaphroditic primarily male (HPM) – spermatogonia abundant, some evidence of oocytes, and Hermaphroditic primary female (HPF) – oocyte stages abundantly found, some evidence of spermatogonia, Female – only oocytes found.

3.3.9 Adult spawning

After the first collection period, a subset of oysters was immediately transported to the Kenneth K. Chew Center for Shellfish Research and Restoration at NOAA Manchester Research Station. Oysters were separated by cohort, placed in mesh bags, and suspended in flow-through 19 L tanks with flow rates of 4 L/min. Seawater was UV sterilized, filtered to 1 µm, and fed into a series of 379 L header tanks with submersible heaters (Teco Aquarium Chiller TK-500 and Finnex HC 810-M, ±0.1°C). Oysters were fed a constant supply of a cultured live mixed algal diet (brown and green phytoplankton) *ad libitum* using an Iwaki dosing pump attached to the inflow waterline. To stimulate spawning, the water temperature was raised 1°C daily until 18°C was reached. We monitored the oysters daily for up to 45 days for sperm release and maternal release of larvae. Outflow was emptied into a smaller 7.5 L tank with 100 µm screens to catch any veligers. Larvae from each cohort were collected and placed in 189 L flow through-tanks fed by the same header

tanks containing seawater that the adults received. All flow-through tanks received constant aeration using an air stone and were emptied bi-weekly for cleaning using a strong stream of freshwater.

3.3.10 Larvae counts growth and survival

A subset of larvae from each cohort were stocked in 1 L plastic tripour beakers (jar) with 800 mL FSW (fresh seawater) at a density of ~1 larvae mL^{-1}. Each jar was fitted with a 100 µm screen insert made of PVC and nitex mesh, so the larvae can be easily filtered during water changes. The jar was emptied and filled daily with 800 mL of FSW containing a mixed culture fresh live phytoplankton. To thermally challenge the larvae, jars were placed in water baths heated or cooled to 14 or 20°C ± 0.1. Each cohort had n = 6 replicate jars in each water bath temperature. We performed counts to assess survival and growth two to three times per week for 14 days. To obtain samples for survival and growth, larvae from each tripour were rinsed using a steady stream of seawater and filtered down to 100 mL volume. We used a "plunger" (device consisting of a circular disk with a handle) to evenly homogenize the larvae within the seawater. We used a micropipette to extract six 1 mL samples and placed each sample into a well within a 6-well plate. We used a dissecting microscope to count total larvae within each well and recorded mortalities. We used an Amscope MD35 digital microscope camera to capture photos of larvae, and ImageJ v1.51 to measure shell height (Gurr et al. 2021).

3.3.11 Larvae Respirometry

Additional larvae collected from site specific broodstock populations were allowed to grow in the 189 L flow-through stock tanks at 18°C until they reached pediveliger stage. On April 26, 2019, pediveliger larvae ranging from 180 – 200 µm from each stock tank were sorted and placed in 19 L tanks using a series of nitex mesh filters. Subsequently, larvae were homogenized within seawater and serial dilutions were prepared at densities of 0.1 mL, 1 mL, 2 mL, 3 mL, and 4 mL from the stock tanks. Dilutions of larvae from each cohort were placed in 4 mL glass vials containing a Planar Trace Oxygen Sensor Spot SP-PST6, topped off with filtered seawater if needed, and sealed with a cap. Vials were placed in a 24 well plate and placed on a PreSens Sensor Dish Reader (SDR) to measure oxygen consumption rate (Gurr et al. 2021, Maboloc and Chan 2021). The sensor was calibrated using the corresponding PreSens SDR software in a similar fashion to the fiberoptic Presens sensors. The sensor spot fixed to the bottom of the vial contains a luminescent dye. When dye is excited by the lasers below, luminescence signal based on oxygen partial pressure is emitted back to the sensor and interpreted by the software. The PreSens SDR plate containing serial larval dilutions from each cohort along with blanks of 0 and 100% saturated seawater were placed in a dark incubator and oxygen consumption was measured overnight at five temperatures (5, 10, 15, 20, 25°C) to create a thermal performance curve for each larval population. Following the respirometry trial, larvae from each vial were preserved in 70% ethanol and counted using a dissecting microscope. Respiration rate was calculated in a similar fashion to the adult oysters, but oxygen consumption was normalized by number of larvae in each vial instead of dry weight.

3.3.12 Data analysis

All analyses were performed in *R* version 1.3.959 (R Core Team, 2020) with a significance threshold of $\alpha < 0.05$. A Shapiro-Wilk Test was performed to assess normality and if needed, values of analysis were log, arcsine, or square root transformed to achieve normality assumptions before a model was run. ANOVAs were performed and post-hoc with Tukey-HSD tests for multiple comparisons for growth, shell strength, lipids, stable isotopes, and respiration rates. A Pearson's Chi-square test based on 10,000 replicates with a Bonferroni correction for multiple comparisons was performed to evaluate sex ratio and gonad maturation (da Silva et al. 2009, Spencer et al. 2021). A correlation plot was created using oceanographic data and larval survival hazard ratio with *R* package *corrplot version 0.87* (Taiyun 2014). R^2 and p-values correlating shell strength and growth were performed. When trials used multiple replicates from a single population, we ran a linear mixed-effects model, using *R* package *lme4 version 1.1-28* (Bates et al. 2015), where each response variable is a fixed effect, and individual the replication variable as a random effect.

To evaluate the effect of temperature on survival of the four larval populations across time, we used the *survival version 3.3-0* (Therneau 2020) and *survminer version 0.4.8* (Kosinski et al. 2020) packages in *R* (R Core Team, 2022.02.2). The functions *Surv and survfit* were used to format data for the models. A non-parametric Kaplin-Meier survival analysis with right censoring (Pernet et al. 2015, Maboloc and Chan 2021) determined overall significance between treatments. Our target stock density was calculated to 800 larvae per jar, but to account for uncertainty and noise of larval subsampling and equal stock density, we evaluated the chances of sampling a larva in a binomial process. We used Bayes Theorem assuming uniform prior (Rish 2001) to predict the number of

larvae in a jar given actual count input. We simulated time series data for each of our 48 jars, selecting only for monotonically decreasing iterations until we had 500 replicates per jar. With high simulated replication, we can approach uniform assumption, and reduce uncertainty around sampling probability. Larval mortalities were assigned a binary status of 1 on the day of death and larvae who remained alive by the end of the 14 days were considered right censored and assigned a binary status of 0. To further explore differences between larval cohorts, we ran a multivariate Cox proportional hazards regression model (Cox 1972, Maboloc and Chan 2021) with the *coxph* function using temperature and parental acclimatization location as covariates in the model. We looped all 500 x 48 replicate jars into the model and extracted the log hazard ratios (lnHR, mean of coefficients) and 5% confidence intervals (two tailed, 2.5, 97.5% quantiles) from the model output to evaluate 27 significance tests for each possible temperature/parental site interaction. We performed an exponential transformation on the lnHR and confidence intervals (95%) before plotting their interactions in a forest plot and heatmap using *ggplot2 version 3.3.6*. Data and *R* codes used for the analysis are publicly available in a supplemental GitHub repository (Alma et al. 2022b).

3.4 RESULTS

3.4.1 Environmental variability

There were clear differences in oceanographic conditions between study sites and between study periods (Appendix Table S3-1, Figure 3-2, Figure 3-3). At all sites, temperature was on average higher in July 2018-January 2019 (T1) when compared to January - July 2019 (T2). DB had the highest variation in temperature at both time periods while CI20 had the lowest. The maximum

temperature of 18.1°C was reached at DB on June 14th, 2019, and the lowest temperature of 6.9°C was also seen at DB on February 14th, 2019. At all sites, T1 had higher average salinities than T2 (Table S3-1, Figure 3-2, Figure 3-3). DB has the lowest salinity at both time periods, with a salinity reading recorded as low as 20.7 PSU on January 18, 2019, and CI20 registered the highest salinity at 31.0 PSU on December 17, 2018. CI20 had a higher salinity than CI5 at both time periods. Average chlorophyll-*a* (chl-*a*) was highest at CI5 for both time periods. On average, there was higher chl-*a* in T2 than there was in T1. The highest variation of chl-*a* occurred at DB in the T2 time period (0.64 - 37.8 mg m^{-3}). On average, dissolved oxygen (DO) was higher at all sites in T2 compared to T1. CI5 had the highest average DO levels during T1, and DB had the highest in T2 (8.32 mg/L and 10.48 mg/L, respectively). At both time periods, CI20 had the lowest average DO levels (6.18mg/L for T1 and 8.28 mg/L for T2, respectively). Average pH was higher at all sites during T2 compared to T1 (Table S3-1, Figure 3-2, Figure 3-3). pH had the highest variation at both time periods at DB, and the lowest variation at CI20. Aragonite saturation state was higher in T2 than T1. In both time periods DB had the highest variation of Ωara and CI20 the lowest. The lowest Ωara and pH recorded during this experiment was 0.62 and 7.51, respectively at DB on October 14, 2018. pCO_2 was, on average, higher in T1 than T2. DB had the highest variation of pCO_2 in both time periods, and CI20 had the lowest variation. Correlations comparing oceanographic parameters at each site were performed (Figure 3-4). At all sites chl-*a* was positively correlated with DO, pH, and Ωara and negatively correlated with salinity and pCO_2. DO was positively correlated with Ωara and pH, and negatively correlated with salinity and pCO_2 at all sites. Ωara was highly correlated with pCO_2 and pH. Ωara was highly correlated with temperature at DB, but negatively correlated at CI20. pCO_2 was highly correlated with pH and correlated with salinity at all sites except DB. pCO_2 also had a negative correlation to temperature

at DB, PW, and CI5, but a strong positive correlation at CI20. pH was negatively correlated with salinity at all locations except DB. pH was positively correlated with temperature at all locations except CI20, where it is negatively correlated. Finally, salinity had a weak positive correlation with temperature at all locations except CI5.

3.4.2 Shell Growth and Strength

Shell height growth rates (height – hinge to apex) differed depending on site and the time of collection ($p < 0.001$) (Figure 3-5A, B, Table 3-1). In T1, CI20 grew slower than all other cohorts, and oysters in CI5 and DB had significantly faster growth rates compared to the other sites. In T2, CI20 and PW cohorts grew slower, and oysters in CI5 grew faster than the other cohorts. Overall, oysters grew 61.6% faster in the T1 time period compared to the T2 time period. Shell length (anterior to posterior) growth rates also differed by site and time of collection ($p < 0.001$) (Figure 3-5C, D, Table 3-1). Slower lengthwise growth rates were observed in oysters at CI20 and PW in T1 and higher growth rates were observed in oysters from CI5 and DB. In T2 oysters from CI20 grew significantly less lengthwise than oysters in CI5, but the oysters from other sites did not differ from each other. Oyster lengthwise growth was 59.7% faster in T1 compared to T2.

Shell strength only differed between time periods ($p < 0.001$) (Figure 3-5E, F, Table 3-1). In T1, shell strength in oysters from CI20 were significantly lower than oysters in PW, but not DB and CI5. In T2 there was no significant difference in shell strength between cohorts. T2 shells were on average 74% stronger than T1 shells, presumably because these oysters are older and grew thicker. Shell strength was not correlated with growth rates (Figure S3-1).

3.4.3 Lipid and Isotopic Composition

Lipid content did not differ between sites ($p = 0.08$) or collection period ($p = 0.41$) (Figure S3-2, Table 3-1). There was no significant correlation between lipids and growth rates. The only cohort to have a relationship between lipids and shell strength was with DB in T1 which had a negative correlation, $R^2 = 0.48$, $p = 0.025$.

$\delta^{13}C$ signatures varied between sites in the different collection times ($p = 0.006$, Figure 3-6, Figure S3-3, Table 3-1). $\delta^{13}C$ signatures were higher in the CI locations compared to the other sites whereas the DB cohorts had the lowest values in both collection times. Between collection periods, CI5 and CI20 signatures did not differ. $\delta^{15}N$ signatures varied between sites in the different collection times ($p = 0.004$, Figure 3-6, Figure S3-3, Table 3-1). In T1, $\delta^{15}N$ signatures in DB were lowest, and the highest in CI20. In contrast, there were no site differences of $\delta^{15}N$ levels in T2 oysters. CI20 $\delta^{15}N$ signatures were higher in T1 than T2. C:N differed between sites in the different collection periods ($p < 0.001$, Table 3-1, Figure S3-3). Oysters in CI5 had the highest C:N ratios during both collection times. Oysters in DB experienced seasonal differences in C:N. Oysters collected in T1 had higher C:N ratios than in T2. In T1, C:N ratios at CI20 and PW were significantly lower than CI5. In T2, C:N ratios at DB were significantly lower than all other cohorts.

3.4.4 Effects of Temperature and pH on Adult Oyster Metabolism

Oysters collected in T1 had a higher respiration rate than those from T2 (Figure 3-7, Table 3-1) when challenged with temperature stress. Rates increased with temperature at all sites during both time periods. The only exception occurred in oysters collected at T2 from DB, which had lower

respiration rates at temperatures above 14°C. CI20, CI5 and DB cohorts had higher respiration rates in T1 compared to T2. PW cohort showed similar respiration rates both time periods ($p = 0.31$). Respiration rates were higher in T1 than T2 under different pH levels (Figure 3-8: Short-term metabolic response to pH challenge at each collection period.T1 = January 2019 [darker colors], T2 = July 2019 [lighter colors]) and study site (CI20 = Carr Inlet at 20 m [green], CI5 = Carr Inlet at 5 m [blue], DB = Dabob Bay at 5 m [orange], and PW= Point Wells at 5 m [purple]). Vertical dotted lines represent temperatures at the collection sites one week prior to collecting the oysters (in January, CI20 and CI5= 7.76, DB = 7.84, and PW = 7.89; in July CI20 = 7.83, CI5 = 8.07, DB = 8.19, PW = 7.98). pH trials were run at 11°C., Table 3-1). Oysters from CI (5 and 20m) did not change respiration rates under different pH levels. DB and PW significantly increased respiration rates at the lowest pH level (pH = 6.6). Notably, respiration rates of oysters under different pH levels never exceeded 10 mg/l g DW^{-1} h^{-1}.

3.4.5 *Reproductive Characteristics: Gamete Development and Sex Ratio*

Gonad maturation stage differed for the different sites ($p = 0.003$) and collection times ($p = 0.048$) (Figure 3-9A). Before the start of the experiment (T_0) 30% were at advanced reproduction, 50% were mature, and 20% were resorbing. In T1, 80% of oysters at CI20 had spawned (either spawned or resorbing states), while only 20% of oysters had spawned at CI5, 50% at DB, and 70% at PW. In T2, 40% of CI20 oysters had spawned, 20% at CI5, 100% at DB, and 10% at PW. When considering oysters at advanced and mature stages (i.e., developed gametes) we found different seasonal patterns. At T1 oysters from CI20 had 0% develop gametes, CI5 had 70%, DB had 50%, and PW had 30%. At T2 oysters from CI20 had 50% developed gametes, CI5 had 80%, DB had 0%, and PW had 90%. Oysters from CI20 appeared to have spawned sometime between July 2018 and January 2019, and they began to develop gametes again between January 2019 and July 2019.

Oysters from CI5 appeared not to have spawned much between July 2018 – January 2019 because their maturation patterns in T1 are still similar to T_0. CI5 oysters likely spawned soon after our T2 collection, as 80% of oysters had advanced/mature gametes. Oysters collected in T1 from DB were primarily still developing gametes, however in T2 none of the oysters were developing gametes, suggesting recent spawning. Finally, at PW 60% of the oysters had spawned by T1, and oysters appear to be redeveloping gametes in T2. When maturation stages were binned into "pre-spawn" and "post-spawn" (Figure S3-4), there were several differences between collection times, but interestingly, there was a difference between DB in T2 and all the other T2 cohorts ($p = 0.04$, 0.002, and < 0.001 at CI20, CI5 and PW, respectively).

There were no differences in sex ratios between site or collection times ($p = 0.84$, 0.14, respectively, Figure 3-9B). 44.4% of oysters were classified as fully male, 37.7% hermaphroditic primarily male (HPM), and 17.8% hermaphroditic primarily female (HPF). We did not observe any oysters that were exclusively female. When comparing differences in hermaphrodism patterns, there were no significant differences across sites ($p = 0.69$) but there were differences between collection period ($p = 0.042$). Before the experiment 50% were male and 50% hermaphrodites. In T1, 60% were hermaphrodites in CI20 and PW, CI5 had 70%, and DB had 90%. In T2, there were fewer hermaphrodites and more males, with CI20, CI5 and PW displaying 40%, and DB had 50% hermaphrodites. The oysters collected in T1 from the DB population had the highest amount of HPF individuals. If sexes are grouped by the dominant sex, the sex ratio is highly skewed toward male/HPM at 82%, and HPF at 18%. The ratios are equal (50%) when grouped by hermaphrodites and full males.

3.4.6 Larval Growth

After running a liner mixed-effects model, we found no significant "tank" effect between replicates from the same cohort. There was a significant effect of parental origin ($p < 0.001$) and temperature ($p < 0.001$) on larval growth (Figure 3-10, Table 3-1). Larvae grew ~138% faster at 20°C than those challenged to 14°C. At 20°C larvae whose parents were from CI5, and DB grew significantly larger than CI20 and PW. At 14°C, larval growth at PW was lower than at CI5.

3.4.7 Larval Survival

Larval cohorts had a higher survival at 20°C than 14°C. CI5 larvae had a lower chance of survival than larvae from DB and PW (HR (hazard ratio), 0.63; CI (confidence interval), 0.50, 0.82, and HR, 0.60; CI 0.48, 0.76, respectively, Figure 3-10, Figure 3-11). At 14°C, larvae from CI5 had a lower chance of survival than larvae from DB and PW (HR, 0.55; CI, 0.44, 0.68, and HR, 0.66; CI 0.54, 0.80, respectively). At 14°C, CI20 larvae also had a reduced probability of survival than DB and PW (HR, 0.58; CI, 0.46, 0.71, and HR, 0.70; CI 0.50, 0.84, respectively). Larvae from CI20, CI5, and PW had higher survival at 20°C vs 14°C (HR, 0.54; CI, 0.43, 0.67, HR, 0.71; CI 0.58, 0.89, and HR, 0.62; CI 0.50, 0.77, respectively). At 20°C, CI20 had a higher chance of survival than CI5 at 14 and 20°C, and PW at 14°C (HR, 1.97; CI, 1.58, 2.47, HR, 1.64; CI 1.35, 2.05, and HR, 1.29; CI 1.04, 1.64, respectively). At 14°C, CI20 had higher survival than DB at 20°C (HR, 1.54; CI 1.14, 2.06)

3.4.8 Larval Respirometry

The response of larvae to different temperatures depended on parental site (Figure 3-13, Table 3-1, $p < 0.001$). Maximum respiration rates for all locations were observed at 20°C. However, larval respiration rates at 20°C were higher in larvae from CI20 and PW parents compared to CI5 and

DB. The lowest respiration rates were found at 5-10°C. Respiration at 15 and 30°C did not differ from each other.

3.5 DISCUSSION

This multidisciplinary study examines how temporal and spatial environmental variability influences phenotypic changes and carryover effects in the Olympia oyster. Our results show high acclimatization potential and phenotypic responses in growth, metabolism, and reproduction in oysters outplanted to different locations in Puget Sound, Washington. Larvae whose parents were acclimatized to Dabob Bay in Hood Canal, were more resilient than others, having the highest survival, growth, and low metabolic stress when exposed to thermal stress. Our results provide important information to support restoration efforts to increase the abundance of this native species and to support shellfish growers' efforts focused on improving broodstock and offspring quality and resilience.

3.5.1 Oceanography

Puget Sound is a remarkably complex and dynamic fjord estuary system which experiences large fluctuations between season, location, and depth (Feely et al. 2010, Reum et al. 2014, Thom et al. 2018). We used long-term monitoring buoys to profile this oceanographic complexity at our sites over a one-year period. We found more extreme and variable temperatures in DB (Hood Canal), while CI20 (South Puget Sound at 20 m), and PW (Central Puget Sound) experienced lower and less variable temperatures. Higher temperatures in the warmer T1 period (July 2018 – Jan 2019) were associated with lower oxygen values, especially at CI20 and PW. At the CI location (5 or 20

m depth) water was well mixed late October (~13°C) to early March (~8°C), so temperatures were very similar at both our shallow and deep sites. In fact, there were 113 days where the 20 m depth was warmer than the 5 m depth at CI due to strong vertical mixing in the colder months. Salinity was lower during the T2 period (January 2019 – July 2019), which is likely due to winter and spring rainfall/runoff. DB site showed extreme low values of salinity compared to the other sites. This site has historically exhibited high freshwater inflow (Newton et al. 2007, Conway-Cranos et al. 2015), which can be exemplified in our data by short periods of low salinity at this site. CI20 had the lowest pH and the DB site had the highest variability in pH. Hood Canal is especially prone to episodic upwelling (Newton et al. 2007), which may explain the environmental variability in our data at this site. During upwelling old deep-water blobs are carried to the surface, bringing cold nutrient rich water with low pH and DO. Many hatcheries, like Taylor Shellfish Farms, whose hatchery is located near the DB site, are already feeling the effects of OA on their bottom line, and they have begun to buffer their water with sodium carbonate to increase the carbonate availability to their larval shellfish (Barton et al. 2015, Washington Sea Grant 2015). CI5 had the highest variability in chlorophyll values during the summers of 2018 and 2019. These high values may have been associated with toxic dinoflagellate algal blooms (*Protoceratium reticulatum* and *Akashiwo sanguinea*) that resulted in mass mortality of shellfish in different parts of Puget Sound (King et al. 2021). In both 2018 and 2019 the combination of stress due to increased environmental variability and exposure to yessotoxin (affects metabolic and immune pathways) from the algae resulted in many cultured and wild bivalve mortalities in Puget Sound within a matter of weeks (King et al. 2021).

3.5.2 Shell Growth and Strength

Growth rates of adult *O. lurida* were higher in the beginning half of our experiment when the temperatures were higher compared to the second half. The internal body temperature of ectotherms varies depending on the environmental temperature so as temperature is reduced, the organism's metabolism, and consequently growth, slows (Pörtner et al. 2000, Brockington and Clarke 2001, Schulte 2015). During T2, oysters experienced more favorable carbonate chemistry levels for calcification, higher DO, and greater chl-*a* levels compared to T1. However, they also experienced a greater number of days in colder than average temperatures which may explain the reduced growth rates during this period. Oysters located in CI20 had the lowest growth likely due to low levels of chlorophyll, oxygen, and pH, associated with stratification and upwelling during warmer months.

Unlike growth rates, shell strength of *O. lurida* did not differ much between sites but there was a clear difference in strength between collection times. Shell strength was higher in T2 when the oysters were older and had thicker shells. Shell strength was not correlated with shell growth (Figure S3-1). This is consistent with studies that show no correlation between growth and shell strength in blue mussels *M. edulis,* and clams *Arctica islandica,* after being exposed to temperature and pH stress (Hiebenthal et al. 2013). It may be hypothesized that oyster growth is prioritized when the individuals are young and as they age, growth rates decrease, and shell strength is prioritized. Ontogenetic increase in shell strength was also observed in acclimatized *Mytilus edulis* (Nagarajan et al. 2006). Alternatively, more favorable carbonate chemistry parameters (high pH, aragonite saturation, and low pCO_2), and higher oxygen levels in the second half of the field experiment may be responsible for changes in calcification and subsequently increased shell

strength. It is important to note that shell strength by T2 remained the same for all sites, despite the high variability in environmental characteristics and differences in shell growth rates between sites. Thus, allocation of energy to shell strength is an important process that is prioritized in *O. lurida*, regardless of external conditions. Not having a strong shell may be detrimental as oysters may become more vulnerable to predators and shell boring parasites (Duckworth and Peterson 2013, Coleman 2014, Mostofa et al. 2015). In future studies, more frequent collection of organisms throughout the year would allow the implementation of linear models to quantify what environmental variables best predicts shell growth and integrity at the different locations and time periods.

3.5.3 Lipid and Isotopic Composition

Oysters from different sites and collection periods had the same total lipid content. This was surprising considering the seasonal and spatial variability of our collection sites. This suggests that oysters from different sites may be mobilizing glycogen (main storage form of glucose) for energy similarly and/or may not need to tap into their fat reserves (Berthelin et al. 2000, Hassan et al. 2018b). Similar results were seen in several lab-based climate change related experiments. There was no significant difference in lipid content between developmental stages in urchin *Strongylocentrotus purpuratus* acclimated to pCO_2 365, 1030, or 1450 μatm for six days (Matson et al. 2012). Conversely, environmental variation with season did cause differences in *C. gigas* total lipid profile in Kali Estuary, India, suggesting different metabolic trade-offs between species and environments (Subasinghe et al. 2019). Performing specific fatty acid assays may elucidate differences in saturation, and distribution of fatty acids to better understand diet source and environmental stress responses (Berthelin et al. 2000, Alma et al. 2022a).

Isotopic signatures were used to trace carbon and nitrogen sources and dietary composition. The present study demonstrates that oysters acclimatized to different locations and time periods are accessing different sources of nitrogen and carbon and assimilating that isotopic signature into their tissue. Carbon isotopic signatures show that *O. lurida* mainly consumes phytoplankton with some evidence that they may consume POM or SPOM from other primary production sources (phytobenthos) depending on biogeographic availability (Hill and McQuaid 2008). Oysters from T1 collected at CI20 had higher $\delta^{15}N$ signatures compared to the other sites. Enriched $\delta^{15}N$ signals are often associated with higher consumer trophic position (Malet et al. 2007, McMahon et al. 2021). It is likely that oysters in this location and time period are consuming more zooplankton, animal-based POM and/or sinking POM (SPOM). High $\delta^{15}N$ signature may also be indicative of heavy nitrates associated with upwelling, which are consumed by primary producers which shellfish feed on (Emery 2015, Feddern et al. 2021). The primary consumers from the southwest/west facing coasts in South Africa: nematode *Trichuris serrata*, gastropod *Oxystele variegate*, and limpet *Scutellastra cochlear* also had enriched $\delta^{15}N$ and $\delta^{15}C$ due to biogeographic location and upwelling when compared to east facing locations (Hill and McQuaid 2008). Similarly, native mussel *Mytilus trossulus* isotopic signatures were tied closely to seasonal changes, and differences between locations in Puget Sound (Howe and Simenstad 2015).

The differences between T1 and T2 $\delta^{15}N$ signatures between sites indicate that the driver of nitrogenous sources for some sites (CI20 and DB) shifts seasonally (likely upwelling). Temperature and metabolic rate may also affect $\delta^{15}N$ as shown in oyster *Crassostrea virginica* in Chesapeake Bay, where tissue $\delta^{15}N$ values decreased during warmer months when the oysters were

more metabolically active, and tissue turnover is higher (Fertig et al. 2010). Coastal nitrogenous sources may come from rivers, runoff (Feeley et al 2012), anthropogenic sources like stormwater, agriculture, or upwelling (Khangaonkar et al 2018). Runoff, containing nitrates from synthetic fertilizers, have a low $\delta^{15}N$ signature (Fertig et al. 2010), and increased runoff may explain the decreased $\delta^{15}N$ signature in oyster at DB during T1. However, this signature is not present in T2 when runoff is more likely to increase due to high precipitation, suggesting that this may not be the largest contributing factor.

3.5.4 Effects of Temperature and pH on Adult Oyster Metabolism

With increasing fluctuations in our oceans due to climate change, it is critical that we examine the tolerance and metabolic plasticity of marine organisms. We used short-term experiments to examine temperature and pH tolerance of adult *O. lurida* from different sites and seasons (Jan vs. Jul).

Higher respiration rates were found in oysters from T1 than T2 for all sites across temperatures. In January, oysters were cold-acclimatized and thus were more responsive to increases in temperature. Oysters from PW had the lowest differences in respiration rates between seasons suggesting that oysters from this site did not express as much plasticity as the other cohorts. Oysters from the deep location (CI20) were more sensitive to increased temperatures. Respiration rates of these oysters increase dramatically at 8.5°C, whereas the other cohorts did not increase substantially until 14°C.

Oysters from DB, the site with the highest temperature levels and variability, showed the highest respiration rates, specifically during the winter. Similar responses were observed in the adult oysters *C. gigas* and *C. gigas angulate* collected in either Qingdao (northern site, colder) or Xiamen (south site, warmer) off the coast of China (Li et al 2017). Southern oysters had higher metabolic rates and tended to have a higher plasticity than the northern oysters. It is interesting to note that we did not see evidence of metabolic depression due to high temperatures (maximum temperature tested 25 °C) in any of the cohorts even though the maximum temperature experienced in the field was 18°C (at DB); suggesting lethal temperature may be greater than 25°C (Lefevre 2016). This has also been observed in arctic blue mussels *Mytilus edulis*, whose metabolic rate continued to rise past 7°C, despite their lowest environmental temperature being around 5°C (Thyrring et al. 2015). We must consider that these measurements are due to acute stress (1 hour exposure) and may not be reflect *in situ* resting metabolic rate. It is also important to note that oxygen consumption is a proxy but not necessarily a perfect indicator of cellular respiration (Schulte 2015) or long-term response. Thermal optimum or maximum tolerance levels may also be breached in the near future due to heightened extreme weather events and heatwaves associated with climate change (Frölicher and Laufkötter 2018, Gobler 2020, Scanes et al. 2020). For example, within the Northeastern Pacific warm-water anomaly of 2015 ‘the blob” (Khangaonkar et al. 2021) resulted in water temperatures of up to 21.5°C, and the Pacific Northwest heat wave of 2021 which resulted in air temperatures of up to 49.4°C, killing many cultured and wild bivalves in the intertidal zone. Our high temperatures exceed levels predicted for year 2100 (IPCC 2019), which may potentially indicate that these bivalves are equipped to survive these warmer temperatures. It may also suggest that their thermal tolerance deviates from the traditional bell shaped TPC or does not follow the oxygen and capacity limitation of thermal tolerance (OCLTT)

hypothesis (Schulte 2015, Pörtner et al. 2017, Jutfelt et al. 2018). This may suggest that metabolic rate may increase until right before complete molecular dentition due to inability to transport oxygen through the body (Lefevre 2016).

It has been well documented that, similar to temperature, OA causes bioenergetic trade-offs, narrowing the aerobic scope, and thermal breadth of an organism (Pörtner 2008, Sokolova et al. 2012). Our results show seasonal differences in respiration rates under different pH levels for all the sites. Oysters collected in T1, which were experiencing lower pH at the time collection than oysters collected at T2, showed lower respiration rates across pH levels. OA exposure is thought to directly affect ectotherms' metabolism by inducing hypercapnia and increasing the amount of ATP needed to maintain homeostasis and ion regulation. Increased metabolic rate in July may be indicative of short-term acidosis followed by release of stress hormones which can temporarily increase oxygen intake and delivery to cells (Lefevre 2016). Seasonal respiration patterns may also reflect differences in pH response between cold and warm acclimatized oysters. DB and PW showed a strong increase in respiration rates below pH 6.9 both seasons but this trend was not observed for CI. We exposed oysters to very low pH levels (6.6 and 6.9) and pH levels of 7.5 and 7.2 are nearest to the Representative Concentration Pathway (RCP) 8.5 climate change scenario predicted for year 2100 (IPCC 2019). It must be recognized that respiration rates were tested with single stressor experiments, but stressors will not occur in isolation; meaning that to better predict responses, interactive responses will need to be explored.

3.5.5 *Reproductive Characteristics: Gamete Development and Sex Ratio*

Gametogenesis in *O. lurida* begins in the winter, where typically, a cold thermal cue triggers a reproductive quiescence (Coe 1932). Spawning is stimulated by warmer water temperatures; extending from the spring to early fall but differences in environmental cues due to abnormally warm waters may cause gametogenesis to continue through the winter (Coe 1932). In our study we examined gamete development and sex ratio of *O. lurida* transplanted to different sites in Puget Sound. All oysters were raised in the same hatchery conditions before the outplants (broodstock consisted of ~100 individuals) and therefore, any differences in reproductive maturity can be attributed to plasticity based on the differences in field conditions.

At the start of the experiment, 80% of oysters had mature gametes, but after the first six months (June to January) of acclimatization in the different environments, oysters showed different reproductive characteristics. In T1, oysters from all shallow sites had gametes in advanced or mature stages, which was not the case for CI20. CI5 and DB sites had the largest proportion of oysters with gametes, and at these sites we also found the largest shell growth rates and C:N ratios. Oysters from the deep location (CI20), the site with lowest oyster growth, only showed gametes in early stages, recently spawned, or being resorbed. Reproduction is an energy demanding processes that depends on physical, chemical, and biological characteristics. Slower gametogenesis at greater depth may be due to changes in temperature, food quantity and quality, and stressors like carbonate chemistry or lower oxygen content (Coe 1932, Neto et al. 2013, Barber and Blake 2016, Xu et al. 2016, Silliman et al. 2018). A ripe gonad found in winter may persist until the water warms, potentially leaving an abnormal amount of mature stage gonads for CI20 at T1. A similar result was found in *Ostrea edulis* from different geographic regions across Europe

where there was a asynchrony in gonad maturation and differences in thresholds for initiation of gametogenesis based on the location of collection and acclimatization (da Silva et al. 2009). Interestingly, a large proportion of oysters from all sites (except for CI5) showed resorbed eggs which may be a strategy to preserve energy in times of low food or stress in bivalves (Hassan et al. 2018b).

By the end of T2 (12 months after the outplants), the CI20 cohort appeared to be reproducing actively with a larger proportion of oysters with gametes in advanced and mature stages. PW and CI5 showed the largest proportions of oysters with gametes in advanced stages. These two sites showed similar temperature values and variability throughout the year. At T2, oysters from DB had recently undergone a spawning event and were in a phase of inactive gametogenesis (based on excessive connective tissue), suggesting that they were able to go through another full gametogenesis cycle in less than 6 months. The temperature at DB during T2 was the highest and extremely variable, possibly accelerating the rate of gonad development at this site. *O. lurida* and an oyster within the same genus, *O. edulis*, have been seen to undergo a second round of gametogenesis within a year (Joyce et al. 2013, Grossman et al. 2020, Spencer et al. 2021). Evidence of reproductive maturation during post-summer months may be beneficial for the cultivation of the species and may be a favorable trait that restoration and commercial aquaculture farms may select for.

We have shown that the reproductive phenology of *O. lurida* is plastic with gamete development and spawning timing changing depending on environmental conditions. As climate change progresses, we will likely see more extreme differences in reproductive timing across geographic

zones and between depths. This may be of concern because asynchrony in gonad maturation may lead to asynchrony in spawning, which may affect the fate of this species (Hassan et al. 2018a). A larvae who was born in one location, may travel and settle in a different habitat where locally adapted populations have evolved different reproductive phenology (da Silva et al. 2009, Barber et al. 2016, Hassan et al. 2018a). It was long thought that *O. lurida* needed to be subjected to least 12.5°C to spawn and brood, however Barber et al. (2016) found that, in Puget Sound, they may spawn in conditions as low as 10.5°C. The authors suggest that this result could signify a widening of their tolerance threshold to parallel the recent dramatic variations experienced in the environment. With predicted increase in environmental variation due to climate change, it is probable that *O. lurida* will experience shifts in reproductive phenology with important consequences for future oyster populations throughout Puget Sound.

The *Ostrea* genus is unique compared to most other oysters because they exhibit sequential hermaphrodism, in which there are sexual phases that oscillate between male and female; individuals are often found to be in transition, making them appear as simultaneous hermaphrodites (Coe 1932, Hassan et al. 2018a). All oysters start as male, and sequence of sex determination is genetic, however, the reproductive patterns and speed progression between sexual phases are strongly controlled by environmental conditions. Lower food availability and temperature reduces metabolic scope and favors spermatogenesis because it is less energetically demanding than oogenesis (Coe 1932, Ingle 1951, Ruiz et al. 1992, da Silva et al. 2009, Joyce et al. 2013). In our study, sex ratios of *O. lurida* were not significantly different between sites. Similarly, *O. lurida* from Puget Sound did not exhibit differences in sex ratio after being exposed to pH and temperature stress in the lab (Spencer et al. 2019). It is worth noting, there were more

males/hermaphroditic primarily males than hermaphroditic primarily females sampled in all cohorts throughout the year, and we did not observe any individuals that were fully female. Reduction in the female phenotype due to sub-lethal stress may result in reduced fertilization and may be detrimental to the species. Notably, in January (six months after acclimatization) oysters at the DB site had substantially more HPF, and fewer males, which deviated greatly from the ratio of other sites. A ratio skewed toward male dominance was also observed in *Ostrea angasi*, that were similar in size to our oysters (Hassan et al. 2018a). The authors suggest that this pattern may be due to oyster's young age. Skewed sex ratios and timing of cyclical sex turnover should be considered in aquaculture and restoration, as they may affect the reproductive success of oysters that are outplanted as part of restoration efforts and of breeding programs who use younger oysters who are male dominant (Joyce et al. 2013).

3.5.6 Evidence of Carryover Effects: Larval Growth, Survival and Physiological Performance

When organisms experience stress, energetic trade-offs occur likely resulting in a phenotypic response (e.g. smaller body size) and/or reduced energy allocation toward reproduction (Bayne 2004, Pörtner et al. 2005, Fitzgerald-Dehoog et al. 2012, Sokolova et al. 2012, Silliman et al. 2018). Energetic trade-offs can be reflected in offspring through the process of maternal provisioning and/or epigenetic inheritance (Ross et al. 2016). In our study we examined offspring's growth, survival, and physiology from parents outplanted to different sites in Puget Sound. At 14°C we did not find notable differences in larval growth between sites. However, when challenged to 20°C, larvae from DB and CI5 oysters had higher growth rates compared to the CI20 and PW sites and at this temperature larval growth patterns closely resembled the growth patterns of their parents. Consistent with our findings, previous studies have shown that larvae of *O. lurida*

have higher growth rates in warm and variable environments (Lawlor and Arellano 2020, Spencer et al. 2020), like DB in our study. A similar result was found by Parker et al. (2021) who found that larvae of oyster *S. glomerata* from parents acclimatized to the highly variable intertidal habitat had faster growth than deeper subtidal populations with more homogenous conditions, suggesting that parents exposed to shallower sites and high variation would yield more resilient larvae. Conversely, elevated temperature reduced larval size of *C. gigas,* indicating that carryover effects are variable and can be species specific (Gibbs et al. 2021).

Larvae from CI20 and PW with slow growth rates may have higher energetic costs to reach settlement size since they likely need to spend longer time as plankton, increasing opportunities for environmentally related mortality, starvation, and predation (Ross et al. 2016). Differences in larval growth rates between different sites at 20°C could have also been attributed to differences in gamete quality. Artificially stimulated spawns may result in premature gamete release, regardless of reproductive maturity. Our gonad maturation data shows that, at the time the oysters were stimulated to spawn, both CI20 and PW populations appear to have spawned recently and were in the process of resorbing tissue, while DB and CI5 had a larger percentage of developing gametes.

It has been proven that sub-lethal temperature stress can promote energetic trade-offs between bivalve larval survival and growth (Fitzgerald-Dehoog et al. 2012, Peng et al. 2016, Silliman et al. 2018, Pan et al. 2021). Our study found differences in larvae survival depending on site and temperature. Interestingly larvae from CI5 parents had lower survival when compared to all other sites at both temperatures, despite having high growth rates. PW and CI20 oyster larvae had high

survival but slower growth which may suggest an adaptive energetic trade-off based on parental environmental history, favoring phenotypes with higher maternal provisioning or epigenetic changes that may increase the likelihood of offspring survival (Parker et al. 2015). It is important to monitor the long-term survival to understand beneficial and negative carryover effects of calcifiers like *O. lurida* across multiple generations.

There is evidence that temperature and environmental variability experienced by parents shape the physiological performance and tolerance of offspring (Cavieres et al. 2019). It has also been shown that bivalve larval physiology is more sensitive to environmental stressors than in adults (Waldbusser and Salisbury 2014) and climate change stress is predicted to breech larval temperature thresholds pushing early life history stages to metabolic collapse (Byrne 2011).We found that, when tested under five temperature levels, we were able to create a classic thermal performance curve following the concept of OCLTT (Pörtner 2008, Sokolova et al. 2012, Schulte 2015), but unlike parental tolerances, larval oxygen consumption rate peaked at 20°C, and are more vulnerable to thermal stress than adults. Larvae from all sites reduced respiration drastically at 25°C whereas adults did not show any evidence of metabolic decrease at 25°C. In recent years, summer highs in Puget Sound have surpassed 20°C, and it is possible that future ocean warming and short-term extreme weather events may affect the metabolism and survival of future oyster offspring with important consequences for dispersal and settlement (Stamps 2006, O'Connor et al. 2007). Our results highlight the importance of examining carryover effects under different scenarios to better assess the potential and limitations of parental investment in providing resilience to offspring performance. This information is beneficial for harnessing the parental

effects to help aquaculturists selectively breed offspring that are more resilient to climate change (Joyce et al. 2013, Parker et al. 2015, Foo and Byrne 2016).

3.6 CONCLUSION

This study takes a multidisciplinary approach to report acute and long-term physiological differences in Olympia oyster *O. lurida* in response to *in situ* oceanographic conditions in a dynamic inland sea. By coupling geochemical and biological metrics, we were able to explore a dynamic environment and the biological consequences on the performance of *O. lurida*. With a more extreme climate, calcifiers will experience higher stress, and tolerance thresholds may be surpassed (Cai et al. 2021). We found that *O. lurida* show high phenotypic plasticity across different sites and seasons in Puget Sound giving this species high potential acclimatization capacity and phenotypic plasticity. Despite its plasticity, *O. lurida* is still outcompeted by other bivalves (namely, *C. gigas*) for space, and predated upon, especially by non-native animals (Peter-Contesse & Peabody 2005). Anthropogenic pollution and urbanization have reduced viable habitat for recruitment, and population density has remained sparse after overharvesting and pollution early last century, making it difficult to reproduce (Bible and Sanford 2016, Ridlon et al. 2021).

Oyster growth was lowest in oysters at the 20 m deep site in both the warmer and colder months. Overall, oyster growth was lower during the colder months, but shell strength increased during this time, suggesting an energetic trade-off as oysters got older. Distinct separations in $\delta^{15}N$ and $\delta^{15}C$ isotopic signatures suggests that bivalve diet sources are spatiotemporally unique, however physiological differences at different sites may also be influencing the isotopic patterns. Respiration rates under an array of temperature and pH levels differed between seasons and sites.

Environmental and seasonal differences did not affect sex ratios; however, our results show asynchronization in gametogenesis based on acclimatization conditions, which may be detrimental to local populations, reducing probability of fertilization of already sparse local populations.

We found evidence of parental carryover in *O. lurida* six months after acclimatization to different sites. When challenged at 20°C temperature, offspring from parents who sustained high and variable thermal conditions had faster growth, while there were no major differences in larval growth at 14°C. Larval survival was higher at 20°C compared to 14°C, but survival rates were not consistent with growth rates. Offspring with higher growth rates did not always show higher survival (i.e., larvae whose parents were outplanted at CI20 and PW had higher survival than CI5, but not higher growth). Although adults can tolerate temperatures that exceed climate change predictions in the Salish Sea for 2100 (~1.5°C increase) (Khangaonkar et al. 2019), our results suggest that future temperatures may exceed physiological tolerance thresholds for larvae, causing a bottleneck for the species. We found evidence that oysters cultured at deeper depths grew more slowly than at shallow depths and that trait is also found in the offspring. However, it is important to note that shell strength, lipid content, and sex ratio are conserved traits that did not change due to location or depth.

Extreme climate events like heat waves and warm water anomalies will become more common due to unstable atmospheric and ocean convection associated with climate change (Frölicher and Laufkötter 2018), and are predicted to quickly destabilize bivalve spawn synchronization (Shanks et al. 2020), intensify processes like upwelling (Feely et al. 2010, Reum et al. 2014), increase the expansion and abundance of invasive species (Ferreira-Rodríguez et al. 2018, Crespo et al. 2021),

and increase mass mortality events (e.g. 2021 Pacific Northwest heatwave). Considering that bivalves provide food security, support jobs, and are ecosystem engineers, it is vital that we continue to monitor their acclimatization capacity and potential for adaptation to ensure the continuation of these important services.

Although field-based studies can more reliably predict real-world phenotypic plasticity compared to controlled laboratory experiments, it is still very difficult to infer causation considering the interaction of countless co-occuring drivers (Forsman 2015). Thus, it is very important that more multigenerational and field-based experiments are performed in the field to better project how multiple environmental factors will affect the adaptive plasticity of economically and ecologically important bivalve species. This will improve the resilience of future generations, ecosystem services, and the productivity of commercial and restoration aquaculture in the next century.

3.7 FIGURES

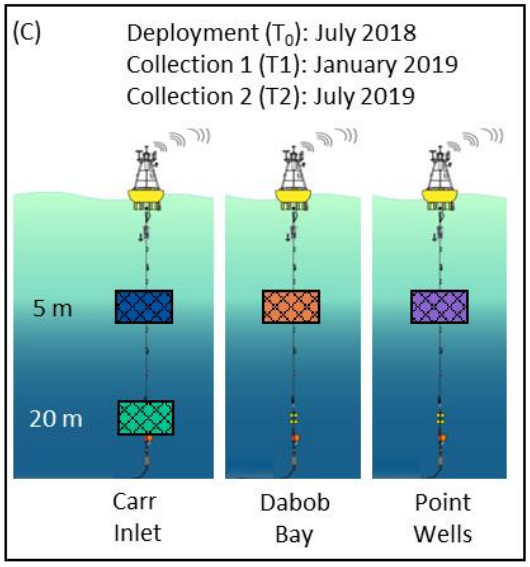

(D) Site	Deployment (T_0)	January Collection (T1)	July Collection (T2)
Carr Inlet 20 m	7/13/2018	1/8/2019	7/11/2019
Carr Inlet 5 m	7/13/2018	1/8/2019	7/11/2019
Dabob Bay	7/12/2018	1/15/2019	7/18/2019
Point Wells	7/12/2018	1/23/2019	7/23/2019

Figure 3-1 (A) Map of Puget Sound in Northwest Washington State showing the study sites where the Oceanic Remote Chemical-Optical Analyzer (ORCA) buoys are deployed. The map also shows Clam Bay where Olympia oysters Ostrea lurida were breed and grown-out before the experiment, and Seattle for reference. (B) O. lurida, marked with numbered tags (photo by Dr. Julieta Martinelli). (C) A study design schematic, outlining the deployment and collection dates, location, and depth of shellfish cages. Cages are color-coded to coordinate with other figures: Carr Inlet at 5 m is blue, Carr Inlet at 20 m is green, Dabob Bay at 5 m is orange, and Point Wells at 5 m is purple. (D) Specific dates of deployment and collections at each site.

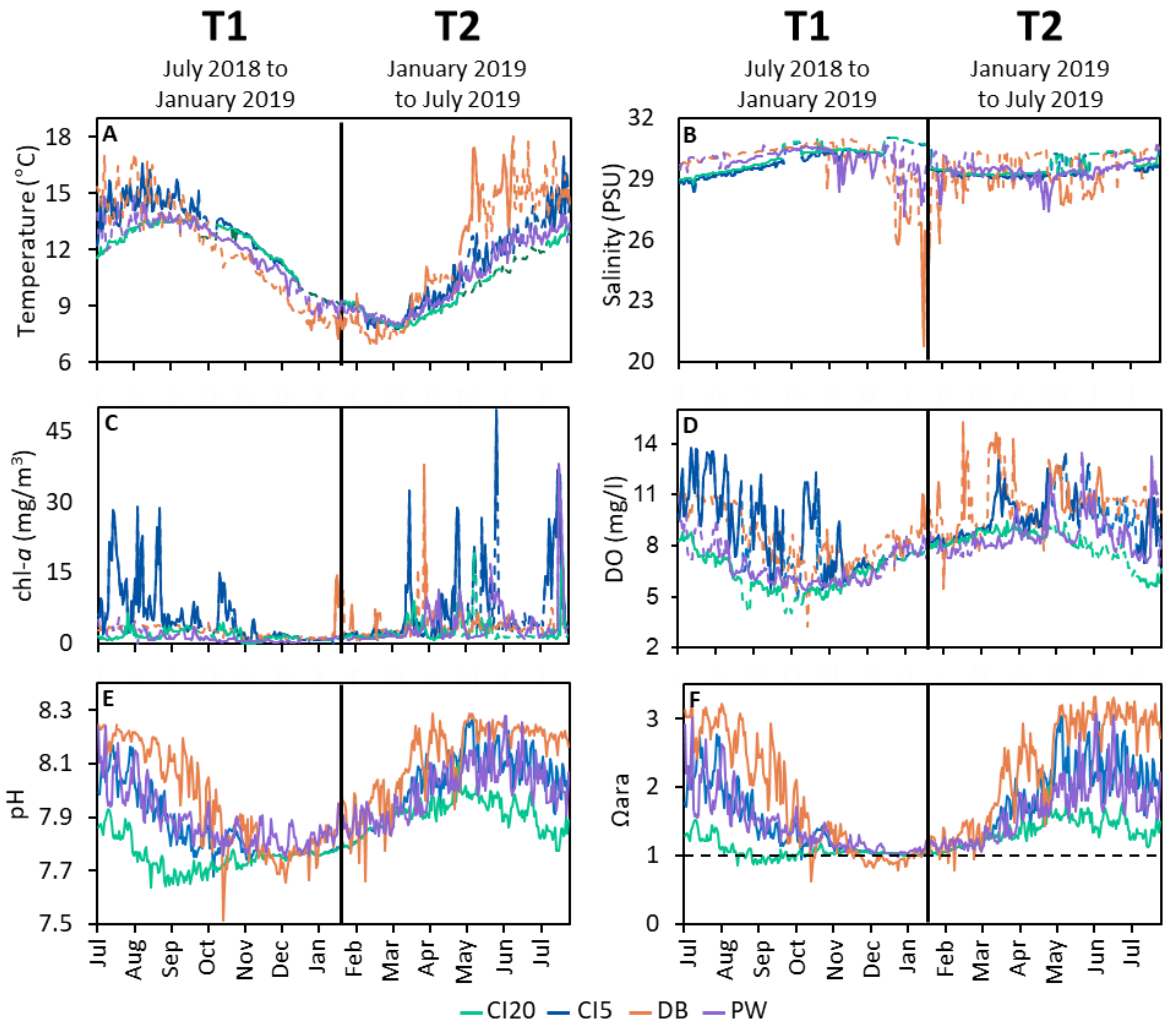

Figure 3-2: Timeseries of oceanographic conditions at four study sites in Puget Sound, Washington, USA. CI20 represents Carr Inlet at 20 m, and CI5 at 5 m. DB is Dabob bay at 5 m, and PW is Point Wells at 5 m. (A) temperature, (B) salinity, (C) chlorophyll-*a*, (D) dissolved oxygen, (E) pH, and (F) aragonite saturation state (horizontal dotted line represents aragonite saturation horizon). Colors correspond to the different sites. Data from ORCA buoys and the LiveOcean Model were combined and one reading per day at 12:00 PM was plotted. In panels A-D, solid lines indicate that the data was collected in situ from the ORCA buoy locations. Dotted lines represent data from the LiveOcean Model which were added to the graphs during times when the buoys were malfunctioning. Carbonate chemistry (panels E and F) are comprised entirely of LiveOcean data. On each panel, the vertical line down the middle represents the midpoint collection (January 2019) that separates the first (T1) and second half (T2) of the one-year outplant.

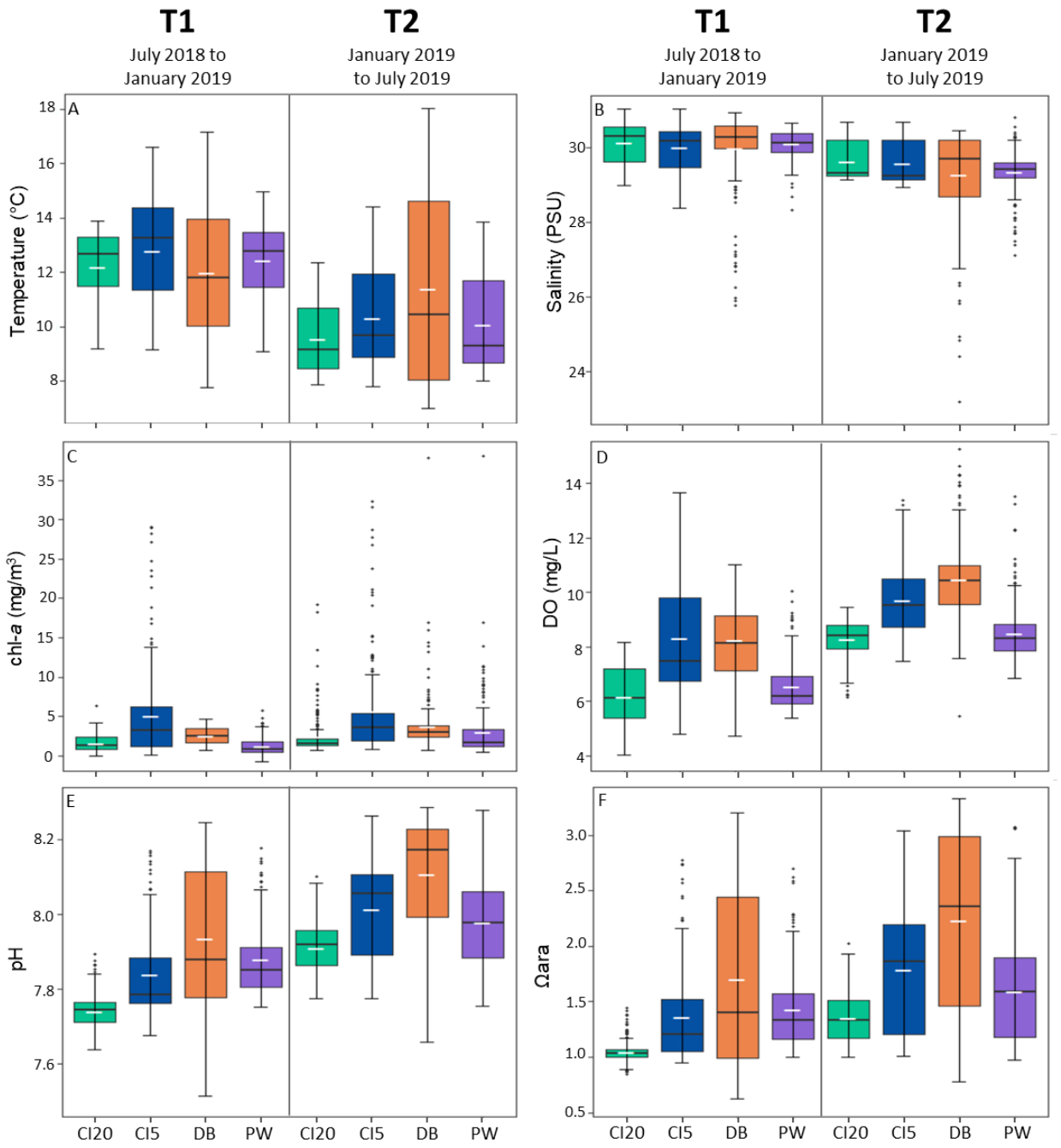

Figure 3-3: Boxplots that summarize oceanographic data at each site (CI20: Carr Inlet at 20 m, CI5: Carr Inlet at 5 m. DB: Dabob Bay at 5 m, PW: Point Wells at 5 m) during the study period. Parameters represented in each panel are as follows: (A) temperature, (B) salinity, (C) chlorophyll-a, (D) dissolved oxygen (E) pH, (F) aragonite saturation state. Each panel is separated by collection time, with data from shellfish deployment in July 2018 to the first collection in January 2019 (T1) on the left half and data from the second half of the experiment

which ran from January 2019 to July 2019 (T2) is represented in the right half of the panel. The median is represented by a crossbar within each box and mean is plotted on the box using a small white dash. Upper and lower parts of the box represent third (75th percentile, Q3) and first quartile (25th percentile, Q1). The upper limit for outliers (top and bottom of the whiskers) are calculated by multiplying the interquartile range (IRQ) by Q1-1.5 or Q3+1.5, respectively. Outliers are depicted by dots beyond the bounds of the whiskers. The wider the data spreads, the more variation there is at that location.

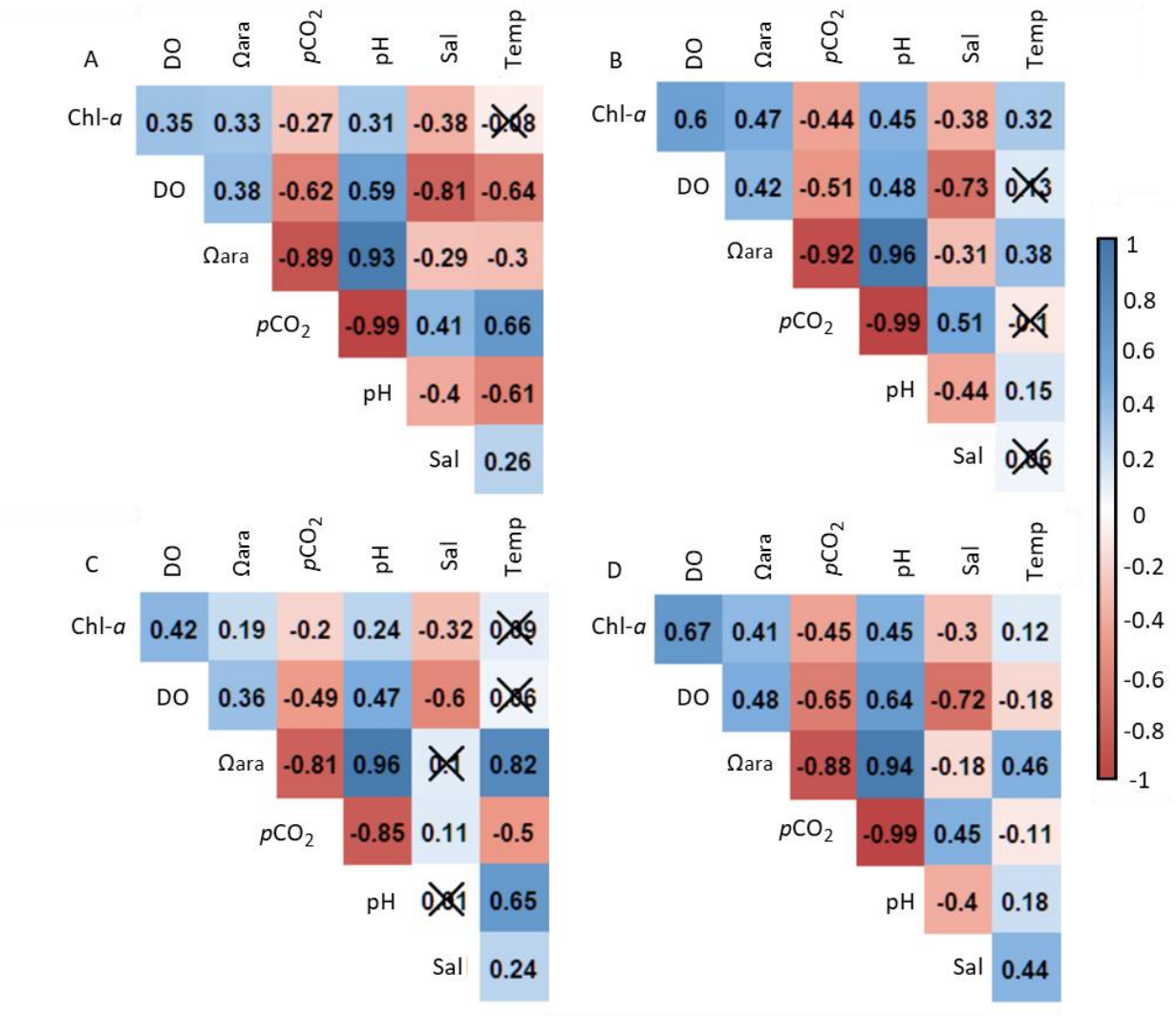

Figure 3-4: Correlation matrix using oceanographic data from each site: (A) CI20, Carr Inlet at 20 m; (B) CI5, Carr Inlet at 5 m; (C) DB, Dabob bay at 5 m; and (D) PW, Point Wells at 5 m. Parameter abbreviations and units are as follows: chl-a is chlorophyll-a (mg/m3), DO is dissolved oxygen (mg/L), Ωara is aragonite saturation state, pCO_2 (µatm), pH, Sal is salinity

(PSU), and Temp is temperature (°C). Values within boxes represent Pearson correlation coefficient. Darker shades of blue signify a higher positive correlation and darker shades of red represent a strong negative correlation. As the coefficient approaches zero, the color gets lighter, which signifies a weak correlation. Boxes signified with an “X” have no correlation with a p-value > 0.05.

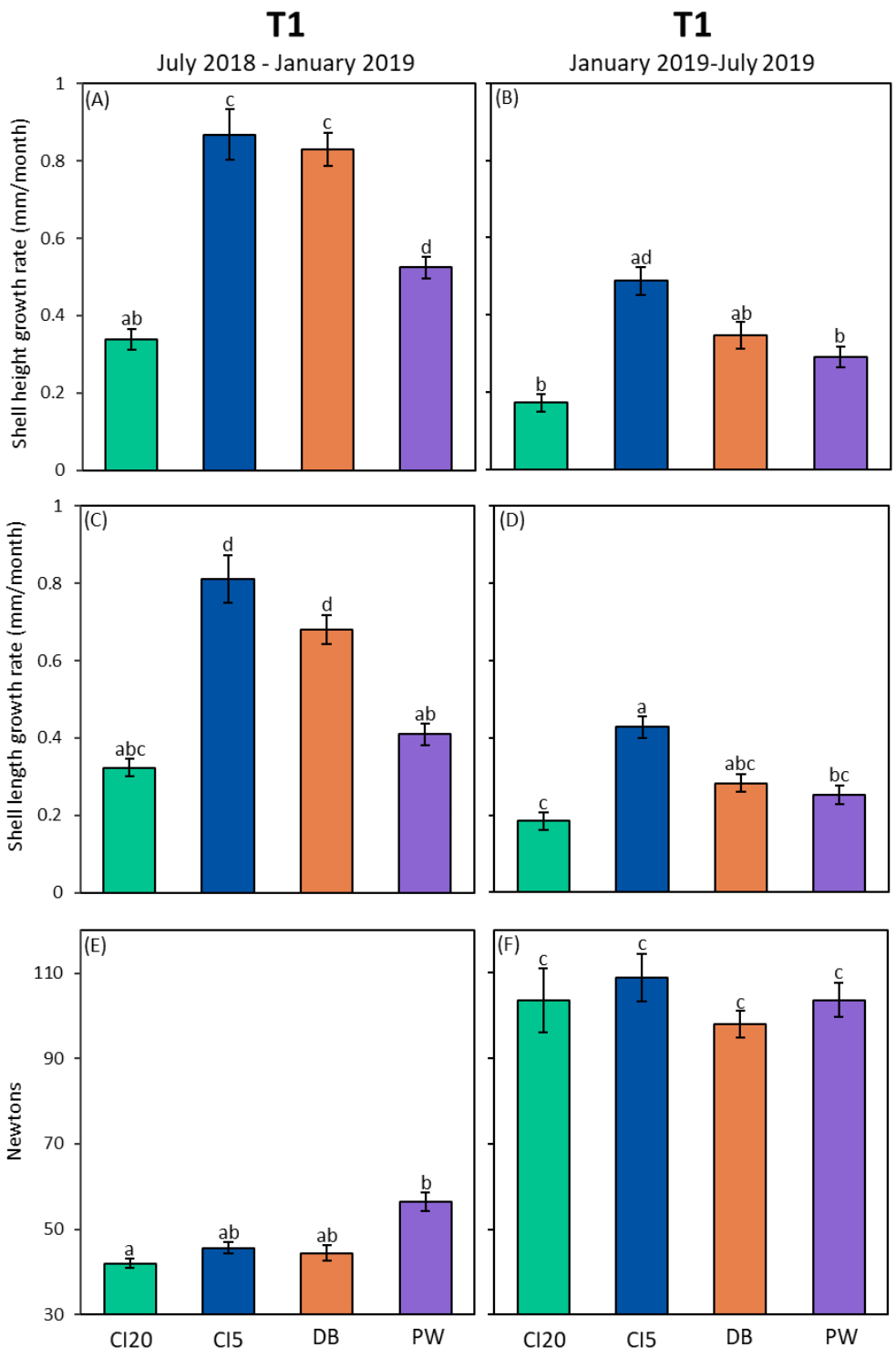

Figure 3-5: Adult Olympia oyster growth and shell strength in Puget Sound. CI20 represents Carr Inlet at 20 m, and CI5 at 5 m. DB is Dabob bay at 5 m, and PW is Point Wells at 5 m. Panels on the left (A, C, E) show results of oysters acclimatized for six months (July 2018 to January

2019), while panels on the right (B, D, F) represent oysters which were allowed to acclimatize for an additional six months (January 2019 to July 2019). A and B show shell height growth rate, and C and D depict lengthwise growth rate. E and F show shell strength. Error bars represent standard error. Post-hoc statistics were run on both collection periods together and are represented with letters. Bars with no common letters indicate significant differences ($p < 0.05$).

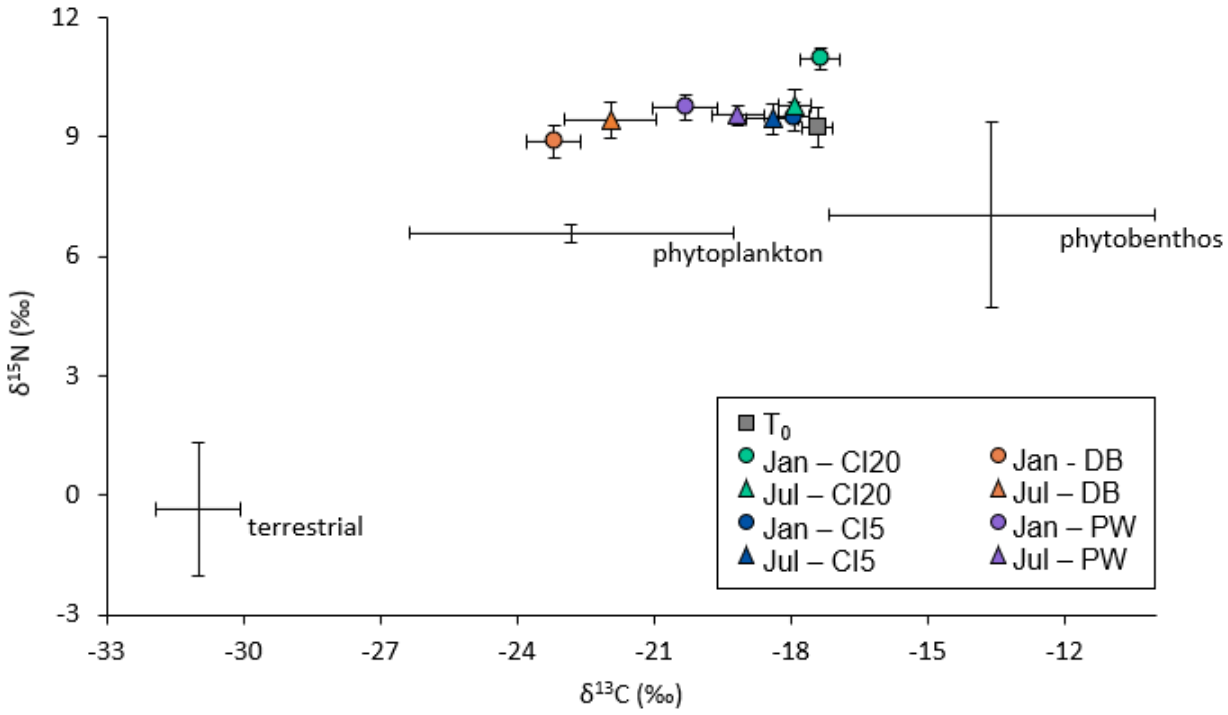

Figure 3-6: Isospace plot showing $\delta^{15}N$ and $\delta^{13}C$ stable isotopic signatures of consumer cohorts (*O. lurida* from different sites and collection times, colored dots) and end members (diet sources: phytoplankton, phytobenthos, terrestrial). Consumer signatures were not adjusted for trophic enrichment factor (ΔTEF) in this plot.

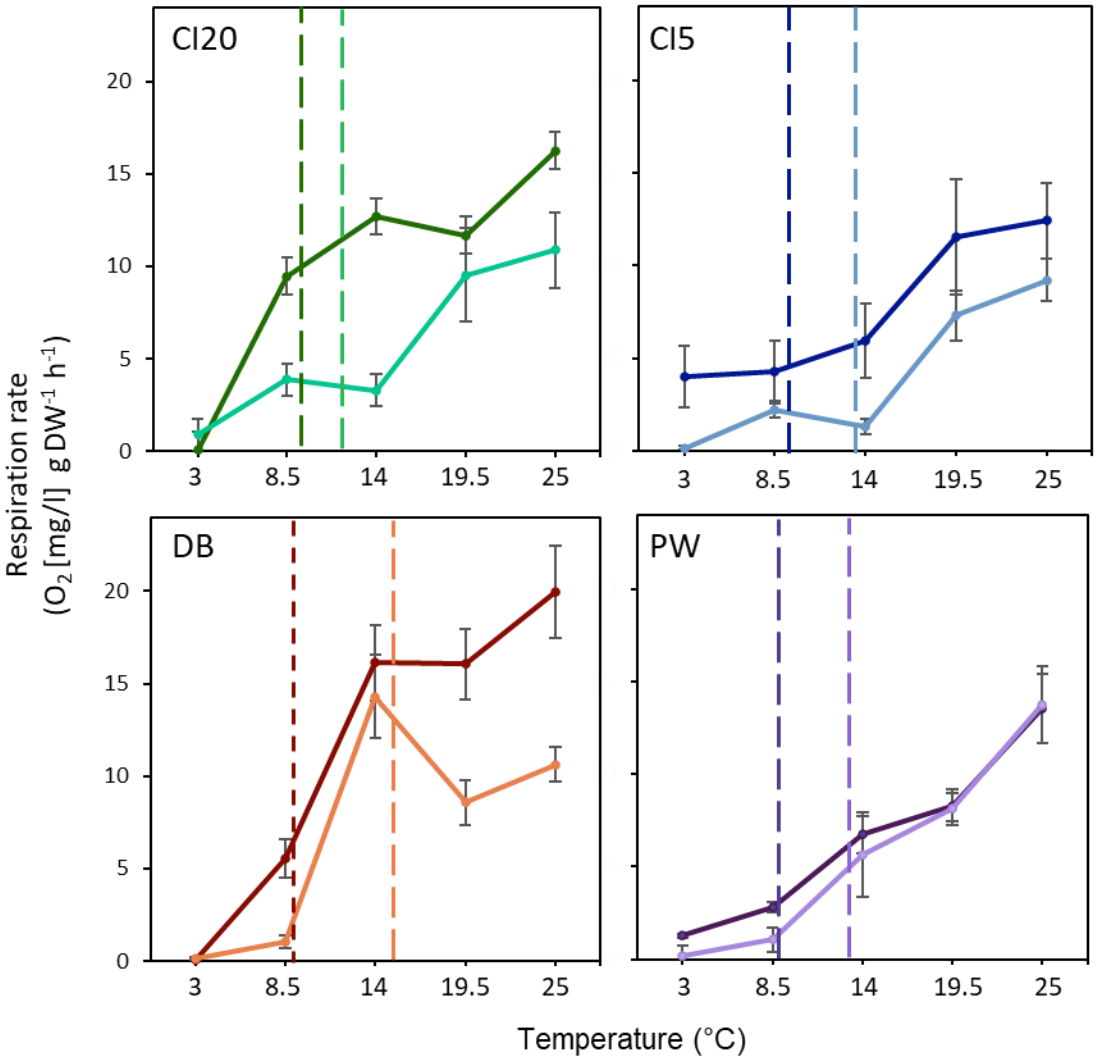

Figure 3-7: Short-term metabolic response to temperature at each collection period (T1 = January 2019 [darker colors], T2 = July 2019 [lighter colors]) and study site (CI20 = Carr Inlet at 20 m [green], CI5 = Carr Inlet at 5 m [blue], DB = Dabob Bay at 5 m [orange], and PW= Point Wells at 5 m [purple]). Vertical dotted lines represent temperatures at the collection sites one week prior to collecting the oysters (in January CI20 = 7.8°C, CI5 = 8.1°C, DB = 8.2°C, and PW = 8.0°C; in July CI20 = 11.9°C, CI5 = 13.4°C, DB = 15.2°C, and PW = 13.2°C).

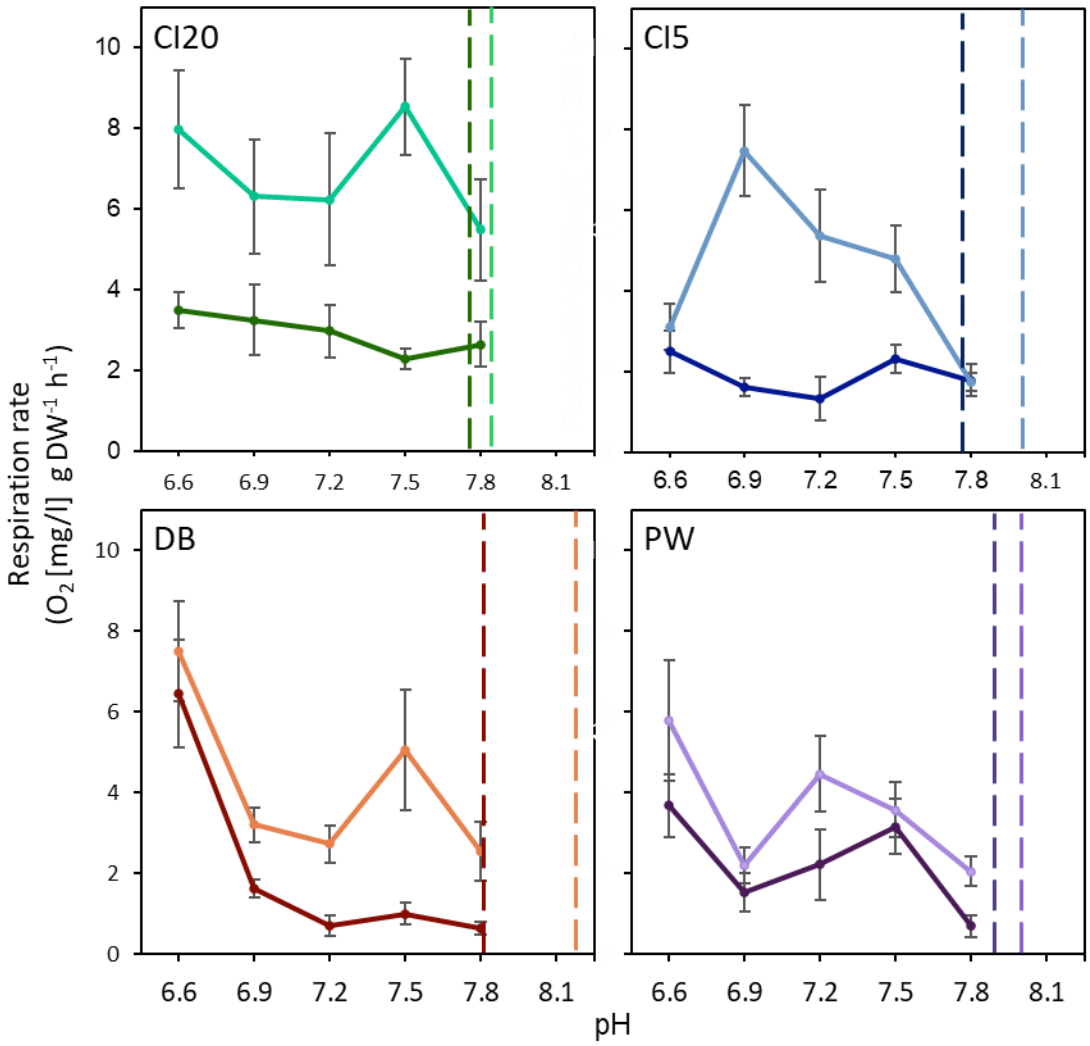

Figure 3-8: Short-term metabolic response to pH challenge at each collection period.T1 = January 2019 [darker colors], T2 = July 2019 [lighter colors]) and study site (CI20 = Carr Inlet at 20 m [green], CI5 = Carr Inlet at 5 m [blue], DB = Dabob Bay at 5 m [orange], and PW= Point Wells at 5 m [purple]). Vertical dotted lines represent temperatures at the collection sites one week prior to collecting the oysters (in January, CI20 and CI5= 7.76, DB = 7.84, and PW = 7.89; in July CI20 = 7.83, CI5 = 8.07, DB = 8.19, PW = 7.98). pH trials were run at 11°C.

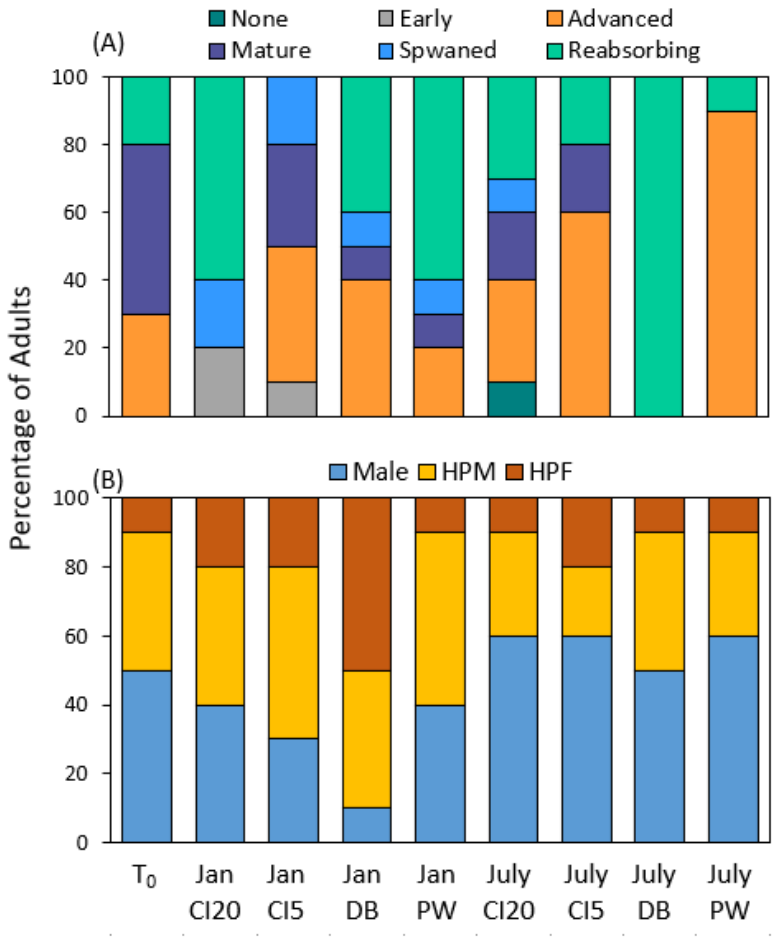

Figure 3-9: Stacked bar plot showing histological data from Olympia oyster (*Ostrea lurida,* n=10) gonads. (A) Percentage of adult at each gametogenesis maturation stage, and (B) sex ratio. T_0 indicates oysters from before the start of the experiment (July 2018). Oysters were outplanted to four sites (CI20: Carr Inlet at 20 m, CI5: Carr Inlet at 5 m, DB: Dabob Bay at 5 m, PW: Point Wells at 5 m) for either 6 months (Jan = January 2019, T1) or 1 year (Jul = July 2019, T2). HPM: hermaphrodite primary male and HPF: hermaphrodite primary female.

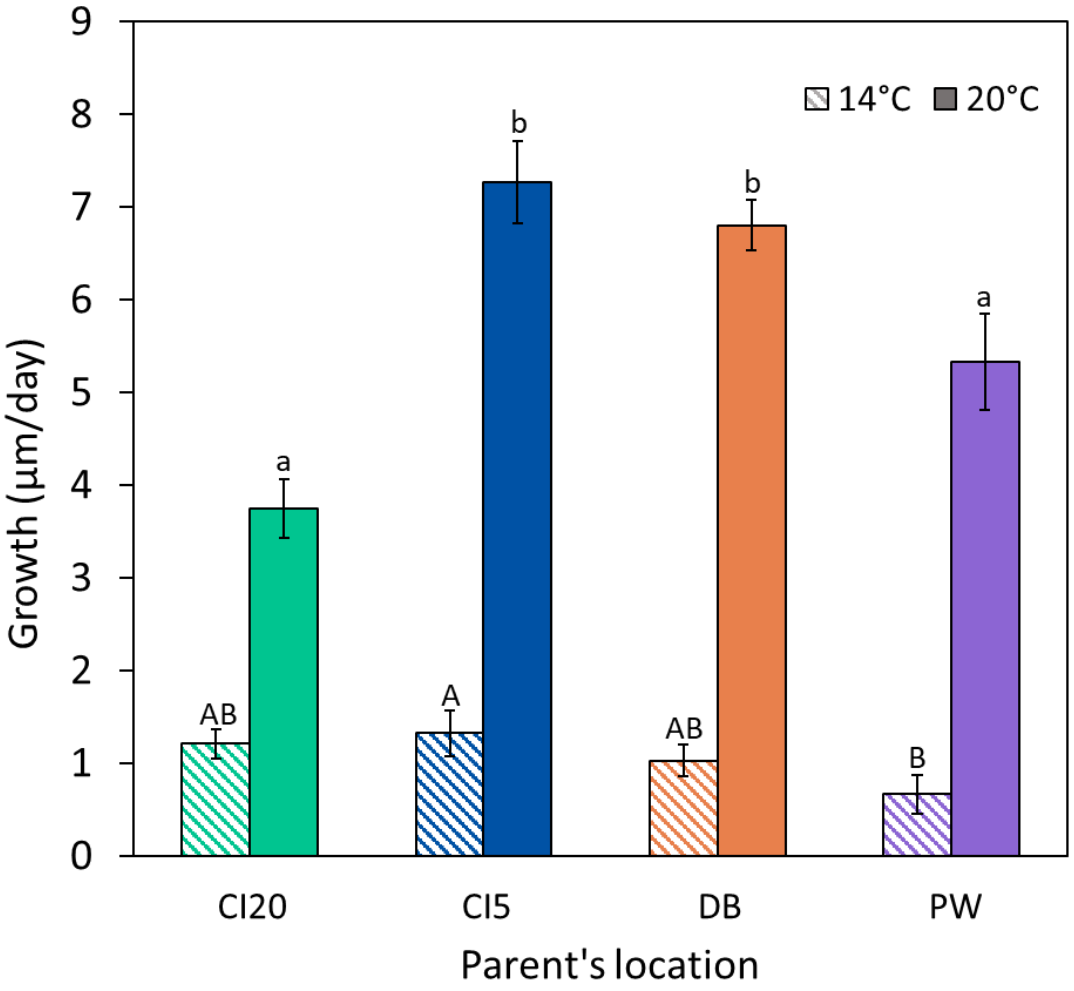

Figure 3-10: Growth rate of Olympia oyster (Ostrea lurida) larvae from parents outplanted to four locations (CI20: Carr Inlet at 20 m, CI5: Carr Inlet at 5 m. DB: Dabob Bay at 5 m, PW: Point Wells at 5 m). Oyster larvae from all locations were exposed to 14°C or 20°C for two weeks. Post-hoc statistics were performed on both thermal challenge levels separately, with capital letters representing differences at 14°C and lowercase letters for 20°C. Bars with no common letter/capitalization indicate significant differences ($p < 0.05$).

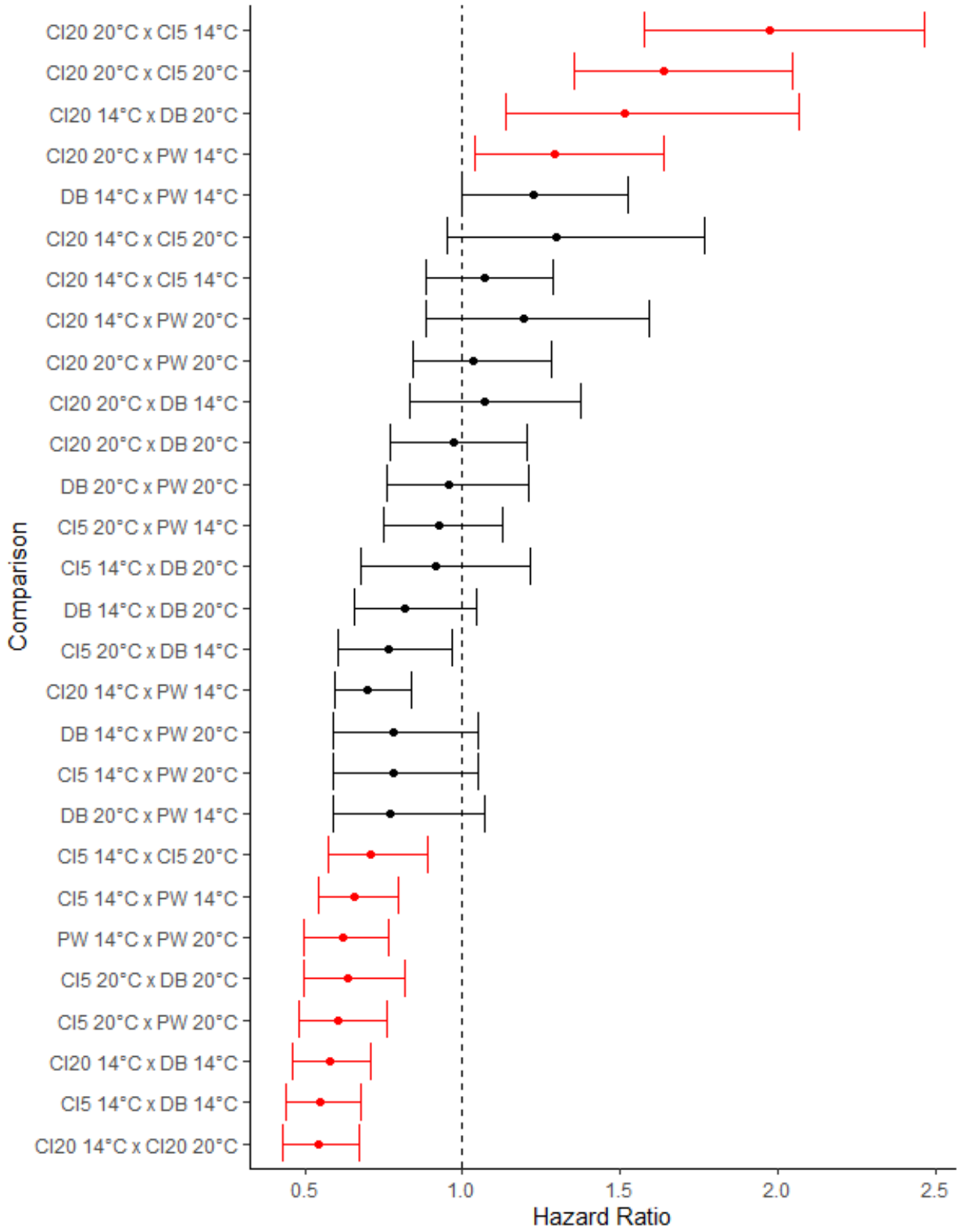

Figure 3-11: Forest plot summarizing survival results of multivariate Cox regression analysis. Points represent hazard ratio (HR, the ratio of the rates of death between the two) with error bars

signifying 95% confidence interval (CI). Larvae from different parental families were exposed to thermal challenges of either 14°C or 20°C for 14 days. Each identifier on the y-axis represents a comparison between two *O. lurida* cohorts of larvae, spawned from parents acclimatized to various environmental conditions. Points are sorted based on the lower limit confidence interval value. Comparisons can be considered significantly different from each other when the HR and CI values are greater than or less than 1. Points highlighted in red represent a treatment pairing that are statistically significant.

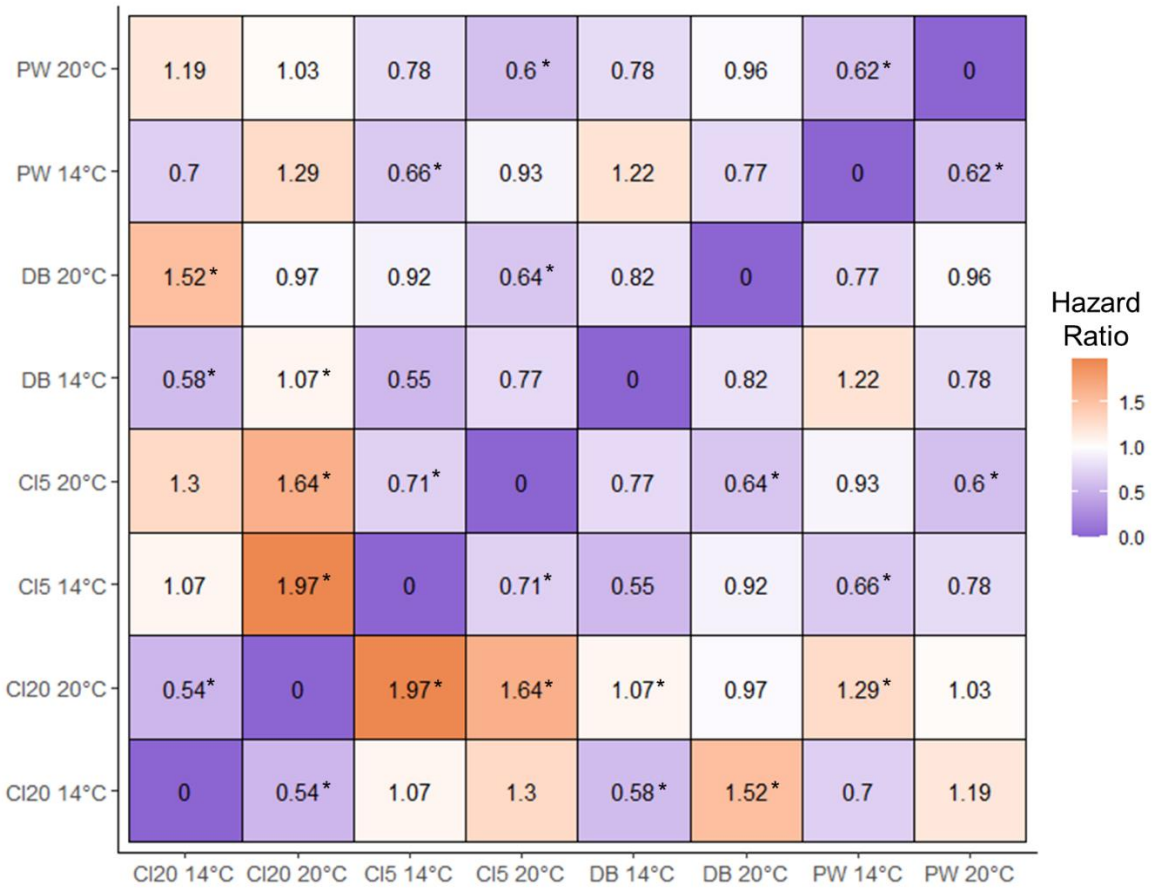

Figure 3-12: Matrix depicting hazard ratio (HR) values for each comparison between two *O. lurida* cohorts of larvae, spawned from parents acclimatized to various environmental conditions. Results summarize survival outcomes of multivariate Cox regression analysis. Larvae from different parental families were exposed to thermal challenges of either 14°C or 20°C for two weeks. Asterisks (*) next to the HR value represent a significant relationship between the two cohorts. When considering the values above the row of zeros, significant HR (± CI, *) >1 (more orange) depicts a relationship in which the cohort on the horizontal has a higher chance of

survival than the vertical axis, and a significant relationship < 1 (more purple) denotes a greater chance of survival on the vertical axis.

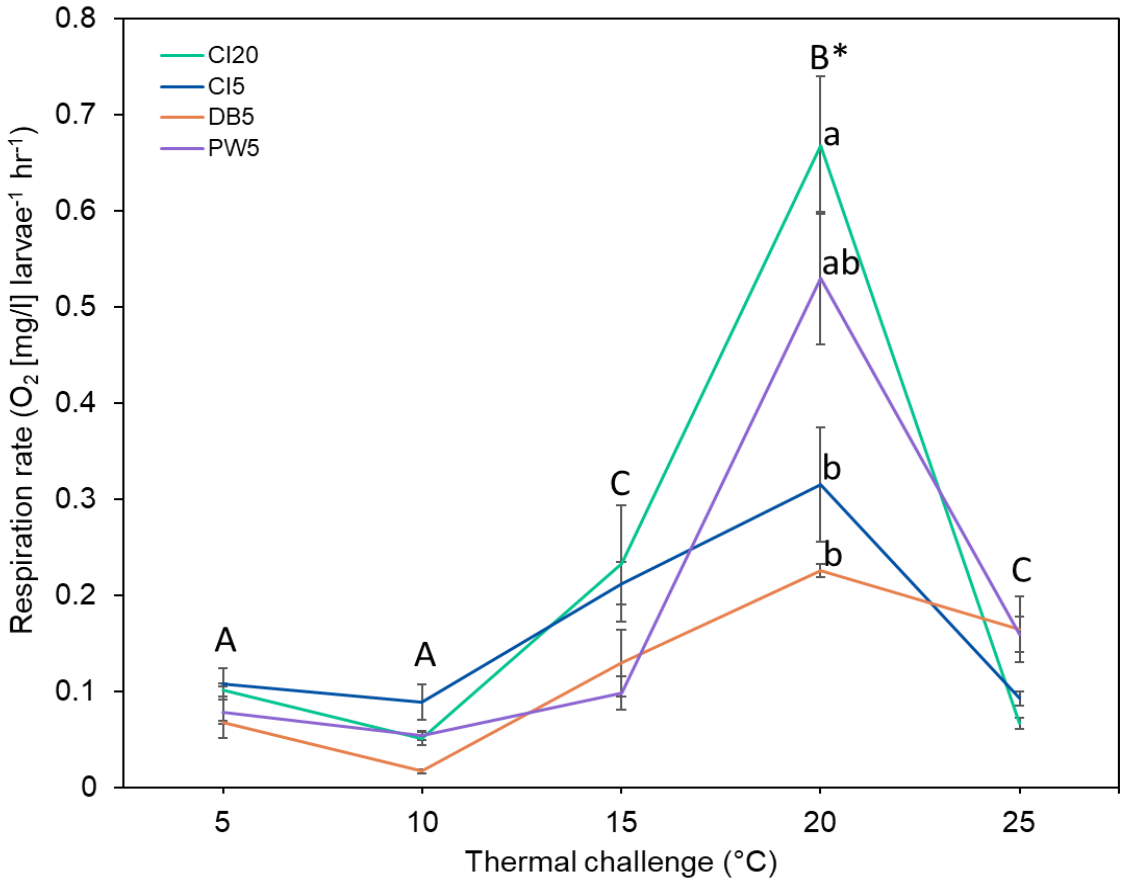

Figure 3-13: Short-term respiration rate of Olympia oyster (*Ostrea lurida*) larvae. Oxygen consumption (mg/l) of larvae per hour and larval count, were measured at five temperature levels. Parents were conditioned for six-months at various sites within Puget Sound, Washington. Different colors represent different parental acclimatization sites (CI20: Carr Inlet at 20 m, CI5: Carr Inlet at 5 m, DB: Dabob Bay at 5 m, PW: Point Wells at 5 m). Capital letters signify differences between temperatures. If a temperature does not include lowercase letters, then there were no differences between site at that temperature ($P < 0.05$). Lowercase letters indicate differences between sites at that temperature (only at 20°C).

Table 3-1: Summary of ANOVA statistics used in this study. Significant codes: *** < 0.001, ** 0.001-0.01, ** 0.01-0.05, · 0.05-0.10.

	df	Mean Sq	F	p	Significance
Growth Rate (Height)					
Site	3	5.74	39.40	< 0.001	***
Date	1	18.32	125.71	< 0.001	***
Site:Date	3	0.84	5.73	< 0.001	***
Growth Rate (Length)					
Site	3	4.54	37.17	< 0.001	***
Date	1	13.71	112.36	< 0.001	***
Site:Date	3	0.81	6.67	< 0.001	***
Residuals	694	0.12			
Shell Strength					
Site	3	6974.00	2.71	0.0436	*
Date	1	1306844.00	508.25	< 0.001	***
Site:Date	3	5774.00	2.25	0.0812	.
Residuals	1659	2571.00			
Total Lipids					
Site	2	0.01	2.55	0.0853	.
Date	1	0.00	0.69	0.4084	
Site:Date	2	0.01	2.08	0.1319	
Residuals	71	0.00			
$\delta^{13}C$					
Date	2	26.58	82.73	< 0.001	***
Site	3	102.84	320.09	< 0.001	***
Date:Site	3	5.82	18.12	< 0.001	***
Residuals	105	0.32			
$\delta^{15}N$					
Date	2	1.45	10.42	< 0.001	***
Site	3	4.99	35.88	< 0.001	***
Date:Site	3	2.95	21.24	< 0.001	***
Residuals	105	0.14			
Respiration - Temperature					
Site	3	194.00	12.05	< 0.001	***
Date	1	829.10	51.52	< 0.001	***
Treatment	4	1487.40	92.43	< 0.001	***
Site:Date	3	61.70	3.84	0.0103	*
Site:Treatment	12	88.30	5.49	< 0.001	***
Date:Treatment	4	32.00	1.99	0.0963	.
Site:Date:Treatment	12	35.30	2.19	0.0124	*
Residuals	262	16.10			
Respiration - pH					
Site	3	64.10	11.47	< 0.001	***
Date	1	487.70	87.20	< 0.001	***
Treatment	4	69.00	12.34	< 0.001	***
Site:Date	3	23.50	4.21	0.0062	**
Site:Treatment	12	22.80	4.08	< 0.001	***

Date:Treatment	4	7.90	1.41	0.2317	
Site:Date:Treatment	12	8.00	1.43	0.1522	
Residuals	269	5.60			
Larval Growth					
Site	3	77.60	19.24	< 0.001	***
Temperature	1	2204.10	546.18	< 0.001	***
Site:Temperature	3	35.00	8.67	< 0.001	***
Residuals	366	4.00			
Larval Respiration					
Temperature	4	0.28	50.27	< 0.001	***
Site	3	0.03	5.00	0.0049	**
Temperature:Site	12	0.03	5.28	< 0.001	***
Residuals	40	0.01			

3.8 REFERENCES

Alma, L., C. J. Fiamengo, S. R. Alin, M. Jackson, K. Hiromoto, and J. L. Padilla-Gamiño. 2022a. Physiological Responses of Scallops and Mussels to Environmental Variability: Implications for Future Shellfish Aquaculture. SSRN Electronic Journal.

Alma, L., K. E. Kram, G. W. Holtgrieve, A. Barbarino, C. J. Fiamengo, and J. L. Padilla-Gamiño. 2020. Ocean acidification and warming effects on the physiology, skeletal properties, and microbiome of the purple-hinge rock scallop. Comparative Biochemistry and Physiology -Part A : Molecular and Integrative Physiology 240.

Alma, L., P. McElhany, and J. L. Padilla-Gamiño. 2022b. Parental Carryover in Olympia Oysters - Survival Analysis.

Barber, B. J., and N. J. Blake. 2016. Reproductive Physiology. Page Developments in Aquaculture and Fisheries Science.

Barber, J. S., J. E. Dexter, S. K. Grossman, C. M. Greiner, and J. T. McArdle. 2016. Low Temperature Brooding of Olympia Oysters (*Ostrea lurida*) in Northern Puget Sound. Journal of Shellfish Research.

Barton, A., G. G. Waldbusser, R. A. Feely, S. B. Weisberg, J. A. Newton, B. Hales, S. Cudd, B. Eudeline, C. J. Langdon, I. Jefferds, T. King, A. Suhrbier, and K. McLaughlin. 2015. Impacts of coastal acidification on the Pacific Northwest shellfish industry and adaptation strategies implemented in response. Oceanography 28:146–159.

Bates, D., M. Mächler, B. M. Bolker, and S. C. Walker. 2015. Fitting linear mixed-effects models using lme4. Journal of Statistical Software.

Bayne, B. L. 2004. Phenotypic flexibility and physiological tradeoffs in the feeding and growth of marine bivalve molluscs. Page Integrative and Comparative Biology.

Becker, B. J., M. D. Behrens, B. Allen, M. Hintz, H. Parker, M. M. McCartha, and S. M. White. 2020. Spatial and Temporal Distribution of the Early Life History Stages of the Native Olympia Oyster *Ostrea lurida* (Carpenter, 1864) in a Restoration Site in Northern Puget Sound, Wa. Journal of Shellfish Research.

Bednaršek, N., J. A. Newton, M. W. Beck, S. R. Alin, R. A. Feely, N. R. Christman, and T. Klinger. 2021. Severe biological effects under present-day estuarine acidification in the seasonally variable Salish Sea. Science of the Total Environment.

Benson, B. B., and D. Krause. 1984. The concentration and isotopic fractionation of oxygen dissolved in freshwater and seawater in equilibrium with the atmosphere. Limnology and Oceanography.

Berthelin, C., K. Kellner, and M. Mathieu. 2000. Storage metabolism in the Pacific oyster (*Crassostrea gigas*) in relation to summer mortalities and reproductive cycle (West Coast of France). Comparative Biochemistry and Physiology - B Biochemistry and Molecular Biology.

Bible, J. M., and E. Sanford. 2016. Local adaptation in an estuarine foundation species: Implications for restoration. Biological Conservation.

Blake, B., and A. Bradbury. 2012. Washington Department of Fish and Wildlife Plan for Rebuilding Olympia Oyster (*Ostrea lurida*) Populations in Puget Sound with a Historical and Contemporary Overview:1–26.

Bligh, E. G., and W. J. Dyer. 1959. a Rapid Method of Total Lipid Extraction and Purification. Canadian Journal of Biochemistry and Physiology 37:911–917.

Brockington, S., and A. Clarke. 2001. The relative influence of temperature and food on the metabolism of a marine invertebrate. Journal of Experimental Marine Biology and Ecology.

Byrne, M. 2011. Impact of ocean warming and ocean acidification on marine invertebrate life history stages: Vulnerabilities and potential for persistence in a changing ocean. Oceanography and Marine Biology: An Annual Review 49:1–42.

Cai, W. J., R. A. Feely, J. M. Testa, M. Li, W. Evans, S. R. Alin, Y. Y. Xu, G. Pelletier, A. Ahmed, D. J. Greeley, J. A. Newton, and N. Bednarscaronek. 2021. Natural and Anthropogenic Drivers of Acidification in Large Estuaries. Annual Review of Marine Science.

Carnarius, K. M., K. M. Conrad, M. G. Mast, and J. H. Macneil. 1996. Relationship of eggshell ultrastructure and shell strength to the soundness of shell eggs. Poultry Science 75:656–663.

Cavieres, G., J. M. Alruiz, N. R. Medina, J. M. Bogdanovich, and F. Bozinovic. 2019. Transgenerational and within-generation plasticity shape thermal performance curves. Ecology and Evolution 9:2072–2082.

Coe. 1932. Development of the Gonads and the Sequence of the Sexual Phases in the California Oyster (*Ostrea Lurida*). Bulletin of the Scripps Institution of Oceanography 3:119–144.

Coleman, S. E. 2014. The effects of boring sponge on oyster soft tissue, shell integrity, and predator-related mortality.

Conway-Cranos, L., P. Kiffney, N. Banas, M. Plummer, S. Naman, P. MacCready, J. Bucci, and M. Ruckelshaus. 2015. Stable isotopes and oceanographic modeling reveal spatial and trophic connectivity among terrestrial, estuarine, and marine environments. Marine Ecology Progress Series 533:15–28.

Core R Team. 2019. A Language and Environment for Statistical Computing.

Costalago, D., I. Forster, N. Nemcek, C. Neville, R. I. Perry, K. Young, and B. P. V. Hunt. 2020. Seasonal and spatial dynamics of the planktonic trophic biomarkers in the Strait of Georgia (northeast Pacific) and implications for fish. Scientific Reports.

Cox, D. R. 1972. Regression Models and Life-Tables. Journal of the Royal Statistical Society: Series B (Methodological) 34:187–202.

Crespo, D., S. Leston, L. D. Rato, F. Martinho, S. C. Novais, M. A. Pardal, and M. F. L. Lemos. 2021. Does an Invasive Bivalve Outperform Its Native Congener in a Heat Wave Scenario? A Laboratory Study Case with *Ruditapes decussatus* and *R. philippinarum*. Biology 2021, Vol. 10, Page 1284 10:1284.

Dickson, A. G., C. L. Sabine, and J. R. Christian. 2007. Guide to Best Practices for Ocean CO_2 measurements. PICES Special Publication. Page Guide to Best Practices for Ocean CO_2 measurements. PICES Special Publication.

Doney, S. C., V. J. Fabry, R. A. Feely, and J. A. Kleypas. 2009. Ocean acidification: The other CO_2 problem. Annual Review of Marine Science 1:169–192.

Duarte, C. M., I. E. Hendriks, T. S. Moore, Y. S. Olsen, A. Steckbauer, L. Ramajo, J. Carstensen, J. A. Trotter, and M. McCulloch. 2013. Is Ocean Acidification an Open-Ocean Syndrome? Understanding Anthropogenic Impacts on Seawater pH. Estuaries and Coasts 36:221–236.

Duckworth, A. R., and B. J. Peterson. 2013. Effects of seawater temperature and pH on the boring rates of the sponge *Cliona celata* in scallop shells. Marine Biology 160:27–35.

Dumbauld, B. R., J. L. Ruesink, and S. S. Rumrill. 2009. The ecological role of bivalve shellfish aquaculture in the estuarine environment: A review with application to oyster and clam culture in West Coast (USA) estuaries.

Eccles, J., C. M. Greene, K. Sobocinski, B. Stevik, H. Carson, and ... 2018. Reconstructing historical patterns of primary production in Puget Sound using growth increment data from shells of long-lived geoducks (Panopea generosa).

Emery, K. A. 2015. Coastal bivalve aquaculture carbon cycling, spatial distribution and resource use in Virginia, USA and Baja California, Mexico:97.

Fassbender, A. J., S. R. Alin, R. A. Feely, A. J. Sutton, J. A. Newton, C. Krembs, J. Bos, M. Keyzers, A. Devol, W. Ruef, and G. Pelletier. 2018. Seasonal carbonate chemistry variability in marine surface waters of the US Pacific Northwest. Earth System Science Data.

Feddern, M. L., G. W. Holtgrieve, and E. J. Ward. 2021. Stable isotope signatures in historic harbor seal bone link food web-assimilated carbon and nitrogen resources to a century of environmental change. Global Change Biology.

Feely, R. A., S. R. Alin, J. Newton, C. L. Sabine, M. Warner, A. Devol, C. Krembs, and C. Maloy. 2010. The combined effects of ocean acidification, mixing, and respiration on pH and carbonate saturation in an urbanized estuary. Estuarine, Coastal and Shelf Science 88:442–449.

Ferreira-Rodríguez, N., I. Fernández, M. L. Cancela, and I. Pardo. 2018. Multibiomarker response shows how native and non-native freshwater bivalves differentially cope with heat-wave events. Aquatic Conservation: Marine and Freshwater Ecosystems 28:934–943.

Fertig, B., T. J. B. Carruthers, W. C. Dennison, E. J. Fertig, and M. A. Altabet. 2010. Eastern oyster (*Crassostrea virginica*) $\delta^{15}N$ as a bioindicator of nitrogen sources: Observations and modeling. Marine Pollution Bulletin 60:1288–1298.

Fitzgerald-Dehoog, L., J. Browning, and B. J. Allen. 2012. Food and heat stress in the California mussel: Evidence for an energetic trade-off between survival and growth. Biological Bulletin.

Foo, S. A., and M. Byrne. 2016. Acclimatization and Adaptive Capacity of Marine Species in a Changing Ocean. Page Advances in Marine Biology.

Forsman, A. 2015. Rethinking phenotypic plasticity and its consequences for individuals, populations and species.

Frölicher, T. L., and C. Laufkötter. 2018. Emerging risks from marine heat waves.

Fry, B., F. J. Mersch, K. Tholke, R. Garritt, and W. Brand. 1992. Automated Analysis System for Coupled $\delta^{13}C$ and $\delta^{15}N$ Measurements. Analytical Chemistry 64:288–291.

Gattuso, J.-P., J.-M. Epitalon, and H. Lavigne. 2016. seacarb: Seawater Carbonate Chemistry R package version 3.0.14.

Ghalambor, C. K., J. K. McKay, S. P. Carroll, and D. N. Reznick. 2007. Adaptive versus non-adaptive phenotypic plasticity and the potential for contemporary adaptation in new environments. Functional Ecology.

Gibbs, M. C., L. M. Parker, E. Scanes, M. Byrne, W. A. O'Connor, and P. M. Ross. 2021. Adult exposure to ocean acidification and warming leads to limited beneficial responses for oyster larvae. ICES Journal of Marine Science.

Gibert, P., V. Debat, and C. K. Ghalambor. 2019. Phenotypic plasticity, global change, and the speed of adaptive evolution.

Gobler, C. J. 2020. Climate Change and Harmful Algal Blooms: Insights and perspective. Harmful Algae.

Grossman, S. K., E. E. Grossman, J. S. Barber, S. K. Gamblewood, and S. C. Crosby. 2020. Distribution and Transport of Olympia Oyster Ostrea lurida Larvae in Northern Puget Sound, Washington. Journal of Shellfish Research.

Gurr, S. J., J. Goleski, F. P. Lima, R. Seabra, C. J. Gobler, and N. Volkenborn. 2018. Cardiac responses of the bay scallop *Argopecten irradians* to diel-cycling hypoxia. Journal of Experimental Marine Biology and Ecology 500:18–29.

Gurr, S. J., S. A. Trigg, B. Vadopalas, S. B. Roberts, and H. M. Putnam. 2021. Repeat exposure to hypercapnic seawater modifies growth and oxidative status in a tolerant burrowing clam. Journal of Experimental Biology.

Hassan, M. M., J. G. Qin, and X. Li. 2018a. Gametogenesis, sex ratio and energy metabolism in *Ostrea angasi:* Implications for the reproductive strategy of spermcasting marine bivalves. Journal of Molluscan Studies 84:38–45.

Heare, J. E., B. Blake, J. P. Davis, B. Vadopalas, and S. B. Roberts. 2017. Evidence of *Ostrea lurida* Carpenter, 1864, population structure in Puget Sound, WA, USA. Marine Ecology.

Hettinger, A., E. Sanford, T. M. Hill, J. D. Hosfelt, A. D. Russell, and B. Gaylord. 2013. The

influence of food supply on the response of Olympia oyster larvae to ocean acidification. Biogeosciences.

Hettinger, A., E. Sanford, T. M. Hill, A. D. Russell, K. N. S. Sato, J. Hoey, M. Forsch, H. N. Page, and B. Gaylord. 2012. Persistent carry-over effects of planktonic exposure to ocean acidification in the Olympia oyster. Ecology.

Hiebenthal, C., E. E. R. Philipp, A. Eisenhauer, and M. Wahl. 2013. Effects of seawater pCO_2 and temperature on shell growth, shell stability, condition and cellular stress of Western Baltic Sea *Mytilus edulis* (L.) and *Arctica islandic*a (L.). Marine Biology.

Hill, J. M., and C. D. McQuaid. 2008. δ13C and δ15N biogeographic trends in rocky intertidal communities along the coast of South Africa: Evidence of strong environmental signatures. Estuarine, Coastal and Shelf Science.

Howe, E., and C. A. Simenstad. 2015. Using Isotopic Measures of Connectivity and Ecosystem Capacity to Compare Restoring and Natural Marshes in the Skokomish River Estuary, WA, USA. Estuaries and Coasts 38:639–658.

Ikejima, I., R. Nomoto, and J. F. McCabe. 2003. Shear punch strength and flexural strength of model composites with varying filler volume fraction, particle size and silanation. Dental Materials 19:206–211.

Ingle, R. 1951. Spawning and Setting of Oysters in Relation to Seasonal Environmental Changes. Bulletin of Marine Science.

IPCC. 2019. The Ocean and Cryosphere in a Changing Climate. Intergovernmental Panel on Climate Change.

Joyce, A., T. D. Holthuis, G. Charrier, and S. Lindegarth. 2013. Experimental effects of temperature and photoperiod on synchrony of gametogenesis and sex ratio in the european oyster *Ostrea edulis* (Linnaeus). Journal of Shellfish Research.

Jutfelt, F., T. Norin, R. Ern, J. Overgaard, T. Wang, D. J. McKenzie, S. Lefevre, G. E. Nilsson, N. B. Metcalfe, A. J. R. Hickey, J. Brijs, B. Speers-Roesch, D. G. Roche, A. K. Gamperl, G. D. Raby, R. Morgan, A. J. Esbaugh, A. Gräns, M. Axelsson, A. Ekström, E. Sandblom, S. A. Binning, J. W. Hicks, F. Seebacher, C. Jorgensen, S. S. Killen, P. M. Schulte, and T. D. Clark. 2018. Oxygen- and capacity-limited thermal tolerance: Blurring ecology and physiology.

Kasai, A., and A. Nakata. 2005. Utilization of terrestrial organic matter by the bivalve *Corbicula japonica* estimated from stable isotope analysis. Fisheries Science.

Khangaonkar, T., A. Nugraha, W. Xu, and K. Balaguru. 2019. Salish Sea Response to Global Climate Change, Sea Level Rise, and Future Nutrient Loads. Journal of Geophysical Research: Oceans.

Khangaonkar, T., A. Nugraha, S. K. Yun, L. Premathilake, J. E. Keister, and J. Bos. 2021. Propagation of the 2014–2016 Northeast Pacific Marine Heatwave Through the Salish Sea. Frontiers in Marine Science 8.

King, T. L., N. Nguyen, G. J. Doucette, Z. Wang, B. D. Bill, M. B. Peacock, S. L. Madera, R. A. Elston, and V. L. Trainer. 2021. Hiding in plain sight: Shellfish-killing phytoplankton in Washington State. Harmful Algae.

Kornbluth, A., B. D. Perog, S. Crippen, D. Zacherl, B. Quintana, E. D. Grosholz, and K. W. Id. 2022. Mapping oysters on the Pacific coast of North America : A coast-wide collaboration to inform enhanced conservation.

Kosinski, A. K. M., P. Biecek, and S. Fabian. 2020. Package 'survminer.' The Comprehensive R Archive Network.

Lancaster, L. T., R. Y. Dudaniec, B. Hansson, and E. I. Svensson. 2015. Latitudinal shift in thermal niche breadth results from thermal release during a climate-mediated range expansion. Journal of Biogeography.

Lawlor, J. A., and S. M. Arellano. 2020. Temperature and salinity, not acidification, predict near-future larval growth and larval habitat suitability of Olympia oysters in the Salish Sea. Scientific Reports.

Lefevre, S. 2016. Are global warming and ocean acidification conspiring against marine ectotherms? A meta-analysis of the respiratory effects of elevated temperature, high CO_2 and their interaction. Conservation Physiology.

Li, L., A. Li, K. Song, J. Meng, X. Guo, S. Li, C. Li, P. De Wit, H. Que, F. Wu, W. Wang, H. Qi, F. Xu, R. Cong, B. Huang, Y. Li, T. Wang, X. Tang, S. Liu, B. Li, R. Shi, Y. Liu, C. Bu, C. Zhang, W. He, S. Zhao, H. Li, S. Zhang, L. Zhang, and G. Zhang. 2018. Divergence and plasticity shape adaptive potential of the Pacific oyster. Nature Ecology and Evolution.

Liedtke, T., C. Smith, and D. Rondorf. 2011. Stable isotopes of nitrogen and carbon as tools to monitor eutrophication and trophic dynamics. Hydrography of and biochemical Inputs to Liberty Bay, a small urban embayment in Puget Sound, Washington:69–84.

Maboloc, E. A., and K. Y. K. Chan. 2021. Parental whole life cycle exposure modulates progeny responses to ocean acidification in slipper limpets. Global Change Biology.

MacCready, P., R. M. McCabe, S. A. Siedlecki, M. Lorenz, S. N. Giddings, J. Bos, S. Albertson, N. S. Banas, and S. Garnier. 2021. Estuarine Circulation, Mixing, and Residence Times in the Salish Sea. Journal of Geophysical Research: Oceans 126.

Malet, N., P. G. Sauriau, N. Faury, P. Soletchnik, and G. Guillou. 2007. Effect of seasonal variation in trophic conditions and the gametogenic cycle on δ13C and δ15N levels of diploid and triploid Pacific oysters Crassostrea gigas. Marine Ecology Progress Series.

Matson, P. G., P. C. Yu, M. A. Sewell, and G. E. Hofmann. 2012. Development under elevated pCO_2 conditions does not affect lipid utilization and protein content in early life-history stages of the purple sea urchin, S*trongylocentrotus purpuratus*. Biological Bulletin.

McIntyre, B. A., E. E. McPhee-Shaw, M. B. A. Hatch, and S. M. Arellano. 2021. Location Matters: Passive and Active Factors Affect the Vertical Distribution of Olympia Oyster (*Ostrea lurida*) Larvae. Estuaries and Coasts.

McMahon, K. W., W. G. Ambrose, M. J. Reynolds, B. J. Johnson, A. Whiting, and L. M. Clough. 2021. Arctic lagoon and nearshore food webs: Relative contributions of terrestrial organic matter, phytoplankton, and phytobenthos vary with consumer foraging dynamics. Estuarine, Coastal and Shelf Science.

Mostofa, K. M. G., C. Q. Liu, W. D. Zhai, M. Minella, D. Vione, K. Gao, D. Minakata, T. Arakaki, T. Yoshioka, K. Hayakawa, E. Konohira, E. Tanoue, A. Akhand, A. Chanda, B.

Wang, and H. Sakugawa. 2015. Reviews and Syntheses: Ocean acidification and its potential impacts on marine ecosystems. Biogeosciences Discussions 12:10939–10983.

Mueller, S. 2017. Morphological and trophic differences between kelp crabs (*Pugettia producta*) inhabiting kelp and pilings

Nagarajan, R., S. E. G. Lea, and J. D. Goss-Custard. 2006. Seasonal variations in mussel, *Mytilus edulis* L. shell thickness and strength and their ecological implications. Journal of Experimental Marine Biology and Ecology 339:241–250.

Neto, R. M., T. O. Zeni, S. Ludwig, A. Horodesky, M. V. F. Girotto, G. G. Castilho-Westphal, and A. Ostrensky. 2013. Influence of environmental variables on the growth and reproductive cycle of *Crassostrea* (Mollusca, Bivalvia) in Guaratuba Bay, Brazil. Invertebrate Reproduction and Development.

Newton, J., C. Bassin, A. Devol, M. Kawase, W. Ruef, M. Warner, D. Hannafious, and R. Rose. 2007. Hypoxia in Hood Canal: an overview of status and contributing factors. Page Proceedings of the 2007 Georgia Basin Puget Sound Research Conference.

O'Connor, M. I., J. F. Bruno, S. D. Gaines, B. S. Halpern, S. E. Lester, B. P. Kinlan, and J. M. Weiss. 2007. Temperature control of larval dispersal and the implications for marine ecology, evolution, and conservation. Proceedings of the National Academy of Sciences of the United States of America 104:1266–1271.

O'Neill, B. C., M. Oppenheimer, R. Warren, S. Hallegatte, R. E. Kopp, H. O. Pörtner, R. Scholes, J. Birkmann, W. Foden, R. Licker, K. J. MacH, P. Marbaix, M. D. Mastrandrea, J. Price, K. Takahashi, J. P. Van Ypersele, and G. Yohe. 2017. IPCC reasons for concern regarding climate change risks. Nature Climate Change.

Oates, M. S. 2013. Obervations of Gonad Structure and Gametogenic Timing in a recovering population of *Ostrea lurida* (Carpenter, 1864). Thesis Univ. Oregon:56 p.

Pan, F. T. C., S. L. Applebaum, and D. T. Manahan. 2021. Differing thermal sensitivities of physiological processes alter ATP allocation. Journal of Experimental Biology.

Parker, L. M., W. A. O'Connor, D. A. Raftos, H. O. Pörtner, and P. M. Ross. 2015. Persistence of positive carryover effects in the oyster, *Saccostrea glomerata*, following transgenerational exposure to ocean acidification. PLoS ONE 10:1–19.

Parker, L. M., P. M. Ross, W. A. O'Connor, L. Borysko, D. A. Raftos, and H. O. Pörtner. 2011. Adult exposure influences offspring response to ocean acidification in oysters. Global Change Biology.

Parker, L. M., E. Scanes, W. A. O'Connor, R. A. Coleman, M. Byrne, H. O. Pörtner, and P. M. Ross. 2017. Ocean acidification narrows the acute thermal and salinity tolerance of the Sydney rock oyster *Saccostrea glomerata*. Marine Pollution Bulletin 122:263–271.

Parker, L. M., E. Scanes, W. A. O'Connor, and P. M. Ross. 2021. Transgenerational plasticity responses of oysters to ocean acidification differ with habitat. Journal of Experimental Biology.

Pelletier, G., M. Roberts, M. Keyzers, and S. R. Alin. 2018. Seasonal variation in aragonite saturation in surface waters of Puget Sound - A pilot study. Elementa.

Peng, T. C., T. Vengatesen, and A. T. S. Hwai. 2016. Assessment of temperature effects on early larval development survival of hatchery-reared tropical oyster, *Crassostrea iredalei*. Tropical Life Sciences Research.

Pernet, F., D. Tamayo, and B. Petton. 2015. Influence of low temperatures on the survival of the Pacific oyster (*Crassostrea gigas*) infected with ostreid herpes virus type 1. Aquaculture.

Peter-Contesse & Peabody. 2005. Reestablishing Olympia oyster populations in Puget Sound, Washington. Washington Sea Grant.

Pörtner, H. O. 2008. Ecosystem effects of ocean acidification in times of ocean warming: A physiologist's view. Marine Ecology Progress Series 373:203–217.

Pörtner, H. O., C. Bock, and F. C. Mark. 2017. Oxygen- & capacity-limited thermal tolerance: Bridging ecology & physiology.

Pörtner, H. O., P. L. M. Van Dijk, I. Hardewing, and A. Sommer. 2000. Levels of Metabolic Cold Adaptation: Tradeoffs in Eurythermal and Stenothermal Ectotherms. Page Antarctic Ecosystems: Models for Wider Ecological Understanding.

Pörtner, H. O., D. Storch, and O. Heilmayer. 2005. Constraints and trade-offs in climate-dependent adaptation: Energy budgets and growth in a latitudinal cline. Scientia Marina.

Pritchard, C. E., R. N. Rimler, S. S. Rumrill, R. B. Emlet, and A. L. Shanks. 2016. Variation in larval supply and recruitment of *Ostrea lurida* in the Coos Bay estuary, Oregon, USA. Marine Ecology Progress Series.

Pritchard, C., A. Shanks, R. Rimler, M. Oates, and S. Rumrill. 2015. The olympia oyster *Ostrea lurida*: Recent advances in natural history, ecology, and restoration.

Raymond, W. W., J. S. Barber, M. N. Dethier, H. A. Hayford, C. D. G. Harley, T. L. King, B. Paul, C. A. Speck, E. D. Tobin, A. E. T. Raymond, and P. S. McDonald. 2022. Assessment of the impacts of an unprecedented heatwave on intertidal shellfish of the Salish Sea. Ecology:1–7.

Reum, J. C. P., S. R. Alin, R. A. Feely, J. Newton, M. Warner, and P. McElhany. 2014. Seasonal carbonate chemistry covariation with temperature, oxygen, and salinity in a fjord estuary: Implications for the design of ocean acidification experiments. PLoS ONE 9.

Ridlon, A. D., A. Marks, C. J. Zabin, D. Zacherl, B. Allen, J. Crooks, G. Fleener, E. Grosholz, B. Peabody, J. Toft, and K. Wasson. 2021. Conservation of Marine Foundation Species: Learning from Native Oyster Restoration from California to British Columbia. Estuaries and Coasts.

Rish, I. 2001. An empirical study of the naive Bayes classifier. IJCAI 2001 workshop on empirical methods in artificial intelligence.

Ross, P. M., L. Parker, and M. Byrne. 2016. Transgenerational responses of molluscs and echinoderms to changing ocean conditions.

Rossi, G. S., and V. Tunnicliffe. 2017. Trade-offs in a high CO_2 habitat on a subsea volcano: Condition and reproductive features of a bathymodioline mussel. Marine Ecology Progress Series.

Ruiz, C., D. Martinez, G. Mosquera, M. Abad, and J. L. Sánchez. 1992. Seasonal variations in

condition, reproductive activity and biochemical composition of the flat oyster, *Ostrea edulis*, from San Cibran (Galicia, Spain). Marine Biology.

Sanford, E., B. Gaylord, A. Hettinger, E. A. Lenz, K. Meyer, and T. M. Hill. 2014. Ocean acidification increases the vulnerability of native oysters to predation by invasive snails. Proceedings of the Royal Society B: Biological Sciences.

Scanes, E., L. M. Parker, W. A. O'Connor, M. C. Dove, and P. M. Ross. 2020. Heatwaves alter survival of the Sydney rock oyster, *Saccostrea glomerata*. Marine Pollution Bulletin.

Schulte, P. M. 2015. The effects of temperature on aerobic metabolism: Towards a mechanistic understanding of the responses of ectotherms to a changing environment. Journal of Experimental Biology 218:1856–1866.

Shanks, A. L., L. K. Rasmuson, J. R. Valley, M. A. Jarvis, C. Salant, D. A. Sutherland, E. I. Lamont, M. A. H. Hainey, and R. B. Emlet. 2020. Marine heat waves, climate change, and failed spawning by coastal invertebrates. Limnology and Oceanography.

Silliman, K. E., T. K. Bowyer, and S. B. Roberts. 2018. Consistent differences in fitness traits across multiple generations of Olympia oysters. Scientific Reports.

da Silva, P. M., J. Fuentes, and A. Villalba. 2009. Differences in gametogenic cycle among strains of the European flat oyster *Ostrea edulis* and relationship between gametogenesis and bonamiosis. Aquaculture.

Sokolova, I. M., M. Frederich, R. Bagwe, G. Lannig, and A. A. Sukhotin. 2012. Energy homeostasis as an integrative tool for assessing limits of environmental stress tolerance in aquatic invertebrates. Marine Environmental Research 79:1–15.

Spencer, L. H., E. Horkan, R. Crim, and S. B. Roberts. 2021. Latent effects of winter warming on Olympia oyster reproduction and larval viability. Journal of Experimental Marine Biology and Ecology.

Spencer, L. H., Y. R. Venkataraman, R. Crim, S. Ryan, M. J. Horwith, and S. B. Roberts. 2020. Carryover effects of temperature and pCO_2 across multiple Olympia oyster populations. Ecological Applications.

Stamps, J. A. 2006. The silver spoon effect and habitat selection by natal dispersers. Ecology Letters 9:1179–1185.

State of California Water Resources Control Board. 2011. Status and Understanding of Groundwater Quality in the San Diego Drainages Hydrogeologic Provice, 2004: California GAMA Priority Basin Project.

Stevens, A. M., and C. J. Gobler. 2018. Interactive effects of acidification, hypoxia, and thermal stress on growth, respiration, and survival of four North Atlantic bivalves. Marine Ecology Progress Series.

Stott, P. A., N. Christidis, F. E. L. Otto, Y. Sun, J. P. Vanderlinden, G. J. van Oldenborgh, R. Vautard, H. von Storch, P. Walton, P. Yiou, and F. W. Zwiers. 2016. Attribution of extreme weather and climate-related events. Wiley Interdisciplinary Reviews: Climate Change.

Subasinghe, M. M., B. K. K. K. Jinadasa, A. N. Navarathne, and S. Jayakody. 2019. Seasonal variations in the total lipid content and fatty acid composition of cultured and wild

Crassostrea madrasensis in Sri Lanka. Heliyon.

Sultan, S. E. 2000. Phenotypic plasticity for plant development, function and life history.

Taiyun, W. 2014. Visualization of a correlation matrix. CRAN.

Therneau, T. M. 2020. survival: A Package for Survival Analysis in R. R package version 2.38.

Thom, R., J. Gaeckle, K. Buenau, A. Borde, J. Vavrinec, L. Aston, D. Woodruff, T. Khangaonkar, and J. Kaldy. 2018. Eelgrass (*Zostera marina L.*) restoration in Puget Sound: development of a site suitability assessment process. Restoration Ecology.

Thyrring, J., S. Rysgaard, M. E. Blicher, and M. K. Sejr. 2015. Metabolic cold adaptation and aerobic performance of blue mussels (*Mytilus edulis*) along a temperature gradient into the High Arctic region. Marine Biology.

Todgham, A. E., and J. H. Stillman. 2013. Physiological responses to shifts in multiple environmental stressors: Relevance in a changing world. Integrative and Comparative Biology 53:539–544.

USDA. 2018. 2018 Census of Aquaculture. 2017 Census of Agriculture 3:AC-17-SS-2.

Waldbusser, G. G., and J. E. Salisbury. 2014. Ocean acidification in the coastal zone from an organism's perspective: Multiple system parameters, frequency domains, and habitats. Annual Review of Marine Science.

Wallace, R. B., H. Baumann, J. S. Grear, R. C. Aller, and C. J. Gobler. 2014. Coastal ocean acidification: The other eutrophication problem. Estuarine, Coastal and Shelf Science.

Washington Sea Grant. 2015. Shellfish Aquaculture in Washington State:1–84.

Washington Sea Grant. 2021. Impacts from the Summer 2021 Heatwave on Washington Shellfish. WSG News Blog.

Washington State Blue Ribbon Panel on Ocean Acidification. 2012. Ocean Acidification : From Knowledge to Action. Washington State's Strategic Response.

Wasson, K., D. J. Gossard, L. Gardner, P. R. Hain, C. J. Zabin, S. Fork, A. D. Ridlon, J. M. Bible, A. K. Deck, and B. B. Hughes. 2020. A scientific framework for conservation aquaculture: A case study of oyster restoration in central California. Biological Conservation.

Wilkie, E. M., and M. J. Bishop. 2012. Differences in shell strength of native and non-native oysters do not extend to size classes that are susceptible to a generalist predator. Marine and Freshwater Research 63:1201–1205.

Xu, X., F. Yang, L. Zhao, and X. Yan. 2016. Seawater acidification affects the physiological energetics and spawning capacity of the Manila clam *Ruditapes philippinarum* during gonadal maturation. Comparative Biochemistry and Physiology -Part A : Molecular and Integrative Physiology.

zu Ermgassen, P. S. E., R. H. Thurstan, J. Corrales, H. Alleway, A. Carranza, N. Dankers, B. DeAngelis, B. Hancock, F. Kent, I. McLeod, B. Pogoda, Q. Liu, and W. G. Sanderson. 2020. The benefits of bivalve reef restoration: A global synthesis of underrepresented species. Aquatic Conservation: Marine and Freshwater Ecosystems.

4 CHAPTER 4

ENVIRONMENTAL VARIATION INFLUENCES PHENOTYPIC PLASTICITY IN THE MUSSEL *MYTILUS GALLOPROVINCIALIS*

Lindsay Alma, Paul McElhany, Jan Newton, Michael Mahar, John Mickett, Jacqueline L. Padilla-Gamiño

4.1 ABSTRACT

Cultured shellfish in coastal regions are increasingly more vulnerable to warming, ocean acidification, deoxygenation, weather extremes, and environmental variability. To understand the tolerance and capacity of organisms to respond to these environmental changes it is important to perform field experiments where multiple stressors co-occur. This study investigates how the economically important bivalve, *Mytilus galloprovincialis*, acclimatizes to different environments in Puget Sound, Washington. We deployed hatchery raised mussels with similar age and genetic makeup to South Puget Sound (Carr Inlet at 5m and 20m), Hood Canal (Dabob Bay at 5 m), and Central Puget Sound (Point Wells at 5 m). To couple biological data with environmental data we affixed cages containing mussels onto the mooring line of oceanographic monitoring buoys, which captured continuous high-resolution environmental readings. Phenotypic plasticity and physiological performance were evaluated after the mussels acclimatized for six and twelve months. Our findings indicate that *M. galloprovincialis* has a high capacity to express different phenotypes depending on abiotic factors. Mussels located in the deeper South Sound location had the lowest growth rate and shell strength in the warmer months when waters are highly stratified. $\delta^{13}C$ and $\delta^{15}N$ signatures differed depending on site and collection time, but no differences were observed in lipid content. Higher respiration rates were found during January than July for all sites

across temperatures. There were no differences in sex ratio between sites, but gametogenesis differed depending on location. In January, mussels at 20 m had spawned out, whereas gametes from other sites were still developing. In July, no differences in gamete development were observed between sites. Our study can be used by scientists and managers to integrate phenotypic plasticity in projections and to assist the aquaculture industry in creating breeding programs to select for favorable traits and maximize production, profit, and withstand conditions related to climate change.

4.2 INTRODUCTION

Shifts in environmental conditions due to climate change can impact sensitive trophic dynamics, ecosystem services, and economically important maritime products like bivalves (Carrington et al., 2015; Osland et al., 2016). The Intergovernmental Panel on Climate Change (IPCC) Sixth Assessment Report (*AR6*) under RCP 8.5 projects that by 2100 global average sea surface temperature will increase by over 4°C, pH will decrease by 0.315, and dissolved oxygen (DO) will decrease by 3.9% (IPCC, 2019; Kwiatkowski et al., 2020). To evaluate realistic physiological responses and the ability of an organism to express different phenotypes depending on the environment, it is important to conduct research in a field setting where multiple stressors co-occur (Gunderson et al., 2016). Of 854 climate change related studies conducted between 2010 - 2019, over 90% were lab-based studies and < 10% were conducted in the field. Recent trends seem to be progressing toward field-based research which indicates that scientists are becoming more aware that experiments in the lab are not as realistic and cannot fully capture the dynamics of natural conditions (Bass et al., 2021; Grear et al., 2020; Wernberg et al., 2012). Long-term field-based studies are not as common because of their logistical challenges and because outcomes are inherently challenging to interpret as multiple drivers can impact organisms simultaneously and/or

at different spatial and temporal scales (Bass et al., 2021). Long-term field based acclimatization studies that record spatiotemporal ocean chemistry can contribute to the growing understanding of long-term plasticity in marine organisms as climate change progresses (Cai et al., 2021; Hofmann et al., 2010).

In this study we performed a long-term field experiment to examine how changing environments affect the physiological performance of an economically and ecologically important bivalve, the Mediterranean mussel *Mytilus galloprovincialis*. Our study was performed in several locations in Puget Sound, Washington, USA. Puget Sound is a large and productive coastal estuary in Northwestern Washington state that has unique geology and complex habitats that foster very different environmental conditions. Puget Sound is nestled between the Olympic and Cascade Mountain ranges, sharing part of its eastern coastline with the urban city of Seattle. It is a unique fjord-like system, scoured by glacial retreat at the end of the last ice age which has left narrow channels with unique ocean chemistry. In Puget Sound upwelling occurs during the warmer months, during this period nutrient rich, cold, acidified bottom waters, leading to very different water chemistry with depth (Bianucci et al., 2018; Feely et al., 2008, 2010; Reum et al., 2014). In addition, Puget Sound has exceptionally high freshwater inflow, often containing anthropogenic nutrient sources of pollution, spurring eutrophication and making waters more vulnerable to ocean acidification (OA) and hypoxia (Bianucci et al., 2018). This makes Puget Sound an ideal coastal system to conduct a “natural laboratory” field experiment.

Puget Sound has recently experienced several concerning extreme weather events associated with unusual atmospheric and ocean convection that have affected the wild ecosystem as well as aquaculture operations. In late June 2021 the intertidal organisms in this region were severely impacted by unprecedented temperatures up to 49°C, that cooked bivalves (like mussels) alive

along the coast within hours (Raymond et al., 2022). The NE Pacific warm water anomaly in 2015 created seawater temperatures of up to 21.5°C in Washington (Bond et al., 2015; Khangaonkar et al., 2021). These extreme events are predicted to increase in frequency and intensity, causing financial loss and wreaking environmental havoc. Due to the ever intensifying seasonal variation, aragonite undersaturation, HABs, etc., the fate of calcifying organisms in Puget Sound is of exceptional concern to scientists and shellfish industry leaders in recent decades (Barton et al., 2015; Feely et al., 2010; Gazeau et al., 2013; Grear et al., 2020; Washington Sea Grant, 2015; Washington State Blue Ribbon Panel on Ocean Acidification, 2012).

Washington state is the leading producer of farmed bivalves in the USA, much of it coming from the Puget Sound area. The shellfish aquaculture industry is extremely important, brining $270 million per year into the local economy and supporting over 3200 jobs (Washington Sea Grant, 2015; Washington State Blue Ribbon Panel, 2012). Extreme environmental events and/or coastal anthropogenic stressors may force farms to shift operations or permanently modify practices to keep shellfish alive and healthy. Many hatcheries, like Taylor Shellfish Farms, in Dabob Bay, are already feeling the effects of climate change on their bottom line, and they have begun to buffer their water with sodium carbonate to combat ocean acidification and increase the carbonate availability for shellfish to grow their shell (Barton et al., 2015; Gurr et al., 2018; Wallace et al., 2014; Washington State Blue Ribbon Panel, 2012).

Our field experiment was inspired by longlines, a common aquaculture practice used to grow-out *M. galloprovincialis* in Puget Sound, and around the world. The lines are typically stocked using a long mesh sock which dissolves with time, or juveniles are encouraged to adhere to filamentous rope (Mizuta & Wikfors, 2019; Tamburini et al., 2020). Lines are then attached offshore to a series of cables, suspended using buoy floats and anchors (Goseberg et al., 2017). Lines are usually

around 20 m depth but can be over 100 m, and environmental gradients with depth may lead to uneven cultured product (Mascorda Cabre et al., 2021; Mizuta & Wikfors, 2019). Cultured mussels on longlines are left to mature in the natural environment which is financially favorable in terms of savings on food, hatchery space, and labor. However, in Puget Sound, site specific conditions are important when placing the bivalve longline because food and ocean chemical and physical properties change dramatically depending on season, location, and depth profile (IdHalla et al., 2017). Our research integrates high resolution oceanographic data with a range of physiological metrics of mussels located in different environments across Puget Sound. Results from this study can be used by shellfish growers to select for favorable grow-out locations and choose phenotypes to assist in selective breeding programs, maximize productivity, profit, and quality.

Mytilidae mussels are the fourth most cultured mollusc in the world (FAO, 2020). The most common aquaculturally grown species in Mytilidae is the Mediterranean mussel *Mytilus galloprovincialis* (Lamarck 1819), *however, because they are so commonly cultured worldwide,* they are also listed as one of the top 100 of the world's most invasive species by the International Union for Conservation of Nature (Lowe et al., 2000), and are also a common fouling nuisance for maritime operations (Lins et al., 2021). *M. galloprovincialis* is native to the Mediterranean Sea but was introduced in the early 20th century as an aquaculture product in the Northeast Pacific. This species is in high demand and is an extremely important and profitable product in Puget Sound shellfish farms, but it also plays a valuable ecological role by filtering water, preventing erosion, and providing habitat for recruits (Mascorda Cabre et al., 2021). Unlike other common bivalves that build shell completely from aragonite, *Mytilus* spp. uses a form of calcite to build its outer shell. Calcite is less soluble than aragonite and provides shell integrity under acidified conditions. Unlike aragonite, calcite undersaturation is mainly encountered in deep waters in Puget Sound,

Washington (Fitzer et al., 2015; Washington State Blue Ribbon Panel, 2012). *M. galloprovincialis* are diecious broadcast spawners and in Puget Sound they typically spawn in the warmer months (April-May) however, maturation, timing and number of spawn cycles per year varies greatly depending on the environment (Smart et al., 2021). In Puget Sound, growth of wild *M. galloprovincialis* is predominantly found around aquaculture farms or shipyards (Green, 2014), indicating that there is some recruitment outside of a hatchery setting. However, with increased temperature, it is likely that this alien species may outcompete native *Mytilus trossulus*, which is adapted to cooler waters than *M. galloprovincialis* (Braby & Somero, 2006; Lockwood & Somero, 2011).

In this study we transplanted young adult *M. galloprovincialis* from a hatchery setting to four outplant locations in Puget Sound, Washington. Cages containing the shellfish were affixed for either six months or one year beneath profiling buoys that allowed for constant high-resolution environmental monitoring. We examined differences in *M. galloprovincialis* phenotypic plasticity and identified evidence of energetic tradeoffs depending on environmental variation. Our study employs a broad range of multidisciplinary methodologies to assess long-term acclimatization capacity and uses acute short-term experiments to analyze seasonal changes in mussel metabolism across different temperature and pH levels.

4.3 METHODS

4.3.1 Oceanographic monitoring in the field

In situ oceanographic readings of temperature, dissolved oxygen (DO), chlorophyll-*a* (chl-*a*), and salinity were acquired from Oceanic Remote Chemical-Optical Analyzer (ORCA) buoys, managed by University of Washington Applied Physics Laboratory, Northwest Association of Networked Ocean Observing Systems (NANOOS), and Integrated Ocean Observing System (IOOS). Three

ORCA buoys within Puget Sound were used in our study: Carr Inlet (CI) (47° 16.8' N, 122° 43.8' W) in South Puget Sound, Dabob Bay (DB) (47° 48.205' N, 122° 48.175' W) in Hood Canal, and Point Wells (PW) (47° 45.67' N, 122° 23.83' W) in Central Puget Sound (Figure 4-1A). When sensors on ORCA buoys malfunctioned during the course of the study, data from the LiveOcean Model were used instead to estimate a continuous profile of conditions (MacCready et al., 2021). pH, pCO_2, and aragonite saturation state (Ωara) were calculated by entering values for dissolved inorganic carbon (DIC), total alkalinity (TA), temperature, and salinity into *R* package *seacarb version 3.2.14* (Gattuso et al., 2016).

4.3.2 Cage deployment and collection

M. galloprovincialis mussels were acquired from Taylor Shellfish Farm located at the North Totten Inlet (47° 08.52' N, 122° 58.30' W). Here, mussels were allowed to grow-out in natural Puget Sound conditions for one year. All individuals in this study were the same age (shell height ~38.5 ± 6.8 mm, mean ± S.D) and raised in the same conditions before the outplanting to eliminate confounding factors related to environmental history (Byrne, 2011). Furthermore, the native (*M. trossulus)* and non-native (*M. galloprovincialis*) mussels cannot be distinguished without DNA analysis so by obtaining hatchery raised mussels we could ensure that we had the correct species. Mussels were measured and tagged by adhering numbered "bee tags" (Betterbee, Greenwich, NY) to their shells with glue (Pacer Technology Zap-A-Gap Adhesives) (n = 400 per site). Shellfish were placed in four identical rigid mesh plastic bags and secured in cages at each location using cable ties. The cages containing the shellfish were secured with a clamp to the anchor line of the ORCA buoys by SCUBA divers. Cages were affixed to the CI buoy at 5 m (CI5) and 20 m (CI20) below the surface on July 13, 2018 (Figure 4-1B). Cages were affixed to the DB and PW buoys at

5 m below the surface on July 12, 2018 (Figure 4-1D). Cages at 20 m below the surface were affixed at DB and PW, however they sank due to strong current, and were unretrievable by the divers due to the deep depths of the sites (>100 m). After six months, half of the mussels were removed from the cages and brought back to the lab for physiological analysis. Mussels at CI were collected on January 8, 2019, DB were collected on January 15, 2019, and PW were collected on January 23, 2019. The final collections for CI took place on July 11, 2019, for DB on July 18, 2019, and for PW on July 23, 2019. Tagged shellfish were immediately brought to the laboratory at the School of Aquatic and Fishery Sciences at the University of Washington, size was recorded, shellfish were dissected, entire visceral mass was flash frozen, and kept at -80°C for further analysis. Their shell containing the numbered tag was cleaned with terrycloth and preserved at room temperature.

4.3.3 Growth

A digital caliper (0.1 mm precision) was used to measure the shell height (from hinge to apex) and shell length (from anterior to posterior) of the right valve. The value measured was subtracted from the initial shell height and length to obtain total growth. The growth value was divided by the fraction of total months in the field to obtain a growth rate (n = 23 - 94).

4.3.4 Shell Strength

Shell strength was estimated using a modified method from Alma et al. (2022). Dried shells were rehydrated in seawater for 24 hours prior to shell strength tests to mimic the aquatic environment (Ikejima et al., 2003). Hydrated shells were taken to the University of Washington Mechanical Engineering Department where they were point-crushed using an Instron 5585H 250 kN electro-

mechanical test frame (Carnarius et al., 1996; Ikejima et al., 2003; Wilkie & Bishop, 2012). Shells (n = 170 - 236) were placed on the stage of the Instron and a hydraulic upper mount was pressed down on the shell with one newton of force to hold it in place before crushing. Bluehill Software (v.2) (Illinois Tool Works Inc., IL, USA) recorded newtons it took to create a 2.5 mm puncture hole.

4.3.5 Total Lipids

Total lipids were extracted from whole body tissue (n = 10). Tissue was freeze dried, and ground to a fine powder using a mortar and pestle, then 15 ± 0.2 mg of tissue was weighed or each individual using a microbalance (sensitivity 10 μg), and lipids were extracted using the Bligh Dyer method (Bligh & Dyer, 1959). In short, chloroform:methanol and nanopure water were added to the tissue sample, then vortexed, and sonicated to extract lipids from the cells. The sample was centrifuged, and polar and non-polar metabolites were separated into phases. The bottom most layer containing the lipids suspended in chloroform was removed using a pasture pipette and placed into a metal tin to dry. The Bligh Dyer method was repeated twice for each sample to ensure full lipid extraction. Total lipids were quantified gravimetrically by weighing the lipids and subtracting from the initial tissue weight.

4.3.6 Isotopes

Frozen whole body shellfish tissue (n = 10) was freeze-dried and ground in the same fashion as the lipid analysis. Dry tissue was weighed using a microbalance (sensitivity 10 μg) to obtain weights of 0.6 ± 0.01 mg per sample The tissue was placed into a small tin 8 x 5 mm and the tin was closed and pressed onto itself several times to create a compact sample. Samples of Glutamic Acid I, II, (0.42 μg) and Bristol Bay Salmon (0.339 μg) of known isotopic values were interspersed

with our samples to serve as a reference. Samples were analyzed at the University of Washington Earth and Space Sciences Department Isolab where they were first placed in a Costech Elemental Analyzer, Conflo III, MAT253 with continuous flow, and then to a Finnigan MAT253 mass spectrometer (Fry et al., 1992). Using an algorithm in Matlab, the output data were corrected to the Air-N_2 scale, for $\delta^{15}N$, and to the VPDB scale, for $\delta^{13}C$. C:N ratio was calculated by dividing the mass of carbon by the mass of nitrogen in the sample.

To determine relative proportions of broad diet categories, we found isotopic signatures of diet end members (diet sources) from the literature. All end member data was collected from the literature within the Salish Sea. We clustered primary production sources based on isotopic values, and created three major categories (Kasai & Nakata, 2005); (i) marine phytoplankton and POM (Wright et al. 2011, Conway-Cranos et al. 2015, Eccles et al. 2018, Pelletier et al. 2018, Costalago et al. 2020), (ii) phytobenthos (marine macroalgae, eelgrass) (Costalago et al., 2020; Liedtke et al., 2011; Mueller, 2017), and (iii) terrestrial matter (C3 plant material washed in from land) (Conway-Cranos et al., 2015). Averages and standard deviations were calculated for $\delta^{13}C$ and $\delta^{15}N$ signatures of end members and consumers (mussels). We plotted the end member and consumer data on a biplot to make estimates of diet proportion. We plotted the end member and consumer data on a biplot to make estimates of diet proportion. A Monte Carlo mixing model was performed, but the wide variation of end member signatures prevented reliable results, and thus the model was omitted from the analysis.

4.3.7 Respiration

A subset of outplanted mussels were taken to National Oceanic and Atmospheric Administration (NOAA) Mukilteo Research Station, Mukilteo, Washington (47° 56.56' N, 122°

18.10' W) to perform respiration measurements. Individuals were placed in holding tanks with filtered flow-through seawater. Mussels were starved 24 hours prior to respirometry trials to eliminate signals of metabolic activity due to digestion (Parker et al., 2017). The respirometry system consisted of 625 mL chambers equipped with a temperature and fiberoptic oxygen probes connected to an OXY-10 SMA G2 meter box, which was then connected to a computer with software PreSens Measurement Studio 2 (version 2.0.0.28). Prior to trials, the system was calibrated using a two-point oxygen calibration. 100% oxygen was achieved by leaving a beaker of fresh seawater overnight to equilibrate with the atmosphere. 0% oxygen was achieved by combining 1 g of sodium sulfate (Na_2SO_3) (Sigma-Aldrich) with 50 µl of cobalt standard for ICP ($Co(NO_3)_2$) (Sigma-Aldrich) and 100 mL of DI water. Individuals were placed within airtight chambers filled with seawater heated or chilled to the appropriate experimental temperature, and to maintain temperature, chambers were placed in a water bath controlled by an Aqualogic heat pump (DSHP-4) (± 0.1°C). A magnetic stir bar was also placed into the chamber, and eight chambers were placed onto a custom-made magnetic submersible stir plate. Constant water movement via the stir bar allowed homogenous temperature and oxygen levels within the chamber. Trials were run for one hour, n = 8 individuals per cohort per trial. We ran blank chambers with seawater to determine a baseline oxygen consumption due to microbial respiration, and we subtracted that value from each individual's respiration rate. Respirometry trials were run at five different temperatures (3, 8.5, 14, 19.5, and 25°C), and five different pH levels (6.6, 6.9, 7.2, 7.6, and 7.8). Temperatures were achieved by adjusting the heat pump, and pH was achieved by bubbling CO_2 controlled by a solenoid valve. The pH probe (Honeywell Durafet) was calibrated with tris buffer and verified using a spectrophotometer and m-cresol purple dye in accordance with Dickson et al., (2007). Temperature treatments were performed at a constant pH 7.8 and pH

treatments were performed at a constant 11°C, representing average ambient conditions. After respirometry trials were completed, individuals were dissected, and visceral mass was placed in a labeled metal tin. Mussel visceral mass was dried in a 60°C oven for 48 hours, and individual dry weight was measured. Appropriate start and end points were chosen for each individual's respiration curve, and oxygen consumption was converted from % oxygen saturation to mg/L of oxygen, using an equation (Benson & Krause, 1984) which takes into account temperature and salinity. Standard metabolic rate (SMR) of each individual (mg O_2 g^{-1} DW h^{-1}) was calculated as oxygen consumption in mg/L per hour and gram of dry weight (Li et al., 2017; Montory et al., 2021; Paolucci et al., 2022).

4.3.8 Gonad Histology

A pea-sized piece of gonad (~3 – 12 cm^2) was excised from the visceral mass (n = 10) the day of collection, fixed for 24 hours in 10% formalin and subsequently preserved in with 70% ethanol. Fixed samples were sent to Histology Consultation Services (Everston, Washington) for staining with hematoxylin counterstaining with eosin staining, paraffin wax imbedding slicing, and mounting onto slides (da Silva et al., 2009; Hassan et al., 2018a; Spencer et al., 2020). The slides were examined under a high-powered microscope (Nikon Eclipse Ni) and photographed using the program NIS-Elements Basic Research. Mussel gonad development was assigned a ranking of 1-8 (Ford & Figueras, 1988) as follows: (1) indeterminate, (2) early development: new evidence of gamete and follicular formation, (3) mid-development: expanding follicles with developing gametes, (4) late development: larger follicles with some mature gametes, but connective tissue still abundant, (5) fully developed/ripe: most gametes mature some evidence of development, little connective tissue, (6) spawning: fully developed gametes in full follicles, (7) post-spawn: follicles

emptying, some gametes may remain, and (8) resorbing: follicles empty, unreleased gametes denaturing and resorbing back into tissue. *M. galloprovincialis* is gonochoristic and therefore histological samples were assigned the sex of either male, female, or indeterminate based on presence of spermatogonia, oogonia, or lack of gametes, respectively.

4.3.9 Data Analysis

All analyses were performed in *R* version 2022.02.1 (R Core Team, 2020) with a significance threshold $\alpha < 0.05$. A Shapiro-Wilk Test was performed to assess normality and if needed, values of analysis were log, arcsine, or square root transformed to achieve normality assumptions before a model was run. ANOVAs were performed and post-hoc with Tukey-HSD tests for multiple comparisons for growth, shell strength, lipids, stable isotopes, and respiration rates. A Pearson's Chi-square test based on 10,000 replicates with a Bonferroni correction for multiple comparisons was performed to evaluate sex ratio and gonad maturation (da Silva et al., 2009; Spencer et al., 2021). A correlation plot was created using oceanographic data with *R* package *corrplot version 0.87* (Taiyun, 2014). When experiments used multiple replicates from a single population, we ran a linear mixed-effects model using *R* package *lme4 version 1.1-28'*(Bates et al., 2015), where each response variable is a fixed effect, and each individual replicate is a random effect variable.

4.4 RESULTS

4.4.1 Environmental Variability

There were clear differences in oceanographic conditions between study sites and between study periods (Table 4-1, Figure 4-2, Appendix Figure S4-1). At all sites, temperature was on average higher in July 2018-January 2019 (T1) when compared to January-July 2019 (T2). DB had the

highest variation in temperature at both time periods while CI20 had the lowest. A maximum temperature of 18.1°C was reached at DB on June 14th, 2019, and the lowest temperature of 6.9°C was also seen at DB on February 14th, 2019. When considering the temperature for all days in the study, T1 at CI20 had the most days below the 25th percentile (Q1, 170 days), and in T2, DB had the most days above the 75th percentile (64, Figure 4-3). At all sites, T1 had higher average salinity than T2 (Table 4-1, Figure 4-2). DB has the lowest salinity at both time periods, with a salinity reading recorded as low as 20.7 PSU on January 18, 2019, and CI20 registered the highest salinity at 31.0 on December 17, 2018. CI20 had a higher salinity than CI5 at both time periods. T2DB had low salinity for the most days under Q1 (91), and T1DB had the most days above Q3 (92). Average chl-*a* was highest at CI5 for both time periods. On average, there was higher chl-*a* in T2 than there was in T1. The highest variation of chl-*a* occurred at DB in the January-July 2019 time period (0.64 - 37.8 mg m^{-3}). In T1, PW had the most days of chl-*a* below Q1 (130), and T1 and T2CI5 had the most days above Q2 (91 and 90, respectively). On average, dissolved oxygen was higher at all sites in T2 than T1. CI5 had the highest average DO levels January 2018 and DB had the highest in T2 (8.32 mg/L and 10.48 mg/L, respectively). At both time periods, CI20 had the lowest average DO levels (6.18mg/L and 8.28 mg/L, respectively). T1CI20 had the most days with DO below Q1 (128), and T2DB had the most days above Q3 (144).

Average pH was higher at all sites during T2 compared to the T1 (Table A1, Figure 4-2, Figure 4-3). pH had the highest variation at both time periods at DB, and the lowest variation at CI20. Aragonite saturation state was higher in T2 than T1. In both time periods DB had the highest variation of Ωara and CI20 the lowest. T1 at CI20 had the most days with pH and Ωara below Q1 (170, 156, respectively) and T2 at DB had the most days above Q3 (122, 113, respectively). The lowest Ωara and pH recorded during this experiment was 0.62 and 7.51, respectively at DB on

October 14, 2018. pCO_2 was, on average, was higher in T1 than T2. DB had the highest variation of pCO_2 in both time periods, and CI20 had the lowest variation.

4.4.2 Shell Growth and Strength

Growth rate for both height (hinge to apex) and length (left to right) had significant differences depending on site and collection time ($p < 0.001$). At the T1 collection, mussels at CI5 had significantly higher heightwise growth rate compared to other cohorts, and mussel growth at CI20 had slower growth lower compared to mussels from all other sites (Figure 4-4A, Table 4-2). Lengthwise for T1, a similar pattern occurred where mussels at CI20 had the lowest growth rate and mussels at CI5 had the highest growth rates (Figure 4-4C, Table 4-2). In T2, there was no significant differences in heightwise growth rates between sites (Figure 4-4B), but for lengthwise growth rates, CI20 mussels had lower rates than all other cohorts (Figure 4-4D). We detected 58% faster heightwise growth in T1 compared to T2 and 48% higher lengthwise growth in T1 compared to T2 ($p < 0.001$).

Mussel shell integrity changed depending on both the time of collection and site of acclimatization ($p < 0.001$, Figure 4-4E, F, Table 4-2). In T1 and T2, mussels at CI20 had the weakest shells. Mussels from shallow environments had similar shell strength during both collection periods. In T2, mussel shells at PW were stronger than DB, while CI5 mussels had similar shell strength to mussels at DB and PW. On average, mussel shells were 84.3% stronger in T2 compared to T1, which is likely due to normal strengthening with age.

4.4.3 Lipids and Isotopic Composition

There were no differences in total lipid signatures between sites ($p = 0.75$) or collection time ($p = 0.52$) (Figure S4-2, Table 4-2). $\delta^{13}C$ and $\delta^{15}N$ signatures differed depending on site and collection

time ($p < 0.001$, Figure 4-5, Table 4-2). After the T1 collection, $\delta^{13}C$ in the two CI sites were significantly higher than the other sites and no different than T_0 (-17.3, -17.3, -17.8 ‰, respectively). The $\delta^{13}C$ signatures for mussels at the DB and PW sites were lower than mussels at the CI site (-22.7, -19.6‰, respectively). At T2, CI20 mussels has the greatest $\delta^{13}C$ signature (-17.6 ‰), followed by CI5 and PW which were not different from each other (-18.8, -18.5‰, respectively). Similar to the T1 collection, DB $\delta^{13}C$ mussel signatures from T2 were lower than all sites (-20.5‰). $\delta^{13}C$ signatures from CI20 mussels remained the same across seasons, at CI5 higher $\delta^{13}C$ signatures were found in T1, and at DB and PW $\delta^{13}C$ signatures increased in T2.

We found that CI20 mussels had the highest $\delta^{15}N$ in T1 (10.1‰). $\delta^{15}N$ signatures of mussels at CI5 and PW were lower than CI20 (9.1, 9.2‰, respectively) and DB had the lowest $\delta^{15}N$ value (8.7‰). For T2, $\delta^{15}N$ mussel's signatures were very similar between sites. The only difference in $\delta^{15}N$ values occurred between CI5 and CI20, where mussels at CI20 had greater $\delta^{15}N$ values than mussels at CI5. When comparing the $\delta^{15}N$ signatures across seasons, CI20 is the only cohort that had different $\delta^{15}N$ signatures between collection periods. C:N ratios differed between sites and collection periods ($p < 0.001$, Table 4-2). For T1, all cohorts had similar C:N ratios except CI5, which was greater than all other sites. For T2, mussels from the shallow depths showed similar values. C:N ratios in mussels at CI20 were lower compared to the shallow CI5 site in T1 and T2.

4.4.4 Effects of Temperature and pH on Mussel Metabolism

After one hour exposure to one of five temperatures, results indicate that mussel metabolic performance changed depending on the season ($p = 0.001$), and site ($p = 0.002$, Figure 4-6, Table 4-2) Higher respiration rates were found during T1 than T2 for all sites across temperatures. In January mussels are cold-acclimatized and thus are more responsive to increases in temperature. Mussels from CI5 had the lowest differences in respiration rates between seasons. Mussels from

the deep location (CI20) were more sensitive to increased temperatures and had the highest respiration rates both seasons (7.44, 5.36 O_2 [mg/l] g DW^{-1} h^{-1}). Mussel respiration in most sites increased sharply above 14°C (both collection times). Our study did not find evidence of metabolic depression due to elevated temperature stress. There were no differences in respiration between time periods at CI20 ($p = 0.44$). Respiration rates were higher in T1 than T2 under different pH levels (Figure 4-7, Table 4-2). Mussels from CI20 were the only cohort to show seasonal differences in respiration rates across pH levels ($p < 0.001$). There was no clear pattern between pH levels, and respiration rates under the pH levels never exceeded 3 mg O_2 g^{-1} DW h^{-1}.

4.4.5 Reproductive Characteristics: Gamete Development and Sex Ratio

There was a significant difference in maturation stage when comparing both site and collection time ($p < 0.001$, Figure 4-8A). All mussels started the experiment with late or mature gametes. By January 2019, CI20 mussel gonad tissue appeared to be resorbed and had excessive connective tissue. Mussels at CI5 had a mix of gamete development stages. Mussel gamete stages at DB remained virtually unchanged from T_0. PW mussels were mainly in the later stages of gametogenesis. In July, we found CI20 mussels had released gametes, the majority of CI5 mussels were developing gametes, DB mussels has also spawned recently, and PW mussels were split between spawned and mid-development stages. When considering the fraction of mussels undergoing gametogenesis from the January collection, CI20 had 0%, CI5 had 90%, DB had 100%, and PW had 90%. In July 2019, mussels from CI20 had 10% developed gametes, CI5 had 90%, DB had 10%, and PW had 50% undergoing gametogenesis. It appears the cohort from CI20 had a spawning event immediately before both collections. Notably, CI20 mussels were the only cohort to have post-spawn individuals in T2.

We found that there was no difference in sex ratio between seasons ($p = 0.57$) or sites ($p = 0.10$,Figure 4-8V). Overall, 42.2% of mussels were male, 55.6% female, and 2.2% indeterminate (I). Before deployment there was a M:F ratio of 3:7. In January 2019 M:F:(I) ratios were 1:7:(2), 7:3, 6:4, 4:6 at CI20, CI5, DB, and PW, respectively. In July 2019 M:F:(I) ratios were 6:4, 1:9, 7:3, 3:7 at CI20, CI5, DB, and PW, respectively. Interestingly CI20 in January 2019 is the only cohort which contains 20% of individuals with indeterminate sex.

4.5 DISCUSSION

Mussel aquaculture serves as an important source of protein for humans, it serves as a source of income to coastal communities, and is rapidly increasing globally (Mascorda Cabre et al., 2021). However, inshore shellfish aquaculture is limited due to space and anthropogenic impacts in the coastal zone (i.e., biological and chemical pollution, ocean warming and acidification). Longline offshore shellfish farms have the potential to overcome these challenges and provide alternatives to mitigate the effects of climate change and coastal development on commercial bivalves currently grown in the intertidal zone. Previous studies have shown that Mytilidae mussels under stressful environmental conditions have a very high capacity for phenotypic plasticity and can exhibit energetic trade-offs between growth, reproduction and physiological tolerance (Fly et al., 2015; Petes et al., 2008; Reusch, 2014; Sebens et al., 2018, Roberts et al. 2021) which may affect cultured mussel production and the communities that depend on them. When choosing the location of offshore farms and projecting the success of shellfish production is important to examine mussel phenotype-environment interactions. In our study we assessed growth, shell strength, metabolism, isotopic signatures, and reproduction of the commercially important Mediterranean mussel *M.*

galloprovincialis at four offshore sites in Puget Sound, Washington. Information from this study can be used by shellfish growers to understand the physiological responses of mussels growing under different environmental conditions and select grow-out locations that optimize favorable characteristics.

4.5.1 Shell Growth and Strength

Mussels grew faster between July 2018 - January 2019 (T1) when temperatures in the field were warmer. A similar result was seen in *M. trossulus* in Puget Sound, whose growth also differed across season and location (Howe & Simenstad, 2015). CI5 had the highest average temperatures and growth rates, but just 15 m deeper, mussels at CI20 had the lowest growth rates. Environmental differences between these two depths may have influenced differences in metabolic scope and growth rates (Gunderson et al., 2016; H. Pörtner, 2001; Schulte, 2015). A strong stratification during the warmer months resulted in CI20 mussels being below the pycnocline with lower food availability (chl-*a*), cooler temperatures, lower oxygen, and pH levels than the shallow locations (Figure 4-2). In the January - July 2019 season (T2), temperature was lower and more variable at all sites and aragonite saturation state was more favorable for mussel shell building. Slowed metabolism due to colder conditions in this time period resulted in slower growth than T1.

Similar to growth rates, shell strength differed between site and season. Older mussels had stronger shells and, in both collection seasons, the deeper CI20 site had the weakest shells. Shell strength of *M. edulis* also showed differences between seasons, potentially due to predation or fluctuation in environmental stressors (Nagarajan et al., 2006). It has been well documented that ocean acidification, food concentration, and dissolved oxygen levels greatly affect bivalve shell integrity by affecting the energy budget, extra and intercellular processes associated with calcification

(Fitzer et al., 2018; Gazeau et al., 2013; Melzner et al., 2020; Tan & Zheng, 2020). When *M. edulis was subjected to low food and high pCO_2 for seven* weeks, starvation *in* combination with acidification stress reduced energy available to dedicate toward shell integrity and reallocated ATP to more vital processes like somatic maintenance (Melzner et al., 2011).

4.5.2 Mussel Lipids, Isotopic Composition, and Dietary Sources

Total lipid content of mussels did not differ between site or collection period. This suggests that, regardless of environmental conditions, *M. galloprovincialis* prioritizes the maintenance of lipid reserves. It is also important to note that lipid content remained the same between the two collection periods despite significant environmental and biological (i.e., mussel growth, reproduction) differences between these two periods. A similar result was seen in mussel *M. edulis* collected in Northern Germany, where seasonal environmental differences did not affect mussel lipid content (Wu et al., 2021). Our result was contrary to other lipidomic analysis of *M. galloprovincialis* in Puget Sound, where total lipids decreased with warmer conditions, suggesting lipid catabolism or peroxidation (Alma et al., 2022 in prep). Further investigation of specific fatty acids and other metabolites may provide insights into the biochemistry, metabolism, and nutrition of this economically important species.

$\delta^{13}C$ and $\delta^{15}N$ signatures were used to gain insight into physiological processes and estimate mussel dietary contributions. Nitrogen stable isotope signatures are generally used as a trophic indicator, and carbon isotopic signatures are used as a primary production food source indicator (Fry, 2006). We found that both location and collection period affected $\delta^{13}C$ and $\delta^{15}N$ isotopic signatures. In mussels from the January 2019 collection, both CI sites had high $\delta^{13}C$, and DB was lowest. A possible explanation for lower $\delta^{13}C$ signatures at DB is excessive runoff from freshwater,

snowmelt, and anthropogenic sources associated with terrestrial matter (Michener & Lajtha, 2008; Millo et al., 2021; Piola et al., 2006). During January 2019 we found extreme low salinity values at DB (Figure 4-2) and previous work has shown that during this period $\delta^{13}C$ signatures of phytoplankton (mussel diet) can be up to 8‰ lower due to freshwater input (Conway-Cranos et al., 2015; Howe & Simenstad, 2015; Simenstad & Wissmar, 1985). However, it should be noted that the $\delta^{13}C$ signal in DB increases in the second collection period, which could indicate quick tissue turnover and a shift away from terrestrial to marine diets in the warm spring and summer months. Higher $\delta^{13}C$ signatures found in CI may be due to preferential uptake of heavier $\delta^{13}C$ through assimilation, combined with increased respiration rates which results in loss of lighter $\delta^{12}C$ isotopes to the environment (Michener & Lajtha, 2008).

CI20 mussels had higher $\delta^{15}N$ compared to all other sites in the first collection period and was higher than the shallower CI5 site in the second period. Increased $\delta^{15}N$ is associated with a higher trophic level (McMahon et al., 2021), which may be the result of a greater dietary fraction of zooplankton or animal based POM (particulate organic matter) and less phytoplankton available at depth. Uptake of dissolved inorganic nitrogen due to summer upwelling is also likely a major factor for the deep site $\delta^{15}N$ signature (Michener & Lajtha, 2008). The process of denitrification via bacteria at very deep depths results in a high content of $\delta^{15}N$ in the seawater, which, when upwelled, brings POM and leaves phytoplankton also enriched (Schlesinger & Bernhardt, 2013). This is likely the case especially for CI20 from T1 which has the highest $\delta^{15}N$, and the more conspicuous evidence of upwelling (lowest DO and pH). Based on the increased $\delta^{15}N$ signature of Oysters from T1 at CI20 relative to other cohorts, we suggest that the deep acclimatized individuals are retaining heavier isotopes in their bodies due to tissue turnover rate, stress response, or high metabolic rate without substantial growth (Fertig et al., 2010; Michener & Lajtha, 2008). These

assumptions can be corroborated with our growth rate and respiration data. Higher growth rates would result in higher assimilation, and less carbon and nitrogen lost to the environment.

By plotting end member and consumer data on a biplot, we can speculate differences in physiology based on feeding patterns. Based on our end member signatures, it is very likely that most of the mussel's diet consists of phytoplankton. The $\delta^{13}C$ signature of phytoplankton in the Salish sea is very broad (-22.8 ± 6.6‰) which, if adjusted for trophic enrichment factor, would very closely reflect all consumer values. Interpretation of isotopic signatures can be quite complex due to the countless number of environmental and physiological factors at play in a field-based study. To further expand this investigation, it would be important to collect physical end member samples (i.e., terrestrial matter from around the study site, plankton tows, and samples of different algae and eelgrass) to reduce uncertainty of *a priori* end member signatures. A species specific trophic enrichment factor can be estimated with acclimation experiments in the laboratory where mussels are only fed one food source of known isotopic composition (Dubois et al., 2007).

4.5.3 Effects of Temperature and pH on Mussel Metabolism

When organisms are subjected to less favorable environments there are energetic trade-offs between various metabolic processes (Bednaršek et al., 2021; Hofmann & Todgham, 2009; Kooijman, 2010; Pouvreau et al., 2006; Sebens et al., 2018). The oxygen and capacity limitation of thermal tolerance (OCLTT) hypothesis states that oxygen supply capacity (aerobic scope) is limited by temperature (H. O. Pörtner, 2008; H. O. Pörtner et al., 2018). Climate change related stressors like ocean acidification and warming are expected to reduce ectotherm's aerobic scope and narrow the thermal tolerance window because the organisms will need to dedicate more energy toward stress response (Lannig et al., 2010; Lefevre, 2016). However, when applying the OCLTT

hypothesis, it should be considered that modulations in oxygen limitation may not be directly related to external temperature because countless other physiological mechanisms are at play (Jutfelt et al., 2018; Lefevre, 2016).

Mussels from the T1 collection had overall higher metabolic rates compared to mussels in T2. Recent cold acclimatization is likely the biggest contributing factor for higher metabolic rates with increased temperature. A similar result was found when *M. galloprovincialis* were collected in Spain in summer, fall and winter (Múgica et al., 2015). Authors found strong seasonal differences, with reduced aerobic scope in the fall and summer, but not winter suggesting energetic reallocation to maintain vital processes.

Our study showed that at 3 and 8.5°C, there was not much difference in mussel respiration between sites and time periods, however at higher temperatures we see different respiration rates between cohorts. DB and CI20 mussels had the largest respiration rates, especially during the winter. DB mussels' physiological response was more sensitive to temperature. These mussels increased respiration greatly beyond 8.5°C in the winter, and they showed the largest seasonal differences in respiration. Large seasonal differences in respiration in DB mussels may be result of high variability in temperature at this site. Large seasonal physiological plasticity may enable mussels to better cope with adverse environmental conditions and enhance tolerance to stressful events (Buckley et al., 2001) which is a desirable trait for the aquaculture industry. Conversely, CI20 also had very high metabolic rates, but unlike DB, CI20 has a very narrow difference between the two collection periods. This may suggest reduced plasticity and high metabolic stress, especially during the T2 time period when other sites showed lower metabolic rates. This is likely a result of cold *in situ* temperatures in the spring and summer due to strong stratification and upwelling at depth. Although the maximum temperature experienced in the field experiment was 18°C (at DB), we

did not see any evidence of metabolic depression in our short-term experiments, except possibly CI5 at 25°, although this signal is likely due to variation and small sample size (H. O. Pörtner, 2008; Schulte, 2015). These results could be elaborated upon by experimenting with warmer acclimation temperatures and longer exposure times, to examine long-term thermal physiological thresholds and lethal temperatures (Schulte, 2015).

Ocean acidification can impact the metabolism of calcifying molluscs, however responses are extremely variable (Breitburg et al., 2015; Doney et al., 2009; Gazeau et al., 2013). Our results showed differences in respiration for all sites and seasons, but not under different pH levels. Mussels collected in January 2019 had lower respiration rates than in July 2019 across all sites, suggesting that mussels that were recently acclimatized to lower pH (in January) were more tolerant to low pH and had lower metabolic demand. Observed differences between site and season provide evidence that mussels have the capacity to acclimatize to different environments, and may be suggestive of short-term trade-offs between different bioenergetic functions (Kellermann et al., 2019). Similar to our results, metabolic rates of *M. edulis* from the Gulf of Maine increased with temperature, but not with pH (Matoo et al., 2021). In our respiration study, we used very low pH levels that greatly exceed any current and near future levels, and our mussels were able to withstand those levels in the short-term. This capacity to tolerate low pH may be due to the fact that mussels are intertidal species and are adapted to tolerate large fluctuations in their environment, including large natural daily fluctuations in pH. However, it should be noted that there is growing evidence that OA will greatly affect the physiology of marine organisms, and our short-term experiment may not be adequate to project long-term in situ responses (Melzner et al., 2020; Parker et al., 2013; Tan & Zheng, 2020)

4.5.4 Reproductive Characteristics: Gamete Development and Sex Ratio

There is strong evidence supporting the fact that gamete development and spawning times for *M. galloprovincialis* are plastic and can very rapidly become asynchronized depending on physiological state, geography, and environmental conditions (Smart, 2019). Mussels in our study were similar in age, and were hatchery raised so they had a similar genetic and environmental history, so any observed reproductive or physiological shifts between cohorts is an environmentally induced plastic change acquired within six months or one year. At the T1 collection, we found very different patterns in gamete development. Mussels from the deep 20 m site had spawned out, whereas gametes in mussels from the other three sites were still developing. Since mussels at CI20 exhibited physiological responses indicative of stress, they may have forgone reproduction in order to allocate energy to more essential survival functions (Hatzonikolakis et al., 2017; Rosland et al., 2009; Sokolova et al., 2012). It is likely that CI20 mussels were not able to start a new gametogenic cycle and instead resorbed reproductive tissue into undifferentiated mantle tissue in order to obtain energy (Hassan et al., 2018). However, at T2, this pattern no longer exists, and CI20 is similar to cohorts, potentially due to more favorable conditions (higher pH, oxygen, etc.) due to weaker stratification in the water column. A study conducted in New Zealand found that when wild *M. galloprovincialis* were collected, spawning patterns and maturation state varied between sites and collection periods (Smart, 2019). In a similar study conducted in Spain, *M. galloprovincialis* showed accelerated gametogenesis in mussels exposed to increased temperature (Múgica et al., 2015). In addition to warm temperatures the effect of food availability plays a substantial role in the seasonal progression of gametogenesis for *M. galloprovincialis* (Domínguez et al., 2010; Suárez et al., 2005). Temperature and chl-*a* profiles

may explain our differences in maturation stage, especially when comparing the stark difference in reproductive cycle between the two CI sites.

Our study shows that mussels can quickly exhibit reproductive plasticity in response to its surroundings to strategically allocate energy toward or away from reproduction (Villalba, 1995). This plastic capacity may be beneficial for *M. galloprovincialis* and the aquaculturists that grow them (Smart et al., 2021). Reproductive asynchronization and stress responses attributed to environmental profiles and stratification are important factors to consider when raising cultured mussels on longlines at depth. Additionally, climate change will lead to more environmental variation and extremes, and we suggest that rapid changes in phenotypic plasticity may cause changes in reproductive energy allocation in this species, which will further affect the spawning synchronization with unpredictable outcomes. Similar to oysters, mussels have a different flavor profile, and the texture becomes softer and less desirable when gametes mature. Many shellfish aquaculture farms harvest non-ripe mussels to maximize product quality year-round (Alma *peronal communication with Taylor Shellfish aquaculturist*), however our results indicate that it may be difficult to predict the maturation stage with rapidly changing environments.

Although reproductive maturation was affected by site and season in the field, we did not see any differences in sex ratio between sites or collection periods. There is evidence that sex ratio does not vary much for this species, regardless of external factors since they are gonochoristic. In a previous study, there was no spatial difference in sex ratio of *M. galloprovincialis* when outplanted ~ one year on longlines at five different sites in Northwest Spain (Villalba, 1995). Additionally, there were no temporal differences in sex ratios of wild *M. galloprovincialis* sampled monthly for one year in New Zealand (Smart, 2019). Our only cohort whose reproductive stage was asynchronized from the other sites (CI20 at T1) is also the only site to have indeterminate sexed

individuals. Thus, it is likely that these mussels resorbed their gametes and failed to begin a new reproductive cycle due to environmental stress.

4.6 CONCLUSION

In order to improve our understanding of economically important species like *M. galloprovincialis*, it is essential that we recognize the link between abiotic drivers and the physiological mechanisms that impact phenotypic plasticity. By coupling high resolution environmental data with an evaluation of sub-lethal responses, we aim to understand this relationship at multiple timescales and levels of biological organization, spanning from the molecular to ecosystem level (Breitburg et al., 2015; Fey et al., 2021). Dynamic ocean conditions may trigger a unique stress response in calcifiers, and unlike single and multi-stressor acclimatory experiments performed in the laboratory, long-term field experiments reveal the complexities of processes like growth, reproduction, metabolism, and skeletogenesis (Byrne, 2011; Todgham & Stillman, 2013). Although field-based studies can more reliably predict real-world phenotypic plasticity compared to controlled laboratory experiments, it is still very difficult to infer causation considering the interaction of countless co-occurring drivers (Forsman, 2015).

In a complex coastal setting like Puget Sound, Washington, habitats that are very close together often have substantial variations in environmental stressors between season and depth that are predicted to greatly affect shellfish aquaculture operations (Gunderson et al., 2016). Our study outplanted mussels at four sites and collected them after six and twelve months. Mussels grew faster in the warmer months, and the deeper population at 20 m differed greatly during that time, but not in the cooler months. Mussels from CI20 also had the weakest shell strength at both collection periods. Carbon stable isotope signatures indicated that DB had lighter signatures at both time periods, and CI20 had the highest nitrogen isotope signature at both time periods. We

found strong seasonal differences in respiration rates in response to temperature, but not for pH stress. There were larger differences in gamete maturation between sites in the T1 collection compared to T2, and there were no differences in sex ratio or total lipid content.

As proposed by Tan & Zheng, (2020), our results show that having different shellfish cultivation sites can help to mitigate climate change effects on mussel product and yield different desirable phenotypes. Physically moving grow-out operations can be a good short-term solution to increase mussel production quantity and quality, however rapid environmental change may push an animal closer to its physiological tolerance window, resulting in increased energy demand, which can reduce resources available for somatic growth (Hofmann & Todgham, 2009) and reproduction (Hofmann & Todgham, 2009; Sokolova, 2013). This study provides the aquaculture industry with valuable information regarding *M. galloprovincialis* phenotypic plasticity, ecophysiology and reproduction, so that farmers may select locations to obtain favorable phenotypes to assist in selective breeding programs, maximize productivity, profit, and product quality (Tan et al., 2020). Mussel longlines are a common practice, however the environmental gradient with depth should be strongly considered since it can significantly influence the growth, tolerance and quality of the shellfish product (Díaz-Puente et al., 2016).

4.7 FIGURES

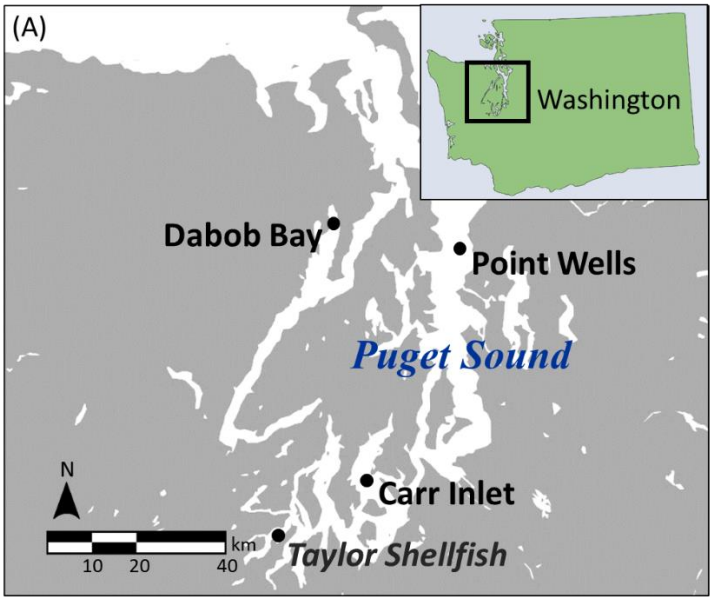

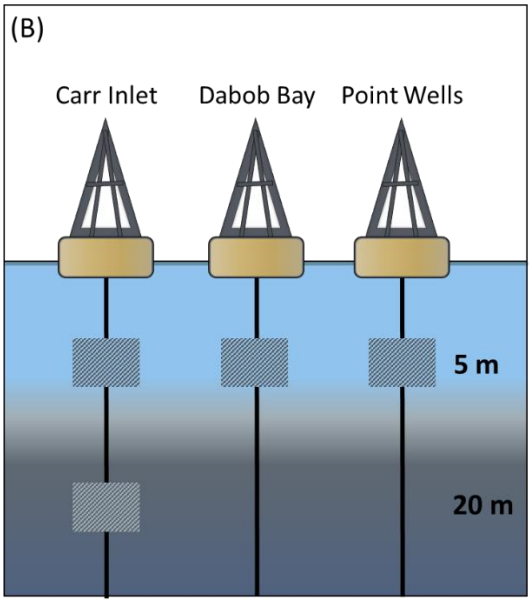

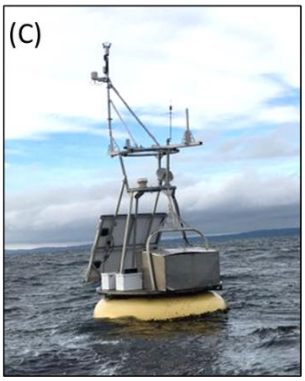

(D)

Site	Deployment (T_0)	January Collection (T1)	July Collection (T2)
Carr Inlet 20 m	7/13/2018	1/8/2019	7/11/2019
Carr Inlet 5 m	7/13/2018	1/8/2019	7/11/2019
Dabob Bay	7/12/2018	1/15/2019	7/18/2019
Point Wells	7/12/2018	1/23/2019	7/23/2019

Figure 4-1: (A) Map depicting locations of Taylor Shellfish Farm (origin location of mussels) and study sites (Dabob Bat, Point Wells and Carr Inlet) in Puget Sound, Washington (B) Schematic depicting location of cages containing mussels at three buoys, with the Carr Inlet buoy having cages at both 5 and 20 m. (C) Photo of an Oceanic Remote Chemical-Optical Analyzer (ORCA) buoy, which collects high-resolution oceanographic data. (D) Dates of deployment and collection periods at each site.

Table 4-1: Average ± S.D. of oceanographic parameters at each site and collection period. Post-hoc results are depicted by lowercase letters. Values that have different letters between sites indicate a significant difference.

	July 2018 - January 2019				January 2019 - July 2019			
	CI20	CI5	DB	PW	CI20	CI5	DB	PW
Temperature (°C)	12.19 ± 1.40^{ab}	12.78 ± 1.93^{a}	11.97 ± 2.47^{bc}	12.45 ± 1.29^{ab}	9.55 ± 1.30^{c}	10.31 ± 1.89^{d}	11.38 ± 3.33^{c}	10.08 ± 1.72^{de}
Salinity (PSU)	30.14 ± 0.58^{a}	30.02 ± 0.63^{a}	29.99 ± 1.02^{a}	30.11 ± 0.37^{a}	29.64 ± 0.52^{b}	29.58 ± 0.55^{bc}	29.26 ± 1.33^{d}	29.37 ± 0.54^{cd}
Chlorophyll-a (mg/m^3)	1.58 ± 1.08^{ab}	5.05 ± 5.84b^{c}	2.51 ± 0.98^{ad}	1.25 ± 1.09^{b}	2.44 ± 2.59^{abd}	5.64 ± 6.77^{c}	3.79 ± 3.54^{e}	3.03 ± 3.65^{b}
DO (mg/L)	6.18 ± 1.03^{a}	8.32 ± 2.17^{b}	8.27 ± 1.56^{b}	6.55 ± 0.96^{a}	8.28 ± 0.68^{b}	9.71 ± 1.29^{c}	10.48 ± 1.56^{d}	8.49 ± 1.05^{b}
pH	7.74 ± 0.05^{a}	7.84 ± 0.11^{b}	7.94 ± 0.18^{c}	7.88 ± 0.10^{d}	7.91 ± 0.07^{cd}	8.01 ± 0.13^{e}	8.11 ± 0.14^{f}	7.98 ± 0.11^{e}
Ωara	1.05 ± 0.1^{a}	1.37 ± 0.42^{b}	1.71 ± 0.79^{cd}	1.43 ± 0.37^{be}	1.35 ± 0.21^{b}	1.79 ± 0.57^{c}	2.23 ± 0.78^{f}	1.59 ± 0.46^{de}
pCO_2 (µatm)	872 ± 101^{a}	703 ± 161^{b}	871 ± 103^{a}	626 ± 134^{c}	566 ± 93^{d}	454 ± 154^{e}	570 ± 94^{d}	481 ± 127^{3}

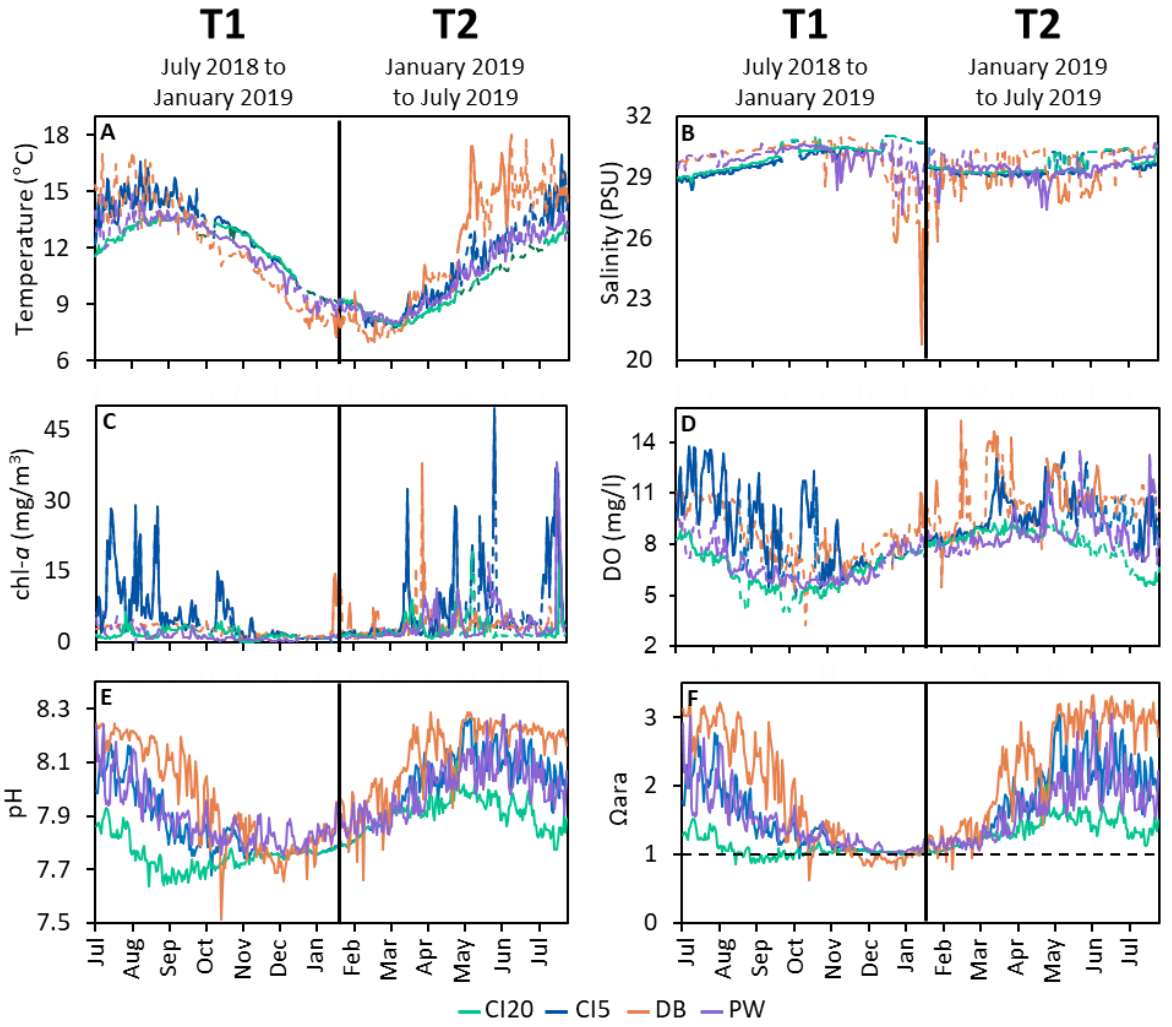

Figure 4-2: Timeseries of oceanographic conditions at four study sites in Puget Sound, Washington, USA. CI20 represents Carr Inlet at 20 m, and CI5 at 5 m. DB is Dabob bay at 5 m, and PW is Point Wells at 5 m. (A) temperature, (B) salinity, (C) chlorophyll-*a*, (D) dissolved

oxygen, (E) pH, and (F) aragonite saturation state (horizontal dotted line represents aragonite saturation horizon). Colors correspond to the different sites. Data from ORCA buoys and the LiveOcean Model were combined and one reading per day at 12:00 PM was plotted. In panels A-D, solid lines indicate that the data was collected in situ from the ORCA buoy locations. Dotted lines represent data from the LiveOcean Model which were added to the graphs during times when the buoys were malfunctioning. Carbonate chemistry (panels E and F) are comprised entirely of LiveOcean data. On each panel, the vertical line down the middle represents the midpoint collection (January 2019) that separates the first (T1) and second half (T2) of the one-year outplant.

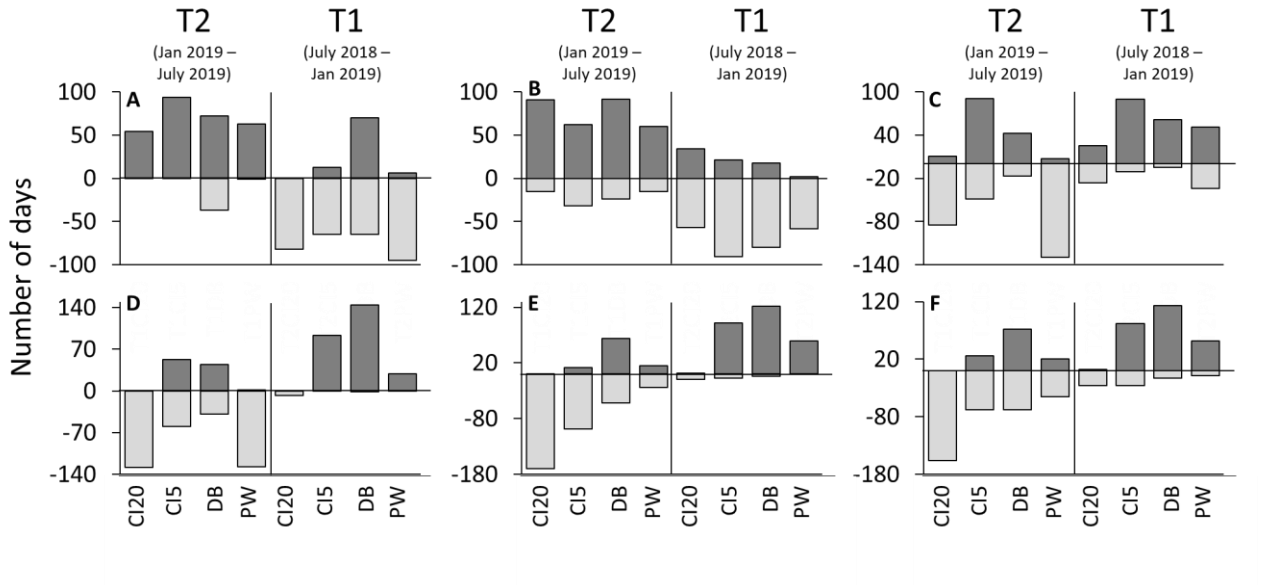

Figure 4-3: Number of days each site was above or below an environmental threshold, chosen with first and third quartiles. Parameters for each panel read as follows: (A) temperature, (B) salinity, (C) chlorophyll-*a*, (D) dissolved oxygen, (E) pH, and (F) aragonite saturation state.

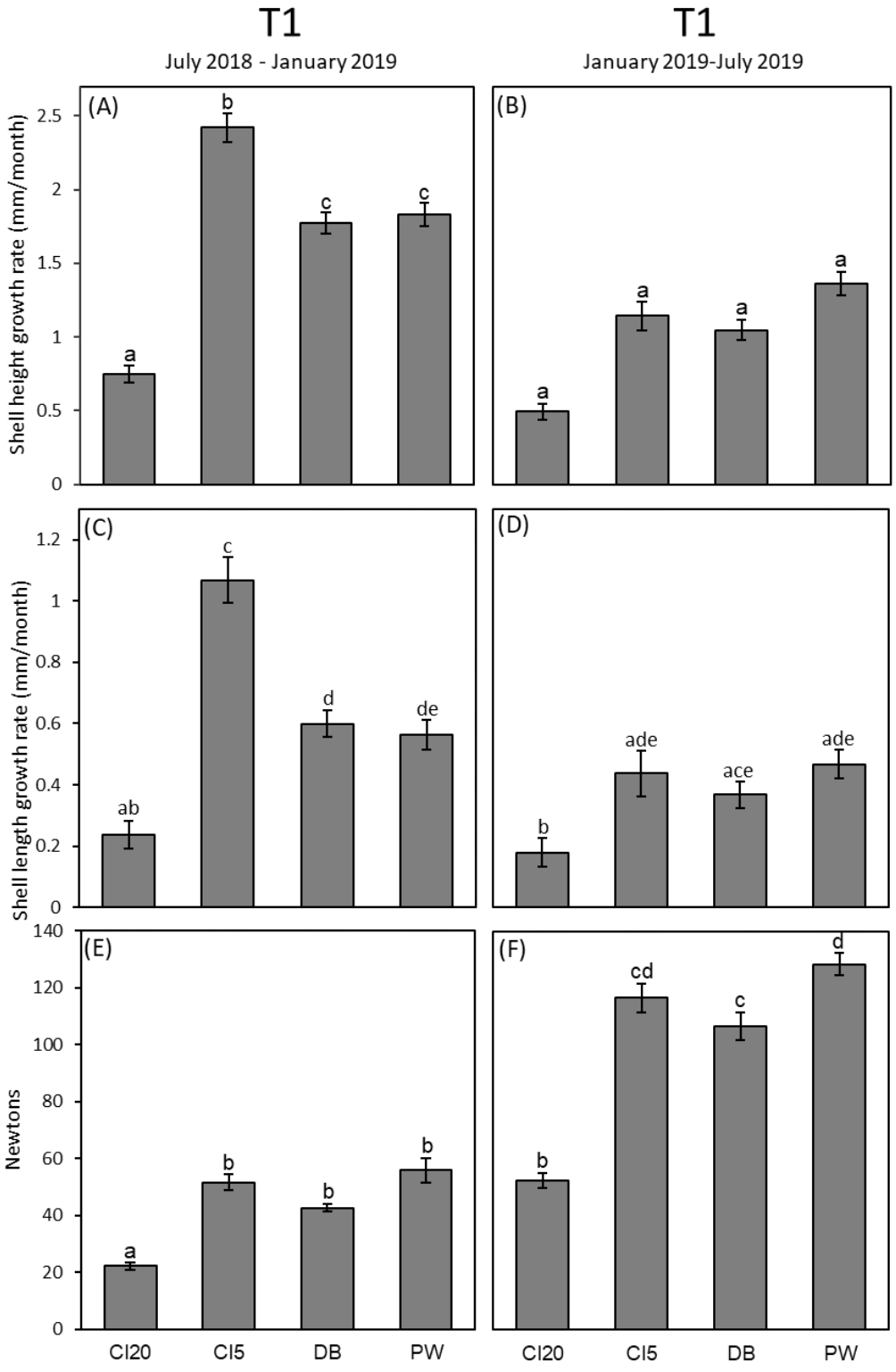

Figure 4-4: *M. galloprovincialis* shell properties at different field sites during two time periods (A, C, E between July 2018-January 2019, and B, D, F between January to July 2019). Shell growth

was measured both heightwise (from hinge to apex, A, B) and lengthwise (anterior to posterior, C, D). Force needed to point-crush a shell (shell strength) was measured using a hydraulic press (E, F). Bars depicted mean with error bars as ± S.E.

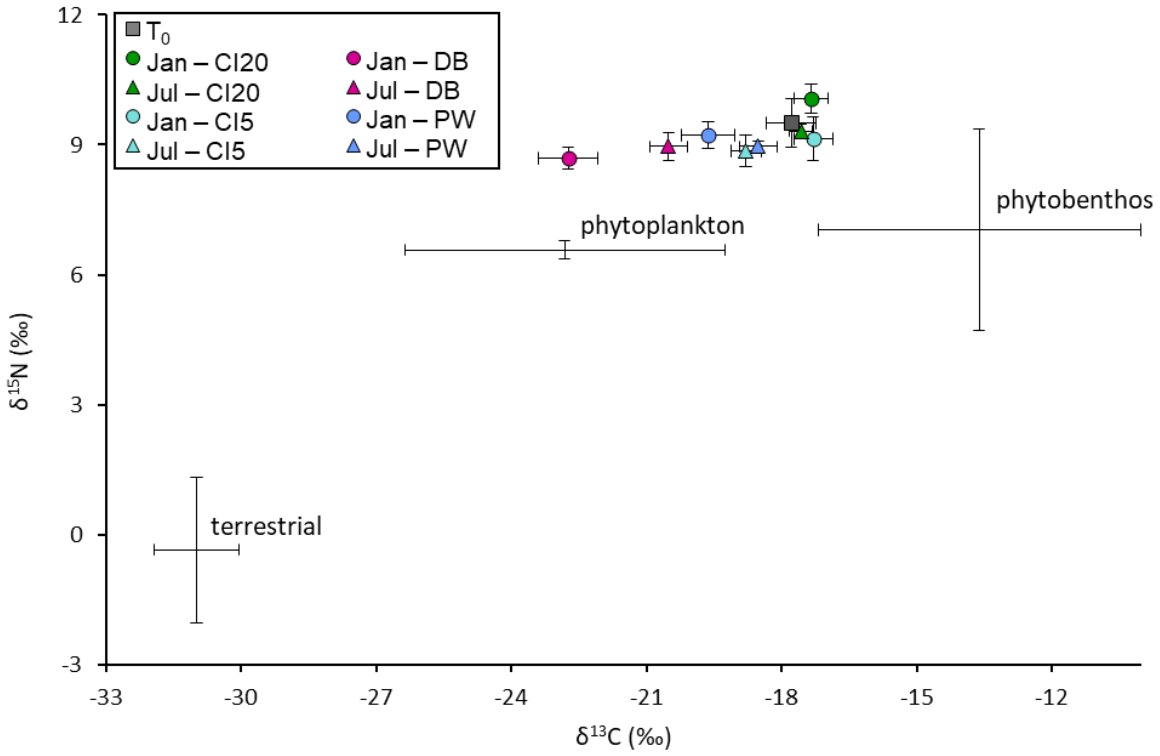

Figure 4-5: Stable isotope C-N biplot depicting $\delta^{15}N$ and $\delta^{13}C$ values (mean ‰ ± S.D.) of consumers (mussels, colored dots represent site, and shapes represent time periods) and end members (diet: terrestrial matter, phytoplankton, and phytobenthos, black crosses). Consumer signatures were not adjusted for trophic enrichment factor in this plot.

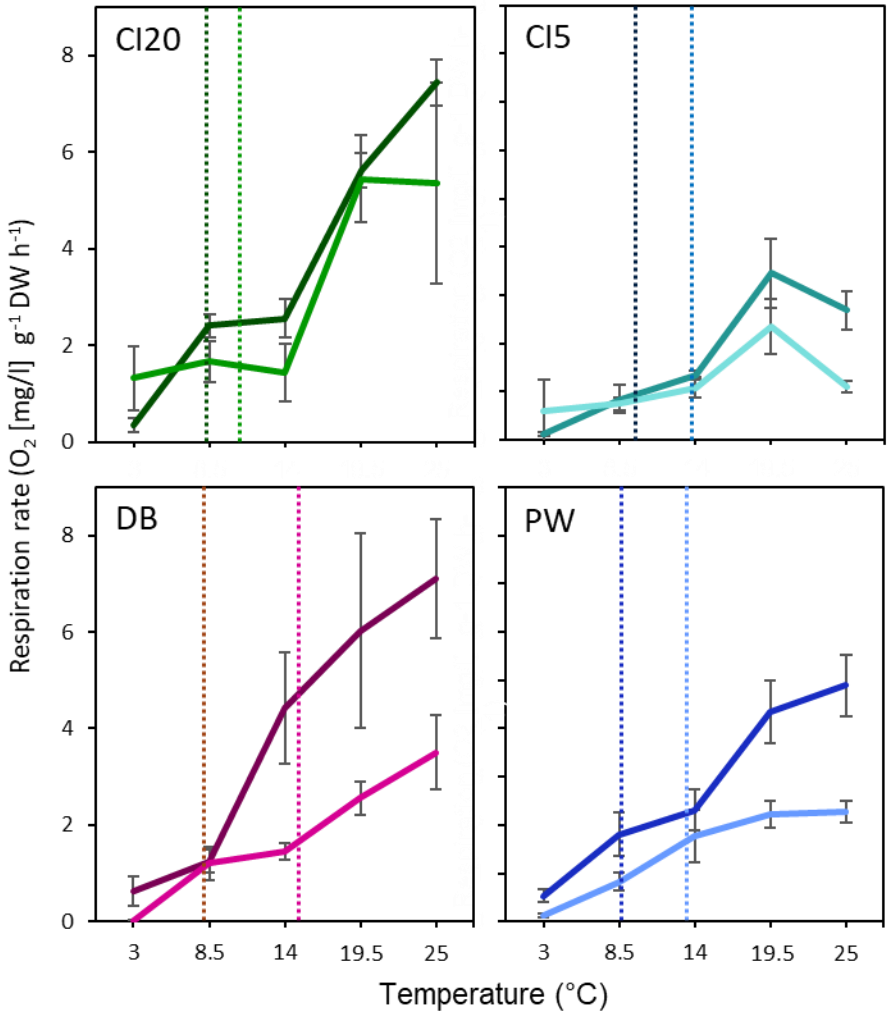

Figure 4-6: Metabolic response of *M. galloprovincialis* to an array of acute (1 hour) temperature scenarios (3 - 25°C). Each panel represents one of the four study sites. Dark colors = January 2019 (T1); light colors = July 2019 (T2). Vertical dotted lines represent temperatures at the collection sites one week prior to collecting the oysters (in January CI20 = 7.8°C, CI5 = 8.1°C, DB = 8.2°C, and PW = 8.0°C; in July CI20 = 11.9°C, CI5 = 13.4°C, DB = 15.2°C, and PW = 13.2°C). Temperature trials were run at pH 7.8. Graph shows mean with standard error (± SE).

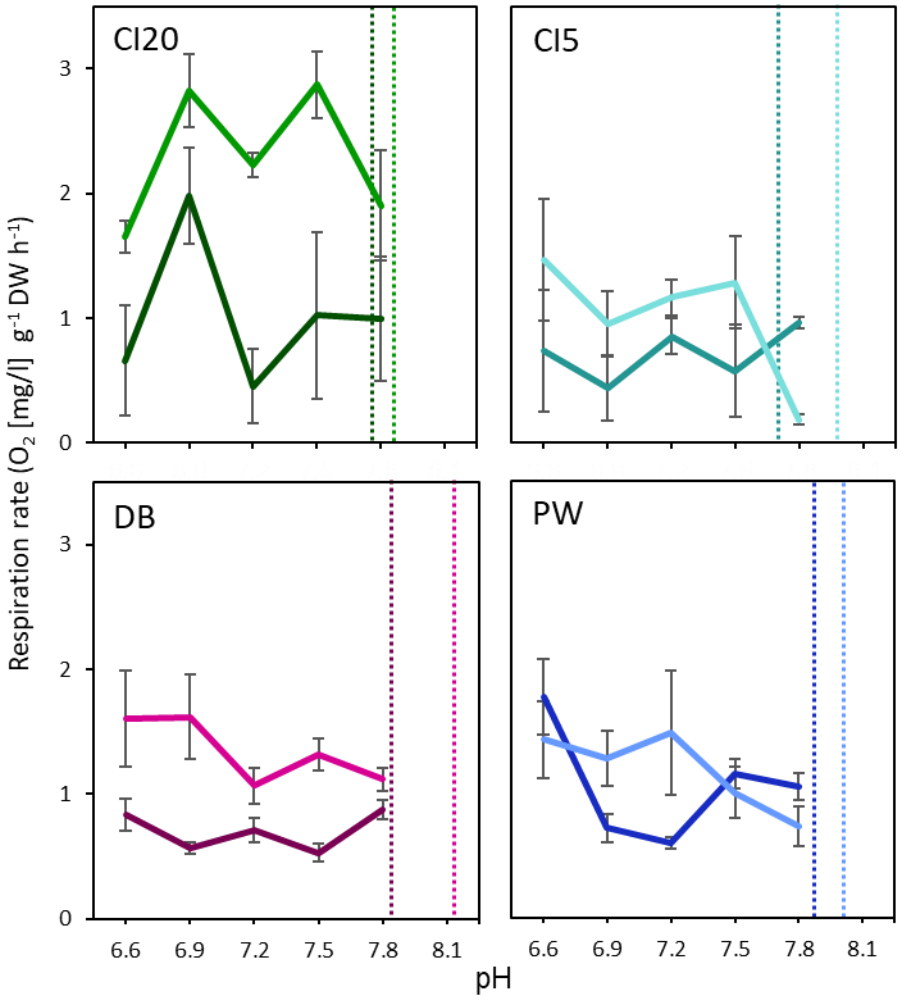

Figure 4-7: Metabolic response of *M. galloprovincialis* to an array of acute (1 hour) pH scenarios (6.6 – 7.8). Each panel represents one of the four study sites. Dark colors = January 2019 (T1); light colors = July 2019 (T2). Vertical dotted lines represent temperatures at the collection sites one week prior to collecting the oysters (in January, CI20 and CI5= 7.76, DB = 7.84, and PW = 7.89; in July CI20 = 7.83, CI5 = 8.07, DB = 8.19, PW = 7.98). pH trials were all run at 11°C. Graph shows mean with standard error (± SE).

Table 4-2: Summary of two and three-way ANOVA statistics used in this study. Significant codes: *** < 0.001, ** 0.001-0.01, ** 0.01-0.05, · 0.05-0.10.

	df	Mean Sq	F	p	Significance
Growth Rate (Height)					
Site	3	5.74	39.40	< 0.001	***
Date	1	18.32	125.71	< 0.001	***

Site:Date	3	0.84	5.73	< 0.001	***
Residuals	688	0.15			
Growth Rate (Length)					
Site	3	4.54	37.17	< 0.001	***
Date	1	13.71	112.36	< 0.001	***
Site:Date	3	0.81	6.67	< 0.001	***
Residuals	694	0.12			
Shell Strength					
Site	3	280921.00	114.03	< 0.001	***
Date	1	1026869.00	416.84	< 0.001	***
Site:Date	3	31945.00	12.97	< 0.001	***
Residuals	1366	2463.00			
Total Lipids					
Site	2	0.00	0.29	0.75	
Date	1	0.01	3.90	0.052	.
Site:Date	2	0.00	0.07	0.93	
Residuals	73	0.00			
$\delta^{13}C$					
Date	2	6.82	31.71	< 0.001	***
Site	3	65.64	305.23	< 0.001	***
Date:Site	3	13.34	62.02	< 0.001	***
Residuals	83	0.22			
$\delta^{15}N$					
Date	2	1.23	9.64	< 0.001	***
Site	3	2.79	21.79	< 0.001	***
Date:Site	3	0.86	6.73	< 0.001	***
Residuals	83	0.13			
C:N					
Date	2	0.99	5.02	0.0088	**
Site	3	4.13	20.98	< 0.001	***
Date:Site	3	0.35	1.75	0.16	
Residuals	83	0.20			
Respiration Rate - Temperature					
Site	3	70.90	19.32	< 0.001	***
Date	1	99.62	27.14	< 0.001	***
Temperature	4	191.43	52.15	< 0.001	***
Site:Date	3	12.71	3.46	0.017	*
Site:Temperature	12	10.04	2.74	0.002	**
Date:Temperature	4	17.44	4.75	0.001	***
Site:Date:Temperature	12	2.33	0.64	0.81	
Residuals	285	3.67			
Respiration Rate - pH					
Site	3	9.02	10.62	< 0.001	***
Date	1	23.77	27.99	< 0.001	***
pH level	4	0.91	1.07	0.37	
Site:Date	3	6.54	7.70	< 0.001	***
Site:pH level	12	2.09	2.46	0.0046	**
Date:pH level	4	1.42	1.67	0.16	
Site:Date:pH level	12	0.64	0.75	0.70	

Residuals	280	0.85	

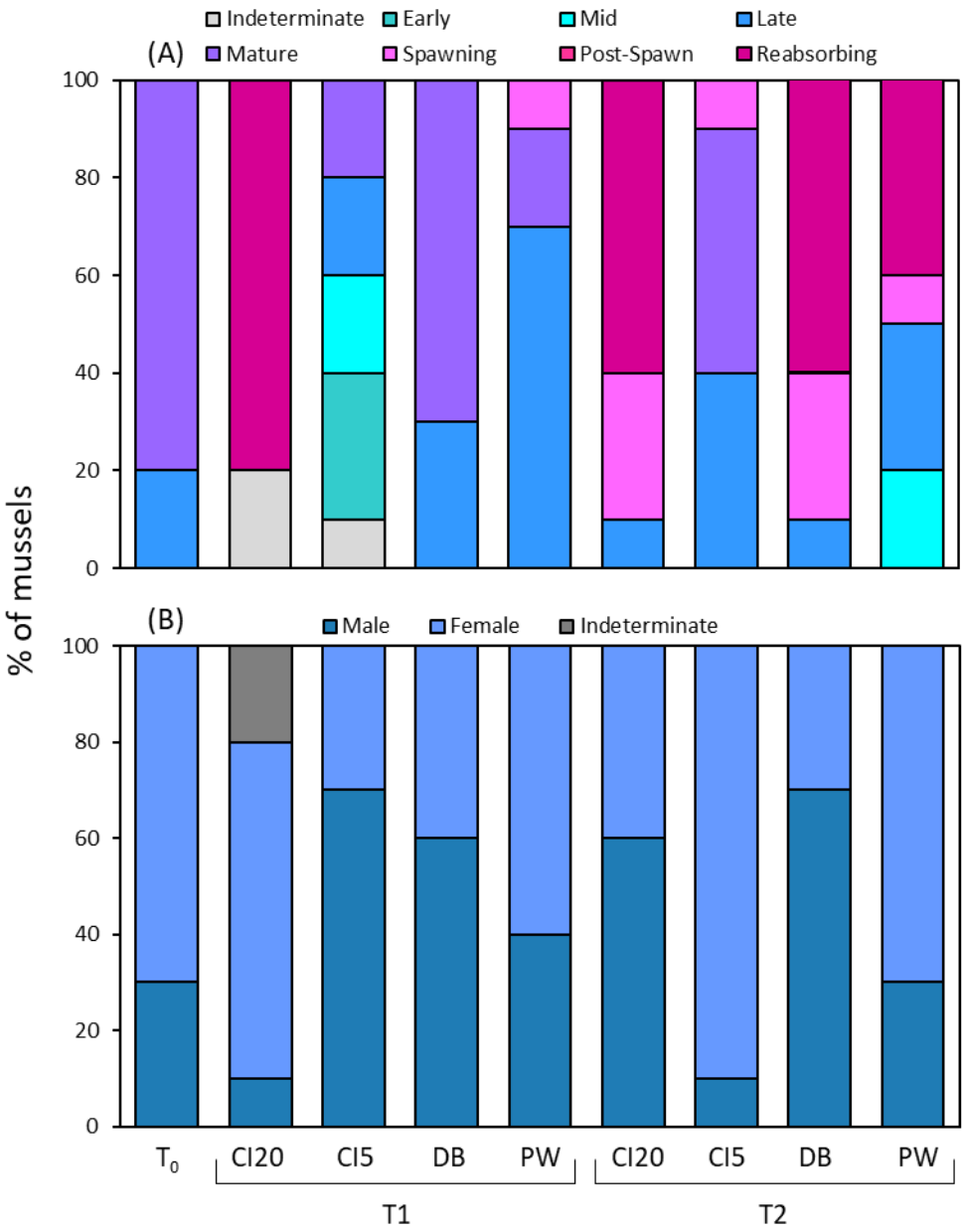

Figure 4-8: (A) Percentage of *M. galloprovincialis* at each ranked gamete maturation ranked stage, sorted by acclimatization site and collection period (n = 10). (B) sex ratio of mussels. T_0 represents mussels evaluated before the study (July 2018). T1 represents the six-month collection period in January 2019. T2 represents the one-year collection period in July 2019. Oysters were outplanted to four sites (CI20: Carr Inlet at 20 m, CI5: Carr Inlet at 5 m, DB: Dabob Bay at 5 m, PW: Point Wells at 5 m).

4.8 REFERENCES

Alma, L., Fiamengo, C. J., Alin, S. R., Jackson, M., Hiromoto, K., & Padilla-Gamiño, J. L. (2022). Physiological Responses of Scallops and Mussels to Environmental Variability: Implications for Future Shellfish Aquaculture. *SSRN Electronic Journal*. https://doi.org/10.2139/ssrn.4033189

Barton, A., Waldbusser, G. G., Feely, R. A., Weisberg, S. B., Newton, J. A., Hales, B., Cudd, S., Eudeline, B., Langdon, C. J., Jefferds, I., King, T., Suhrbier, A., & McLaughlin, K. (2015). Impacts of coastal acidification on the Pacific Northwest shellfish industry and adaptation strategies implemented in response. *Oceanography*, *28*(2), 146–159. https://doi.org/10.5670/oceanog.2015.38

Bass, A., Wernberg, T., Thomsen, M., & Smale, D. (2021). Another Decade of Marine Climate Change Experiments: Trends, Progress and Knowledge Gaps. In *Frontiers in Marine Science*. https://doi.org/10.3389/fmars.2021.714462

Bates, D., Mächler, M., Bolker, B. M., & Walker, S. C. (2015). Fitting linear mixed-effects models using lme4. *Journal of Statistical Software*. https://doi.org/10.18637/jss.v067.i01

Bednaršek, N., Newton, J. A., Beck, M. W., Alin, S. R., Feely, R. A., Christman, N. R., & Klinger, T. (2021). Severe biological effects under present-day estuarine acidification in the seasonally variable Salish Sea. *Science of the Total Environment*. https://doi.org/10.1016/j.scitotenv.2020.142689

Benson, B. B., & Krause, D. (1984). The concentration and isotopic fractionation of oxygen dissolved in freshwater and seawater in equilibrium with the atmosphere. *Limnology and Oceanography*. https://doi.org/10.4319/lo.1984.29.3.0620

Bianucci, L., Long, W., Khangaonkar, T., Pelletier, G., Ahmed, A., Mohamedali, T., Roberts, M., & Figueroa-Kaminsky, C. (2018). Sensitivity of the regional ocean acidification and carbonate system in Puget Sound to ocean and freshwater inputs. *Elementa*. https://doi.org/10.1525/elementa.151

Bligh, E. G., & Dyer, W. J. (1959). a Rapid Method of Total Lipid Extraction and Purification. *Canadian Journal of Biochemistry and Physiology*, *37*(1), 911–917. https://doi.org/10.1139/y59-099

Bond, N. A., Cronin, M. F., Freeland, H., & Mantua, N. (2015). Causes and impacts of the 2014 warm anomaly in the NE Pacific. *Geophysical Research Letters*, *42*(9), 3414–3420. https://doi.org/10.1002/2015GL063306

Braby, C. E., & Somero, G. N. (2006). Ecological gradients and relative abundance of native (*Mytilus trossulu*s) and invasive (*Mytilus galloprovincialis*) blue mussels in the California hybrid zone. *Marine Biology*. https://doi.org/10.1007/s00227-005-0177-0

Breitburg, D. L., Salisbury, J., Bernhard, J. M., Cai, W. J., Dupont, S., Doney, S. C., Kroeker, K. J., Levin, L. A., Long, W. C., Milke, L. M., Miller, S. H., Phelan, B., Passow, U., Seibel, B. A., Todgham, A. E., & Tarrant, A. M. (2015). And on top of all that: Coping with ocean acidification in the midst of many stressors by denise. *Oceanography*, *28*(2), 48–61.

https://doi.org/10.5670/oceanog.2015.31

Buckley, B. A., Owen, M. E., & Hofmann, G. E. (2001). Adjusting the thermostat: The threshold induction temperature for the heat-shock response in intertidal mussels (genus *Mytilus*) changes as a function of thermal history. *Journal of Experimental Biology*. https://doi.org/10.1242/jeb.204.20.3571

Byrne, M. (2011). Impact of ocean warming and ocean acidification on marine invertebrate life history stages: Vulnerabilities and potential for persistence in a changing ocean. *Oceanography and Marine Biology: An Annual Review*, *49*(January), 1–42.

Cai, W. J., Feely, R. A., Testa, J. M., Li, M., Evans, W., Alin, S. R., Xu, Y. Y., Pelletier, G., Ahmed, A., Greeley, D. J., Newton, J. A., & Bednarscaronek, N. (2021). Natural and Anthropogenic Drivers of Acidification in Large Estuaries. *Annual Review of Marine Science*. https://doi.org/10.1146/annurev-marine-010419-011004

Carnarius, K. M., Conrad, K. M., Mast, M. G., & Macneil, J. H. (1996). Relationship of eggshell ultrastructure and shell strength to the soundness of shell eggs. *Poultry Science*, *75*(5), 656–663. https://doi.org/10.3382/ps.0750656

Carrington, E., Waite, J. H., Sarà, G., & Sebens, K. P. (2015). Mussels as a model system for integrative ecomechanics. *Annual Review of Marine Science*, *7*(1), 443–469. https://doi.org/10.1146/annurev-marine-010213-135049

Conway-Cranos, L., Kiffney, P., Banas, N., Plummer, M., Naman, S., MacCready, P., Bucci, J., & Ruckelshaus, M. (2015). Stable isotopes and oceanographic modeling reveal spatial and trophic connectivity among terrestrial, estuarine, and marine environments. *Marine Ecology Progress Series*, *533*, 15–28. https://doi.org/10.3354/meps11318

Core R Team. (2019). A Language and Environment for Statistical Computing. In *R Foundation for Statistical Computing* (Vol. 2, p. https://www.R--project.org). http://www.r-project.org

Costalago, D., Forster, I., Nemcek, N., Neville, C., Perry, R. I., Young, K., & Hunt, B. P. V. (2020). Seasonal and spatial dynamics of the planktonic trophic biomarkers in the Strait of Georgia (northeast Pacific) and implications for fish. *Scientific Reports*. https://doi.org/10.1038/s41598-020-65557-1

da Silva, P. M., Fuentes, J., & Villalba, A. (2009). Differences in gametogenic cycle among strains of the European flat oyster *Ostrea eduli*s and relationship between gametogenesis and bonamiosis. *Aquaculture*. https://doi.org/10.1016/j.aquaculture.2008.10.055

Díaz-Puente, B., Miñambres, M., Rosón, G., Aghzar, A., & Presa, P. (2016). Genetic decoupling of spat origin from hatchery to harvest of *Mytilus galloprovincialis* cultured in suspension. *Aquaculture*, *460*, 124–135. https://doi.org/10.1016/j.aquaculture.2016.04.016

Dickson, A. G., Sabine, C. L., & Christian, J. R. (2007). Guide to Best Practices for Ocean CO_2 measurements. PICES Special Publication. In *Guide to Best Practices for Ocean CO_2 measurements. PICES Special Publication* (Vol. 3, Issue 8).

Domínguez, L., Villalba, A., & Fuentes, J. (2010). Effects of photoperiod and the duration of conditioning on gametogenesis and spawning of the mussel *Mytilus galloprovincialis* (Lamarck). *Aquaculture Research*. https://doi.org/10.1111/j.1365-2109.2010.02601.x

Doney, S. C., Fabry, V. J., Feely, R. A., & Kleypas, J. A. (2009). Ocean acidification: The other CO_2 problem. *Annual Review of Marine Science*, *1*, 169–192. https://doi.org/10.1146/annurev.marine.010908.163834

Dubois, S., Jean-Louis, B., Bertrand, B., & Lefebvre, S. (2007). Isotope trophic-step fractionation of suspension-feeding species: Implications for food partitioning in coastal ecosystems. *Journal of Experimental Marine Biology and Ecology*. https://doi.org/10.1016/j.jembe.2007.06.020

Eccles, J., Greene, C. M., Sobocinski, K., Stevik, B., Carson, H., & ... (2018). Reconstructing historical patterns of primary production in Puget Sound using growth increment data from shells of long-lived geoducks *(Panopea generosa)*. https://cedar.wwu.edu/ssec/2018ssec/allsessions/429/

FAO. (2020). The State of World Fisheries and Aquaculture 2020. Sustainability in action. *FAO*. https://doi.org/https://doi.org/10.4060/ca9229en

Feely, R. A., Alin, S. R., Newton, J., Sabine, C. L., Warner, M., Devol, A., Krembs, C., & Maloy, C. (2010). The combined effects of ocean acidification, mixing, and respiration on pH and carbonate saturation in an urbanized estuary. *Estuarine, Coastal and Shelf Science*, *88*(4), 442–449. https://doi.org/10.1016/j.ecss.2010.05.004

Feely, R. A., Sabine, C. L., Hernandez-Ayon, J. M., Ianson, D., & Hales, B. (2008). Evidence for upwelling of corrosive "acidified" water onto the continental shelf. *Science*, *320*(5882), 1490–1492. https://doi.org/10.1126/science.1155676

Fertig, B., Carruthers, T. J. B., Dennison, W. C., Fertig, E. J., & Altabet, M. A. (2010). Eastern oyster (*Crassostrea virginica*) δ15N as a bioindicator of nitrogen sources: Observations and modeling. *Marine Pollution Bulletin*. https://doi.org/10.1016/j.marpolbul.2010.03.013

Fey, S. B., Kremer, C. T., Layden, T. J., & Vasseur, D. A. (2021). Resolving the consequences of gradual phenotypic plasticity for populations in variable environments. *Ecological Monographs*. https://doi.org/10.1002/ecm.1478

Fitzer, S. C., Torres Gabarda, S., Daly, L., Hughes, B., Dove, M., O'Connor, W., Potts, J., Scanes, P., & Byrne, M. (2018). Coastal acidification impacts on shell mineral structure of bivalve mollusks. *Ecology and Evolution*. https://doi.org/10.1002/ece3.4416

Fitzer, S. C., Zhu, W., Tanner, K. E., Phoenix, V. R., Kamenos, N. A., & Cusack, M. (2015). Ocean acidification alters the material properties of *Mytilus edulis* shells. *Journal of the Royal Society Interface*. https://doi.org/10.1098/rsif.2014.1227

Fly, E. K., Hilbish, T. J., Wethey, D. S., & Rognstad, R. L. (2015). Physiology and biogeography: The response of European Mussels (*Mytilus* spp.) to climate change. *American Malacological Bulletin*. https://doi.org/10.4003/006.033.0111

Ford, S., & Figueras, A. (1988). Effects of sublethal infection by the parasite *Haplosporidium nelsoni* (MSX) on gametogenesis, spawning, and sex ratios of oysters in Delaware Bay, USA. *Diseases of Aquatic Organisms*. https://doi.org/10.3354/dao004121

Forsman, A. (2015). Rethinking phenotypic plasticity and its consequences for individuals, populations and species. In *Heredity*. https://doi.org/10.1038/hdy.2014.92

Fry, B. (2006). Stable isotope ecology. In *Encyclopedia of Ecology*. Springer. https://doi.org/10.1016/B978-0-12-409548-9.10915-7

Fry, B., Mersch, F. J., Tholke, K., Garritt, R., & Brand, W. (1992). Automated Analysis System for Coupled $\delta^{13}C$ and $\delta^{15}N$ Measurements. *Analytical Chemistry*, *64*(3), 288–291. https://doi.org/10.1021/ac00027a009

Gattuso, J.-P., Epitalon, J.-M., & Lavigne, H. (2016). *seacarb: Seawater Carbonate Chemistry R package version 3.0.14* (R package version 3.0.14.). Article R package version 3.0.14. https://cran.r-project.org/package=seacarb

Gazeau, F., Parker, L. M., Comeau, S., Gattuso, J. P., O'Connor, W. A., Martin, S., Pörtner, H. O., & Ross, P. M. (2013). Impacts of ocean acidification on marine shelled molluscs. *Marine Biology*, *160*(8), 2207–2245. https://doi.org/10.1007/s00227-013-2219-3

Goseberg, N., Chambers, M. D., Heasman, K., Fredriksson, D., Fredheim, A., & Schlurmann, T. (2017). Technological approaches to longline- and cage-based aquaculture in open ocean environments. In *Aquaculture Perspective of Multi-Use Sites in the Open Ocean: The Untapped Potential for Marine Resources in the Anthropocene*. https://doi.org/10.1007/978-3-319-51159-7_3

Grear, J., Pimenta, A., Booth, H., Horowitz, D. B., Mendoza, W., & Liebman, M. (2020). In situ recovery of bivalve shell characteristics after temporary exposure to elevated pCO_2. *Limnology and Oceanography*. https://doi.org/10.1002/lno.11456

Green, A. (2014). *Invasive Species Report*. http://media.eol.org/content/2013/07/02/05/62258_260_190.jpg

Gunderson, A. R., Armstrong, E. J., & Stillman, J. H. (2016). Multiple Stressors in a Changing World: The Need for an Improved Perspective on Physiological Responses to the Dynamic Marine Environment. *Annual Review of Marine Science*, *8*, 357–378. https://doi.org/10.1146/annurev-marine-122414-033953

Gurr, S. J., Goleski, J., Lima, F. P., Seabra, R., Gobler, C. J., & Volkenborn, N. (2018). Cardiac responses of the bay scallop *Argopecten irradians* to diel-cycling hypoxia. *Journal of Experimental Marine Biology and Ecology*, *500*, 18–29. https://doi.org/10.1016/j.jembe.2017.12.011

Hassan, M. M., Qin, J. G., & Li, X. (2018a). Gametogenesis, sex ratio and energy metabolism in *Ostrea angasi*: Implications for the reproductive strategy of spermcasting marine bivalves. *Journal of Molluscan Studies*, *84*(1), 38–45. https://doi.org/10.1093/mollus/eyx041

Hatzonikolakis, Y., Tsiaras, K., Theodorou, J. A., Petihakis, G., Sofianos, S., & Triantafyllou, G. (2017). Simulation of mussel *Mytilus galloprovincialis* growth with a dynamic energy budget model in Maliakos and Thermaikos Gulfs (Eastern mediterranean). *Aquaculture Environment Interactions*. https://doi.org/10.3354/aei00236

Hofmann, G. E., Barry, J. P., Edmunds, P. J., Gates, R. D., Hutchins, D. A., Klinger, T., & Sewell, M. A. (2010). The effect of Ocean acidification on calcifying organisms in marine ecosystems: An organism-to-ecosystem perspective. *Annual Review of Ecology, Evolution, and Systematics*. https://doi.org/10.1146/annurev.ecolsys.110308.120227

Hofmann, G. E., & Todgham, A. E. (2009). Living in the now: Physiological mechanisms to tolerate a rapidly changing environment. In *Annual Review of Physiology*. https://doi.org/10.1146/annurev-physiol-021909-135900

Howe, E., & Simenstad, C. A. (2015). Using Isotopic Measures of Connectivity and Ecosystem Capacity to Compare Restoring and Natural Marshes in the Skokomish River Estuary, WA, USA. *Estuaries and Coasts*, *38*(2), 639–658. https://doi.org/10.1007/s12237-014-9831-4

IdHalla, M., Nhhala, H., Kassila, J., Ait Chatou, E. M., Orbi, A., & Moukrim, A. (2017). Comparative production of two mussel species (*Perna perna* and *Mytilus galloprovincialis*) reared on an offshore submerged longline system in Agadir, Morocco. *International Journal of Scientific & Engineering Research*.

Ikejima, I., Nomoto, R., & McCabe, J. F. (2003). Shear punch strength and flexural strength of model composites with varying filler volume fraction, particle size and silanation. *Dental Materials*, *19*(3), 206–211. https://doi.org/10.1016/S0109-5641(02)00031-3

IPCC. (2019). The Ocean and Cryosphere in a Changing Climate. *Intergovernmental Panel on Climate Change*.

Jutfelt, F., Norin, T., Ern, R., Overgaard, J., Wang, T., McKenzie, D. J., Lefevre, S., Nilsson, G. E., Metcalfe, N. B., Hickey, A. J. R., Brijs, J., Speers-Roesch, B., Roche, D. G., Gamperl, A. K., Raby, G. D., Morgan, R., Esbaugh, A. J., Gräns, A., Axelsson, M., … Clark, T. D. (2018). Oxygen- and capacity-limited thermal tolerance: Blurring ecology and physiology. In *Journal of Experimental Biology*. https://doi.org/10.1242/jeb.169615

Kasai, A., & Nakata, A. (2005). Utilization of terrestrial organic matter by the bivalve *Corbicula japonic*a estimated from stable isotope analysis. *Fisheries Science*. https://doi.org/10.1111/j.1444-2906.2005.00942.x

Kellermann, V., Chown, S. L., Schou, M. F., Aitkenhead, I., Janion-Scheepers, C., Clemson, A., Scott, M. T., & Sgrò, C. M. (2019). Comparing thermal performance curves across traits: How consistent are they? *Journal of Experimental Biology*, *222*(11). https://doi.org/10.1242/jeb.193433

Khangaonkar, T., Nugraha, A., Yun, S. K., Premathilake, L., Keister, J. E., & Bos, J. (2021). Propagation of the 2014–2016 Northeast Pacific Marine Heatwave Through the Salish Sea. *Frontiers in Marine Science*, *8*. https://doi.org/10.3389/FMARS.2021.787604

Kooijman, S. (2010). Dynamic Energy Budget Theory for Metabolic Organization. *Zhurnal Eksperimental'noi i Teoreticheskoi Fiziki*.

Kwiatkowski, L., Torres, O., Bopp, L., Aumont, O., Chamberlain, M., R. Christian, J., P. Dunne, J., Gehlen, M., Ilyina, T., G. John, J., Lenton, A., Li, H., S. Lovenduski, N., C. Orr, J., Palmieri, J., Santana-Falcón, Y., Schwinger, J., Séférian, R., A. Stock, C., … Ziehn, T. (2020). Twenty-first century ocean warming, acidification, deoxygenation, and upper-ocean nutrient and primary production decline from CMIP6 model projections. *Biogeosciences*. https://doi.org/10.5194/bg-17-3439-2020

Lannig, G., Eilers, S., Pörtner, H. O., Sokolova, I. M., & Bock, C. (2010). Impact of ocean acidification on energy metabolism of oyster, *Crassostrea gigas* - Changes in metabolic

pathways and thermal response. *Marine Drugs*. https://doi.org/10.3390/md8082318

Lefevre, S. (2016). Are global warming and ocean acidification conspiring against marine ectotherms? A meta-analysis of the respiratory effects of elevated temperature, high CO_2 and their interaction. *Conservation Physiology*. https://doi.org/10.1093/conphys/cow009

Li, A., Li, L., Song, K., Wang, W., & Zhang, G. (2017). Temperature, energy metabolism, and adaptive divergence in two oyster subspecies. *Ecology and Evolution*. https://doi.org/10.1002/ece3.3085

Liedtke, T., Smith, C., & Rondorf, D. (2011). Stable isotopes of nitrogen and carbon as tools to monitor eutrophication and trophic dynamics. *Hydrography of and Biochemical Inputs to Liberty Bay, a Small Urban Embayment in Puget Sound, Washington*, 69–84.

Lins, D. M., Zbawicka, M., Wenne, R., Poćwierz-Kotus, A., Molina, J. R. A., Alves, L. P., & Rocha, R. M. (2021). Ecology and genetics of *Mytilus galloprovincialis*: A threat to bivalve aquaculture in southern Brazil. *Aquaculture*. https://doi.org/10.1016/j.aquaculture.2021.736753

Lockwood, B. L., & Somero, G. N. (2011). Invasive and native blue mussels (genus *Mytilus*) on the California coast: The role of physiology in a biological invasion. *Journal of Experimental Marine Biology and Ecology*, *400*(1–2), 167–174. https://doi.org/10.1016/j.jembe.2011.02.022

Lowe, S., Browne, M., Boudjelas, S., & De Poorter, M. (2000). 100 of the world's worst invasive species. *Aliens*.

MacCready, P., McCabe, R. M., Siedlecki, S. A., Lorenz, M., Giddings, S. N., Bos, J., Albertson, S., Banas, N. S., & Garnier, S. (2021). Estuarine Circulation, Mixing, and Residence Times in the Salish Sea. *Journal of Geophysical Research: Oceans*, *126*(2). https://doi.org/10.1029/2020JC016738

Mascorda Cabre, L., Hosegood, P., Attrill, M. J., Bridger, D., & Sheehan, E. V. (2021). Offshore longline mussel farms: a review of oceanographic and ecological interactions to inform future research needs, policy and management. In *Reviews in Aquaculture*. https://doi.org/10.1111/raq.12549

Matoo, O. B., Lannig, G., Bock, C., & Sokolova, I. M. (2021). Temperature but not ocean acidification affects energy metabolism and enzyme activities in the blue mussel, *Mytilus edulis*. *Ecology and Evolution*. https://doi.org/10.1002/ece3.7289

McMahon, K. W., Ambrose, W. G., Reynolds, M. J., Johnson, B. J., Whiting, A., & Clough, L. M. (2021). Arctic lagoon and nearshore food webs: Relative contributions of terrestrial organic matter, phytoplankton, and phytobenthos vary with consumer foraging dynamics. *Estuarine, Coastal and Shelf Science*. https://doi.org/10.1016/j.ecss.2021.107388

Melzner, F., Mark, F. C., Seibel, B. A., & Tomanek, L. (2020). Ocean Acidification and Coastal Marine Invertebrates: Tracking CO_2 Effects from Seawater to the Cell. In *Annual Review of Marine Science*. https://doi.org/10.1146/annurev-marine-010419-010658

Melzner, F., Stange, P., Trübenbach, K., Thomsen, J., Casties, I., Panknin, U., Gorb, S. N., & Gutowska, M. A. (2011). Food supply and seawater pCO 2 impact calcification and internal

shell dissolution in the blue mussel *Mytilus edulis*. *PLoS ONE*, *6*(9). https://doi.org/10.1371/journal.pone.0024223

Michener, R., & Lajtha, K. (2008). Stable Isotopes in Ecology and Environmental Science: Second Edition. In *Stable Isotopes in Ecology and Environmental Science: Second Edition*. https://doi.org/10.1002/9780470691854

Millo, C., Bravo, C., Covelli, S., Pavoni, E., Petranich, E., Contin, M., De Nobili, M., Crosera, M., Otero Sutti, B., Das Mercês Silva, C., & Braga, E. de S. (2021). Metal binding and sources of humic substances in recent sediments from the cananéia-iguape estuarine-lagoon complex (South-eastern brazil). *Applied Sciences (Switzerland)*. https://doi.org/10.3390/app11188466

Mizuta, D. D., & Wikfors, G. H. (2019). Depth selection and in situ validation for offshore mussel aquaculture in Northeast United States federal waters. *Journal of Marine Science and Engineering*. https://doi.org/10.3390/jmse7090293

Montory, J. A., Chaparro, O. R., Salas-Yanquin, L. P., Buchner-Miranda, J. A., Pechenik, J. A., & Cubillos, V. M. (2021). Impact of Intertidal Distribution on the Physiological Performance of the Filter-Feeder Bivalve *Perumytilus purpuratus* (Bivalvia, Mytilidae) from Southern Chile. *Malacologia*. https://doi.org/10.4002/040.064.0108

Mueller, S. (2017). Morphological and trophic differences between kelp crabs (Pugettia producta) inhabiting kelp and pilings

Múgica, M., Sokolova, I. M., Izagirre, U., & Marigómez, I. (2015). Season-dependent effects of elevated temperature on stress biomarkers, energy metabolism and gamete development in mussels. *Marine Environmental Research*, *103*, 1–10. https://doi.org/10.1016/j.marenvres.2014.10.005

Nagarajan, R., Lea, S. E. G., & Goss-Custard, J. D. (2006). Seasonal variations in mussel, *Mytilus edulis* L. shell thickness and strength and their ecological implications. *Journal of Experimental Marine Biology and Ecology*, *339*(2), 241–250. https://doi.org/10.1016/J.JEMBE.2006.08.001

Osland, M. J., Enwright, N. M., Day, R. H., Gabler, C. A., Stagg, C. L., & Grace, J. B. (2016). Beyond just sea-level rise: Considering macroclimatic drivers within coastal wetland vulnerability assessments to climate change. In *Global Change Biology*. https://doi.org/10.1111/gcb.13084

Paolucci, E. M., Ron, L., & Thuesen, E. V. (2022). Metabolic response to increasing environmental temperature in the invasive mussel Limnoperna fortunei. *Austral Ecology*, 1–10. https://doi.org/10.1111/aec.13161

Parker, L. M., Ross, P. M., O'Connor, W. A., Pörtner, H. O., Scanes, E., & Wright, J. M. (2013). Predicting the response of molluscs to the impact of ocean acidification. In *Biology*. https://doi.org/10.3390/biology2020651

Parker, L. M., Scanes, E., O'Connor, W. A., Coleman, R. A., Byrne, M., Pörtner, H. O., & Ross, P. M. (2017). Ocean acidification narrows the acute thermal and salinity tolerance of the Sydney rock oyster *Saccostrea glomerata*. *Marine Pollution Bulletin*, *122*(1–2), 263–271.

https://doi.org/10.1016/j.marpolbul.2017.06.052

Pelletier, G., Roberts, M., Keyzers, M., & Alin, S. R. (2018). Seasonal variation in aragonite saturation in surface waters of Puget Sound - A pilot study. *Elementa*. https://doi.org/10.1525/elementa.270

Petes, L. E., Menge, B. A., & Harris, A. L. (2008). Intertidal mussels exhibit energetic trade-offs between reproduction and stress resistance. *Ecological Monographs*. https://doi.org/10.1890/07-0605.1

Piola, R. F., Moore, S. K., & Suthers, I. M. (2006). Carbon and nitrogen stable isotope analysis of three types of oyster tissue in an impacted estuary. *Estuarine, Coastal and Shelf Science*, *66*(1–2), 255–266. https://doi.org/10.1016/j.ecss.2005.08.013

Pörtner, H. (2001). Climate change and temperature-dependent biogeography: Oxygen limitation of thermal tolerance in animals. In *Naturwissenschaften* (Vol. 88, Issue 4, pp. 137–146). https://doi.org/10.1007/s001140100216

Pörtner, H. O. (2008). Ecosystem effects of ocean acidification in times of ocean warming: A physiologist's view. *Marine Ecology Progress Series*, *373*, 203–217. https://doi.org/10.3354/meps07768

Pörtner, H. O., Bock, C., & Mark, F. C. (2018). Connecting to ecology: A challenge for comparative physiologists? Response to "Oxygen- and capacity-limited thermal tolerance: Blurring ecology and physiology." In *Journal of Experimental Biology*. https://doi.org/10.1242/jeb.174185

Pouvreau, S., Bourles, Y., Lefebvre, S., Gangnery, A., & Alunno-Bruscia, M. (2006). Application of a dynamic energy budget model to the Pacific oyster, *Crassostrea gigas*, reared under various environmental conditions. *Journal of Sea Research*, *56*(2), 156–167. https://doi.org/10.1016/j.seares.2006.03.007

Raymond, W. W., Barber, J. S., Dethier, M. N., Hayford, H. A., Harley, C. D. G., King, T. L., Paul, B., Speck, C. A., Tobin, E. D., Raymond, A. E. T., & McDonald, P. S. (2022). Assessment of the impacts of an unprecedented heatwave on intertidal shellfish of the Salish Sea. *Ecology, December 2021*, 1–7. https://doi.org/10.1002/ecy.3798

Reum, J. C. P., Alin, S. R., Feely, R. A., Newton, J., Warner, M., & McElhany, P. (2014). Seasonal carbonate chemistry covariation with temperature, oxygen, and salinity in a fjord estuary: Implications for the design of ocean acidification experiments. *PLoS ONE*, *9*(2). https://doi.org/10.1371/journal.pone.0089619

Reusch, T. B. H. (2014). Climate change in the oceans: Evolutionary versus phenotypically plastic responses of marine animals and plants. *Evolutionary Applications*, *7*(1), 104–122. https://doi.org/10.1111/eva.12109

Rosland, R., Strand, Alunno-Bruscia, M., Bacher, C., & Strohmeier, T. (2009). Applying Dynamic Energy Budget (DEB) theory to simulate growth and bio-energetics of blue mussels under low seston conditions. *Journal of Sea Research*, *62*(2–3), 49–61. https://doi.org/10.1016/j.seares.2009.02.007

Schlesinger, W. H., & Bernhardt, E. S. (2013). Biogeochemistry: An Analysis of Global Change,

Third Edition. In *Biogeochemistry: An Analysis of Global Change, Third Edition*. https://doi.org/10.1016/C2010-0-66291-2

Schulte, P. M. (2015). The effects of temperature on aerobic metabolism: Towards a mechanistic understanding of the responses of ectotherms to a changing environment. *Journal of Experimental Biology*, *218*(12), 1856–1866. https://doi.org/10.1242/jeb.118851

Sebens, K. P., Sarà, G., & Carrington, E. (2018). Estimation of fitness from energetics and life-history data: An example using mussels. *Ecology and Evolution*, *8*(11), 5279–5290. https://doi.org/10.1002/ece3.4004

Simenstad, C., & Wissmar, R. (1985). $\delta^{13}C$ evidence of the origins and fates of organic carbon in estuarine and near-shore food webs. *Marine Ecology Progress Series*, *22*, 141–152. https://doi.org/10.3354/meps022141

Smart, D. C. (2019). *Local Adaptation of the Blue Mussel (Mytilus galloprovincialis) in Southern New Zealand*. *May*.

Smart, D. C., Heenan, S., Lokman, P. M., & Lamare, M. D. (2021). Seasonal reproduction of the blue mussel (*Mytilus galloprovincialis*) from two locations in southern New Zealand. *New Zealand Journal of Marine and Freshwater Research*. https://doi.org/10.1080/00288330.2020.1757472

Sokolova, I. M. (2013). Energy-limited tolerance to stress as a conceptual framework to integrate the effects of multiple stressors. *Integrative and Comparative Biology*, *53*(4), 597–608. https://doi.org/10.1093/icb/ict028

Sokolova, I. M., Frederich, M., Bagwe, R., Lannig, G., & Sukhotin, A. A. (2012). Energy homeostasis as an integrative tool for assessing limits of environmental stress tolerance in aquatic invertebrates. *Marine Environmental Research*, *79*, 1–15. https://doi.org/10.1016/j.marenvres.2012.04.003

Spencer, L. H., Horkan, E., Crim, R., & Roberts, S. B. (2021). Latent effects of winter warming on Olympia oyster reproduction and larval viability. *Journal of Experimental Marine Biology and Ecology*. https://doi.org/10.1016/j.jembe.2021.151604

Spencer, L. H., Venkataraman, Y. R., Crim, R., Ryan, S., Horwith, M. J., & Roberts, S. B. (2020). Carryover effects of temperature and pCO_2 across multiple Olympia oyster populations. *Ecological Applications*. https://doi.org/10.1002/eap.2060

State, C., Resources, W., & Board, C. (2011). *Status and Understanding of Groundwater Quality in the San Diego Drainages Hydrogeologic Provice, 2004: California GAMA Priority Basin Project*.

Suárez, M. P., Alvarez, C., Molist, P., & San Juan, F. (2005). Particular aspects of gonadal cycle and seasonal distribution of gametogenic stages of Mytilus galloprovincialis cultured in the estuary of Vigo. *Journal of Shellfish Research*. https://doi.org/10.2983/0730-8000(2005)24[531:PAOGCA]2.0.CO;2

Taiyun, W. (2014). Visualization of a correlation matrix. *CRAN*. http://cran.r-project.org/web/packages/corrplot/

Tamburini, E., Turolla, E., Fano, E. A., & Castaldelli, G. (2020). Sustainability of Mussel (*Mytilus galloprovincialis*) farming in the Po River delta, northern Italy, based on a life cycle assessment approach. *Sustainability (Switzerland)*. https://doi.org/10.3390/su12093814

Tan, K., Zhang, H., & Zheng, H. (2020). Selective breeding of edible bivalves and its implication of global climate change. In *Reviews in Aquaculture*. https://doi.org/10.1111/raq.12458

Tan, K., & Zheng, H. (2020). Ocean acidification and adaptive bivalve farming. In *Science of the Total Environment*. https://doi.org/10.1016/j.scitotenv.2019.134794

Todgham, A. E., & Stillman, J. H. (2013). Physiological responses to shifts in multiple environmental stressors: Relevance in a changing world. *Integrative and Comparative Biology*, *53*(4), 539–544. https://doi.org/10.1093/icb/ict086

Villalba, A. (1995). Gametogenic cycle of cultured mussel, *Mytilus galloprovincialis*, in the bays of Galicia (N.W. Spain). *Aquaculture*. https://doi.org/10.1016/0044-8486(94)00213-8

Wallace, R. B., Baumann, H., Grear, J. S., Aller, R. C., & Gobler, C. J. (2014). Coastal ocean acidification: The other eutrophication problem. *Estuarine, Coastal and Shelf Science*. https://doi.org/10.1016/j.ecss.2014.05.027

Washington Sea Grant. (2015). *Shellfish Aquaculture in Washington State. December*, 1–84. https://wsg.washington.edu/shellfish-aquaculture

Washington State Blue Ribbon Panel on Ocean Acidification. (2012). *Ocean Acidification : From Knowledge to Action. Washington State's Strategic Response.* (Issue November).

Wernberg, T., Smale, D. A., & Thomsen, M. S. (2012). A decade of climate change experiments on marine organisms: Procedures, patterns and problems. In *Global Change Biology* (Vol. 18, Issue 5, pp. 1491–1498). https://doi.org/10.1111/j.1365-2486.2012.02656.x

Wilkie, E. M., & Bishop, M. J. (2012). Differences in shell strength of native and non-native oysters do not extend to size classes that are susceptible to a generalist predator. *Marine and Freshwater Research*, *63*(12), 1201–1205. https://doi.org/10.1071/MF12078

Wu, F., Sokolov, E. P., Dellwig, O., & Sokolova, I. M. (2021). Season-dependent effects of ZnO nanoparticles and elevated temperature on bioenergetics of the blue mussel *Mytilus edulis*. *Chemosphere*. https://doi.org/10.1016/j.chemosphere.2020.127780

5 APPENDEX

5.1 APPENDIX S1

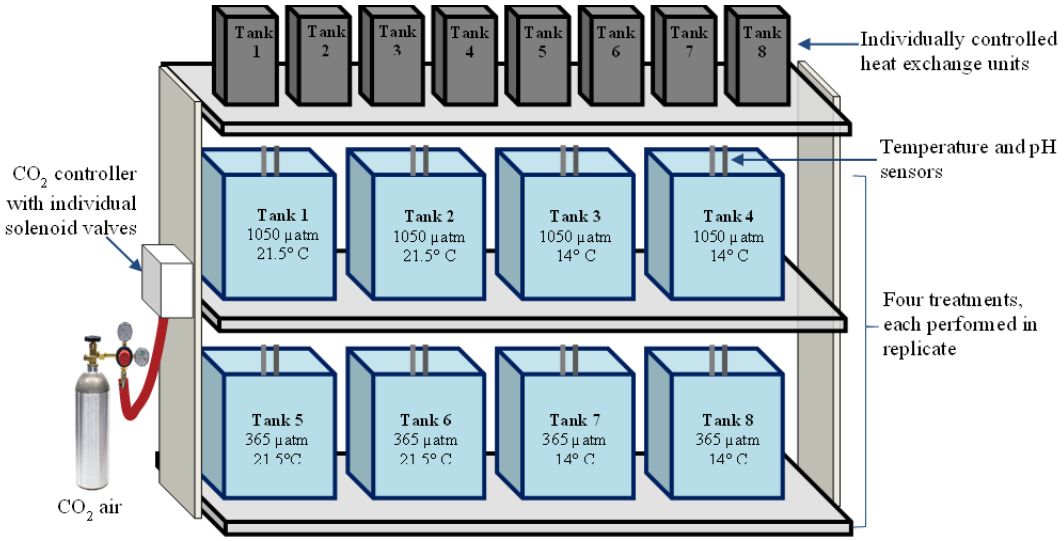

Figure S1-1: Schematic of the experimental system. Each treatment was set up in replicate and individually manipulated/controlled for pCO_2 using a computerized solenoid system, and temperature using multiple heat exchangers.

Table S5-1-1: Seawater chemistry for the six-week experimental treatments of C. gigantea (mean ± s.d.).

Treatment	21.5°C/1050 µatm	21.5°C/365 µatm	14°C/1050 µatm	14°C/365 µatm
Salinity (PSU)	33 ± 0.54	33 ± 0.65	33 ± 0.61	33 ± 0.47
Temperature (°C)	21.5 ± 0.03	21.5 ± 0.03	14 ± 0.03	14 ± 0.02
pH	7.6 ± 0.02	8 ± 0.04	7.6 ± 0.02	8 ± 0.01
pCO2 (µatm)	1027.9 ± 125.7	365.7 ± 40.0	1099 ± 64.4	366 ± 35.6
TA (µmol kg^{-1})	1808.3 ± 125.7	1786.1 ± 64.5	2062.8 ± 37.8	1859.4 ± 37.5
Ω_{cal}	1.46 ± 0.17	3.15 ± 0.41	1.32 ± 0.09	2.63 ± 0.10
Ω_{ara}	0.95 ± 0.16	2.06 ± 0.26	0.84 ± 0.13	1.68 ± 0.17

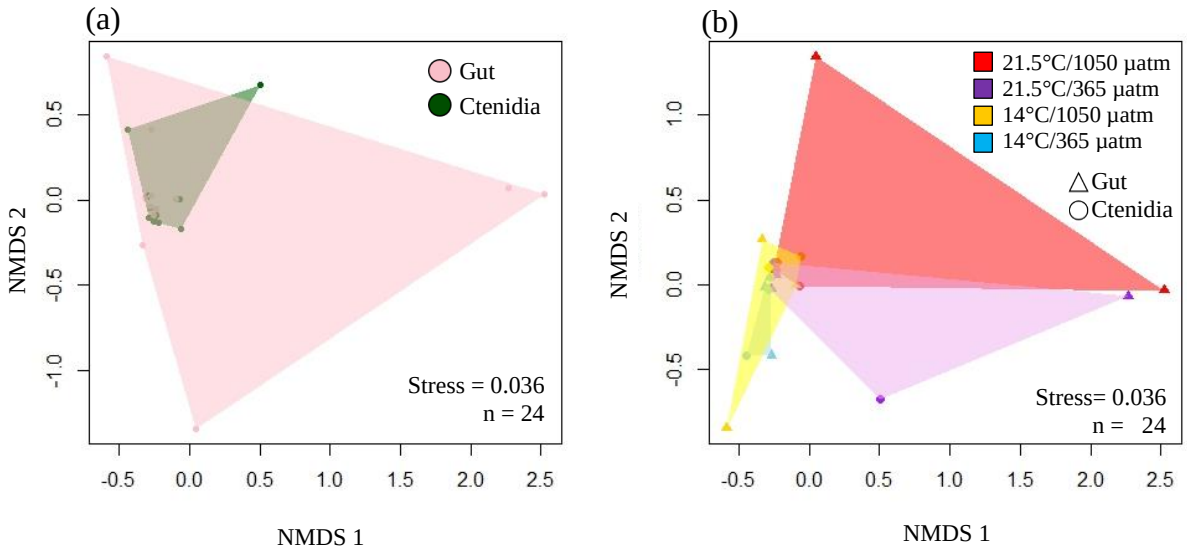

Figure S1-2: NMDS plot of microbial community diversity (a) in gut and ctenidia, regardless of treatment or (b) between treatments.

5.2 APPENDIX S2

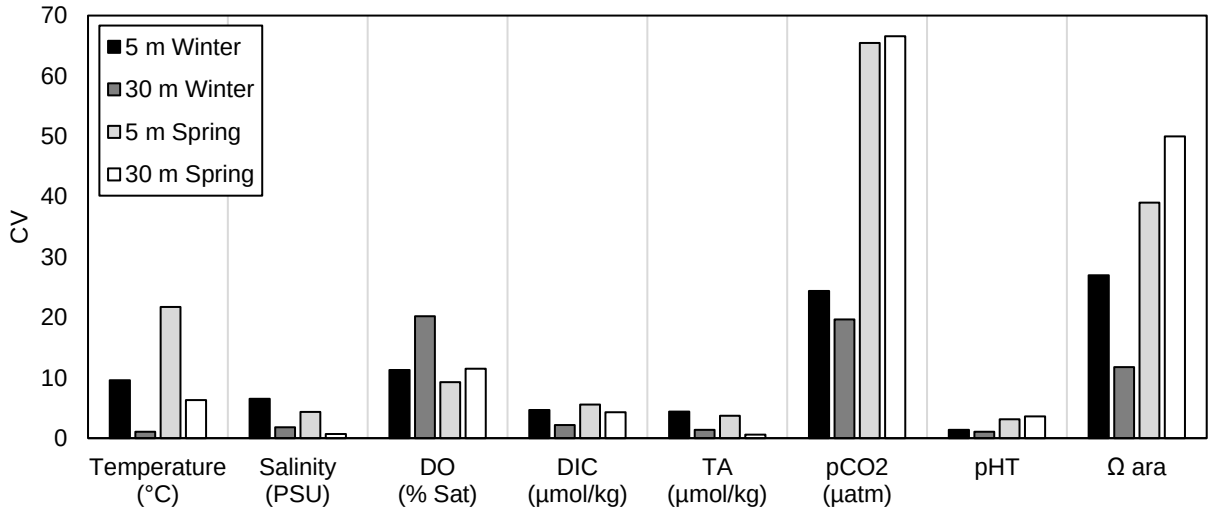

Figure S2-1: Coefficient of variation (CV) of oceanographic parameters. A higher CV value indicates higher environmental variation. Abbreviations are as follows: dissolved oxygen (DO), dissolved inorganic carbon (DIC), total alkalinity (TA), partial pressure of carbon dioxide (pCO_2), and aragonite saturation state (Ωara).

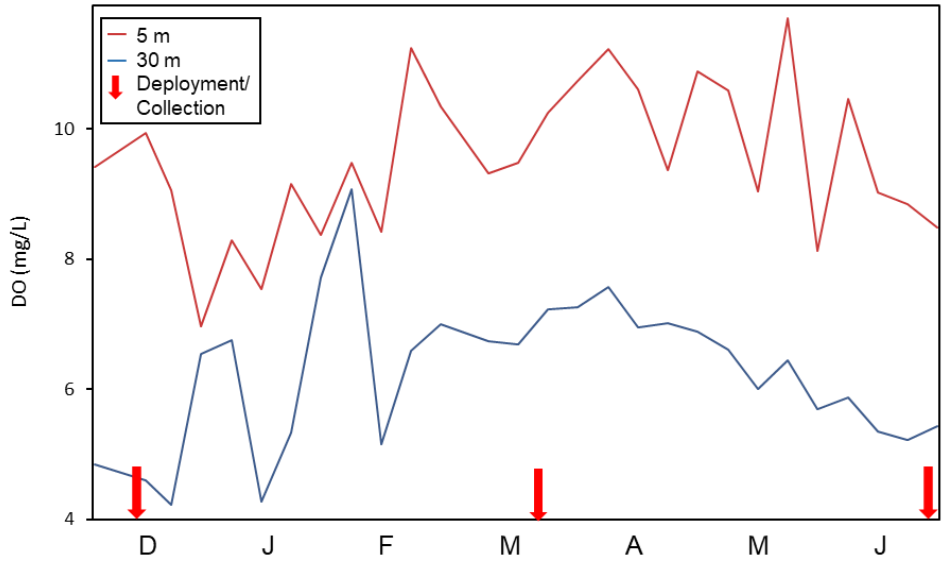

Figure S2-2: This data shows dissolved oxygen levels in mg/L at our study site in Dabob Bay at 5 and 30 m depth. Units were converted from % saturation to mg/L using equation from USGS

(2012), taking into account temperature and salinity. Arrows show the time when organisms were deployed (December 11, 2016) and collected (March 22, 2017 and June 27, 2017).

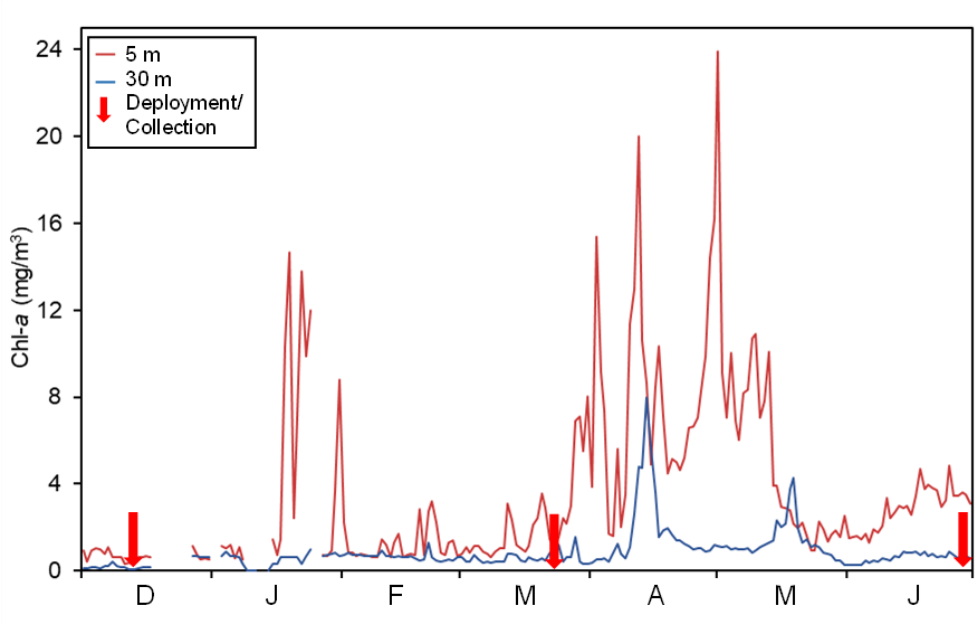

Figure S2-3: Chlorophyll-*a* data collected using a fluorometer attached to the Dabob Bay (Hood Canal) Oceanic Remote Chemical Analyzer (ORCA) buoy located 2.3 km from the study site. This data shows the average chlorophyll data from 2010 to 2021, with some time periods omitted due to technical difficulties. Daily data were averaged at both 5 and 30 m study sites. Arrows show the time when organisms were deployed (December 11, 2016) and collected (March 22, 2017 and June 27, 2017). Data courtesy of Applied Physics Laboratory, University of Washington.

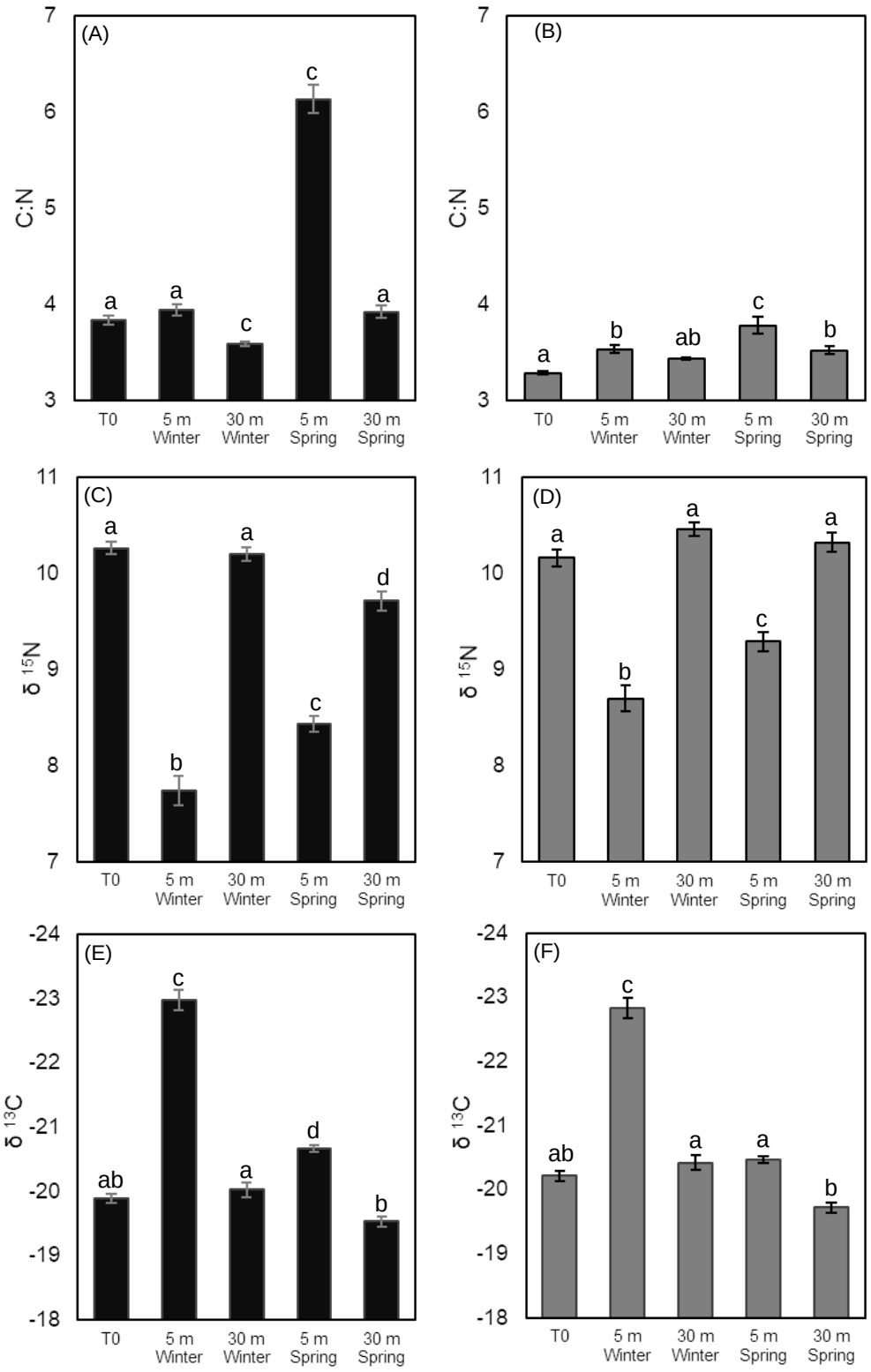

Figure S2-4: Average ± S.E. of (A) Mediterranean mussel (*Mytilus galloprovincialis*) and (B) Purple-hinge rock scallop (*Crassodoma gigantea*) C:N ratio, (C) mussel and (D) scallop δ ^{15}N

signature, and (E) mussel and (F) scallop $\delta^{13}C$ signatures. Bars with no common letters indicate significant differences ($p < 0.05$).

Table S2-1: Summary of stable isotope signatures (Average ± S.E.) of the mussel *Mytilus galloprovincialis* and scallop *Crassadoma gigantea* acclimated to two depths and collected during two seasons.

		Mussel		Scallop	
Season	**Depth**	**$\delta^{13}C$**	**$\delta^{15}N$**	**$\delta^{13}C$**	**$\delta^{15}N$**
T_0		-19.88 ± 0.07	10.26 ± 0.07	-20.21 ± 0.10	10.16 ± 0.09
Winter	**5 m**	-22.97 ± 0.16	7.73 ± 0.15	-22.83 ± 0.17	8.70 ± 0.13
	30 m	-20.02 ± 0.11	10.20 ± 0.07	-20.42 ± 0.07	10.46 ± 0.07
Spring	**5 m**	-20.67 ± 0.05	8.43 ± 0.08	-20.47 ± 0.11	9.29 ± 0.10
	30 m	-19.53 ± 0.08	9.71 ± 0.01	-10.71 ± 0.12	10.32 ± 0.10

5.3 APPENDIX S3

Table S3-1: Puget Sound seawater chemistry at each study site for the first (T1) and second (T2) half of the one-year study. CI20 represents Carr Inlet at 20 m, and CI5 at 5 m. DB is Dabob bay at 5 m, and PW is Point Wells at 5 m. Values are represented as mean and standard error [± S.E.]. Common letters between parameters indicate that there were no significant differences between those sites.

	July 2018 - January 2019 (T1)				January 2019 - July 2019 (T2)			
	CI20	CI5	DB	PW	CI20	CI5	DB	PW
Temperature (°C)	12.19 ± 1.40^{ab}	12.78 ± 1.93^{a}	11.97 ± 2.47^{bc}	12.45 ± 1.29^{ab}	9.55 ± 1.30^{c}	10.31 ± 1.89^{d}	11.38 ± 3.33^{c}	10.08 ± 1.72^{de}
Salinity (PSU)	30.14 ± 0.58^{a}	30.02 ± 0.63^{a}	29.99 ± 1.02^{a}	30.11 ± 0.37^{a}	29.64 ± 0.52^{b}	29.58 ± 0.55^{bc}	29.26 ± 1.33^{d}	29.37 ± 0.54^{cd}
Chlorophyll-a (mg/m^3)	1.58 ± 1.08^{ab}	$5.05 \pm 5.84b^{c}$	2.51 ± 0.98^{ad}	1.25 ± 1.09^{b}	2.44 ± 2.59^{abd}	5.64 ± 6.77^{c}	3.79 ± 3.54^{e}	3.03 ± 3.65^{b}
DO (mg/L)	6.18 ± 1.03^{a}	8.32 ± 2.17^{b}	8.27 ± 1.56^{b}	6.55 ± 0.96^{a}	8.28 ± 0.68^{b}	9.71 ± 1.29^{c}	10.48 ± 1.56^{d}	8.49 ± 1.05^{b}
pH	7.74 ± 0.05^{a}	7.84 ± 0.11^{b}	7.94 ± 0.18^{c}	7.88 ± 0.10^{d}	7.91 ± 0.07^{cd}	8.01 ± 0.13^{e}	8.11 ± 0.14^{f}	7.98 ± 0.11^{e}
Ωara	1.05 ± 0.1^{a}	1.37 ± 0.42^{b}	1.71 ± 0.79^{cd}	1.43 ± 0.37^{be}	1.35 ± 0.21^{b}	1.79 ± 0.57^{c}	2.23 ± 0.78^{f}	1.59 ± 0.46^{de}
pCO_2 (µatm)	872 ± 101^{a}	703 ± 161^{b}	871 ± 103^{a}	626 ± 134^{c}	566 ± 93^{d}	454 ± 154^{e}	570 ± 94^{d}	481 ± 127^{3}

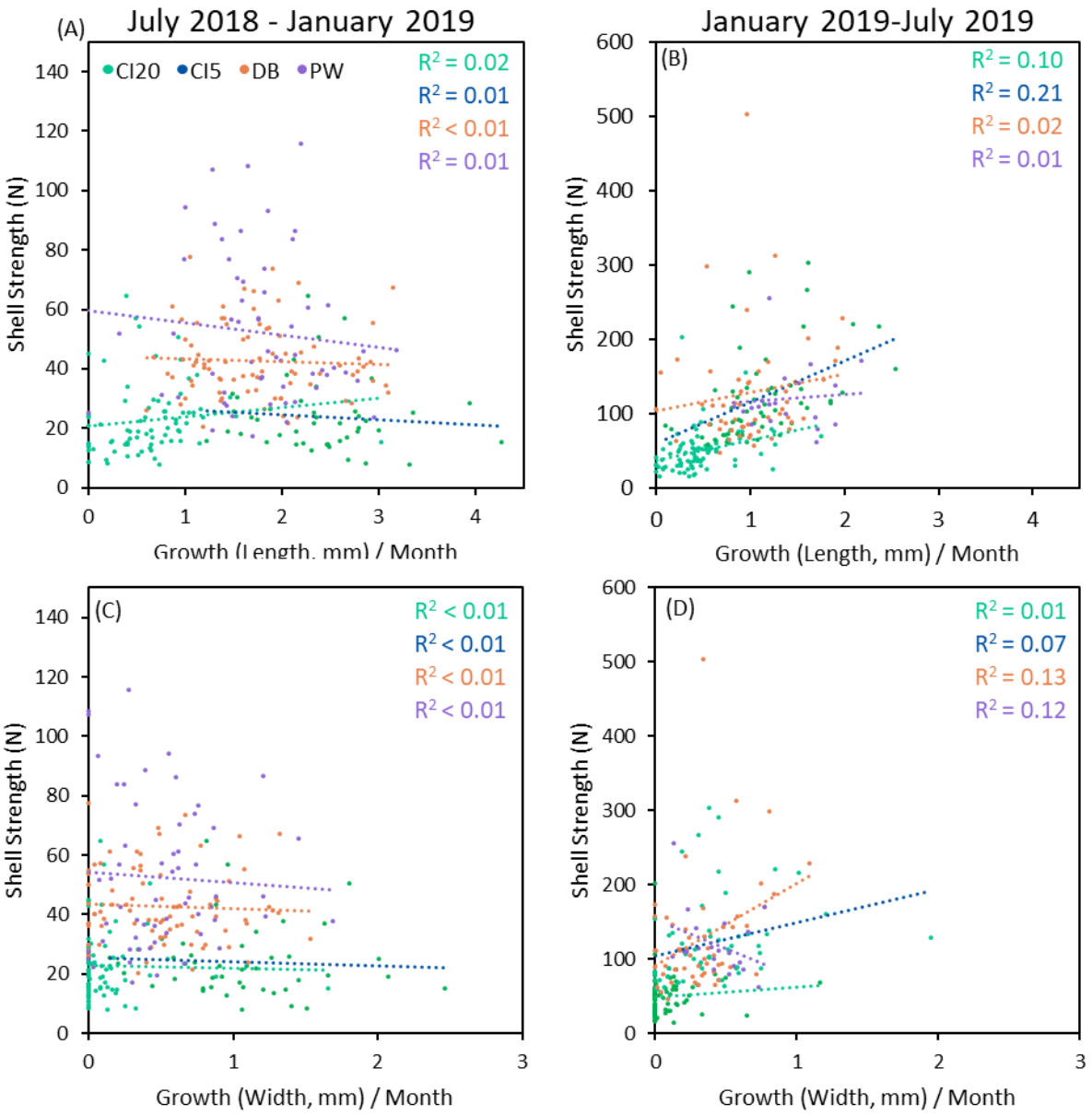

Figure S3-1: Linear regression correlating both height and lengthwise growth rate (mm month^{-1}) with force needed to puncture the shell (N). Each point represents one individual. Each panel represents a different collection time and correlation with shell strength with (A) comparing shell height growth rate with shell strength in July 2019 – January 2019 (T1), (B) is the same as A but for January 2019 – July 2019 (T2), (C) correlates shell strength with lengthwise growth rate in T1, and (D) is the same as C but with the T2 collection period.

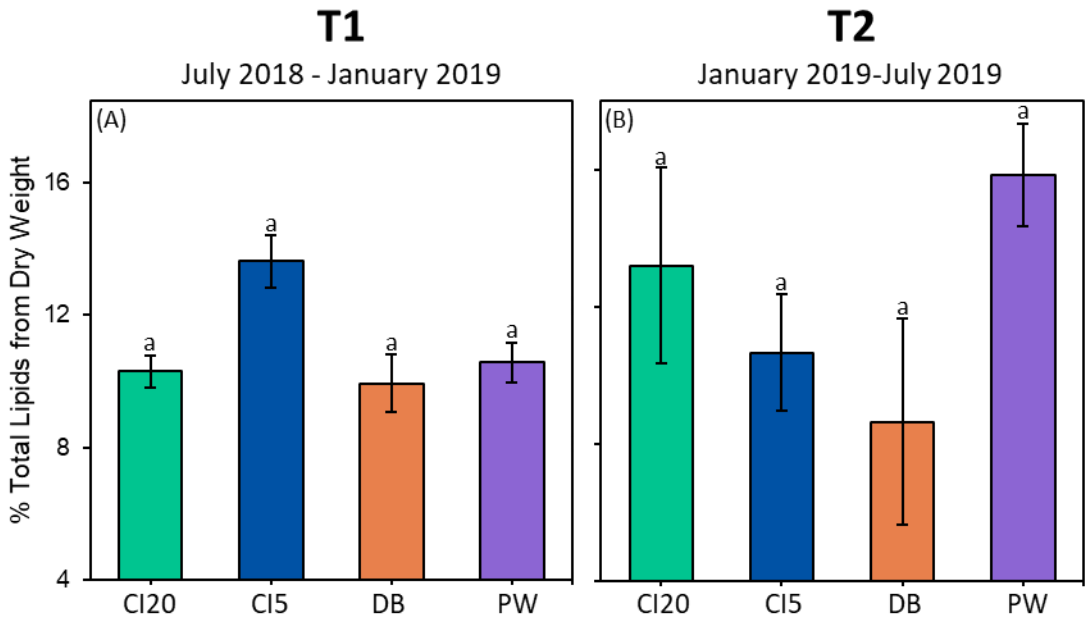

Figure S3-2: Percent of dry weight made up of lipids in Olympia oyster (*Ostrea lurida*) acclimatized to four study sites within Puget Sound, WA (CI20: Carr Inlet at 20 m, CI5: Carr Inlet at 5 m. DB: Dabob Bay at 5 m, PW: Point Wells at 5 m) for either (A) six months (T1) or (B) one year (T2). Post-hoc statistics were run on both collection periods together and are represented with letters. Bars with all common letters indicate that there were no significant differences between site or time of collection.

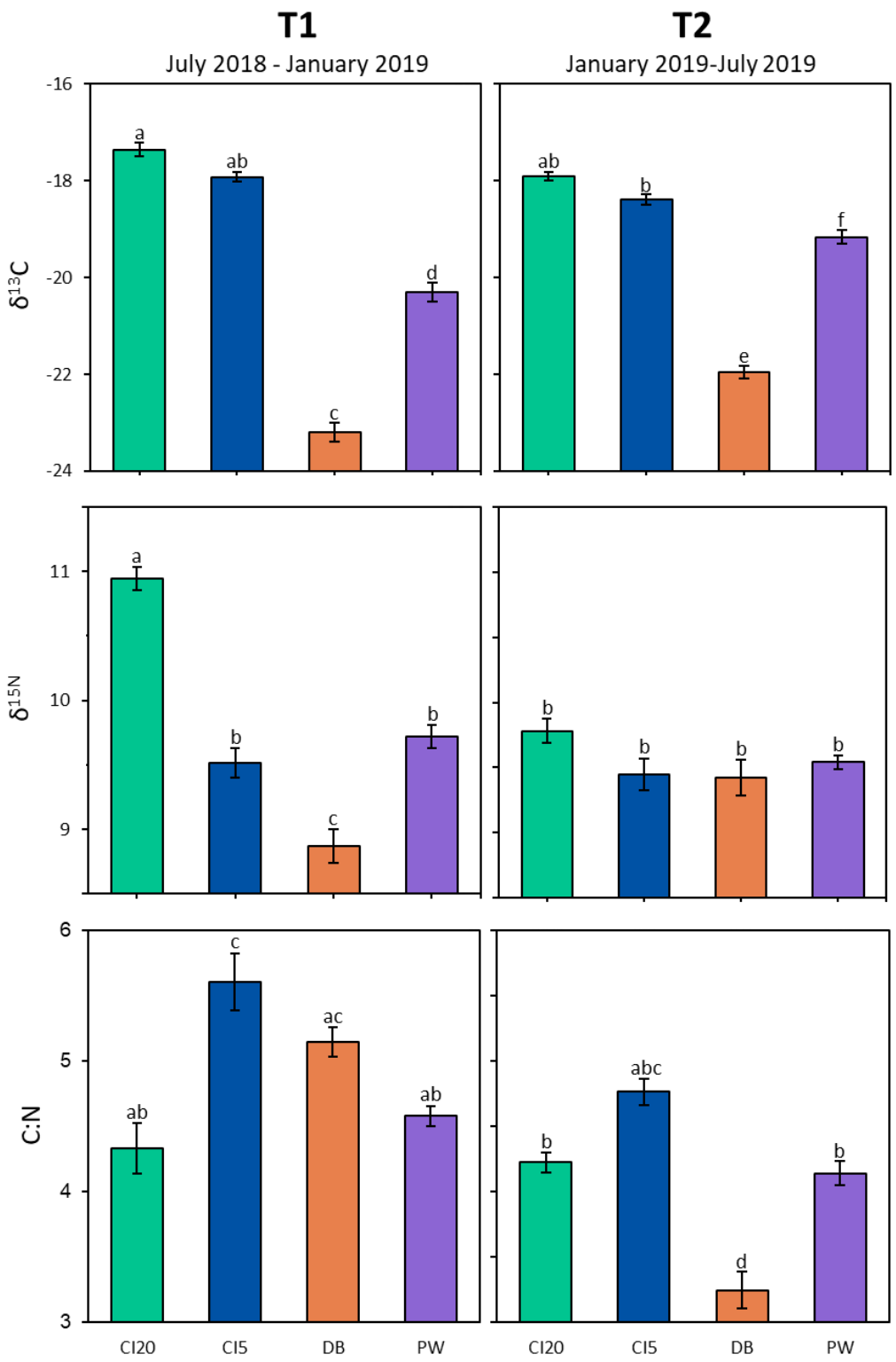

Figure S3-3: Adult Olympia oyster $\delta^{13}C$ and $\delta^{15}N$ signatures and C:N ratio extracted from full-body visceral mass. Panels on the left (A, C, E) show results of oysters acclimatized to Puget Sound, WA for six months from July 2018 to January 2019 (T1), and panels on the right (B, D,

F) represent oysters which were allowed to acclimatize for an additional six months from January 2019 to July 2019 (T2). Sites are as follows: CI20 represents Carr Inlet at 20 m, and CI5 at 5 m. DB is Dabob bay at 5 m, and PW is Point Wells at 5 m. (A and B) represent $\delta^{13}C$ signature, (C and D) represent $\delta^{15}N$ signature, and (E and F) depict C:N ratio. Post-hoc statistics were run on both collection periods together and are represented with letters. Bars with no common letters indicate significant differences ($p < 0.05$).

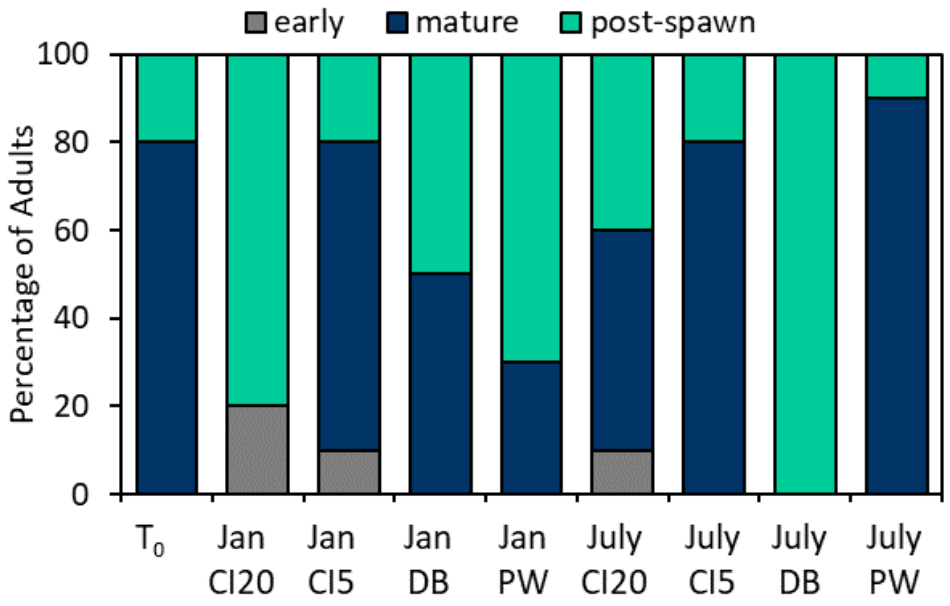

Figure S3-4: Stacked bar plot showing reproductive maturation data from Olympia oyster (*Ostrea lurida*, n=10). T_0 indicates oysters from before the start of the experiment (July 2018). Oysters were outplanted to four sites (CI20: Carr Inlet at 20 m, CI5: Carr Inlet at 5 m, DB: Dabob Bay at 5 m, PW: Point Wells at 5 m) for either 6 months (Jan = January 2019, T1) or 1 year (Jul = July 2019, T2). Maturation stages were binned into three general categories: early, mature (gravid), and post spawn.

5.4 APPENDIX S4

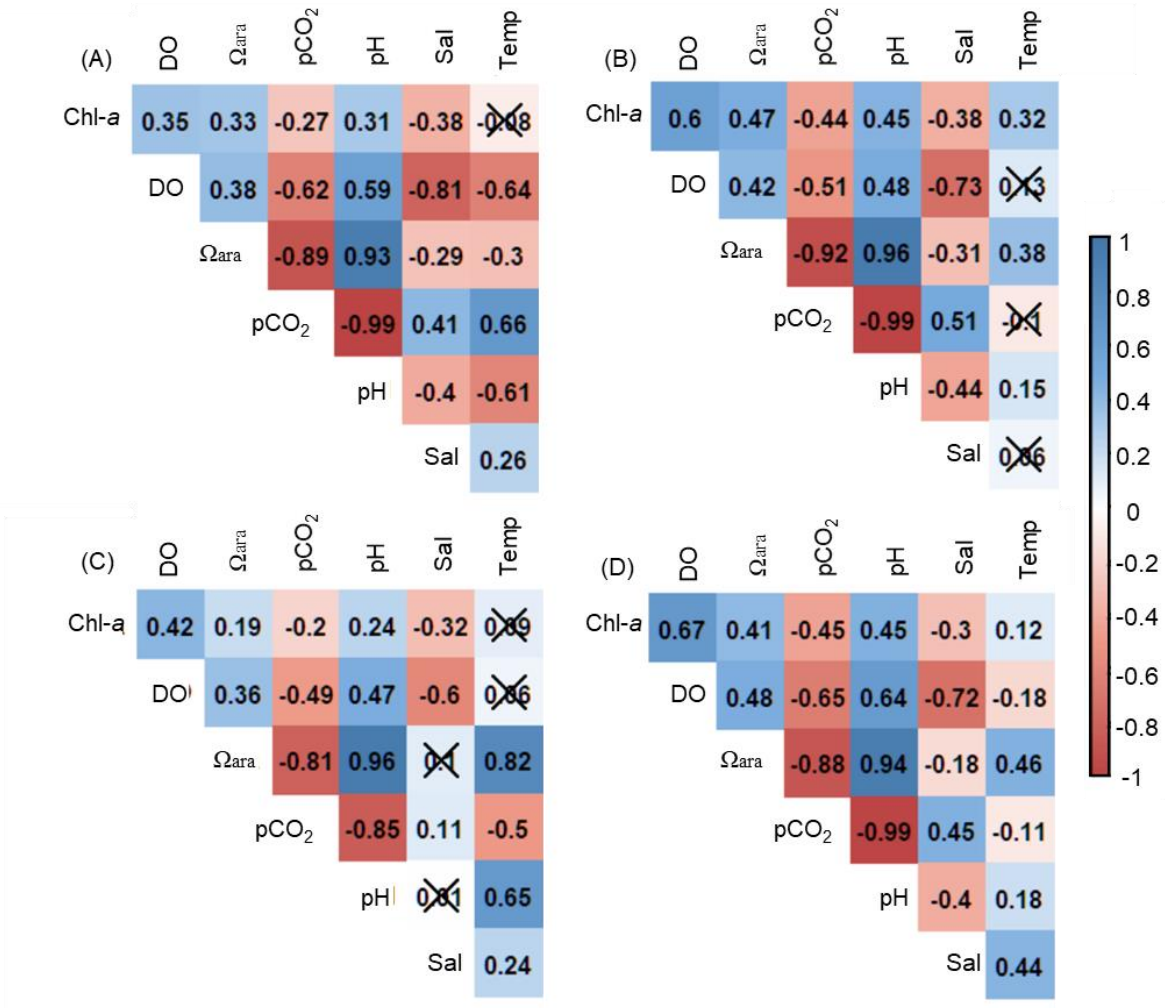

Figure S4-1: Correlations between oceanographic parameters throughout the study at each site: (A) CI20, Carr Inlet at 20 m; (B) CI5, Carr Inlet at 5 ; (C) DB, Dabob bay at 5 m; and (D) PW, Point Wells at 5 m. Parameter abbreviations and units are as follows: chl-*a* is chlorophyll-*a* (mg/m^3), DO is dissolved oxygen (mg/L), Ωara is aragonite saturation state, pCO_2 (µatm), pH, Sal is salinity (PSU), and Temp is temperature (°C). Numbers inside each box represent Pearson correlation coefficient. Darker shades signify a stronger correlation, with red depicting a negative correlation, and blue is positive. Boxes signified with an "X" have no correlation with a p-value > 0.05.

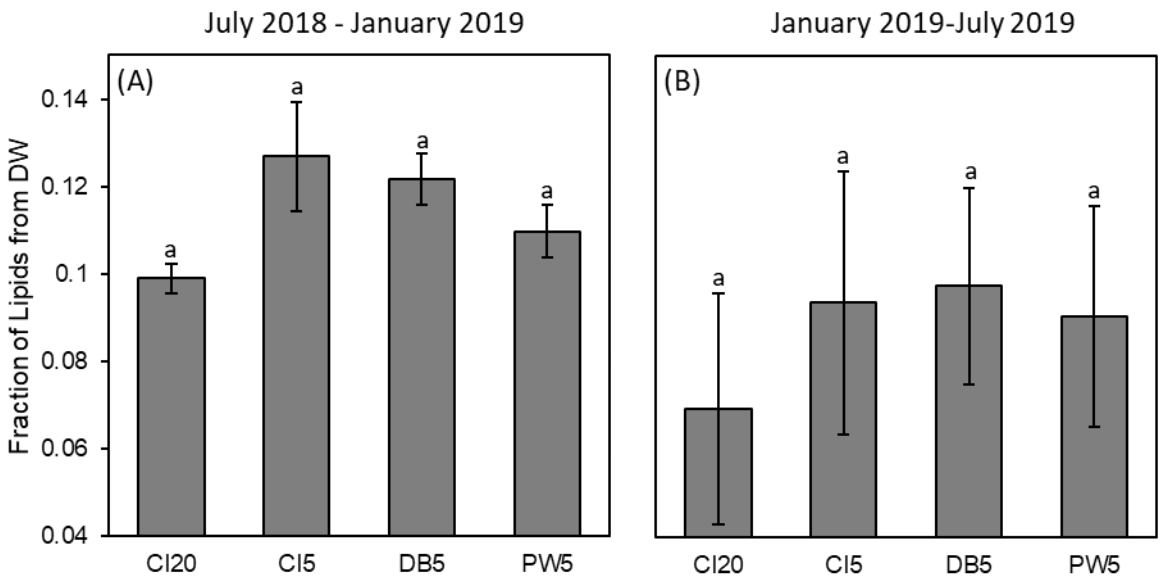

Figure S4-2: Total lipids expressed as a fraction of total dry weight of visceral mass in *M. galloprovincialis* acclimatized to conditions at four sites within Puget Sound, Washinton for either six months (a) or one year (B). Post-hoc statistics were run on both collection periods together and are represented with letters. Bars with all common letters indicate that there were no significant differences between site or time of collection.